ASSESSMENT OF THE DYNAMICS OF SURFACE HYDROLOGY AND WATER QUALITY OF THE BAROTSE FLOODPLAINS, WESTERN ZAMBIA.

By

Anthony Chabala

A thesis submitted to the University of Zambia in fulfilment of the requirements of the Degree in Master of Science in Integrated Water Resources Management.

The University Of Zambia

School Of Mines, Department of Geology

Integrated Water Resources Management Centre

Lusaka

2022

COPYRIGHT

DECLARATION

I, Anthony Chabala do hereby declare that this thesis entitled “Assessment of the dynamics of water quality and surface hydrology of the Barotse Floodplain, Western Zambia” is my own work, that all the sources used or quoted have been indicated and acknowledged by means of complete references. This is in conforming to the regulations required for the award of Master of Science in Integrated Water Resources Management. I further declare that this document has neither in part nor in whole been presented as substance for the award of any degree, either to this or any other University.

Signature of Author: ……..……Date:……..……

APPROVAL

This dissertation of Anthony Chabala is approved as fulfilling the requirements of Degree of Master of Science in Integrated Water Resources Management of the University of Zambia.

Examiner 1:…… ……

Signature:……

Date:……

Examiner 2:……. ……

Signature:……

Date:……

External Examiner:……..…….

Signature:……..

Date:……..

Chairperson Board of Examiners:……

Signature:……

Date:……..

Supervisor:……

Signature:……..

Date:……..

ABSTRACT

The seasonal interactions among rivers, floodplains, vegetation and anthropogenic activities result in highly dynamic systems, which tend to exhibit distinctly different biogeochemical patterns throughout the wet and dry seasons.

An assessment and characterization of the spatial-temporal variability of water quality of the Barotse Floodplain, Western Zambia was based on three major components: biological, physical and chemical properties. Samples were collected and analysed for two successive years for both wet and dry seasons. Further, a hydrological model was developed using the Soil and Water Assessment Tool (SWAT) for predicting sediment yields into the floodplain. This was done to investigate for any heavy metal presence in water and sediments due to upstream mining activities, and nutrient transport mechanisms for the separate seasons.

Results from bacteriological tests indicated that coliforms were highest on the Mongu-Senanga Transect (85.7%), which had Too-Numerous-To-Count (TNTC> 200 coliforms) readings on several points due to a number of human induced activities. Physio-chemical characteristics generally showed a low pH (6.5-6.9) for the dry season as compared to the pH (6.9-7.5) for the wet season. The Luanginga River, at the confluence of the Zambezi River, had the highest turbidity (87.9 NTU), electrical conductivity (EC) and total dissolved solids (TDS).

Results from the hydrological model gave sediment distribution in the floodplain with 0.609 tons/year/subbasin as the highest yield of sediments in the floodplain from the Luanginga River. The model calibrated and validated with its performance monitored by the P and R-factor. The parameters read of: P-factor 0.5 to 0.75; and R-factor 0.56 to 1.36 respectively.

In conclusion, this study shows that the Barotse Floodplain is still in a pristine state and therefore results from this research may be used as baseline information for future work. Due to the upstream large scale copper mining and increased anthropogenic activities via the Luanginga River leading to high turbidly, a proxy to the high sedimentation observed, continuous monitoring is encouraged.

Key Word: Sediments, water quality, Barotse Floodplain, SWAT

ACKNOWLEDGEMENTS

This work is a synergistic product of many minds whose work I have cited and quoted. I am forever grateful to the inspiration and knowledge of the many great scholars who, through their commitment to giving their most valuable time in research on water resources management.

I would also like to thank Prof. Imasiku Nyambe (supervisor of this work), Coordinator, UNZA IWRM Centre, Dr. Kawawa. Banda, Lecturer School of Mines and Head of Department Geology and the entire team of staff at Integrated Water Resource Management Centre (IWRM) for the support during the implementation of this project. This project was carried out with financial support from Southern African Science Service Centre for Climate Change and Adaptive Land Use Management, (SASSCAL), Germany.

DEDICATION

To my father, Felix Katundu Chabala, who has been the essence of my love for education, a personal source of encouragement and inspiration, and a cause for my passionate commitment to finishing every piece of work with excellence. Thank you for teaching me that work is a glimpse/snap short of how well your thoughts are organized;

To my darling wife, Mwaka, your devotion and consistent support during this project while I was away cannot go without mention. I am truly blessed to have you; and

To my University Professor, Imasiku Nyambe, truly your methods of teaching and mentoring students have left a mark on my life, both theoretical and practical approaches. I can simply say that much of how I see and do things today is because of your undying efforts to seek academic perfection.

Table of Contents

Appendices

List of Figures

List of Tables

List of Abbreviations and Acronyms

Abbreviation/Acronym	Full Name
ACC	Archaean Congo Craton
ADCP	Acoustic Doppler Current Profiler
AAS	Atomic Absorption Spectrophotometry
ASTER	Advanced Space-borne Thermal Emission and Reflection Radiometer
BB	Broad Band
BGR	Federal Institute for Geoscience and Natural Resources
BMP	Best Management Practices
CFSR	Climate Forecast System Reanalysis
CH_K2	Effective Hydraulic Conductivity
CMIP3	Climate Model Simulation
CN	Curve Number
CSO	Central Statistics Office
CSV	Comma Separated Values
CU	Commercial Utilities
CUP	Calibration and Uncertainty Programs
DEM	Digital Elevation Model
DGH	Digital Ground Model
DHM	Digital Height Model
DMMU	Disaster Management and Mitigation Unit
DO	Dissolved Oxygen
DTED	Digital Terrain Elevation Data
DTM	Digital Terrain Model
DWA	Department of Water Affairs
DWNP	Department of Wildlife and National Parks
DWRD	Department of Water Resources Development
EC	Electrical Conductivity
ESCO	Evaporation Compensation Coefficient
ESRI	Environmental Systems Research Institute
ET	Evapotranspiration
FAO	Food and Agricultural Organization
FC	Field Capacity
GDB	Geo-Database
GIS	Geographic Information Systems
GLUE	Generalized Likelihood Uncertainty Estimations
GPS	Global Positioning System
GRZ	Government of the Republic of Zambia
GUI	Graphical User Interface
GW_DEPLAY	Groundwater Delay Time
HP	Horse Power
HRU	Hydrologic Response Unit
HWSD	Harmonized World Soil Database
IPCC	Intergovernmental Panel for Climate Change
IRI	International Research Institute
ITCZ	Inter Tropical Convergence Zone

IUCN	International Union for Conservation of Nature
JICA	Japanese International Cooperation Agency
KMB	Kibaran Mobile Belt
LOADEST	Load Estimator
LOD	Limit of Detection
LHB	Left Hand Bank
LH-OAT	Latin Hypercube One-factor-At-Time
MAL	Ministry of Agriculture and Livestock
MCMC	Markov Chain Monte Carlo
MIT	Massachusetts Institute of Technology
MIUB	Meteorological Institute of the University of Bonn
NCEP	National Centre for Environmental Prediction
NDTr	Niton Data Transfer
NGO	Non-Governmental Organization
NOAA	National Oceanic and Atmospheric Administration
NS	Nash-Sutcliffe
NYSKIP	Number of Years to Skip
ParaSOL	Parameter Solution
PBIAS	Percent Bias
PPU	Percentage Prediction Uncertainty
PSO	Particle Swarm Optimization
R^2	Coefficient of Determination
RHB	Right Hand Bank
RMSE	Root Mean Square Error
SADC	Sothern African Development Community
SARDC	Sothern African Research and Documentation Centre
SASSCAL	Southern African Science Service Centre for Adaptive Land Use
SOL_AWC	Soil Available Water Content
SPM	Suspended Particulate Matter
SRTM	Shuttle Radar Topographic Mission
SS	Suspended Solids
SSURGO	Soil Survey Geographic
STATSGO	State Soil Geographic Data Base
SUFI-2	Sequential Uncertainty Fitting Volume 2
SVM	Spectra View Mode
SWAT	Soil and Water Assessment Tool
TDS	Total Dissolve Solids
TNTC	Too-Numerous-To-Count
TS	Total Solids
t-Stat	Statistical Test of Parameter Sensitivity
TSS	Total Suspended Solids
UNESCO	United Nations Educational, Scientific and Cultural Organization
UNZA	University of Zambia
UTC	Universal Time Coordinated
UZB	Upper Zambezi Basin
WARMA	Water Resources Management Authority
WEP	Water and Energy Transfer Processes
WEPP	Watershed Erosion Prediction Project

WGEN	Weather Generator
WGS 84	World Geodetic System 1984
WHO	World Health Organization
WMO	World Meteorological Organization
XRF	X-Ray Fluorescence
ZABS	Bureau Of Standards
ZAWA	Zambia Wildlife Association
ZEMA	Zambia Environmental Management Agency
ZESCO	Zambia Electricity Supply Corporation
ZRA	Zambezi River Authority

CHAPTER 1: INTRODUCTION

1.1 Background

Floodplains are of great cultural and economic importance as most early civilizations arose in fertile flood plains (Nicholas, 2008). Throughout history, people have learned to cultivate and use their rich resources as they served as focal points for urban development and exploitation of their natural functions (Naiman et al., 2005). Flood plains are also described as dynamic systems that are shaped by repeated erosion and deposition of sediments, inundation or prolonged hydro-periods during rising water levels, and complex ground and surface water exchange processes. This dynamic nature makes flood plains among the most biologically productive and diverse ecosystems on earth (Gregory et al., 1991; Naiman & De´camps, 1997; Tockner and Stanford, 2002; Naiman et al., 2005).

Wetlands or floodplains are widely thought to be important locations for the uptake and transformation of nutrients and sediment in fluvial landscapes (Noe and Hupp, 2007). Sediments are probably the most influential determinant of the ability of the system to process and sustain nutrient loads (Ahiablame et al, 2010). This is because floodplains are frequently thought of as sinks of inorganic nutrients and sources of organic nutrients, in other words nutrient transformers (Noe and Hupp, 2007). Moreover, many agrochemicals, heavy metals and nutrients chemically bind to sediments which provide a transport mechanism for these contaminants as well as substrate where they react (Lovett, Price & Edgar, 2007).

All these agrochemical, heavy metal and nutrient contaminants, as described above, may be caused by anthropogenic perturbations which can lead to alterations of the physical, chemical and biological properties of the water body (Bilotta and Brazier, 2008). Nutrient contaminants can be categorized with respect to where they are being discharged or source. Writing on “modelling the relationship between land use and surface water quality”, Tong & Chen (2002) categorize runoff from different types of land use may be enriched with different kinds of contaminants which may come from agricultural lands enriched with nutrients, highly developed urban areas (mines inclusive) enriched with rubber fragments, oil, heavy metals, as well as sodium and sulphates from road deicers. While Lovett, Price and Edgar (2007) refer to sediments as contaminants, Baidu-Foron et al (2014) have a different stance in that they view sediments as deposits composed of silt

and humus from vegetation and decaying aquatic plants which enrich floodplain areas, creating fertile arable land for crop production.

In aquatic systems, alluvial sediments use water in their conveyance and therefore it becomes inevitable to also look at the qualitative aspects of water. Bilotta et al (2012), Gray (2008) and Richter et al (2005) explain that one of the most commonly attributed causes for the impairment of water quality globally is the presence of suspended particulate matter (SPM), ranging from nano-scale particles and colloids to sand-sized sediments. When anthropogenic activities are enhanced, concentrations of suspended solids (SS) also increase having the potential to alter the physical, chemical and biological properties of water bodies. These alterations may include: i) reduced penetration of light, temperature changes, infilling of channels and reservoirs when solids are deposited (physical aspects); ii) release of contaminants such as heavy metals and pesticides and nutrients such as phosphorous from adsorption sites on the sediments (chemical aspects), and iii) depletion of oxygen levels especially when the sediments have a high organic content (biological aspects), (Bilotta and Brazier, 2008).

Bilotta et al (2012) and Flaxman (1975) bring in the aspect of SS and their effects on water quality. According to Flaxman (1975, p.78) sediments probably have their greatest impact on the water used for irrigation as accumulation in canals, laterals and farm ditches require cleanouts while Bilotta and Brazier (2008) add to this by stipulating that SS are an extremely important cause of water quality deterioration leading to aesthetic issues such as high cost of water treatment, a decline of fisheries resource and serious ecological degradation of aquatic environments, for example, re-leveling for efficient water applications due to depositions on fields reducing on permeability.

With all this complex hydrological relationship between sediments and water quality, modelling seems to be one of the best options to comprehending such systems. The Soil and Water Assessment Tool (SWAT) is used to model soil sedimentation yields, identify soil erosion prone areas, and assess the impact of Best Management Practices (BMPs) on sediment reduction (Betrie et al., 2011). SWAT model seems to be robust and can be relied upon as a tool for catchment sediment management in the tropics (Preksedis &Van Griensven, 2011). By robustness, we mean that after specifying the basic input variables and their accurate equilibration, we can expect quality outputs of simulations, even if the full capacity of the input database is not filled (Jozef et al., 2010). Unlike other modelling tools which are either too expensive or have numerous data input

requirements, SWAT is a freeware, and has been used by a number of researchers all over the world in various applications. These applications range from qualitative aspects to quantitative aspects. These may include sediments, river discharge or flows, water quality, nutrients etc. All this is dependent on what the ultimate expectations of the project are, following the objectives (SWAT Documentation, 2009).

This research is part of the Southern African Science Service Centre for Adaptive Land Use Management, (SASSCAL). SASSCAL is a joint initiative of Angola, Botswana, Namibia, South Africa, Zambia, and Germany, responding to the challenges of global change. This study is under a specific task identity number 191 and the research area is in Western Zambia. Western Zambia hosts the Barotse Basin which is part of the larger Zambezi Basin shared by eight (8) countries such as Angola, Botswana and Namibia who will benefit from this task. The major significance of this study is to assist Zambia develop a database to support existing national databases that classifies water resources specifically in the Barotse Basin, in terms of spatial variations in quality and quantity. In spite of the Barotse Basin hosting headwaters of the Zambezi River which have key economic, environmental and social connotation, no standard database is operational. Therefore, this study has a direct contribution to the Zambian Water Sector. This includes the government, cooperating partners, private sector and Non-Governmental Organizations (NGOs).

1.2 Description of the Study Area

The Barotse Floodplain is found within the Upper Zambezi Basin (UZB). This is illustrated in Figure 1.1. The basin lies between latitudes 11^0S -19^0S and longitude 18^0E -27^0E, which covers part of Western Zambia. This includes parts of Angola, Namibia and Botswana.

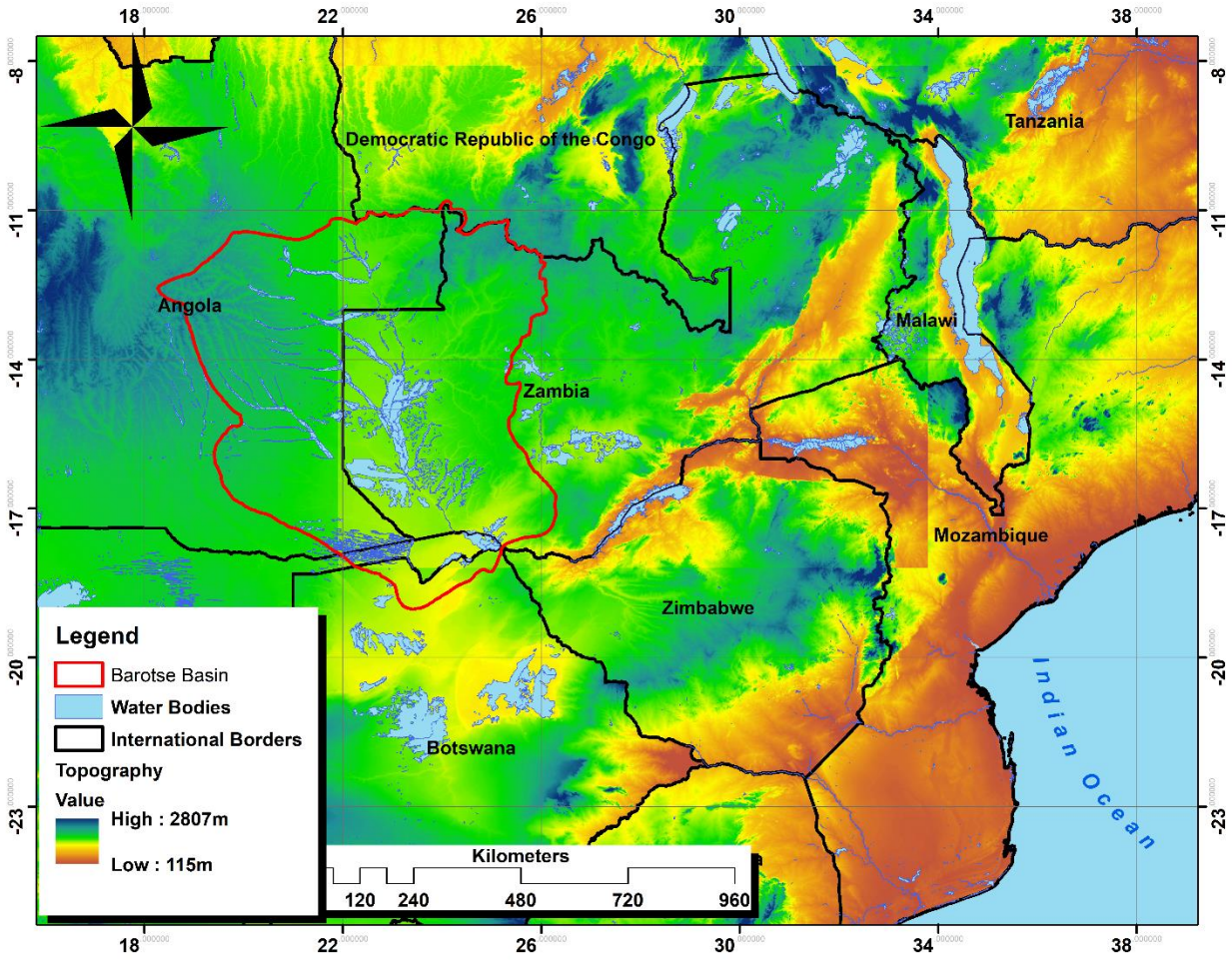

Figure 1.1: Location of the Upper Zambezi Basin (UZB) covering parts of Angola, Namibia and Botswana

The floodplain can be accessed via Mongu-Lusaka Road (M9) which cuts across the Kafue National Park or Livingstone-Lusaka Road (M10) passing through Kazungula District into Sesheke. The extent of the floodplain is described by Turpie et al, (1999), Timberlake (2000) and the report produced by the Ministry of Finance (2013) on an Investment Project for the Barotse and Kafue Sub-basins under the Strategic Programme for Climate Resilience in Zambia. According to (GRZ-Ministry of Finance, 2013), the floodplain measures approximately 240 km long and 34 km wide, extending from Lukulu in the north to Nangweshi in the south. The total wetland area is estimated at 1.2 million hectares (Turpie et al., 1999). This includes the Barotse Floodplain, Lungwebungu Wetlands, Luena Flats, Luanginga River and Liuwa Plains National Park. From the five, the Barotse Floodplain is broadly estimated at 550,000 hectares. It comprises of excessive grasslands from Lukulu, which is located near a confluence of three river systems

namely, Kabompo, Lungwebungu and Zambezi rivers to Senanga District. Part of the wetland that specifically falls in Western Zambia is shown in Figure 1.2.

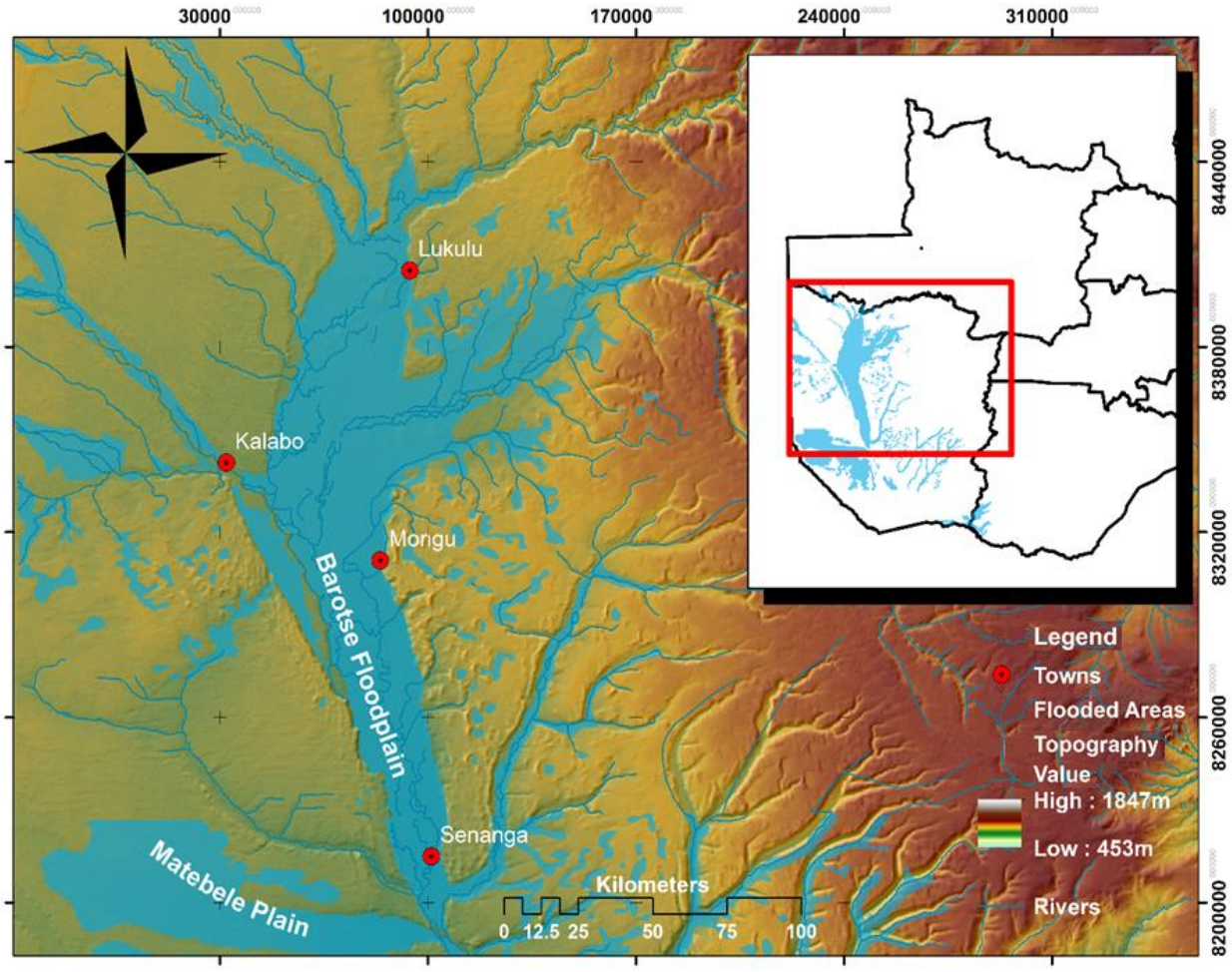

Figure 1.2: Location of the Barotse Floodplain within Western Zambia and its related river systems

Timberlake (2000) further defines the area as extending from Lukulu to downstream of Senanga, and including the Liuwa Plains National Park, Luena Flats, the Barotse Floodplain and the Lungwebungu River Wetlands. The Liuwa Plains National Park and associated areas to the north-west of the floodplain are relatively flat and more water logged during the rainy season while remaining extremely dry during the rest of the year as soils of this region have a high infiltration rate. Baidu-Foron et al, (2014) generalize the floodplain into four categories which are arable land, canals, lagoons and swamps. The estimated area of the Barotse Floodplain and extended wetlands can be viewed in a summary table (Table 1-1). It is flat and influenced by a number of river systems.

Table 1-1: Estimated area of the Barotse Floodplain and extended wetlands (Turpie et. al., 1999)

Wetland	**Area (ha)**
Barotse Floodplain	550,000
Lungwebungu Wetland	70,000
Luena Flats	110,000
Luanginga River	100,000
Liuwa Plains National Park	366,000
Total	**1,196,000**

1.2.1 Climate

The Barotse Floodplain is described to be in a region with an elevation of about 1000m tilting very slightly to the south. The Zambezi and its headwaters rise on the higher ground to the north, which experiences rainfall of about 1400mm annually. However, a map made by the International Research Institute (IRI) Climate Library (satellite rainfall data, http://iridl.ldeo.columbia.edu/SOURCES/) gives the 2014 to 2015 annual rainfall distribution across Zambia and its neighbouring countries (Figure 1.3). Of interest is the annual rainfall pattern in the red bounding box. Rainfall generally ranged from 500mm/year in the Southern parts of Western Zambia to around 1200mm/year in the North near North Western Province and parts of Angola further North West. This clearly shows that the largest contributions to the floodplain inundation emanate from the northern region, particularly North Western Zambia which has pockets of deeper brown, indicating higher precipitation following the colour bar or legend attached to the map.

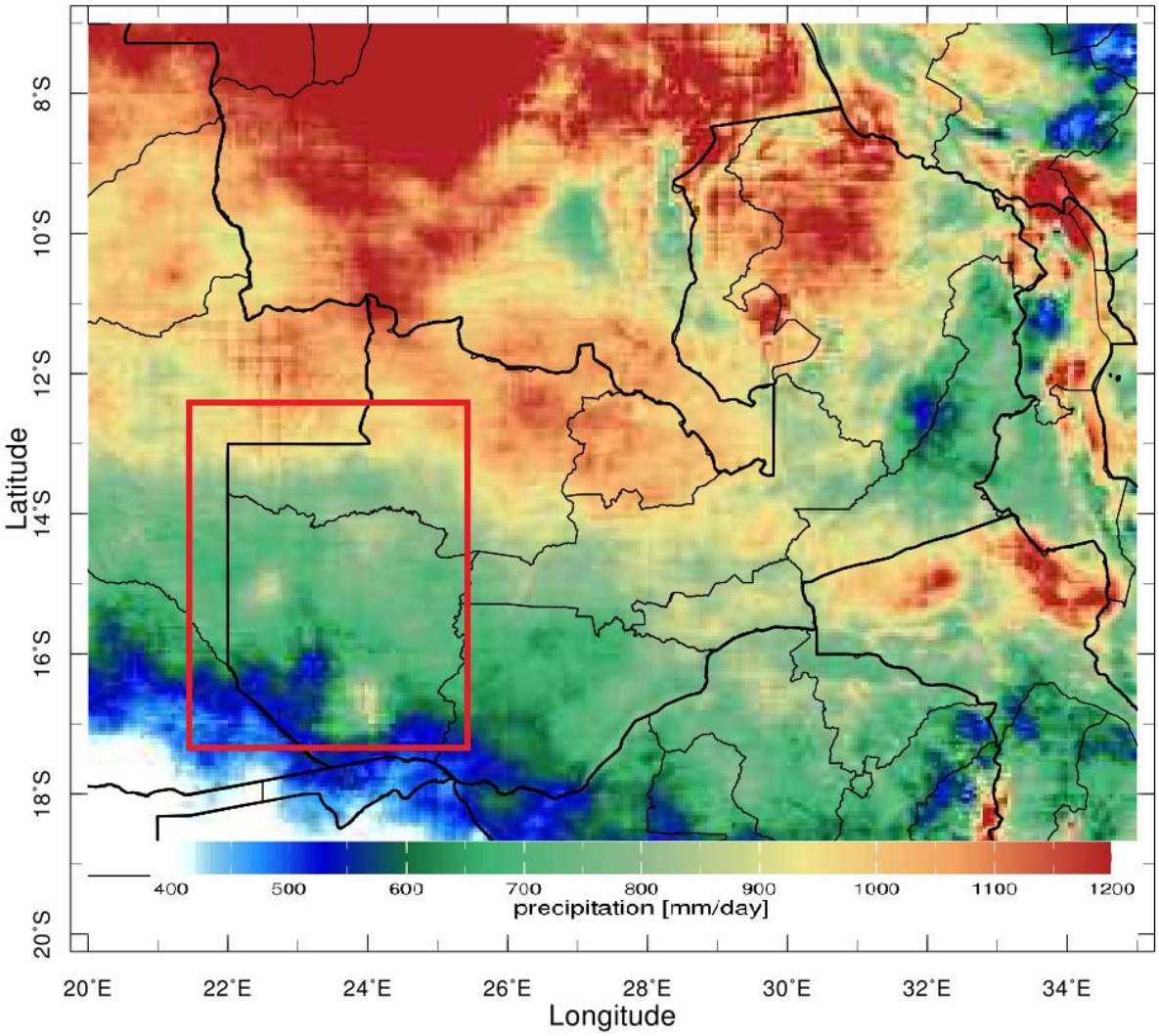

Figure 1.3: Annual rainfall distribution according from satellite imagery for 2014 to 2015 seasons (IRI Climate Library, 2016)

The main wet season runs from November until March, although inundation depends mainly on rainfall in the upper catchment and seepage from the uplands (Zimba et al, 2018). In Mongu, the average annual rainfall is about 945mm leaving the floodplain with green fresh grass capable of feeding 250,000 cattle. The area is hot from September to December, with a mean maximum for October of 41.26^{0}C, and cool from May to August, with a mean maximum in June of 29.67^{0}C and a mean minimum of 8.04^{0}C (National Oceanic & Atmospheric Administration (NOAA), 2016). The climatic features of the study area from January to December 2016 are outlined for some of the weather parameters (Table 1-2).

The climate of a watershed provides the moisture and energy inputs that control the water balance and determine the relative importance of different components of the hydrological cycle (SWAT Documentation, 2009).

Table 1-2: Climatic parameters from January through to August as monitored at Mongu, Western Zambia (NOAA, 2016)

PARAMETER	WS50M	T2M_MAX	T2M_MIN	PRECTOTCORR	PRECTOTCORR_SUM
YEAR	2016	2016	2016	2016	2016
JAN	4.06	35.13	18.62	8.9	274.22
FEB	3.23	34.24	18.69	4.19	89.65
MAR	3.55	30.86	18.19	6.14	189.84
APR	5.17	31.34	12.19	0.63	21.09
MAY	5.22	30.33	9.7	0	0
JUN	5.47	29.67	8.1	0	0
JUL	5.57	32.67	8.04	0	0
AUG	6.64	35.22	9.48	0	0
SEP	6.07	38.74	14.21	0	0
OCT	6.12	41.26	18.12	0.09	0
NOV	4.07	41.05	18.84	2.17	58.01
DEC	3.45	39.15	18.95	4.46	126.56
ANN	4.89	41.26	8.04	2.22	759.38
Parameter(s) Meaning					
WS50M	MERRA-2 Wind Speed at 50 Meters (m/s)				
T2M_MAX	MERRA-2 Temperature at 2 Meters Maximum (C)				
T2M_MIN	MERRA-2 Temperature at 2 Meters Minimum (C)				
PRECTOTCORR	MERRA-2 Precipitation Corrected (mm/day)				
PRECTOTCORR_SUM	MERRA-2 Precipitation Corrected Sum (mm)				

1.2.2 Hydrology

Beilfuss (2012) gives an insight into the hydrology of the Zambezi River Basin, following Balek (1971) who gave the first detailed description. After rising in North-Western Zambia and passing southward through Angola, the Zambezi re-enters Zambia in Western Province and becomes larger and more consolidated, giving rise to a series of floodplains. The onset of annual flooding varies greatly and may occur anywhere between December and March, although northern parts of the floodplain are generally inundated earliest. The maximum flood level is attained in April, after which floodwaters gradually recede over May, June and July (Basin, 2003). The complexity of the hydrological network of the study area is given in Figure 1.4 and Table 1-3.

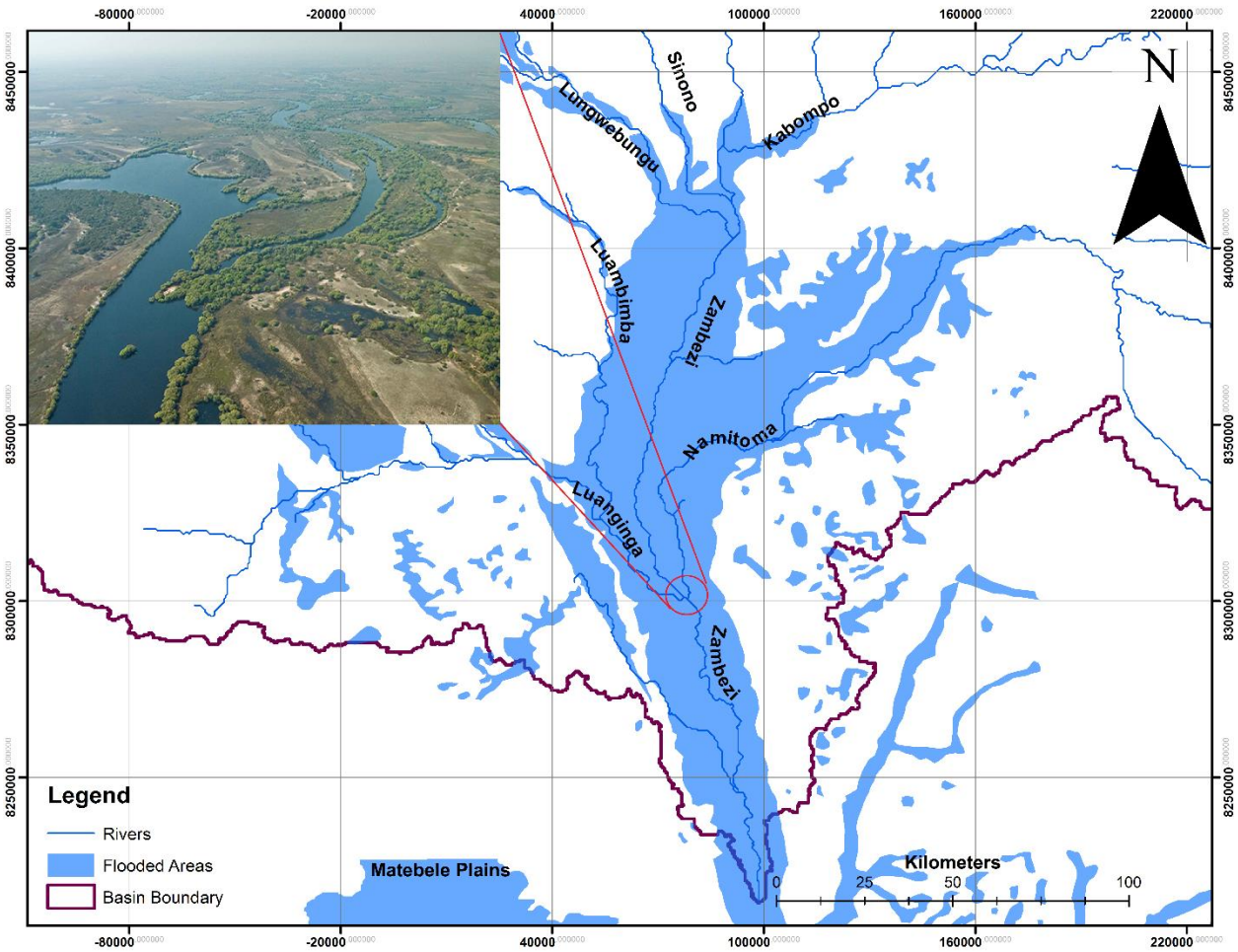

Figure 1.4: The complex river network of the Barotse Floodplain emerging from a series of rivers from the North West clockwise to the North East

Table 1-3: Hydrological variables for natural (unregulated) flows (Beilfuss et al., 2012)

Sub-basin	Area (km^2)	Mean Annual Rainfall(mm)	Potential ET (mm)	Runoff efficiency	Mean annual runoff(mm^3)	Cumulative Zambezi mean annual runoff (Mm^3)
UPPER ZAMBEZI REGION						
Upper Zambezi	91,317	1,225	1,410	0.21	23,411	23,411
Kabompo	78,683	1,211	1,337	0.09	8,615	32,026
Lungwe-bungu	44,368	1,103	1,472	0.07	3,587	35,613
Luanginga	35,893	958	1,666	0.06	2,189	37,802
Cuando/ Chobe	148,994	797	1,603	-	0	37,802
Barotse	115,753	810	1,578	-	553	37,249

Figure 1.4 above shows a stream network made in Arc GIS's spatial analyst under the hydrology tool to give us an impression of where water flows to the main streams and eventually into the inundated areas. A picture is also embedded in the map to give a pictorial overview of the dense vegetation along the river course supporting the tortuous water resources. Sharp changes in vegetation can quickly be noticed as the land immediately after the thick tree riverbanks are grasslands.

1.2.3 Geomorphology

According to the Japanese International Cooperation Agency, JICA (1995), most parts of Zambia are classified as the Central African Plateau. The elevation of the plateau ranges from 600 to 1,850m above mean sea level. The highest parts of the plateau are located in the northern direction and Northwest of Zambia. Elevation gradually reduces in the southwest/south to the Zambezi River. This is the region in which the Barotse Floodplain is found. The region is described to be a flat plateau at an elevation of about 1000m tilting very slightly to the south as shown by the geomorphological flow direction of the Zambezi River.

1.2.4 Geology

The geology of Western Zambia including the Barotse Floodplain which fall within this region was first described by Money (1972). Money (1972), Haddon and McCarthy (2005) elucidate that Western Zambia is predominantly made up of a surficial windblown desert sand cover (the Kalahari Sands) considered to represent the end of the Neogene Erosion surface on the west and

south - east. Thomas & Shaw (1991) describe that these Aeolian Sands have a predominant grain size of 0.2mm and are well sorted. Sandstone with clays, gravels and fine sands typically occurs in deeper Kalahari beds. Alluvium, laterite and colluvium sediments are found in the more central region within rivers systems or terraces; these second order landforms which are due to post-Neogene cycles of erosion and deposition, most of which are probably initiated by a series of down-warps and alternating up-warps (Haddon & McCarthy, 2005). Furthermore, Haddon and McCarthy (2005) describe that the strata constitute the Kalahari Group Formation that varies in depth and may reach up to 450m at its thickest but is more typically 10-100m thick. Surface outcrops of Basement Karoo rocks are infrequent, however, as the Zambezi approaches Senanga Habour, these can be clearly seen.

Other researchers, such as Williams et al. (2009)2, explain that the geology of Zambia is dominated by the northeast-trending Kibaran Mobile Belt (KMB), which separates the Archaean Congo Craton (ACC) to the northwest from the Kalahari and Zimbabwe Cratons to the southeast. Furthermore, the KMB was probably initiated in the Palaeoproterozoic (ca 1800 Ma), but is dominated by Neoproterozoic rocks and structures. However, Western Zambia is underlain predominantly by Palaeozoic to Recent Age Rocks (Figure 1.5). This includes parts of Angola, Namibia and other countries to the south of the area under study. Above it, is the Lufilian Arc, a large dome-like geological structure that dominates the geology of North Western Zambia and extends into the southern part of the Democratic Republic of Congo (ZEMA et al., 2013).

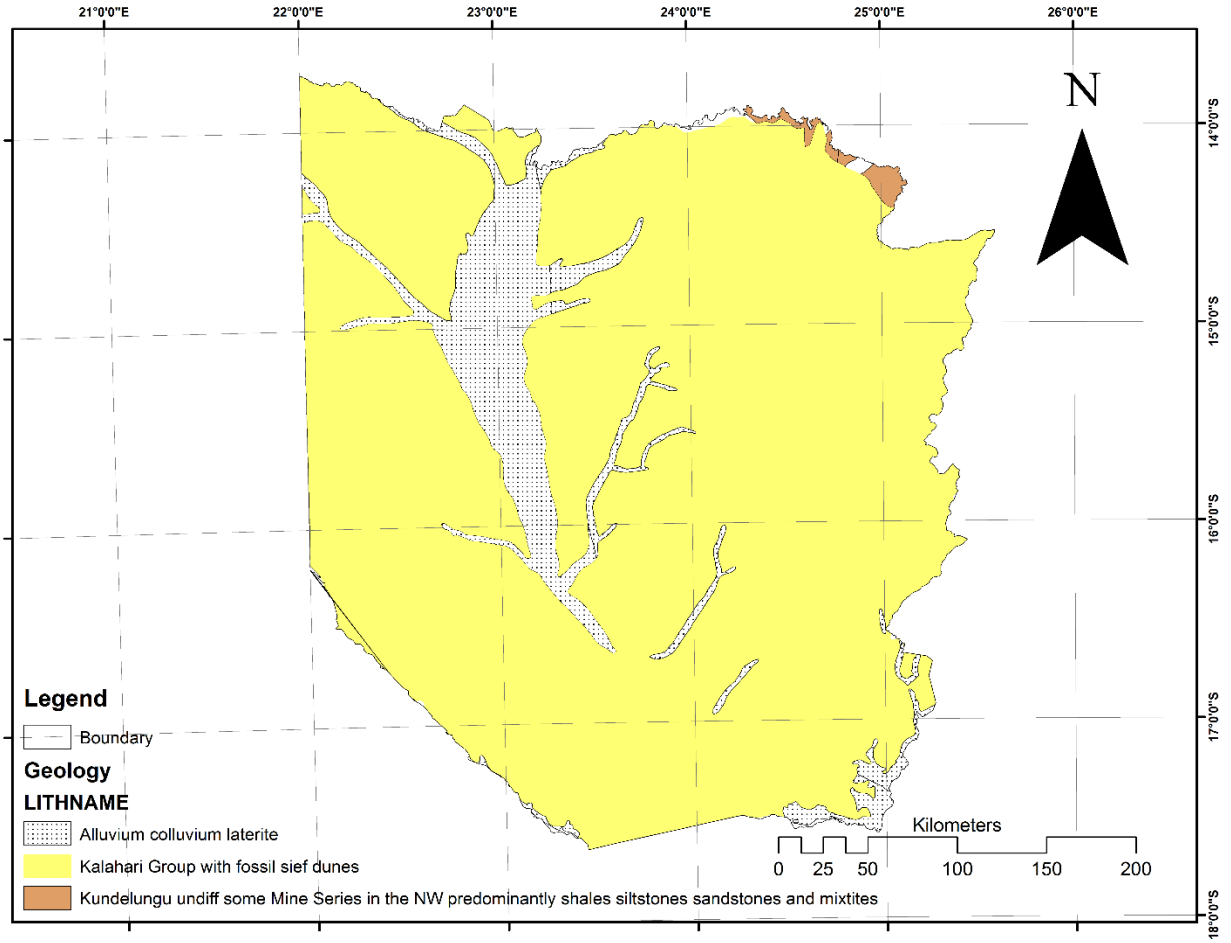

Figure 1.5: Western Province is largely dominated by Kalahari Group with fossil sief dunes with Upper Karoo (Zambezi Valley) Karoo undifferentiated (elsewhere) in the floodplain (Haddon and McCarthy, 2005)

1.2.5 Soils

The soils of Zambia can be classified using three agro-ecological zones. The main soils are loamy-sand or sand alfisols, interspersed with clay (ZEMA et al., 2013). The Kalahari sands are underlined by rocks of the Karoo Supergroup. The sand are a Pleistocene Deposit, the erosion product of Upper Karoo sandstones. They vary in colour from pallid to orange, are moderately acidic and contain 3-12% silt + clay. The sands are not very fertile, the nitrogen content being particularly low where the humus has been disturbed by cultivation. There is no erosion problem as the area is so flat, but heavy population pressure in some areas has resulted in land degradation (Fanshawe, 2010).

According to Muzumara (2014) following after JICA (1995), large parts of Western Province are covered by Acrisols distributed in pan complex zones, while cleysols are distributed in floodplain along main courses and tributaries of the Zambezi River. Pedzils are distributed in the middle of Western Province, namely the eastern part of Mongu. A more detailed spatial view of the soil distribution in Western Zambia is given in Figure 1.6 and Table 1-4 based on FAO/UNESCO classification and soil description following the map units (numbers).

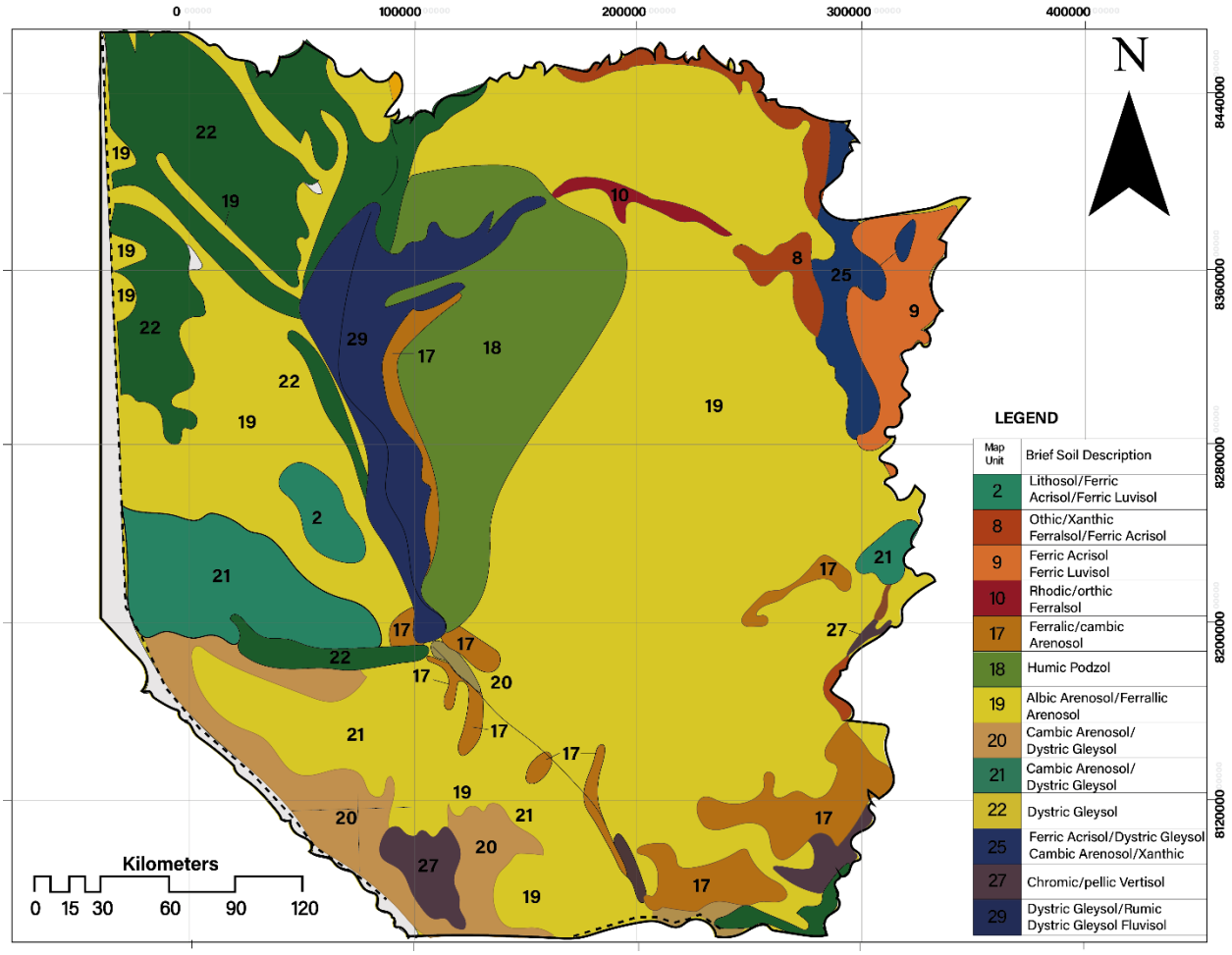

Figure 1.6: Soil distribution of Western Zambia (FAO, 2009)

The main soils types in the floodplain described as the depression land type in Table 1-4 are Dystric Gleysol, Rumic Gleysol and Dystric Fluvisol. These are bordered by Ferric/Cambic Arenosols on the eastern side which fall under the low relief area (western plateau). The mapping units are 29 and 17 for the depressed land type (Dystric Gleysol, Rumic Gleysol and Dystric

Fluvisol) and low relief area (Ferric/Cambic Arenosols), Figure 1.6 above. On the western side of the depression land type area, Ferralic/Cambic Arenosols are under a mapping unit of 19.

Table 1-4: Soil classification for Western Province based on the FAO/UNESCO (2009)

SOIL REFERENCE		F.A.O./UNESCO CLASSIFICATION		
Map Unit	Description of soils (and vegetation)	Major unit(s)	Associated soil unit(s)	Important inclusions
HIGH RELIEF AREAS				
2	Shallow and gravelly soils derived from acid rocks, occurring in rolling to hilly areas, including escarpments ("escarpment zone") (Miombo)	• Lithosol • Ferric Acrisol • Ferric Luvisol		
8	Associated of strongly (60%-map unit 7) and moderately (40 %-map unit 9) leached reddish to brownish clayey to loamy soils derived from acid rocks (Miombo)	• Othic/xanthic Ferralsol • Ferric Acrisol		Dystric Gleysol
9	Moderately leached reddish to brownish clayey to loamy soils, derived from acid rocks (Miombo)	• Ferric Acrisol • Ferric Luvisol	• Orthic/Xanthic Ferralsol	Dyetric/eutric Gleysol
10	Moderately leached reddish to brownish clayey to loamy soils, derived from acid rocks (Miombo)	• Rhodic/orthic Ferralsol	• Ferric Acrisol • Dystric Nitosol	Dyetric Gleysol
LOW RELIEF AREAS (western plateau)				
17	Red sand soils on Kalahari (Balkiaea)	• Ferralic/cambic Arenosol		Dystric Gleysol
18	Podzols on Kalahari sands (Kalahari)	• Humic Podzol	• Ferralic Arenosol • Dystric Gleysol	• Humic Gleysol • Albic Arenosol
19	Non or weakly podzolic sandy soils on Kalahari sands (Kalahari and Cryptosepalum)	• Albic Arenosol • Ferralic Arenosol		Dystric/ humic Gleysol
20	Association of moderately leached reddish clayey to loamy soils, derived from basic rocks, often with acid rock admixture (50%-map unit 9) (Munga) and sandy soils on Kalahari sands (50%-map unit 19) (Kalahari)	• Cambic Arenosol • Dystric Gleysol	• Dystric Gleysol • Ferric Acrisol	
21	Senanga-West floodplain soils (Miombo and termitary associated vegetation)	• Cambic Arenosol • Dystric Gleysol	Humic Gleysol	
22	Hydromorphic sand plain soils or very poorly drained soils in large dambos (Grassland)	• Dystric Gleysol	• Humic Gleysol	Gleyic Cambisol
DEPRESSION				
25	Association of moderately to strongly leached reddish to yellowish loamy to clayey soils (40%-map unit 8) (Miombo) and poorly drained soil in large depressions or valleys (60%-map unit 29) (Termitary associated vegetation)	• Ferric Acrisol • Dystric Gleysol • Cambic Arenosol • Xanthic Ferralsol	• Ferric Luvisol • Orthic Ferralsol	
27	Back swamp soils (Mopane)	• Chromic/pellic Vertisol	• Orthic/gleyic Solonetz	
29	Floodplain soils (Termitary associated and grassland vegetation	• Dystric Gleysol • Rumic Gleysol • Dystric Fluvisol	• Eutric Gleysol • Gleyic Cambisol	• Dystric Histosol • Humic Cambisol

1.2.6 Vegetation

The floodplain is mainly comprised of grasslands. Trees are largely absent from seasonally flooded areas, where only a number of small, wooded areas on higher ground, and swamp forests are scattered over the area (IUCN, 2003). These may be described as shrub-lands especially in the northern parts of the floodplain towards Kalabo. Marine Biologists describe the floodplain as being found in a flooded grassland eco-region, bordered by the slightly higher sandy ground on which grows grass (Western Zambian grasslands fertilized by decayed nutrients of the grass before) with woodlands savanna (Zambian Baikiaea woodlands) to the east and south, and patches the evergreen forest (Cryptosepalum dry forest) in the north and east. As elucidated by IUCN (2003), ZEMA et at, (2013) also adds to the reason why trees are largely absent in these constantly indunated. This is due to the permanently high water table.

1.3. Social Economic Characteristics

In the Barotse Floodplain, inundation is of great importance as it has a cultural and economic benefit. People from around the world and from within Zambia travel to witness a traditional ceremony called 'Kuomboka' which is characterised by the movement of the Litunga (King of Barotse Land) from his lowland capital to his upland capital (ZEMA et al., 2013). This ceremony is dependent on annual flooding. This implies that if the flood levels are low, the ceremony does not take place.

Sefula was identified for its rice fields. After some water has receded from the floodplain in the latter part of the rainy season, the community farms rice. The irrigation network infrastructure was historically used to regulate and manage water levels in flood plains so that communities could grow two crops annually rather than just one utilizing rain fed farming (Chileshe, Trottier and Wilson, 2005).

1.3.1 Population

In total, the four districts (now further subdivided by the new government) of the Barotse Floodplain are estimated to contain just fewer than 225,000 people or 27,500 households. Population density, which is generally low in Western Province with fewer than 5 people per km^2, increases steeply around the floodplain (IUCN, 2003).

1.3.2 Economic Activities

Most of the population in the Barotse Floodplain depends on a mixed livelihood strategy, combining crop farming, livestock keeping (especially cattle) fishing and natural resource exploitation (Basin, 2003). Recession irrigation is widely practiced; crops are planted in moist soils of receding wetlands and emerge at the onset of the dry season. The main growing season in the floodplain is between November and April in which maize, rice, sweet potatoes, sugar cane, fruits and vegetables are produced. In the upland area, the main vegetables are cassava leaves, especially in Kalabo. Floodplain farming systems area diverse, and include raised gardens (Lizulu), rain-fed village gardens (Litongo), seepage gardens (wet Litongo), drained seepage gardens (Sishango), lagoon gardens (Sitapa) and river bank gardens (Litunda) (Basin, 2003).

Other activities that can be tied to the floodplain include the provision of employment to the local people, such as coxswains and traders transporting people and goods across the plains (Figure 1.7). A business of mats, fences, and houses etc. that are made out of dried water reeds (locally called as ‘Mata’) is quite lucrative as the materials are locally sourced.

Figure 1.7: Traders travelling from Kalabo to Mongu via the Luanginga River with a canoe fully loaded with reeds (Credit: Bioversity International/E.Hermanowicz, 2020)

With game parks such as the Liuwa Plain National Park, local people are employed by the Department of Wildlife and National Parks (DWNP) formally known as Zambia Wildlife Association (ZAWA), to assist in discouraging and stopping people from poaching activities.

1.4 Problem Statement

According to the Ministry of Finance Investment Project for the Barotse and Kafue Sub-basins (2013), over the past three or four decades, Zambia has experienced an increased incidence of climatic hazards. Drought, seasonal floods and flush floods, extreme temperatures (such as frost) and dry spells have been the most serious. With increased frequency, intensity and magnitude over the last two decades, these extreme climate events have severely impacted the livelihoods of rural communities (GRZ, 2013). Among those most vulnerable to the effects of climate change are the rural communities in the Barotse Sub-basin. Furthermore, Richard (2012) adds that more than a decade ago, the Intergovernmental Panel on Climate Change, IPCC (Change and Basis, 2001), categorized the Zambezi as the river basin exhibiting the "worst" potential effects of climate change among eleven major African basins, due to the resonating effect of an increase in temperature and decrease in rainfall resulting in the potential for evaporation and runoff. Adding on to the stipulated climatic variability in the Barotse Floodplain (in the Zambezi River Basin), floods leave behind a fertile grey to black soil overlaying the Kalahari Sands, enriched by silt deposited by the flood as well as humus from vegetation that has perished due to long inundation periods by the initial flood, and from decaying aquatic plants left to dry out in the mud. This provides good soils, but in the late dry season, it is baked by the heat of the sun (GRZ, 2013).

Fish is a source of livelihood for about 28,000 households along the Barotse Floodplain, endowed with an estimated 122 fish species (CSO, 2012). However, sedimentation poses a danger in reducing the spawning areas for fish. Further, Southern African Science Service Centre for Climate Change, and Adaptive Land Use, (SASSCAL) Task 191 (2012) asserts that most of the population in Western Zambia is heavily dependent on nutrient load associated with flooding. This heavy dependence on rain-fed riverbank agriculture (including livestock production) and fishing means that the communities in this basins are most exposed to climate change and its impacts, at the same time, have the least capacity to adequately adapt and protect themselves from the adverse effects of weather (GRZ, 2013). The SADC/SARDC et al (2012) further indicated that the main recorded

threats are loss of habitat due to agricultural encroachment into wetland areas and the eutrophication and sedimentation of the riverine habitat.

All these stipulated exacerbating environmental challenges attract a sound scientific intervention. This can only be done by research that allows for a thorough collection of data and its coalescence. Since measurements of key weather and climatic data sets are not done on a continuous basis, there is a paucity of data. It has, therefore, become inevitable to use models that implore remotely sensed data to manage the challenge at hand. The information will be essential in developing watershed management plans and so as to have a picture on climate variability.

This research, therefore, uses SWAT interface to model sedimentation in terms of yields. Water quality and nutrient loading within the sediments and riverbank (alluvial) soils are all taken into account. The goal is to have holistic and scientifically guided decisions on how the Barotse Floodplain can be managed in terms of its land and water resources.

1.5. Overall Objective

The overall objective is to determine the dynamics of water quality and quantity of the Barotse Floodplains.

1.5.1 Specific Objectives

The following specific objectives were framed to aid in achieving the overall objective of the research:

(i) To assess the spatial and temporal variability of water quality parameters in the Barotse Floodplain; and

(ii) To investigate the hotspot areas for sediment deposition due to the floodplain hydrology using Arc-SWAT.

1.6 Research Questions

To achieve the research objectives, two study questions were formulated. Answers to the following questions were sought:

(i) How do the spatial and temporal water quality parameters vary on the Barotse Floodplain during the high and low flow periods?; and

(ii) Can SWAT suitably plot sediment yields and distributions for a flat non-mountainous area such as the Barotse Floodplain?

1.7 Hypothesis

It is assumed that elements and nutrients conveyed by water and sediments increase by some linear relationship during the high flow periods in the Barotse Floodplain.

1.8 Significance of Study and Scientific Contribution

The ever-increasing anthropogenic activities and infrastructure development on water resources such as the construction of Mongu-Kalabo Road, mining in the upstream Kabompo Basin, abstractions by Commercial Utilities (CU), fishing and farming on alluvial have a way of altering and reshaping the hydrological behaviour of the floodplain.

The significance of the study was, therefore, to provide hydraulic and hydrological data and models that can be used by environmental agencies e.g., Zambia Environmental Management Authority ZEMA, Disaster Management and Mitigation Unit (DMMU) for planning to deal with future flooding, drought and food challenges (Ndomba & Griensven, 2010; GRZ, 2003). Furthermore, the target of this research was not only to answer to academic requirements, but to provide baseline data for industry. It was envisioned that Zambia Electricity and Supply Cooperation (ZESCO), Zambezi River Authority (ZRA), Water Resource Management Authority (WARMA) and Zambia Environmental Management Agency (ZEMA) would find this baseline data useful in their day-to-day decision making. According to SASSCAL Task 191 (2012), the basin has had very little or no scientific studies other than ethical and social based studies such as Mutonga (2012) and Banda et al (2015).

Finally, SWAT has the capacity to produce land use, vegetation and soil fertility maps by means of sediment distribution maps since sediments are a sink for nutrients and elements from upstream, that can be used by the farming communities.

1.9 Benefits of Project Outputs

The research is expected to have the following outcomes/outputs:

(i) Improved livelihoods through sustainable agricultural practices by characterizing soil fertility patterns associated with flooding regime through the SWAT model as needed by the Ministry of Agriculture and Livestock (MAL). This also includes grassland areas for cattle grazing;

(ii) Provide status of the chemistry (water quality) within flood waters, sediment and soils to assess potential mining contamination from upstream Kabompo River within proximity to large-scale mining activities. This will be integrated into the catchment management system, including the ZEMA database;

(iii) Following (ii), the water sector in Zambia has undergone several changes since the 2011 Water Act that has seen the birth of the WARMA which is mandated to monitor and manage both ground and surface water resources. Therefore, the information, as well as the database to be developed is a baseline information to WARMA as it regulates the water resources in the (6) catchments of the country; and

(iv) Encourages further research to improve on the database and build long period dataset for future management of water resources and climatic interventions.

CHAPTER 2: LITERATURE REVIEW

This chapter describes the literature by following the order of the two specific objectives of the study mentioned in the previous chapter.

2.1 Water Quality

Wamulume et al, (2011) states that anthropogenic disturbances to flooding regimes can thus substantially alter wetland habitat and biogeochemistry. Conferring to the Ramsar Convention on wetlands, water quality and monitoring are considered part of the basic performance indicators when designing a wetland management plan (Obarrio, 2005; Taylor, 2002). This implies that the water quality samples collected and analyzed is the right step towards fulfilling the requirements of the treaty. The Convention on Wetlands, signed in Ramsar, Iran, in 1971, was an intergovernmental treaty that provided a framework or guide for both national action and international cooperation for the conservation and wise use of wetlands and their resources.

Water quality is simply defined as the measure of the state or condition of water resources relative to the requirements of the biotic species and human needs (Johnson et al., 1997). According to the United Nations (2007), cited by (Ndungu et al, 2014), it is defined as the physical, chemical, biological and organoleptic (taste-related) characteristic of water. Based on this definition, the components of water quality to be studied are defined.

2.1.1 Regulations, Limits and Quality Control

In order to adhere to the water quality standards of the treaty mentioned above, detection limits and regulations have been set. A handbook for the technical supervision of water resources, offers chemical standards to be used in lake investigation programmes and wetlands following after the Ramsar Treaty. It expresses the water quality parameters and regulation limits as:

(i) pH values should range from 7.5 – 9.0;
(ii) Sulphates values should be below 1 mg/l;
(iii) Phosphate values should be below 0.005 mg/l;
(iv) Nitrate values should be below 0.02 mg/l;
(v) Chloride values should be below 5 mg/l;
(vi) Calcium should be below 2 mg/l; and
(vii) Magnesium should be below 1 mg/l (Bayern, 2002).

With these standards set by other scholars and the Ramsar Treaty, our results may be cross referenced to see whether they fall within the required standards or if there is cause for alarm.

In order to inspire confidence in any water quality studies, an ionic balance is inevitable. The ion balance describes the relationships between the equivalent concentration of the different cations and anions. Larger differences indicate that important ions are missing. For these calculations, dominant cations Na, K, Mg and Ca and the anions chloride, sulphate and hydrogen carbonate should be taken into account and should fall within an error limit equal to 5 percent or less (Gray, 2008; Bilotta & Brazier, 2008).

2.1.2 Spatial Variability of Water Quality

Studies on Lake Cuitzeo in Mexico applied geo-statistical analysis methods for sampling points that were in close proximity using Kriging (Obarrio, 2005). This method works on Toblar's "First Law of Geography," which states everything is related to everything else, but near things are more related than distant things. This is from a concept referred to as the friction of distance. In other words, distance itself hinders interaction between places. With the vastness of the floodplain, this method was used to link some water quality parameters by way of creating surfaces that exhibit changes and trends.

Ndungu et al (2014) approaches the concentration and distribution of nutrients loads with seasonal changes, that is, high flow periods, medium and low flow periods for nitrates, nitrites and phosphates to ascertain whether sources are domestic (if presence of NH_4-N is higher) or from agricultural effluents via surface runoff (if NO_3-N, and Total Phosphates (TP) are higher). Using this approach by way of linear graphs, nutrients are to be compared on one graph for the different seasons.

A delineated watershed via GIS is illustrated with the complex river system and inundated areas are emphasized in blue (Figure 2.1). The upstream areas show influence to the quality of water flowing into the Barotse Floodplain other than atmospheric conditions. Transportation of sediments, nutrients and chemicals from upstream areas varies in quantity and quality as will be shown by the different sub-basin contributions having different soils, slopes and land use activities. The red dots (Figure 2.1) are the official hydrometric stations formerly owned by the Department

of Water Affairs (DWA/DWRD), now taken over by WARMA. In this study, Senanga Hydrometric Station (2-400) was used as the model outlet. The data recorded from this station is shared between WARMA and ZRA.

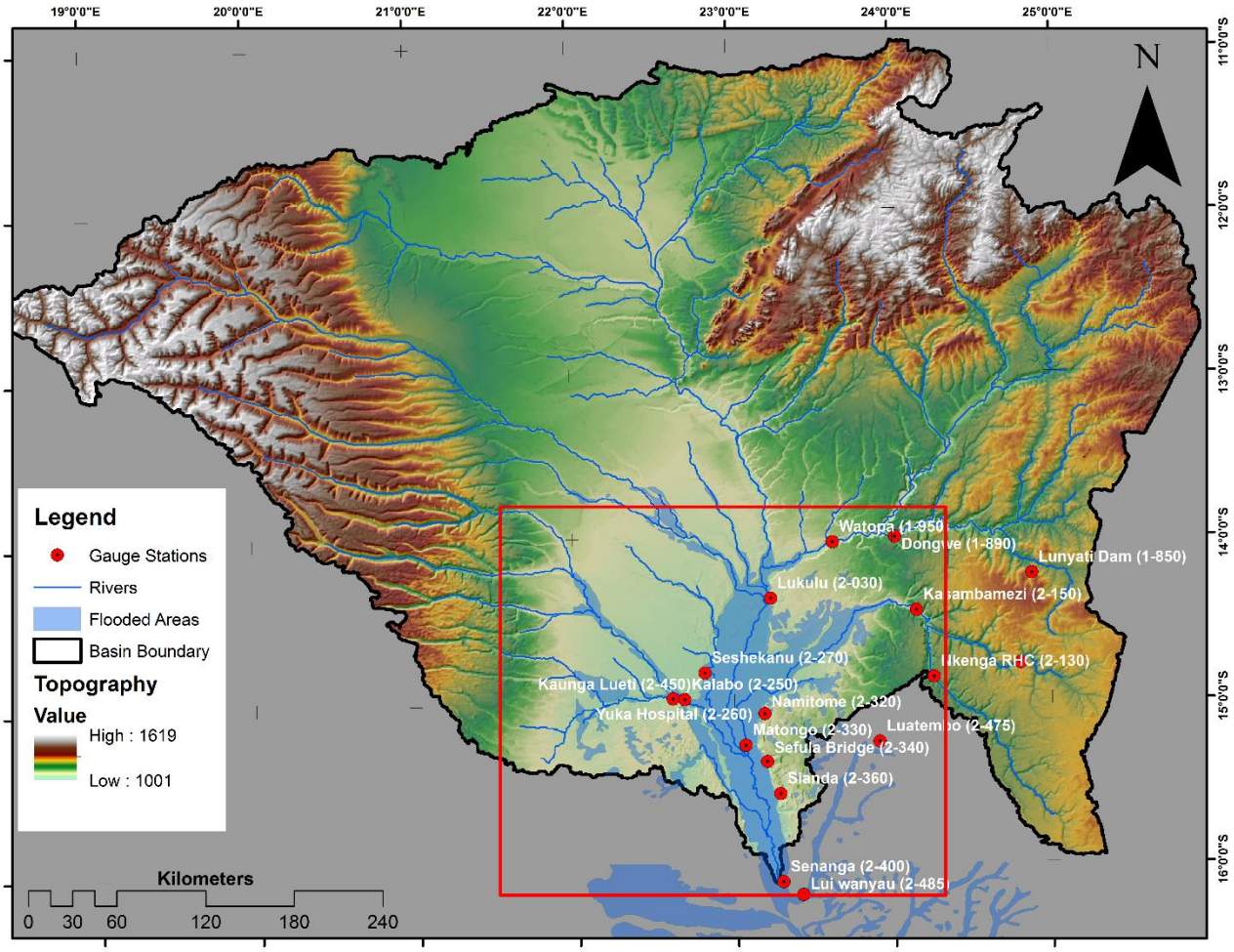

Figure 2.1: Outlet point at Senanga (2-400) receiving water influenced from upstream via surface runoff into the main river course. Each of the sub-basins upstream has some level of influence to the quality of water, Barotse Floodplain, Western Zambia (Source of map, Arc SWAT delineation by researcher/ student, 2015)

2.1.3 Non-Spatial Analysis

Boxplots and histograms were used to present non-spatial data in studies on Lake Cuitze to understand there distribution (Obarrio, 2005). Using a similar approach, data in this research uses boxplots, histograms and linear graphs to reveal relationships that exist between water quality components and sediment constituents. This is because graphs provide crucial information to the data analysis, which is difficult to obtain in any other way because computing statistical measures without looking at a plot is invitation to misunderstanding data. Graphs provide visual summaries

of data that more quickly and completely describe essential information than do tables of numbers (Gotway, Helsel & Hirsch, 1994).

2.2 Hydrological Modelling

Hydrological modelling is a method used to simplify the complex rainfall-runoff processes occurring in the real-world using computer aided environments (Rukuni, 2006). The first step (input data quality) in developing a hydrological model is critical in that all the output results produced will be determined by this (Abbaspour *et al*, 2015). However, a few guiding principles should be based on the objectives of the study at hand, function and level of spatial and temporal resolution. Rukuni (2006) explains why it is essential to be specific with the criterion for model selection. In his argument, he brings out two important things that a researcher requires in order to qualify a model for use after observing that in recent years the number of water resources models available have increased. Some of the preliminary guidelines in the selection phase include the nature of the problem being investigated and the resources available. The following were some of the issues considered in the selection of the model to be used in the Barotse Floodplain as guided by Loucks & Van Beek (2017) and Schulze (1995):

(i) The vastness of the area under study, making it difficult to collect spatial data at every location. This meant that a model that uses remotely sensed data and is capable of using different spatial resolutions coupled with different geo-statistical packages had to be considered. Moreover, the area is largely un-gauged hence the need to generate useful information from limited or missing data;

(ii) The study area falls in an area that experiences three different seasonal changes per annum with various land use types. Hence, the model selection stage had to look at a model that encompasses varying climatic and land use varieties;

(iii) A model that could synthesize hydrological data both measured and remotely sensed in order to produce a coherent and holistic perspective of the behavior of the entire system; and

(iv) A model that is cost effective in the sense that it can assist in making assumptions, predicting impacts, and ultimately aid in decision making in water and land resources (Schulze, 1995).

Besides the spatial and temporal changes in water quality parameters mentioned earlier, this chapter narrows down to the reasons behind the selection of SWAT as the hydrological model

suitable for this research. The suitability of the SWAT model's capacity to be used in huge basins is given by its capability of dividing the large area into Hydrologic Response Units (HRUs), which are simply small pieces of land that experience similar precipitation and have comparable soil, slope and land use distribution (Francos et al., 2001). This is done to evaluate the hydrology with respect to weather, sediment yield, nutrients, pesticides, soil temperature, crop growth, and agricultural management practices at a smaller and precise scale for accuracy and representative results for the entire area (Arnold *et al.*, 2012).

2.3 Selection of an Appropriate Model

The selection of the model to use in this study was made based on the guidelines given in the introductory remarks of the previous sub-section. Hydrological modelling is a powerful technique in the planning and development of an integrated approach for the management of water resources (Bakir and Xingnan, 2008). Consequently, many models have been developed. Some models like the Water and Energy Transfer Processes (WEP), developed to simulate spatially variable water and energy process in watersheds with complex land covers were good enough for what was needed, however, fell out at selection stage as its input requirements was much more. Moreover, sediment modelling is one of the key objectives and it is not included in the WEP, which is more concerned with water allocations and energy processes (Yangwen et al., 2001). The closest software to Arc SWAT was the Watershed Erosion Prediction Project (WEPP) which unfortunately is still under development for use only in America on areas < 2.6m^2 (Brooks et al, 2016).

The Hydrologic Engineering Center's (HEC) River Analysis System (HEC-RAS) software, which allows users to perform one-dimensional steady and 1D and 2D unsteady flow hydraulic calculations, (Brunner, 2016) would have also been ideal for this research. However, HEC-RAS requires a high-resolution DEM. This could have been made using a differential GPS at short interval distances on a square grid; however, the area under study was too large. Downloading from free sites also gave coarse-resolution DEMs. Hence, SWAT being capable of producing results using a 90m DEM was ideal. Literature further revealed that HEC-RAS is more suitable for stream geometries, bridge and culvert design.

The succeeding sub-headings further unearth the hydrological cycle and how it was incorporated into the model, again showing how the SWAT model was the best model suited for the floodplain,

its applications, processing and technical structure. This is because many scholars have written on the applications of SWAT on a number of different watersheds throughout the world. These studies range from predicting impacts of land management practices on water quantity and quality to sedimentation due to slope, land cover and soil type variations. This is because SWAT is a physically based hydrological model that predicts the parameters mentioned above for large and complex watersheds over long periods of time (Inchell, Rinivansan & Uzio, 2010).

2.4 The Hydrological Cycle

In order to fully comprehend what happens in the SWAT model simulation, it is important to review the hydrological cycle. According to Schulze (1995), the hydrological cycle is the pathway of water as it moves in its various forms through the atmosphere to the earth over and through the land, to the ocean and back to the atmosphere. Water is transferred from one environment to another through a system that involves evaporation, transpiration, transportation as water vapour, condensation or transformation from water vapour to rain, which then falls on the surface of the earth and the cycle repeats, hence the name (Shaw, 1983).

Simulation of the hydrological cycle of a watershed in SWAT can be separated into two major divisions. These are land and water or routing phases where the land phase precedes the routing phase. Land phase involves the movement of sediments, nutrients and pesticides (in farming areas) from the land surface into the stream network within a basin. As for the routing phase, water conveys sediments, nutrients etc. through the channel network of the watershed to their respective outlet(s) (Neitsch, *et al* 2005). Water flowing in rivers is the residual of two climatically determined processes, namely precipitation and evapotranspiration. This can be determined by the water-balance equation for a region of interest where P stands for precipitation, Q for runoff, AET for actual evapotranspiration, GW for exchange with groundwater aquifers, and DS for change in soil storage. The water-balance equation is as given by Dingman (2009, p.3) with all terms expressed in mm/year.

$$P = Q + AET + GW + DS \qquad \ldots\ldots\ldots \textit{(eqn 1)}$$

A schematic overview of the hydrological cycle is clearly given showing the land and routing phases of the hydrological cycle including the three parameters making the water balance equation (Figure 2.2). Discharge can further be defined as the sum of the runoff, lateral flow and return flow. This schematic overview shows the model processes which SWAT uses and this will later be looked into when we look at calibration. Please note that simplifying a model to this form may have certain processes ignored due to simplification and as a result may not holistically represent the hydrological cycle as it occurs in nature (Abbaspour et al., 2015).

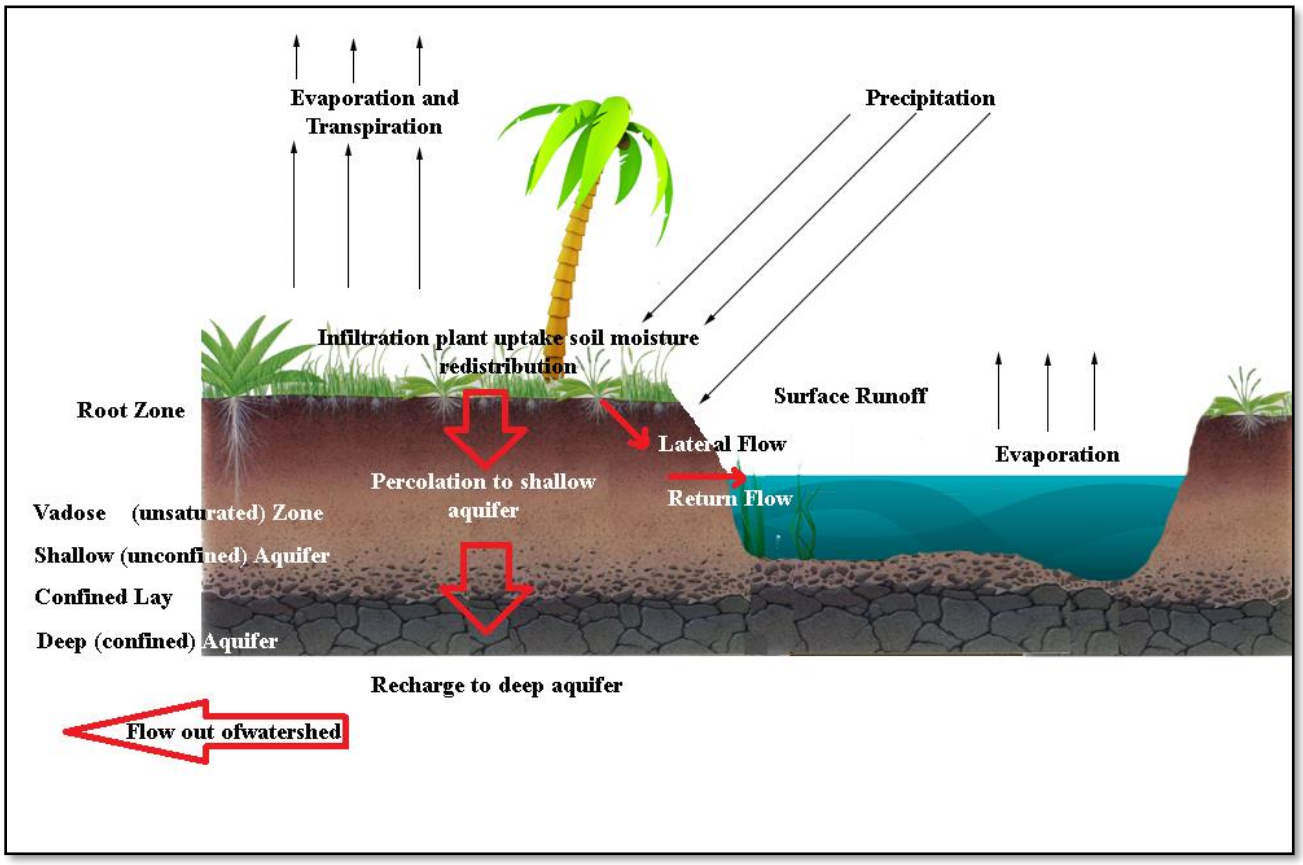

Figure 2.2: Schematic representation of the hydrologic cycle after SWAT Documentation, 2009

2.4.1 Land Phase of the Hydrological Cycle

Unlike the water balance equation introduced earlier in the previous sub-section documented by Dingman (2009) which simplifies the hydrology into three main parameters, SWAT Arnold *et al* (2012) further break down the water balance equation into seven parameters giving more details. According to Arnold *et al* (2012), the hydrologic cycle simulated by SWAT is based on the water balance equation (Neitsch *et al*, 2005):

$$SW_t = SW_o + \sum_{i=1}^{t}(R_{day} - Q_{surf} - E_a - W_{seep} - Q_{gw}) \ldots\ldots\ldots \textit{(eqn 2)}$$

Where $\boldsymbol{SW_t}$ is the final soil water content (mm H_2O), $\boldsymbol{SW_o}$ is the initial soil water content on a day ***i*** (mm H_2O), ***t*** is time (days), $\boldsymbol{R_{day}}$ is the amount of precipitation on a day ***i*** (mm H_2O), $\boldsymbol{Q_{surf}}$ is the amount of surface runoff on a day ***i*** (mm H_2O), $\boldsymbol{E_a}$ is the amount of evapotranspiration on a day ***i*** (mm H_2O), $\boldsymbol{W_{seep}}$ is the amount of water entering the vadose zone from the soil profile on a day ***i*** (mm H_2O), and $\boldsymbol{Q_{gw}}$ is the amount of return flow on a day ***i*** (mm H_2O).

2.4.2 Routing Phase of the Hydrological Cycle

This is a complex phase of the hydrological cycle and has two main divisions for the model. These are routing the main channel (reach) and routing in the reservoir. As mentioned, the phase is complex, and each division has subdivisions to ensure precision in the modelling process. Routing in the main channel has four components namely: water, sediment, nutrient and organic chemical component, which are thoroughly explained by Arnold *et al* (2012).

Routing in the reservoir works on the principle of the continuity equation. The water balance for reservoirs includes inflow, outflow, rainfall on the surface, evaporation, seepage from the reservoir bottom and diversions.

2.5 The SWAT Model and Some Applications

In order to qualify SWAT as being an appropriate model for this study, a literature survey was conducted on some studies that have employed SWAT to model their basins. Fundamentally, the SWAT model is a physical model. The fact that physical models generally respect the physical essence of simulated processes sets these models apart from empirical ones. This is due to their higher accuracy and better representativeness of their outputs and because these models have a wider range of use concerning the parameters being observed in the study area. In contrast to the empirical models, the group of physical models is much more demanding for input data, which logically results from the structure of the model as a complicated system of differential equations. These define the individual factors of complex rainfall -runoff and erosion processes in a simplified way (Jozef et al, 2010).

Betrie et al (2011) uses SWAT to find out the Best Management Practice (BMP) scenario to be applied in the Upper Blue Nile Basin as erosion and sedimentation were reported to be an immense problem that threatened water resources development in this area. Sedimentation and erosion mitigation methods which were compared are:

(i) Maintaining existing conditions;
(ii) Introducing filter strips;
(iii) Applying stone bunds (parallel terraces); and
(iv) Reforestation.

SWAT was used to model soil erosion, identify soil erosion prone areas and evaluate the effect of BMPs on reducing sedimentation. Similarly, Duan, Song & Liu (2007) used SWAT in a mountainous agricultural basin that is semi-arid to monitor or get an understanding of the sources of erosion and the worst affected area by sedimentation. This was done on the Chaohe Basin the main contributing area to Miyun Reservoir, the largest reservoir in North China. Like Betrie et al (2011), Duan, Song and Liu (2007) also concluded that SWAT could be applied in a rugged mountainous region for erosion control and watershed management. This is contrary to the study area at hand, which is generally smooth with an elevation ranging from 1001m to 1619m based on a 90m DEM (Digital Elevation Model). What makes the study by Duan, Song and Liu (2007) interesting is that not only did they plot time-series plots of measured monthly sedimentation at the outlet of the basin, but they also added on a spatial view by developing soil loss class maps. Further studies in 2013 add on to the advantages of using SWAT in that they clearly stipulate that SWAT is designed to simulate management impacts on water and sediment movement for un-gauged rural basins (Habte, Mamo and Jain, 2013). This description properly suits the study area at hand, which has little, or no data measured from the various monitoring points.

In summary, the demand for the SWAT model for input data is quite high as it has the following design advantage; the model has a certain rate of robustness, which means that after specifying the basic input variables and their accurate equilibration we can expect quality outputs of simulations, even if the whole capacity of input database is not filled (Jozef et al, 2010).

2.6 SWAT Processing Stages

In order for the SWAT model to work effectively, one needs two dataset formats. These are thematic layers and database formats. All these have to be in the same coordinate system to avoid

any errors when running the model. The coordinate system to be used is the World Geodetic System 1984 or simply WGS 84. Thematic layers include a digital soil map, a land use map and a DEM. The other format is a database format and this includes rainfall, relative humidity, solar radiation, wind speed and temperature data. Note that these database format data can either be remote sensed or measured depending on the availability of data for your project.

The first step in setting up of SWAT model on any study area is the physiographic analysis based on catchment topography. Then SWAT automatically delineates a watershed into sub-watersheds based on the DEM to account for catchment heterogeneities. It is worth noting that inputs for SWAT are defined at one of the several different levels of detail: watershed, sub-basin, or Hydrologic Response Units (HRUs). Pre-processed 90m resolution DEM of the study area is to be supplied to SWAT for topographic analysis, delineation of sub-watershed and stream network generation as mentioned (Kaleab and Manoj, 2013). A 90m DEM is chosen because the study area is large and choosing a coarse resolution DEM makes the model run faster. By pre-processing, all gaps are closed and the DEM becomes what is called seem-less raster dataset. This helps in the snapping of the stream shapefiles.

In the delineation stage, the DEM is preprocessed for the purpose of calculating the flow directions which are slope or elevation based with respect to the pixel or cell values, and flow accumulations as pits in the DEM are filled so that flow is smooth. Note that the flow accumulation stage precedes the flow direction stage.

In the modelling of sediment yield from Anjeni-gauged Watershed, Ethiopia using the SWAT model, a high-resolution DEM (2m X 2m) was used. This was supplied by a project at the University of Bern, Switzerland, which was used to delineate watershed and sub-basin boundaries, and to calculate sub-basin average slopes and delineate the stream network (Setegn et al, 2010). Such a high-resolution DEM is suitable for a small area; however, in this study we have used a 90m resolution DEM.

Secondly, land use and digital soil maps along with their respective look up tables prepared earlier need to be supplied to the model for reclassification according to the SWAT coding convention (Kaleab and Manoj, 2013). This is during a stage that compounds the slope, soils and land use.

The entire watershed will then need to be classified into appropriate slope categories using the interface based on the elevation differences between the maximum and minimum DEM elevations (heights). All three maps will then need to be overlaid to create HRUs. The catchment is divided into HRUs based on soil type, land use and slope classes that allow a high level of spatial detail simulation (Betrie et al, 2011). Subdividing the area into HRUs enables the model to reflect the evapotranspiration and other hydrologic conditions for different land cover/crops and soil (Kaleab and Manoj, 2013). In a nutshell, SWAT subdivides a watershed into different sub-basins connected by a stream network, and further into HRUs. When land use, soil and slope layers are set for the project, their threshold inputs need not be neglected as they define the level of spatial detail (Setegn et al, 2010).

A location table of weather data that has daily precipitation data files, maximum and minimum temperatures, wind speed and relative humidity should be loaded to link them up with the required files already created for the purpose. This is through appending this data into the database. For example, ten years of precipitation, air temperature, sediment measurements, and river discharge on Minchet River were used for the simulation of the stream flow and sediment yield in Anjeni-gauged Watershed (Setegn et al, 2010). When part of weather data is missing, a Weather Generator abbreviated as WGEN can be used by the model itself. At this stage, two radio buttons are available. These are gauged station button for actual measured or observed data and simulated station radio buttons for estimated weather data.

After loading all the input data and generating the required database files, the SWAT model is to be initially run on a set time basis using default parameter values (Kaleab and Manoj, 2013). As the model is about to be run, the interface prompts the user to set the period of simulation, that is, the starting year and the ending year. The interface requires warm up years for the model. These can be set in the Number of Years to Skip abbreviated as NYSKIP representing the number of years the model has to use to warm up and these will not be included in the report produced eventually (Abbaspour, 2015).

A summary of the spatial data inputs required in order for the SWAT model to run is shown in Table 2-1(Betrie et al., 2011).

Table 2-1: Spatial data sets, other related data sets obtained from government departments and remote sensed (Adapted from Betrie et al., 2011)

Data Type	Description	Resolution	Source
Topographic map	Digital Elevation Map	90m	SRTM
Land use map	Land use classification	1km	GLCC
Soil map	Soil types	10km	FAO
Weather	Daily precipitation and minimum and maximum temperature	10 Stations/ or remotely sensed	Metrological Department of Zambia /http://swat.tamu.edu/

A summary of the processes used by SWAT in form of a flow chart is illustrated giving the datasets needed and the various successive steps (Figure 2.3). Notice that these are the main platforms in a model that is cost effective in the sense that it can assist in making assumptions, predicting impacts, and ultimately aid in decision making in water and land resources (Schulze, 1995).

The flow chart illustrates a summary of the successive steps that must be followed to have a successful Arc SWAT modelling processes (Figure 2.3). From left to right, Shuttle Radar Topographic Mission (SRTM) elevation data (DEM) needs to be downloaded and this will lead to watershed and stream delineation based on the topography. This then is merged with reclassified land use and digital soil maps to form HRUs. Once the land based characteristics are put together, weather parameters (far left) are introduced to the model. At this level, the model can be run.

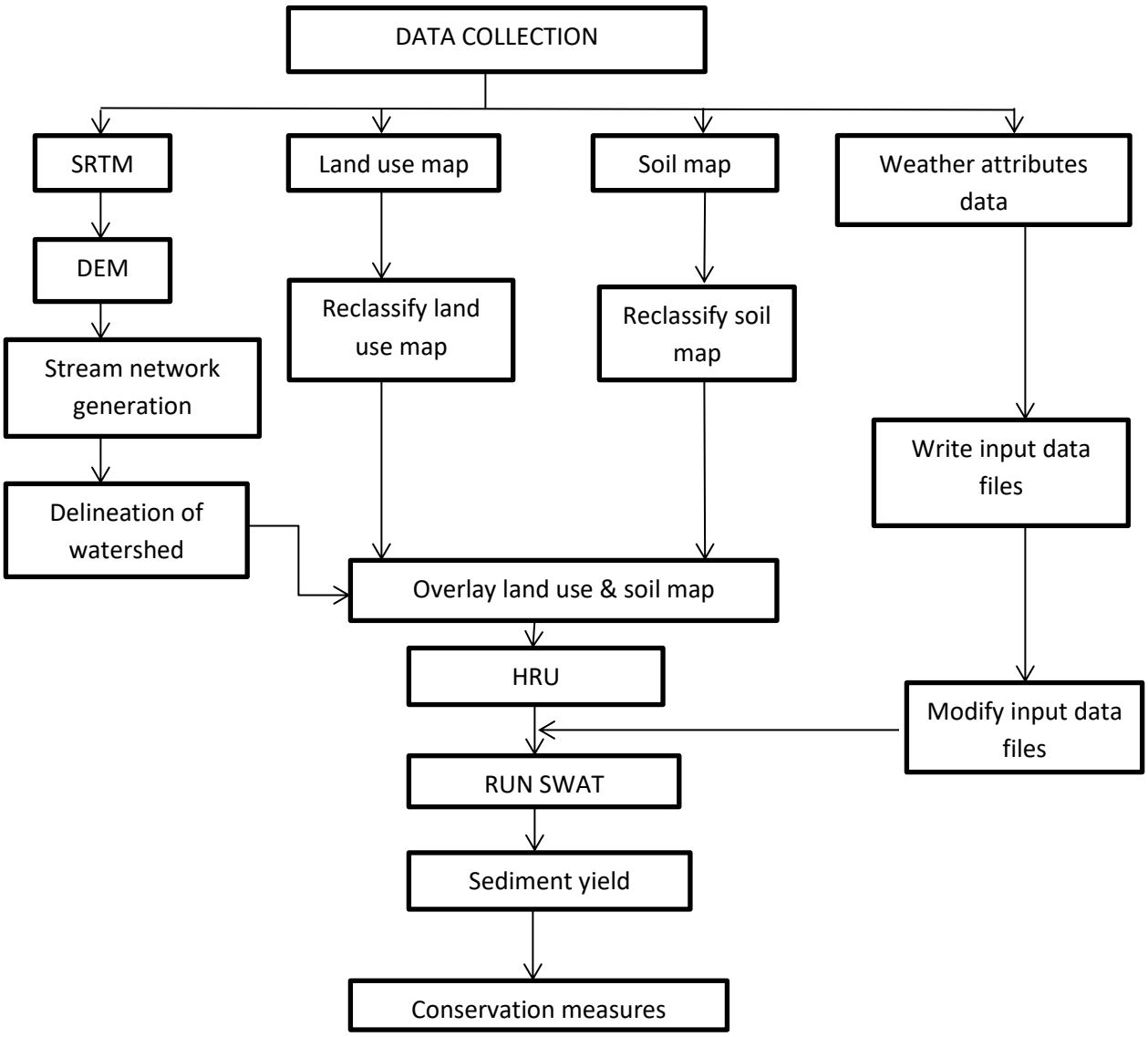

Figure 2.3: Flow chart illustrating the main stages, requirements and processes involved in the Soil and Water Assessment Tool used in this study (Anon, 2012)

2.6.1 Model Inputs

In order for any SWAT model to run, the following are the input data sets and the format in which SWAT can read them.

a) Digital Elevation Model

In order to understand what a DEM is, let us briefly have a look at its history and what Digital Terrain Modelling is.

In the 1950's, two engineers at Massachusetts Institute of Technology (MIT) developed the concept of digital models of a terrain. These were Miller & La Flamme (1958).

A Digital Terrain Model (DTM) is a statistical representation of the continuous surface of the ground by a large number of points with known X-, Y-, and Z- coordinates in an arbitrary coordinate field (Miller & La Flamme, 1958). This basically means that a series of points define the surface, and this surface does not stop abruptly or suddenly (continuity). These points have numerical values assigned to them following a particular coordinate system in 3D. A coordinate system essentially brings out an ordered mathematical representation of a surface (Biagi, Brovelli & Zamboni, 2011).

Nowadays, the information provided by DTM represents a fundamental database for GIS (O' Sullivan & Unwin, 2003) used in a number of large scientific and technical applications. These are geodesy, geomorphology, geology, hydrology, civil and environmental engineering, seismology, geophysics, territorial planning, remote sensing, mapping, etc. Other terms have been used to describe this process and are often used as synonyms, but they are actually used to refer to distinct products. Some of these synonyms are:

(i) DEM: Digital Elevation Model;
(ii) DHM: Digital Height Model;
(iii) DGM: Digital Ground Model; and
(iv) DTED: Digital Terrain Elevation Data.

Essentially, each of these means something else. In DEM the word 'Elevation' emphasizes the measurement of height above a datum in the absolute altitude or elevation in a model. This is the most common among the four. The others are seldom used. This also depends on the geographical region which is under study. DHM originated from Germany and is the same as DEM and DGM. Sometimes the term DTM (Digital Terrain Model) is used. However, this represents a more complex concept involving not only height and elevation, but also other GIS features such as rivers and ridge lines. A DTM can also include other derived data about the terrain such as slope, aspect and visibility (Figure 2.4). Lastly the term DTED is used by the US defense mapping agency and is specifically used for grid based data ((Biagi, Brovelli & Zamboni, 2011).

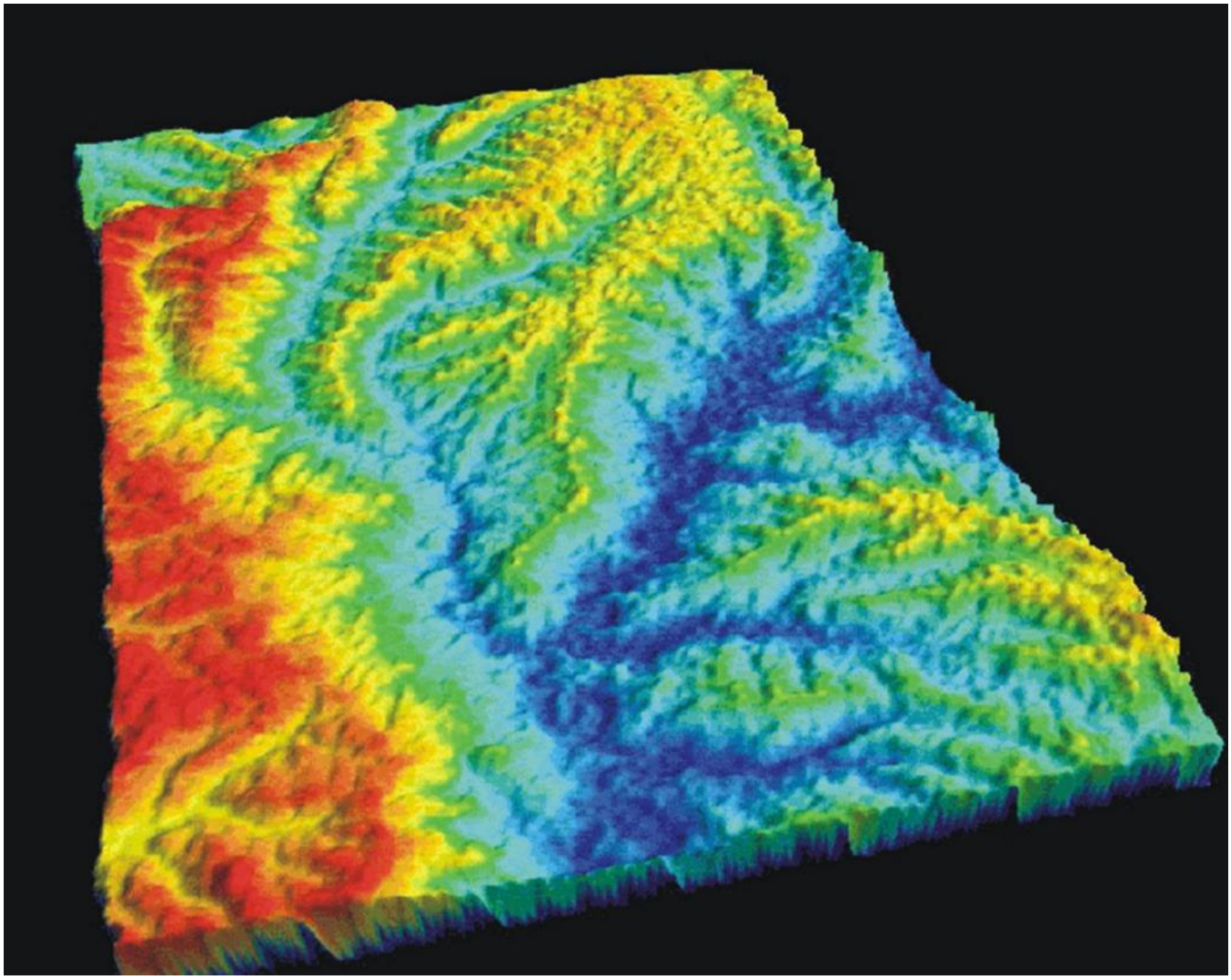

Figure 2.4: Example of a DEM illustrating elevation differences by different pigmentation (alloverthmapproject.blogspot.com, 11th November 2015).

b) Weather Data

The data is loaded using the first command in the "Write Input Table" menu item situated on the Arc SWAT toolbar. This tool allows loading weather station locations into the project and assigns weather data to sub-watersheds (SWAT Documentation, 2009). However, obtaining representative meteorological data for watershed-scale hydrological modelling can be very difficult and time consuming. Land-based weather stations do not always accurately represent the weather occurring over a watershed because they can be far from the watershed of interest and can have gaps in their data series, or recent data are not available (Easton *et al.*, 2008). Moreover, another complication arises in data such as rain gauge, which effectively points measurement, implying that it may poorly present precipitation distribution across a watershed especially in areas exhibiting large

hydro-climatic gradients (WMO, 1985; Ciach, 2003). With this in mind, it is evident that the watershed under study is poorly gauged and exhibits these characteristics of a shifting Inter Tropical Convergence Zone (ITCZ) between the northern and southern parts, hence precipitation is unevenly distributed.

According to Kouwen et al (2005) and Mehta et al, (2004) a common challenge in modelling watershed hydrology is obtaining accurate weather input data which is almost always one of the most important drivers for watershed models. With these challenges, researches have resorted to remotely sensed weather data approaches. Some researchers have utilized radar data to provide precipitation inputs in hydrological modelling studies (Habib et al., 2008; Muzumara, 2014). However, radar data is only available for a small fraction of the world's land surface. Hence, there is a need to consider additional methods to estimate weather conditions for watershed-scale modelling (Fuka et al., 2014). In this research, Climate Forecast System Reanalysis (CFSR) global meteorological datasets were employed. The elimination and qualification criteria used were based on: (i) an openly available global reanalysis dataset that included temperature and precipitation rate; (ii) a spatial resolution on the order of 30km; and the period of record should include adequate historical coverage to allow model calibration and validation (Easton et al., 2010).

The CFSR dataset consists of the hourly weather service's National Centre for Environmental Prediction (NCEP) global forecast system. Forecast models are reinitialized every 6 h (analysis hours = 0000, 0600, 1200 and 1800 UTC) using information from the global weather station network and satellite-derived products. At each analysis hour, the CFSR includes both the forecast data, predicted from the previous analysis hours, and the data from the analysis utilized to reinitialize the forecast models. The horizontal resolution of the CFSR is 38 km. This dataset contains historic expected precipitation and temperatures for each hour for any land located in the world. In addition, as the precipitation is updated in near-real time every 6 h, these data can provide real-time estimates of precipitation and temperature for hydrologic forecasting (Easton *et al.*, 2010).

The CFSR weather datasets where downloaded from the Arc SWAT website for a thirty five (35) year period. This was from 1979 to 2013. A period of 35 years is meteorologically acceptable for monitoring hydro-climatic weather variations.

2.6.2 Model Calibration, Validation and Sensitivity Analysis

Calibration is adjusting model inputs (parameters, structures, variables, etc.) with the purpose of achieving the best simulation match with observation. In other words best match between what the model gives and what you observe. Therefore, calibration boils down to the optimization of an objective function. For example (Abbaspour, 2015, p.57):

$$\text{Minimize: } SSQR = \left(\frac{1}{n}\right)\sum_{i=1}^{n}[Q_{i,m} - Q_{i,s}]^2 \quad \ldots\ldots\ldots \textit{(eqn 3)}$$

It could be some kind of error between the observed data and the simulated data. So the idea is to reduce the error and catch the dynamics of your observations. There are many different types of objective functions (Abbaspour et al, 2015).

Validation is the process of testing the calibrated parameters with an independent set of data without further changes to the parameters. Once you have calibrated your model, you use certain amounts of your observed data. You need to show that your model is not just conditioned on those observations you use for calibration, but it can also simulate beyond the input that you use to calibrate the model. So you need to save part of your data to validate the model. Once you calibrate, there will be no further adjustment to the parameters. You just need to run your model and see how it behaves during the validation period. So validation is sort of an independent dataset to that one you use for calibration (Abbaspour et al, 2015; Betrie et al, 2011; Ndomba & Griensven, 2010).

Sensitivity analysis is the process of determining the significance of one or a combination of parameters with respect to the objective function or a model output, or the process where you define which one of your parameters has the highest impact on the objective function that you are using. Usually this is important to know for many reasons. When this is known, it is easier to interpret and understand the system being modeled because parameters represent processes and so the dominant parameters are the controlling processes. With this one may want to know, for example, what processes are dominant in a particular watershed being modeled. This also includes knowing the most sensitive parameters in the hydrological cycle. Those parameters from

whichever objective function being are used then represents the dominant processes in your watershed. These, with any small change may change the entire system. A good example is Curve Number, abbreviated as CN2. CN2 is the factor that partitions rainfall into infiltration and runoff. It depicts how different land pieces characterized by different soil and land uses accept and or reject water. So, it is a very important parameter. This is the parameter you go to in order to control the peaks in your discharge against the time hydrograph. When one does a sensitivity analysis where adjustments are made to the CN2 value from -0.6 to 0.0 and then finally to +0.6, it can be observed that the changes are evident either in the peaks or the base flow on the hydrograph (Abbaspour et al, 2015).

The sensitivity analysis tool is helpful to model users in identifying parameters that are most influential in governing stream flow or water quality response. Sensitivity analysis allows for two types of analysis:

(i) The first analysis may help to identify parameters that improve a particular process or characteristics of the model; and

(ii) The second analysis identifies the parameter that are affected by the characteristics of the study watershed and those to which a given project is most sensitive (Veith and Ghebremichael, 2009).

The auto-calibration option provides a powerful, labour-saving tool that can be used to substantially reduce the frustration and uncertainty that often characterize manual calibration (Van Liew, Arnold & Bosch, 2005).

CHAPTER 3: METHODOLOGY

In order to answer the research questions as mentioned in Chapter one, a well thought out and carefully planned series of methods had to be put in place. Effective methods to assess spatial-temporal patterns in water quality and sediment yields were essential for possible future remedial or protective management decisions. Therefore, this chapter focuses on the methodology used to achieve these. A summary of the methods used is given in Figure 3.1.

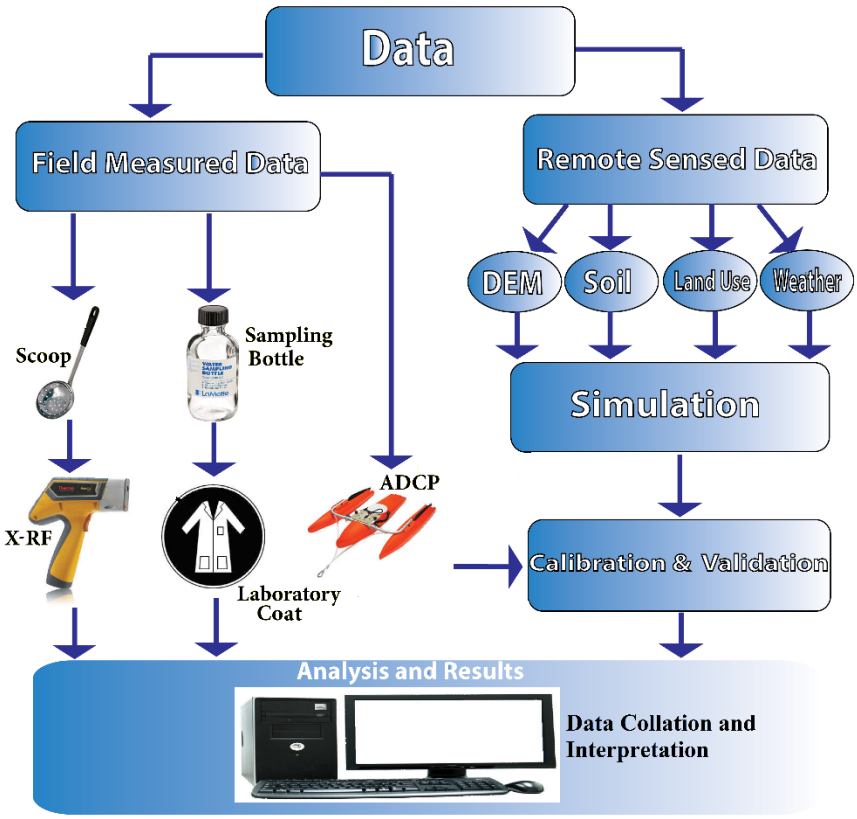

Figure 3.1: Summary of the methodology and the instruments used to capture the data in this study. Calibration and validation incorporated actual flow measurements

Surface water quantity, quality and sediments of the Barotse Floodplain were characterized during low and high flows. Water samples were collected across the floodplain and tested for their physical, bacteriological and chemical characteristics. Stream sediments were only tested for their chemical elements. This was done over a two-year field campaign: during the wet (April to June) and dry (September to October) seasons of 2014 and 2015.

A summary of the instruments/symbols, their purpose and who and where the samples were analysed is given in Table 3-1.

Table 3-1: Instrument/symbol, function and who and where the various samples were analysed

FIELD MEASURED DATA		
INSTRUMENT/SYMBOL	USED FOR	ANALYSED BY
i. Scoop	Used for collecting riverbed sediments	School of Mines, UNZA
ii. Sampling Bottle	Used for collecting water quality samples	School of Engineering, UNZA
iii. XRF/AS	Used for elemental analysis of alluvial sediments	School of Mines, UNZA
iv. Laboratory Coat	Represents the laboratory where water samples were analysed	School of Engineering, UNZA
v. ADCP	Used for measuring river flows	Measurements done by students
REMOTE SENSED DATA		
TYPE	DOWNLOADED FROM	PURPOSE
i. DEM	http://www.cgiar-csi.org/data/srtm-90m-digital-elevation-database-v4-1	Topographic analysis leading to stream and basin delineation
ii. Soil Map	http://www.fao.org/soils-portal/soil-survey/soil-maps-and-databases/en/	Spatial classification of soil types clipped to the study area
iii. Land Use	http://www.mapcruzin.com/free-world-landuse-maps.htm	Spatial classification of land use clipped to the study area
iv. Weather	http://globalweather.tamu.edu/cmip	Inclusion of precipitation, temperature, relative humidity, wind speed and solar radiation to the project

3.1 Conceptual Framework

In order to visualize how each component of our study fits together, a conceptual framework was designed. It was divided into three columns namely field measured parameters (In-Situ), the model used, and remotely sensed thematic data sets (Figure 3.2).

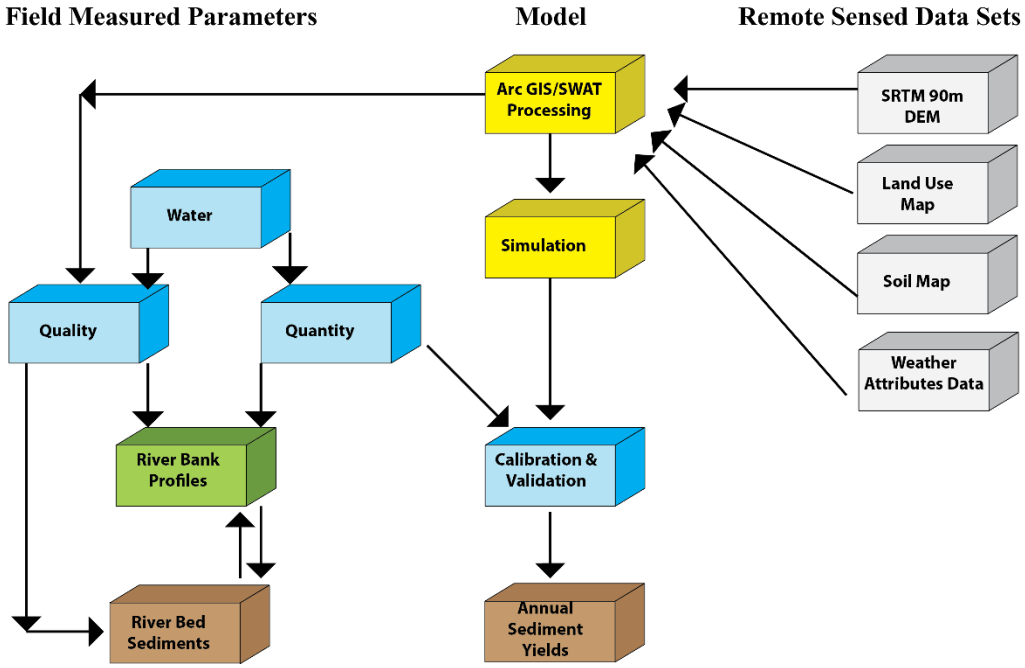

Figure 3.2: Conceptual Framework showing how water quality, quantity and sediments are related

In Figure 3.2, the arrows show the relationships or linkages established in this research, thereby answering the research questions. Remote sensed datasets of topography (DEM), land use, soil and weather attributes fed into the model and these after careful processing gave simulation results. However, in order to bring the results to reality, calibration and validation were done. Both calibration and validation were done using an independent dataset from the discharge measurements, which is fully explained later under the calibration and validation sub-section in order to give a level of confidence in the results. Furthermore, the sediments modeled after calibration and validation are ideally supposed to be compared with actual sediment quantities collected from sediment traps. However, no sediment traps were available. These were now to be compared with the quality results from the field sampled sediments. Before we proceed to the next subsection, it is essential to make it clear that it was planned for water to be analysed in two categories, that is, qualitatively and quantitatively as it was perceived to be intimately linked with the riverbank soil profiles as well as the riverbed sediments. This is because riverbed sediments

act as a sink and hence a signature of what was in the water as it remains in the sediments. The mechanism or link between water and sediments is due to the hydrodynamic forces of water (quantitative part) that detach lose soil and convey it as sediments from upstream. This through repeated action, season after season as water erodes and deposits soils downstream to form sediment banks. However, channelization takes place upstream leading to gullies and eventually formation of reaches over time with riverbanks downstream as historical repository of sediments. This can be clearly observed through a variation of composition (e.g., pigmentation) and grain size variation on a sediment profile.

3.2 Equipment Used

The pieces of equipment used for the in-situ measurements were divided into four categories. These are:

(i) Water quality: These included:

- Multi-metres for physical parameters (with batteries);
- Cooler boxes;
- Sampling bottles, glass for bacteriological samples;
- Ice packs;
- Global Positioning System (GPS);
- Scoop; and
- Syringe (for Nitric Acid addition).

(ii) Water quantity: These included:

- ADCP for discharge measurements;
- Tagline for safety and ensuring that straight path is followed;
- Speed boat with a seating capacity of 8 plus a coxswain;
- Tough book with Broad-Band (BB) Talk software for communicating with ADCP; and
- Life jackets.

(iii) Riverbed sediments: These included:

- A Scoop; and
- Sampling bottles.

(iv) Riverbank profiles: These included:

- A Measuring type;
- Spade;
- Pick;
- Sampling bottles; and
- A Niton XRF for elemental analysis.

Other pieces of equipment included notebooks, stickers, markers, pens and a camera for capturing photographs at locations marked by the GPS.

3.3 Field Measured Parameters

The parameters sampled/measured in the field were water quality and quantity, riverbank soil profiles (1mx1m pits), riverbed sediments and nutrient loading. The following subsections give a detailed description of the field campaigns and the tasks involved in capturing meaningful and representative data.

3.3.1 Water Quality Sampling

Water quality sampling as indicated earlier, were divided into seasonal field trips each with a different number of samples collected depending on stretch or route taken and the nature of tasks involved during that trip. In 2014 and 2015, five separate field campaigns were undertaken. In the first year, three trips were made and two in the second year. The timing of the trips was targeted at capturing the high, and low flow hydro-periods.

a) Field Trip One

The first field trip was in April 2014 during the high flow period. A total of forty-four (44) samples were collected during this field campaign. These samples were collected in triplicates at each point, that is, one sample for anion analysis, the other for cation analysis, and the third one for bacteriological analysis. The capacity of the sampling bottles used was 250 millilitres. When collecting the water samples, the bottles were rinsed three times together with their respective lids. The depth at which the samples were collected was 50 centimetres from the water surface and the same water was used for rinsing. Upon completing each sampling collection procedure, the samples were immediately put into cooler boxes containing ice packs. Photographs and coordinates were captured before moving to the next point. These samples were meant for laboratory analysis and were transported within 48 hours. Two percent (2%) of 250 millilitres of nitric acid was added to water samples meant for cation analysis. Acidification of water samples

preserved most trace metals and reduced precipitation, microbial activity and sorption losses to container walls.

As the samples were being collected, in-situ measurements were simultaneously taken using multi-metres. Multi-metres measured the physical components of the water. The components measured were Dissolved Oxygen (DO) in milligrams per litre, Temperature in degrees celsius, pH and Electrical Conductivity (EC) in micro-siemens per centi-metre. The 44 samples collected, and their respective coordinate of location are shown in Appendices 1a and 1b. This includes both the physical in-situ parameter readings mentioned. The samples were labeled as IB1 through to IB 44 and their spatial locations are shown (Figure 3.3).

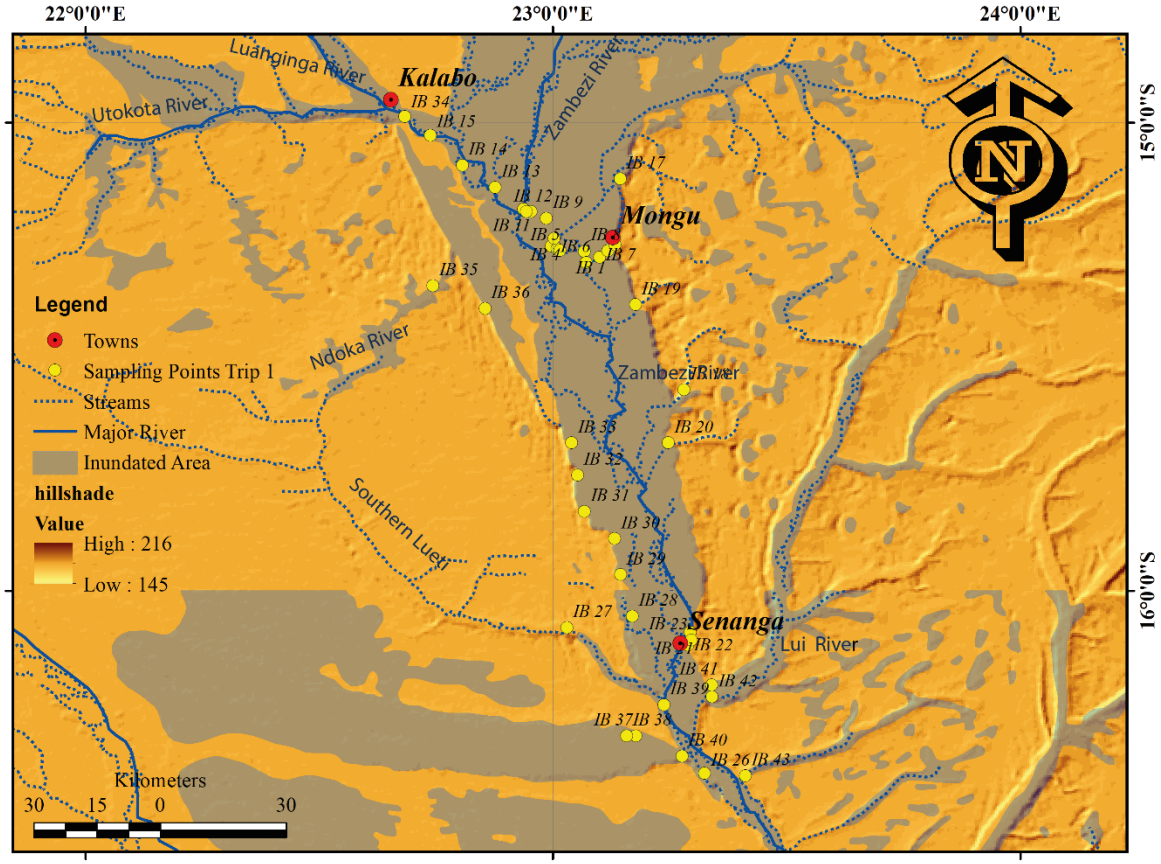

Figure 3.3: Spatial distribution of water quality sampling points during the high flow period, April 2014 (Kalabo-Mongu-Senanga into the mouth of the Matebele Plain and down), Barotse Floodplain, Western Zambia

Sample collection started at Mongu Habour all the way to Kalabo Habour using a 90 Horse Power (HP) speed boat used for transporting people between the two towns (hired public transport). After

this, the route taken was by road (Mongu-Senanga) near the banks of the Zambezi River. Samples collected were on the Zambezi River. This included collecting samples at confluences of tributaries entering the Zambezi River on the eastern bank of the floodplain as we travelled southwards to Senanga. From Senanga, we crossed the Zambezi River using a pontoon at Kalongola into the western bank of the floodplain. Samples were then collected on the western bank of the floodplain while maintaining a north-western direction until Kalabo after Sitoti and Matebele Plain samples. This made a closed loop and therefore marked the end of trip one (see Appendix 1a and b for results). In some instances, river sediments were also simultaneously picked at the same sampling points as the water quality samples for comparisons.

b) Trip Two

This trip was in October 2014, and this was during the low flow period. The same procedure for collecting water samples was followed. A total of thirty (30) water samples were picked with riverbed sediments at appropriate sites where water was shallow. The same in-situ parameters were measured for every sampling point. The labels this time were from IB 45 to IB74, a continuation from where we left off from the first field campaign. The routes used were Mongu-Kalabo and Mongu-Lukulu. A map (Figure 3.4) illustrates the location of the points where samples were picked and Appendix 2a and b gives a tabular display of the samples, parameters and their respective geographic coordinates.

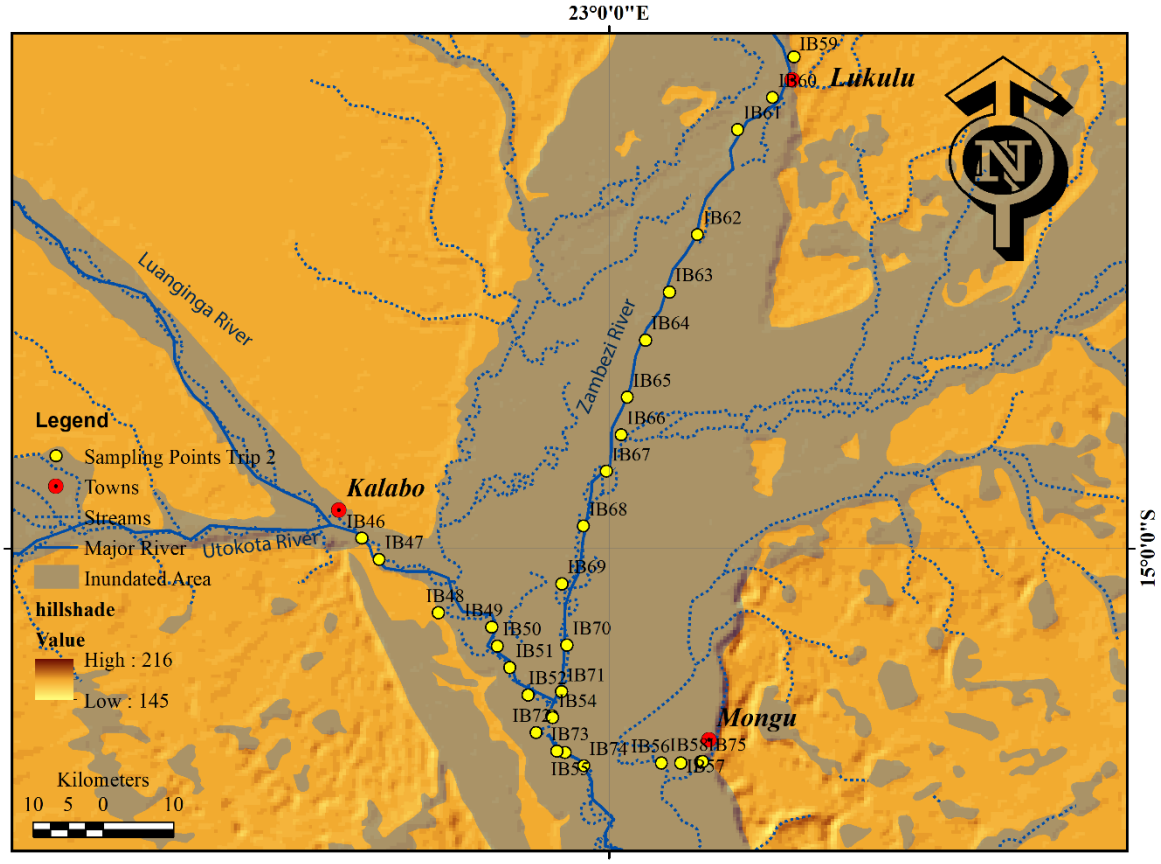

Figure 3.4: Spatial distribution of water quality sampling points during the low flow period, September 2014 (Mongu-Kalabo-Lukulu Transacts), Barotse Floodplain, Western Zambia

c) Trip Three

This trip was in September 2014 and used for collecting water quality samples. A total of thirty-one (31) samples were collected and the same collection/sampling criteria were observed. However, this time around the samples were not sent to The University of Zambia Environmental Engineering Laboratory for analysis like the ones before. They were sent to German at a laboratory called Federal Institute for Geoscience and Natural Resources (BGR).

In-situ parameters were collected following the same routine, and a table containing the field measurements and their respective coordinates is given in Appendix 3. The water levels were very low and hence the boat had to be pushed at a number of sections along the Zambezi River. Another map (Figure 3.5) shows the locations of the sampling points with respect to where these thirty-one (31) samples were collected. The labels on the sampling bottles were IBG 1 to IBG 31. The route taken this time was almost identical to that one for trip two; however, the Mongu-Senanga stretch

was also included so as a way of having low flow reading to be compared with the high flows reading of the first field campaign.

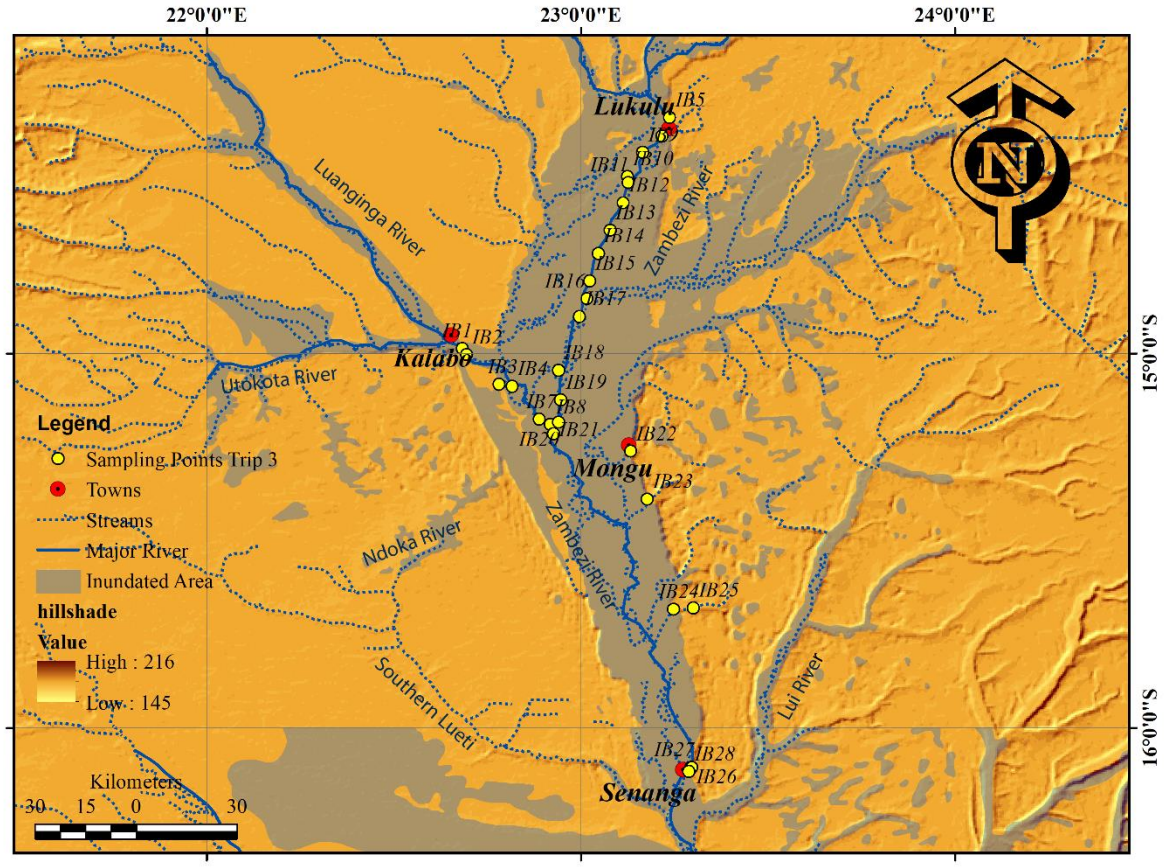

Figure 3.5: Spatial distribution of water quality sampling points during the low flow period, October 2014, Barotse Floodplain, Western Zambia

d) Trip Four

Trip four was in September 2014 and was mostly used for soil moisture sample collection within the Luanginga Basin and flow measurements at Kalabo Hydrometric Station. This was for the development of a rating curve at Kalabo Gauge Station. Several flow measurements were made using the Acoustic Doppler Current Profiler (ADCP) to augment the already existing data obtained from the Department of Water Affairs (DWA). In essence, the exercise acted as ground truthing.

This time the team was joined by a PhD student from Jena University, Germany (cooperating partners) who was also monitoring flows of the Luanginga River at Kalabo Hydrometric Station.

e) Trip Five

The trip was in June 2015 and a total of 21 water samples were collected following the criteria above. These were numbered from IB 76 to IB 96 using the Mongu-Senanga route/transect (Appendix 4a and b). This was during the high flow period and a table showing the results is in Appendices 4a and b. A map that shows the locations and the path taken during this trip is given in Figure 3.6. The path was characterized by a lot of meandering due to the thick density of vegetation mostly reeds called 'Mataka' by the local people.

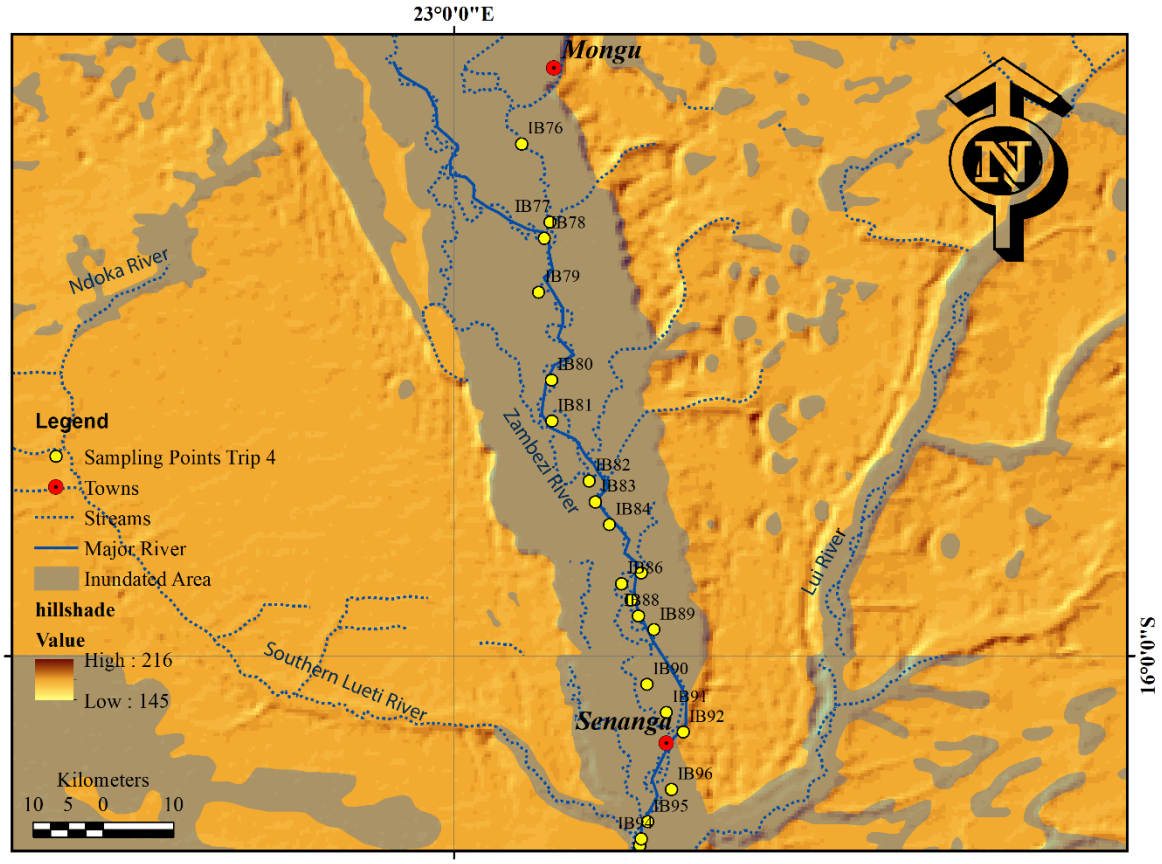

Figure 3.6: Spatial distribution of water quality sampling points during the high flow period, June 2015, Barotse Floodplain, Western Zambia

3.3.2 Water Quantity Measurements

Discharge measurements where done on two main hydrometric stations located in Senanga and Kalabo. As indicated earlier, an Acoustic Doppler Current Profiler (ADCP) was used in these measurements. A tagline was attached to the two ends of a chosen river cross section in order to have a straight line that cuts across the river section. This was to prevent the sagging or curving of the path taken during the flow measurement due to the strong river current of the Luanginga and

the Zambezi. However, the ADCP had inbuilt compensation functionality for curvilinear measurements.

Due to the depth of the two cross sections mentioned, the wadding method was not used and hence the ADCP had to be tied to the boat for the measurements done. Before commencement of the measurement, the ADCP had to be calibrated using what is called a moving riverbed test. After completion of the moving riverbed test, which requires about ten (10) minutes in order for the machine to stabilize, the distance of the ADCP with respect to the nearest bank was taken. This was either the Left-Hand Bank (LHB) or the Right-Hand Bank (RHB). Acoustic signals were sent to the riverbed and the bouncing back signals were captured. These were done in three ensembles. A Win River II ADCP (the model used for this research), makes one ensemble per second. This is plotted in real time on the screen as the measurements are being taken. A photograph was taken on a pontoon in Kalabo to show the tough-book computer and the ADCP alignment as the discharge measurement process was in progress (Figure 3.7).

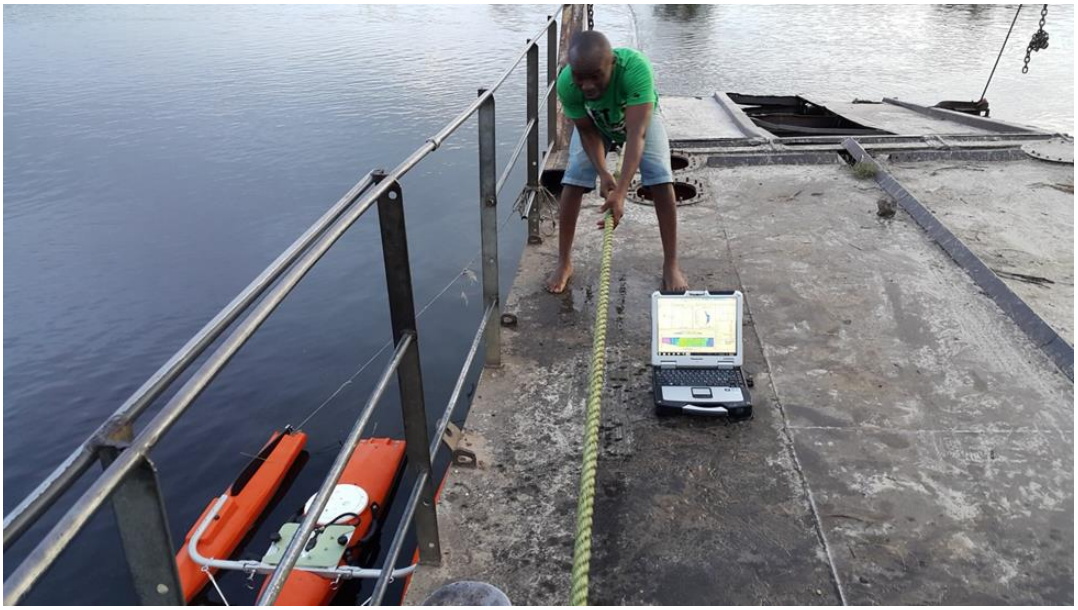

Figure 3.7: Method used in measuring discharge at Kalabo Hydrometric Station using a tagline tied end to end with the ADCP tied to the boat, Barotse Floodplain, Western Zambia

A tough-book computer communicated with the ADCP via Bluetooth settings. This made the reading easier and convenient unlike the serial connections that required cables. The software programme used in the communication between the tough-book and the ADCP is called Broad

Band (BB) Talk. A closer view of the ADCP screen as it plots the river profile with the tracking system display showing the path taken (Figure 3.8).

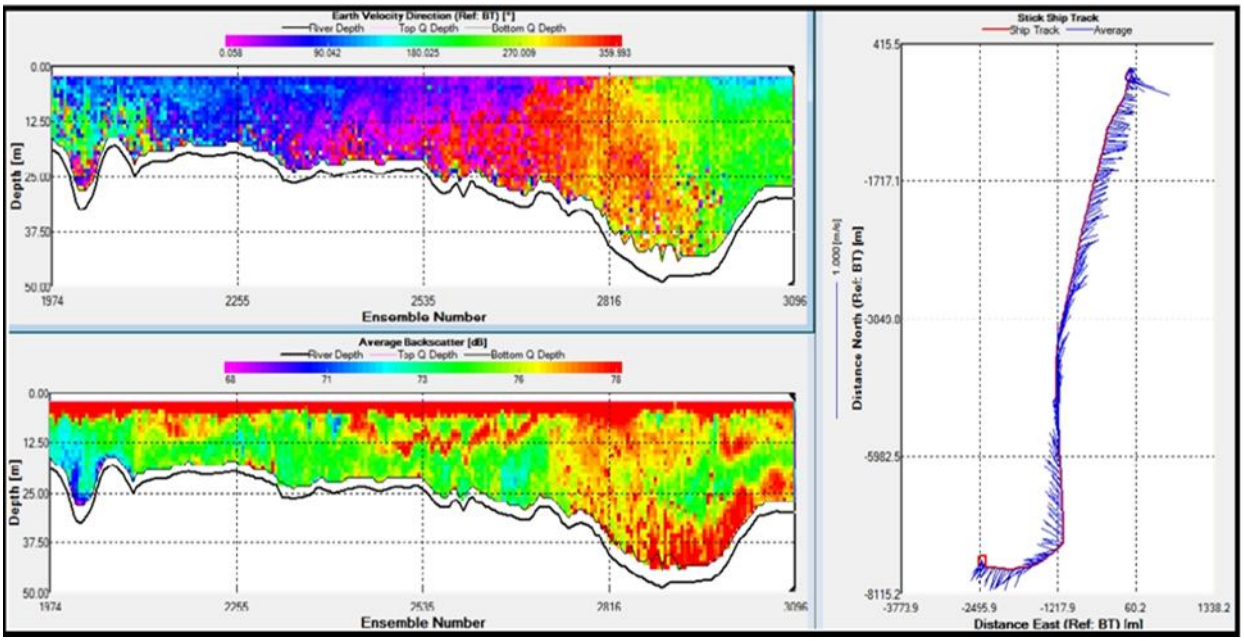

Figure 3.8: River profile of varying depth done in three ensembles. The colour codes show the variation of velocity following the colour bar above (left). A track and its curvature (right) is also given. This measurement was done at Kalabo Gauging Station, Barotse Floodplain, Western Zambia

3.3.3 River Bed Sediment Sampling

Riverbed sediments were collected alongside with water quality samples. This was at the same locations as the water quality samples for the trips mentioned in the previous subsections. They were named as IB1 through to IB96 following the same nomenclature as the water quality samples for easier identification and comparison.

Once collected using a perforated scoop (for draining water), the samples were placed in sampling bottles. This was followed by tightly closing the lid and placing the sample into the cooler box for soil samples. The samples were preserved in this manner until each field campaign came to an end. The samples were then transported to the University of Zambia, School of Mines Geochemical Laboratory for analysis. The samples were analysed using the Atomic Absorption Spectrophotometry (AAS). The results of the elemental constituents of the riverbed sediments are shown in Appendix 5.

3.3.4 River Bank Soil Profiles

Several riverbanks were viewed and those selected samples were collected and taken to the laboratory for analysis. One metre by one metre (1m x 1m) pits were also dug around the floodplain area for qualitative comparisons in terms of spatial changes in elemental constituents, both riverbed sediment and water quality.

For analysis of soil profiles, a Niton XL2 XRF gun given in Figure 3.9 with components such as the X-Ray source that sends the incident irradiation ray that excites the electrons of the material and forces them out of the energy levels for the detector to finally read the reflected irradiation ray.

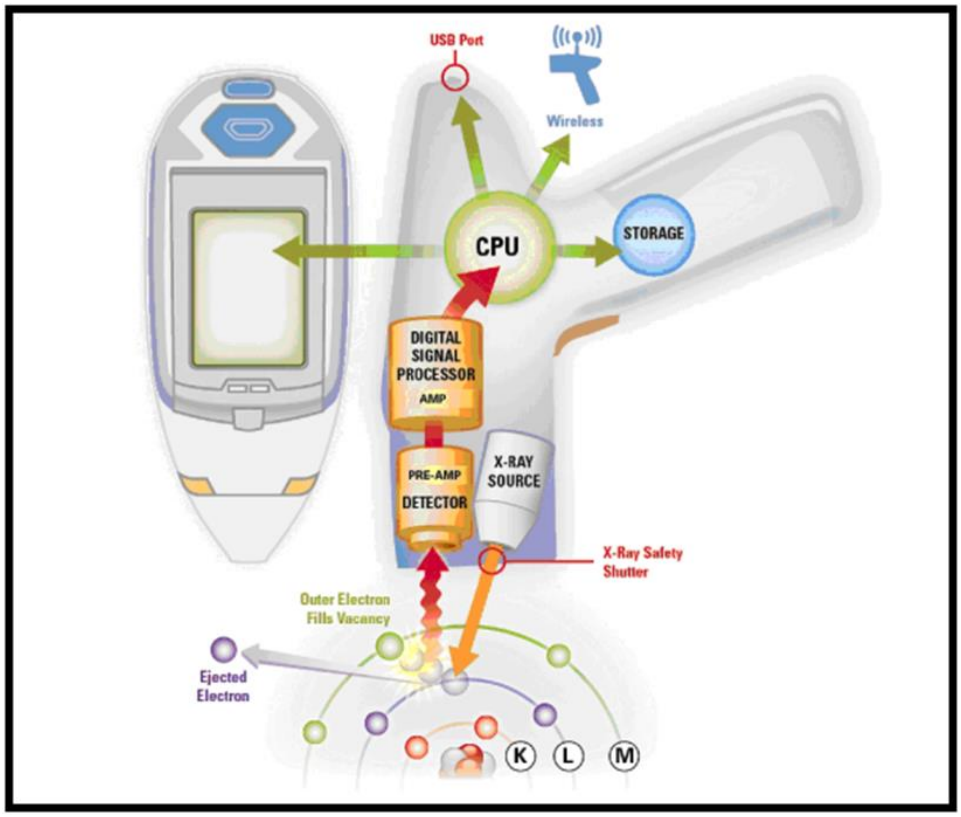

Figure 3.9: XRF analysis diagram showing the interaction of x-rays with matter thereby causing emission of other x-rays that are characteristic of the elements present in the material being irradiated (XL2 User's Guide v 7.1.1, 2010), used in the Barotse Floodplain, Western Zambia

The gun was used on samples having percentage moisture content of 10% and below. The gun had a stand where it was placed for easy handling within the laboratory. Samples were properly ground and mixed in order to have a homogeneous mixture. This also helped increase the surface area for

the sample in order for the XRF gun to shoot on several grains so that the reading is unbiased. Shooting on coarse grains would have led to biased results as only one (1) grain would have produced the irradiation.

An average of three (3) reading was taken for each sample. The sample was given a maximum exposure time possible in the XRF, that is, 120 seconds. In order to protect the lens for the XRF from damage, a thin plastic cover was placed on the sample for the whole period of exposure. An XRF with a tough book computer including the protective case for carrying the gun are given in Figure 3.10. A software called Niton Data Transfer, (NDTr) was installed on the tough book computer for viewing and eventually downloading the results. The results were in two file formats, NDTr (.ndt) and Comma Separated Values (.csv).

Figure 3.10: XRF, case and tough book computer where the NDTr software was installed for downloading readings, used for measurements on the Barotse Floodplain, Western Zambia

Samples for the profile/pits were labelled from top to bottom. For example, if a one (1) metre pit had three (3) layers or horizons, each layer was designated by a letter followed by a number. These were labelled as L1, L2 and L3. A pit at one of locations where three samples were collected as it had three different soil textures and pigmentation is given in Figure 3.11.

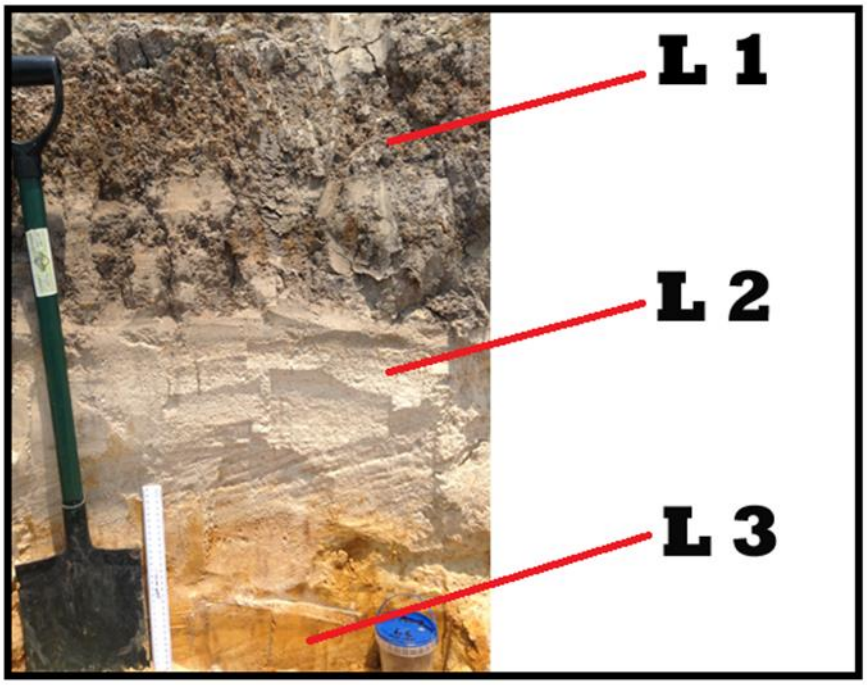

Figure 3.11: Labeling of collected samples from oldest to youngest, we have oxidized sandy soils (L3) at the bottom, followed by sandy soils (L2) in the middle, and finally the clay-rich soils (L1) at the top, Barotse Floodplain, Western Zambia

Some of the useful points taken note of in sample preparation included:

(i) Ensuring that the sample selected from a bulk material and used to prepare the specimen had to be representative of the bulk;

(ii) The prepared specimen had to be representative of the sample;

(iii) The volume of the specimen analyzed had to be representative of the entire specimen; and

(iv) Therefore, the analyzed volume of the specimen was representative of the bulk material.

3.4 Arc SWAT Modelling

The Arc SWAT ArcGIS extension is a graphical user interface for the SWAT model (Arnold et al., 1998). As was described earlier, SWAT is a river basin, or watershed, scale model developed to predict the impact of land management practices on water, sediment and agricultural chemical yields in large, complex watersheds with varying soils, land use and management conditions over long periods of time. The model is physically based and computationally efficient, uses readily

available input and enables users to study long-term impacts (SWAT Documentation, 2009). This model has been extensively tested in mountainous area (Fontaine et al., 2002; Duan et al., 2007 and Mutenyo et al., 2013 etc), however, as was mentioned, this research sought to use this model in flat non-mountainous wetland area to simulate sediments.

Arc SWAT is open source software. It was downloaded from the SWAT website (http://swat.tamu.edu/) and was attached to Arc GIS as a plug-in under the extensions menu by checking the box corresponding to it.

3.4.1 Installing the Arc SWAT Interface

In this study, SWAT 2012/ Arc SWAT Interface was used. The hardware and software specifications were as follows:

(i) A personal computer using Intel(R) Core (TM) i5-4210U CPU @ 1.70GHz 2.40 GHz;
(ii) 4 GB RAM;
(iii) Software (Arc SWAT for 10.0 – 10.2 versions);
(iv) Microsoft Windows 10 operating system;
(v) PDF-X Change viewer for reading the manual was downloaded;
(vi) ArcGIS: ArcView 10.2 was installed as the platform for Arc SWAT; and
(vii) ArcGIS Spatial Analyst extension (ArcGIS 10.2) was checked so that the functionalities were available.

With these basics, we were set for setting up the SWAT project.

3.4.2 Setting up the SWAT Project

The ArcSWAT interface for SWAT2012 is installed by default in the folder C:\SWAT\ArcSWAT\ or in a folder of the user's choosing. Getting full user permission for all users is recommended when installing ArcSWAT (SWAT Documentation , 2009).

To start up a new SWAT Project, six (6) windows were available namely: SWAT Project Setup; Watershed Delineator; HRU Analysis; Write Input Tables; Edit SWAT Input; and SWAT Simulation. These are arranged chronologically, that is, in order for the next window/menu to be accessed, one has to complete the processing in succession. In other words, access to the next stage is dependent on completion of the stage being worked on.

It is during this first step that the SWAT Project was named and saved via a Project Setup Menu with clear indication of the path where the project is stored or located. The Project was named 'Task 191a' after the SASSCAL Task 191 Project name.

3.4.3 Watershed Delineation

This is the menu right after SWAT Project Setup. This menu had five sections and these are:

(i) DEM Setup;
(ii) Stream Definition;
(iii) Outlet and Inlet Definition;
(iv) Watershed Outlet(s) Selection and Definition; and
(v) Calculation of Sub-basin Parameters.

Watershed delineation is derived from the basic premise that water flows downhill, and in so doing it will follow the path with the largest gradient (steepest slope) using a model called the 8-direction pour-point model. The following procedure was followed for the 'Task 191a' Project:

Firstly, when the new project was setup, the Automatic Watershed Delineation command of the Watershed Delineation menu was enabled. A DEM for the region of interest was loaded from the disk. This was a 90m resolution SRTM DEM downloaded from the CGIAR-CSI GeoPortal website (http://srtm.csi.cgiar.org/). The area under study was large and so a coarse resolution DEM was preferred over a fine 30m ASTER DEM which took more processing time and at times did not give the desired results. Once the DEM was successfully loaded, a DEM projection setup was clicked. This is where the Z-coordinate or elevation unit was adjusted to metres with our DEM indicating a cell size of 4.50m and a cell area of 20.25m^2.

Once this was done, the specific area of interest was masked. Masking aids in reducing the processing time as only the masked area will undergo hydrological processing. Three options were available during the masking of the DEM. These were, loading from the disk, or select from the map, or manually delineating. The later one was used. When manually delineating, the outlet point was first selected so that it helps in knowing where the basin will end or pour out its water. After the masking shape file was overlaid on the DEM, it was made hollow for easier visibility.

Next was the "Burn In" function. A "Burn In" stream dataset is used to force the SWAT sub-basin reaches to follow known stream locations. These streams being "Burned In" were made via the

spatial analysis tool of ArcGIS. This was specifically under the hydrology tool which has functions such as sink, fill and flow directions.

When masked area was defined and the streams “Burned In”, streams had to be defined. Two options were offered, and these were to either define the streams based on a drainage threshold, or, importing pre-defined watershed boundaries and streams. The earlier option was used while leaving the radio button named “DEM-based” checked.

The flow direction and accumulation button was clicked and the processing began. This segmented the area under study into 28,686 cells with an area of 580,891.5 hectares. After this, the “Create streams and outlet” function was activated. This was clicked and processing began. At the end of processing, streams were formed. To illustrate this, two DEMs are given. One had a high stream density due to the clipped digital streams overlaid and the other had processed streams at 580, 891.5 hectares threshold. These are given in Figures 3.12 and 3.13, respectively.

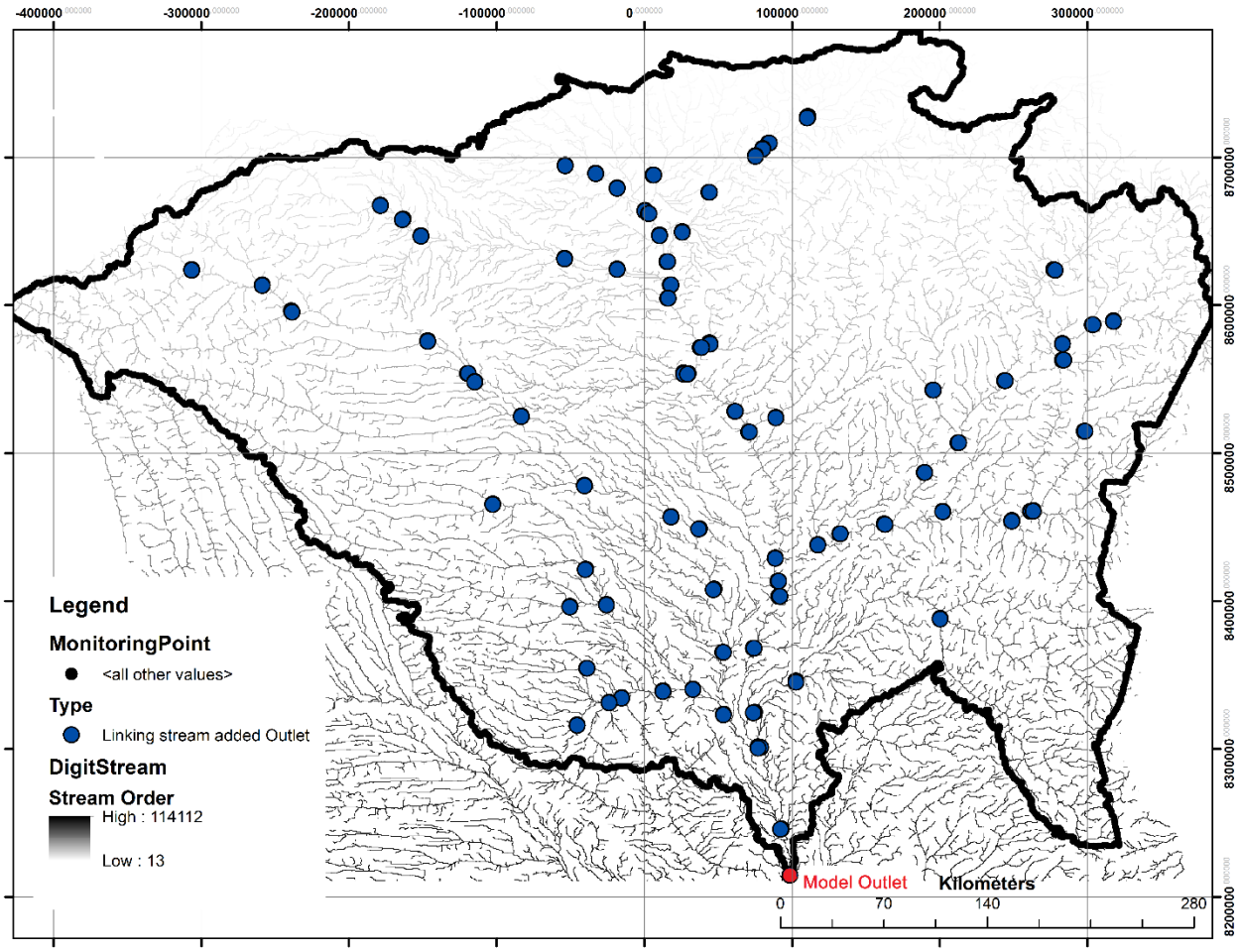

Figure 3.12: Clipping digital streams to the DEM with outlet point coloured in red, Barotse Floodplain, Western Zambia

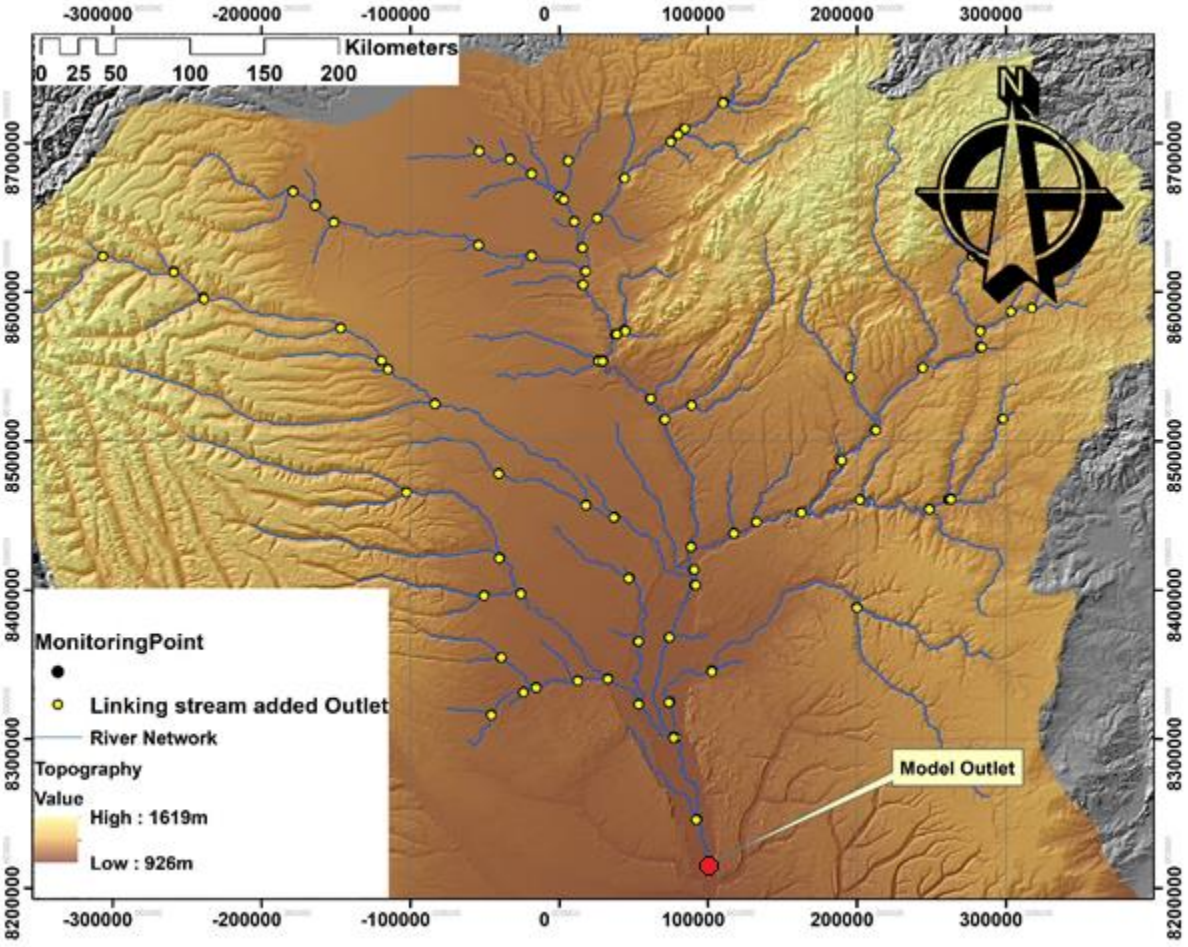

Figure 3.13: Formation of streams on DEM followed by filling in of the sinks to enable proper flow directions based on the elevation differences of the individual cells of the DEM, Barotse Floodplain, Western Zambia

After the streams were delineated, a point for the entire watershed outlet was selected. This is at Senanga Hydrometric Station (red dot in Figures 3.12 and 3.13 above). This point was selected since the floodplain narrows in, there is an already established gauge station with historical data and the river banks/bed become rocky and defined. This point also captures most of the entire flow coming out from the floodplain even though Kalongola would have been the best point. This is because Kalongola would have been ideal for capturing the entire flow from upstream.

Drainage inlets and sub-watershed outlets were automatically added when the "Whole watershed outlet(s)" function was used. This was done by selecting the outlet drawing box around it for automatic selection. All other unnecessary linking stream outlets were deleted via the "Edit

manually" function. A delineated watershed with 159 sub-basins is given in Figure 3.14 and the description of these sub-basins in details from 1989 to 2013 are given in Appendix 6. This is the detailed database generated by SWAT. The delineation was done after selecting the outlet point leading to the activation of the "Delineate watershed" function button when it turned to green from being grayed out. When the delineation was completed, a prompt window appeared stating, "Watershed delineation is done".

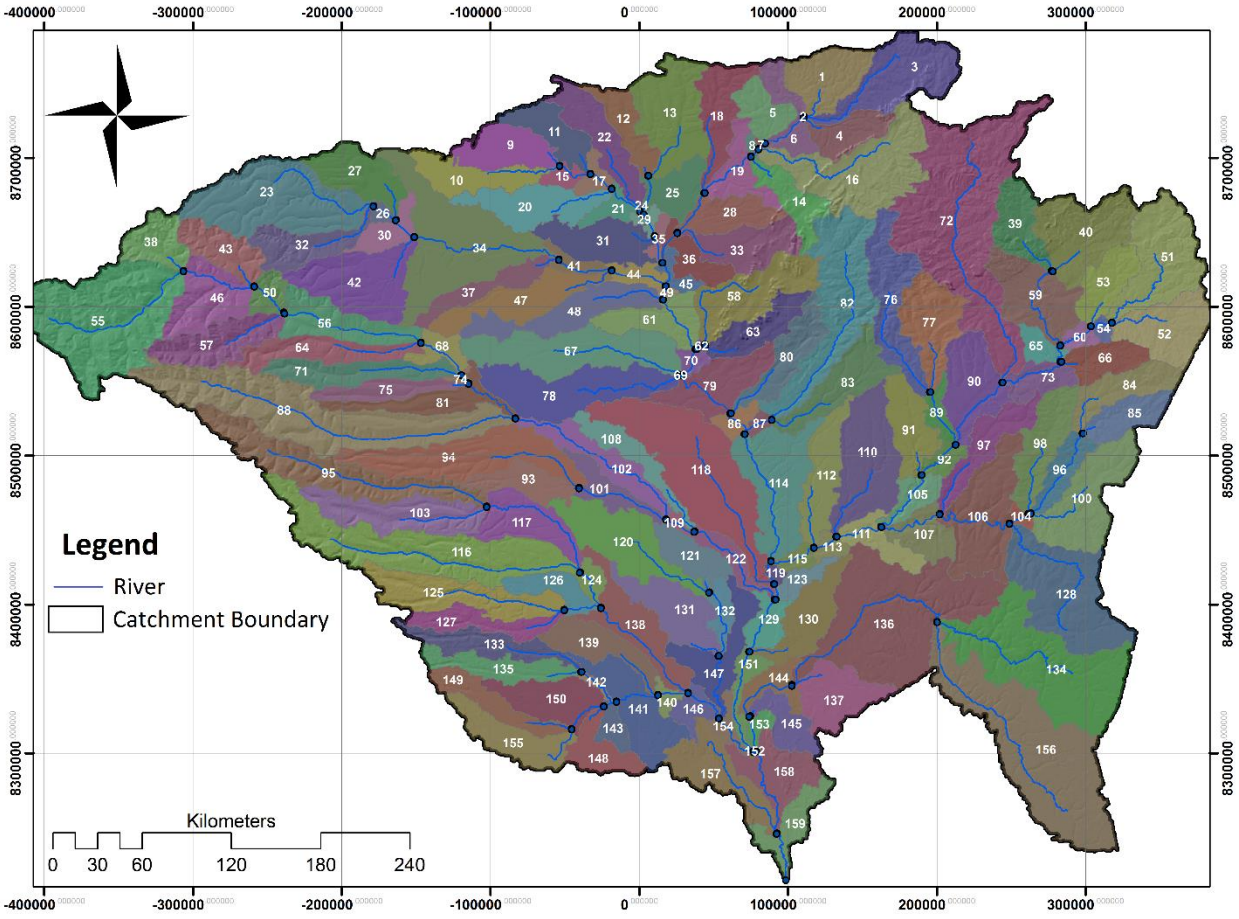

Figure 3.14: Barotse Floodplain delineated into 159 sub-basins following the stream threshold that was set for the model. Sub-basins are coloured differently for distinction

The next stage was the "Calculation of sub-basin parameters". This section of hydrologic processing contained functions that aided in calculating the geomorphic characteristics of the sub-basins and reaches formed in the preceding steps. This step was also important in defining the locations of reservoirs within the watershed. However, in our case we had no reservoirs as water is not impounded at any section of the floodplain as it flows freely (except natural ponding in some isolated sections within which were ignored in the model). When this stage was completed, another

prompt message appeared in form of a pop-up window saying, “Sub-basin parameter calculation successfully done”. When the okay button was clicked, watershed delineation cleanup process began where the data was exported to a “Raster Geodatabase” (GDB). Finally, the watershed delineation was done, and an exit button was clicked to proceed to the next stage.

3.4.4 HRU Analysis

This stage in the SWAT analysis allowed to load land use and soil layers into the project ,‘Task 191a’. It also enabled the evaluation of slope characteristics and determination of land use/soil/slope class combinations and distributions for the delineated watershed and each respective sub-watershed (SWAT Documentation, 2009).

As indicated earlier, HRU can be thought of as a small area within a sub-basin that is expected to behave about the same way to a precipitation event. So within each sub-basin, there will be several HRUs. These for instance may have the same land use and soil cover, but different slopes. These are expected to respond differently to a precipitation event due to the spatial distribution of rainfall and variant land use, slope and soil characteristics.

The first key step was defining the land use dataset. Initiating the Land Use/Soil/Slope Definition tool was done by selecting “Land Use/Soil/Slope Definition” in the HRU Analysis menu. A dialogue box was opened that enabled load the required datasets. These were to be in the same projection as our earlier loaded raster (DEM, in WGS 84). Upon loading the land use raster, it was clipped to our watershed and only showing changes for our region of interest. A land use map with numbers in the legend before reclassification is given in Figure 3.15.

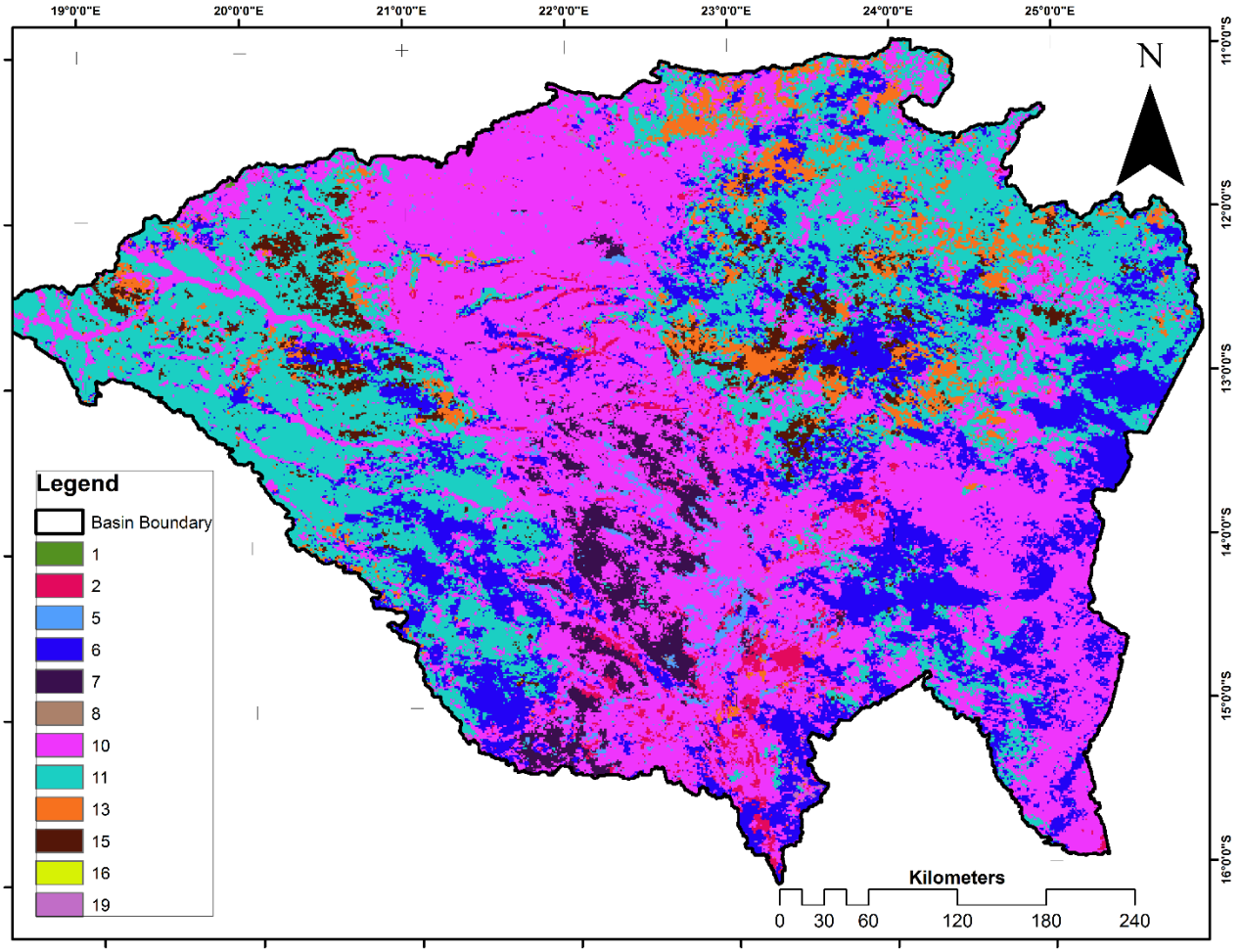

Figure 3.15: Land use characterization based of the FAO 2009 raster classification, Barotse Floodplain, Western Zambia

A "Look-Up Table" was prepared for the actual land use classes based on the options available in the Arc SWAT Model also called Arc SWAT Categories. A "Look-Up Table" offered an advantage of putting land use classes once and for all instead of manually entering them every time we start the project, that is, individually. The "Look-Up Table" used can be viewed from Appendix 7. It was in notepad text format. Please note that this stage requires a personal judgment call. This is because the land classes used in SWAT are predefined (USA), hence, one has to choose a class/classes that are nearer or similar to one's region of interest. The illumination of the new reclassified land use map is displayed in Figure 3.16.

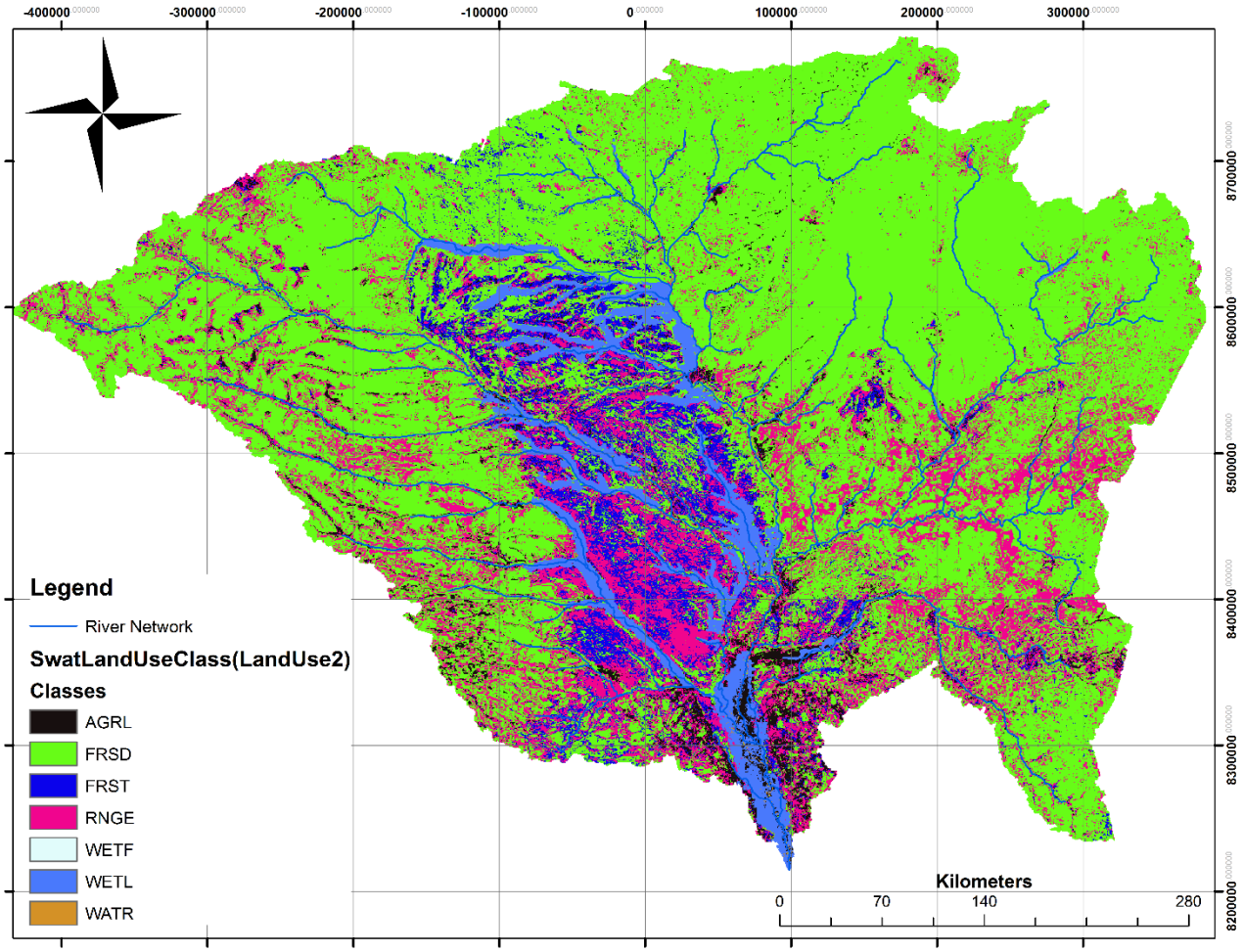

Figure 3.16: Re-classified land use according to this study, Barotse Floodplain, Western Zambia. AGRL = Agricultural Land, FRSD = Forest Deciduous, FRST = Forests, RNGE = Range Grasses, WETF = Wetland Forested, WETL = Wetland and WATR = Water.

Once the land use is reclassified, the next stage is to define our soil type. The soil data was loaded from the disk as the prompt window gave three options. As was before, the projection was put in WGS 84. The soil data was successfully loaded and clipped to the watershed boundary. This was downloaded from the FAO website. The following map is the same map as Figure 3.16, however, a digital soil map has been overlaid on it. This is before re-classification of the soil classes by SWAT (Figure 3.17).

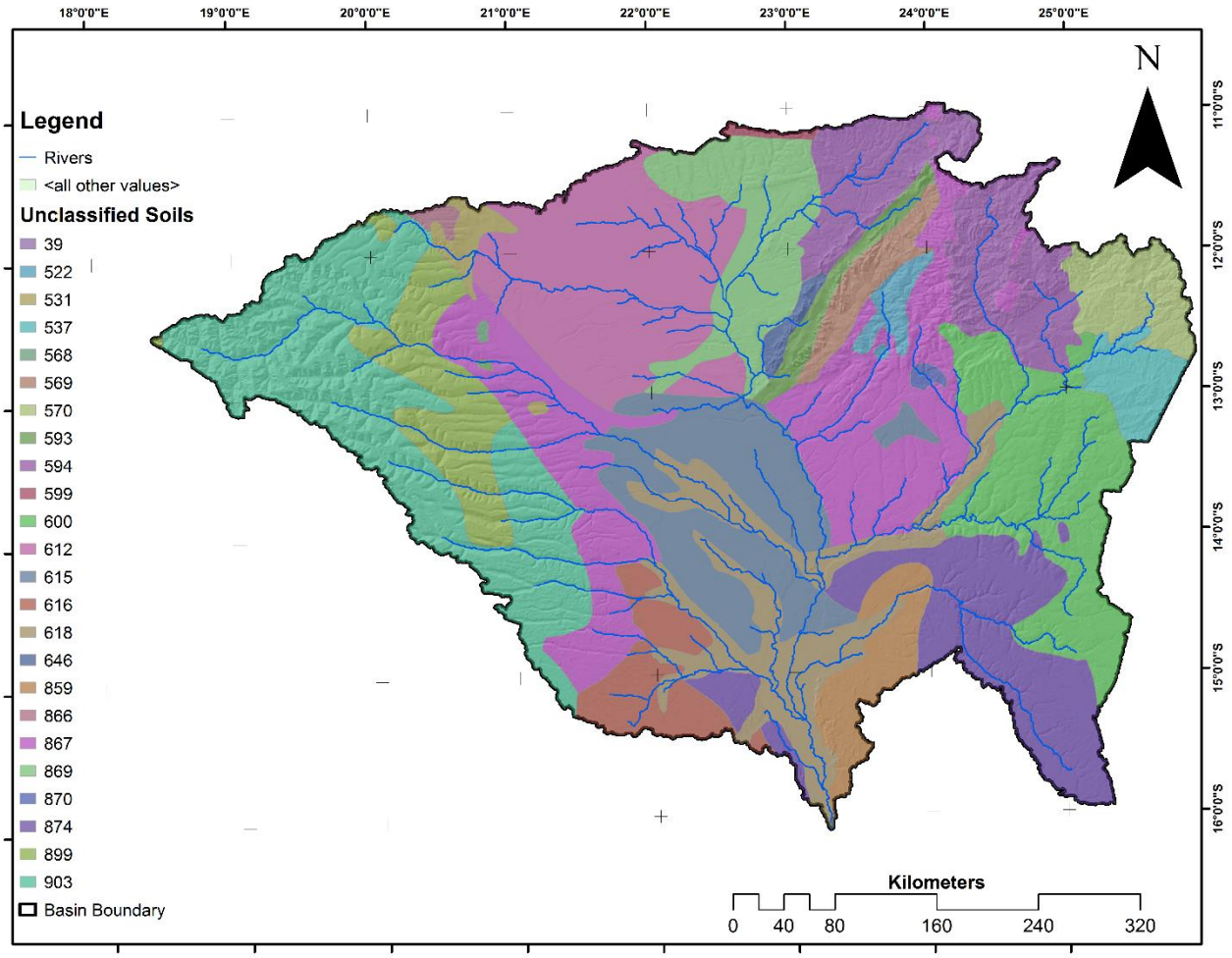

Figure 3.17: Soils data downloaded from the FAO website imported into GIS and clipped to the watershed in the Barotse Floodplain, Western Zambia

In reclassification, the Harmonized World Soil Database (HWSD) was used. This aided in the naming of the soils and giving them their respective soil pedo-transfer codes. This was made possible via software called HWSD Viewer. A display of Figure 3.18 gives the re-classified soil classes according to the HWSD using "Lookup Table" as was done in the land use re-classification.

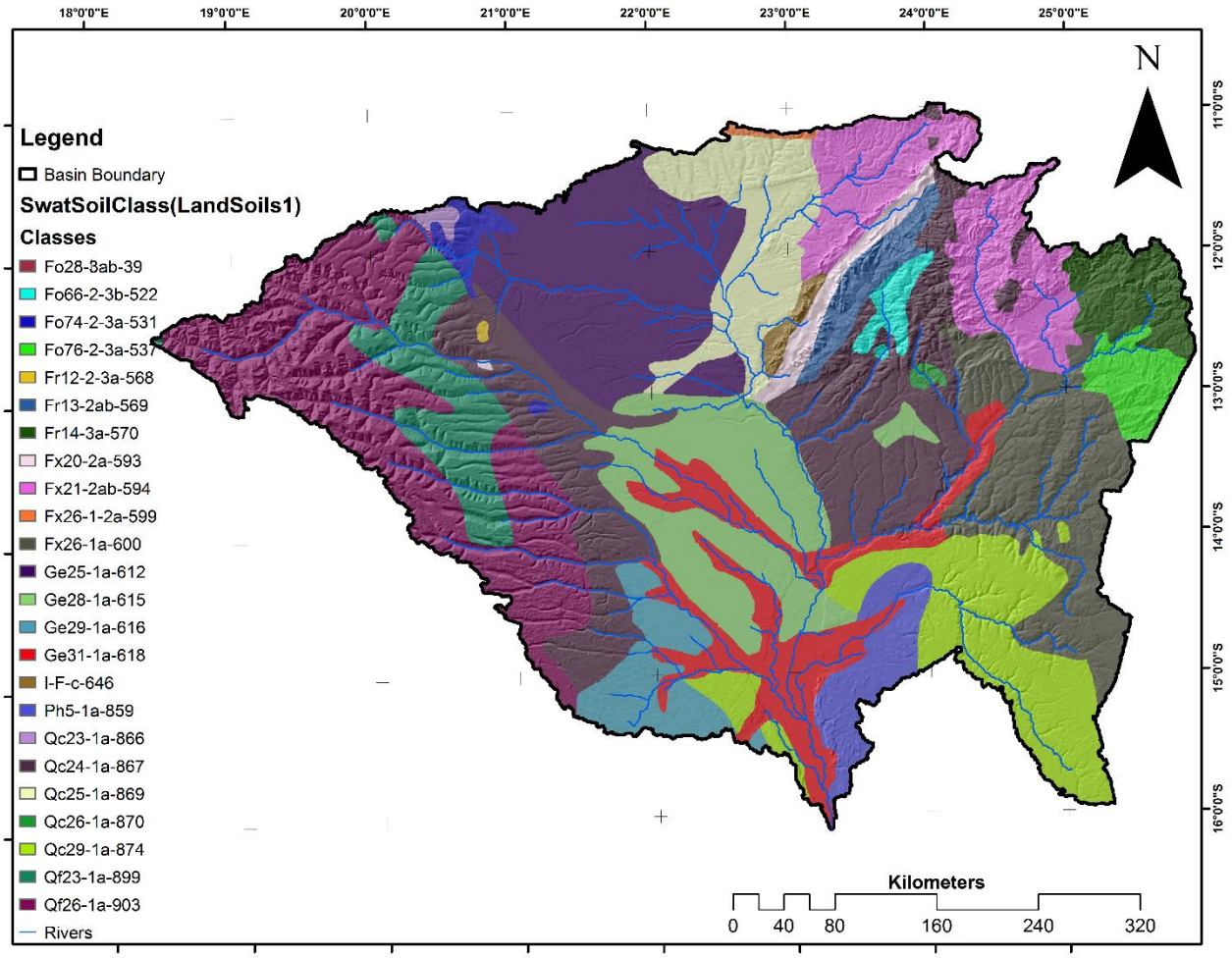

Figure 3.18: Reclassified soil classes according to the HWSD using "Lookup Table" that had all the soil pedo-transfer codes, Barotse Floodplain, Western Zambia

The soil code summaries used in the legend for Figure 3.18 above are in Appendix 7. Meanwhile, Figure 3.19 is a screen captured image of the HWSD-Viewer, which can be used in the naming of the soils and zooming to the region of interest. The purpose of the HWSD-Viewer is to provide a simple geographical tool to query and visualize the Harmonized World Soil Database. The HWSD consists of a 30 arc-seconds (or~1km) raster image and an attribute database in Microsoft Access 2003 format. The raster image file is stored in binary format (ESRI Band Interleaved by Line – BIL) that can directly be read or imported by most GIS and Remote Sensing software. For advanced use or data extraction of the HWSD, it is recommended to use a GIS software tool (Nachtergaele, Velthuizen and Verelst, 2008).

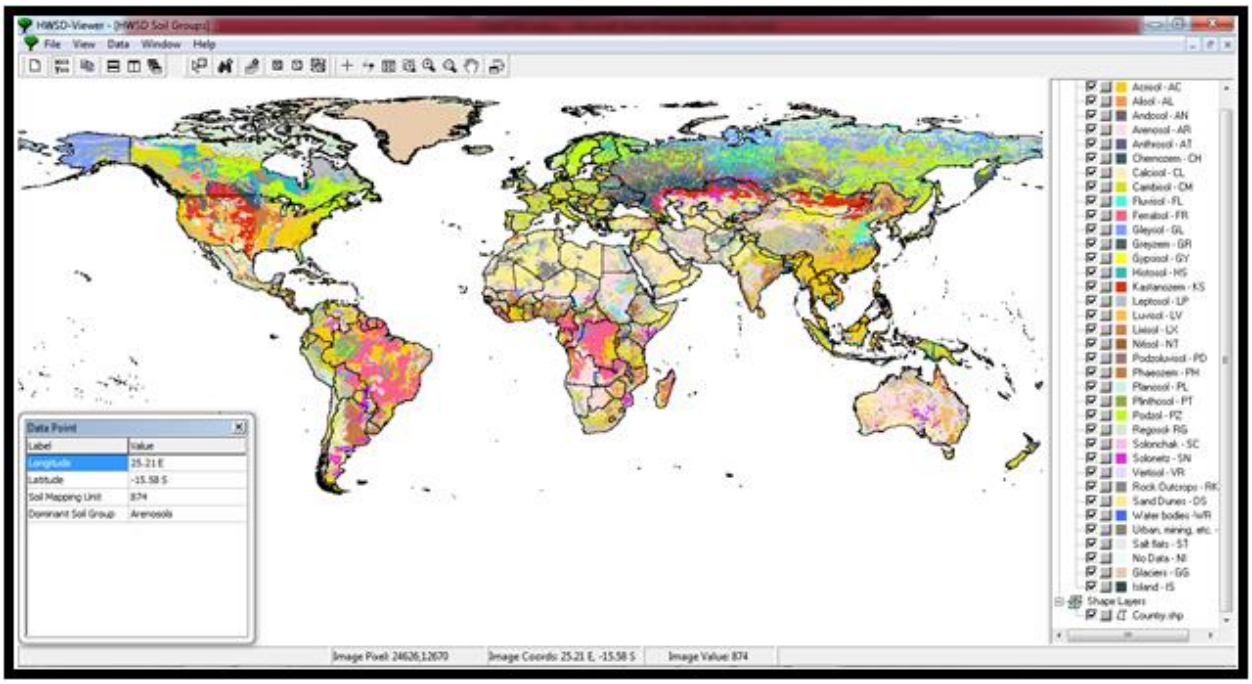

Figure 3.19: Screen shot of HWSD Viewer for the whole world. This was zoomed to the region of interest in order to get the desired results for the Barotse Floodplain, Western Zambia

Upon completion of the soil classification with the aid of FAO Raster and HWSD, the next step undertaken was slope classification. This stage too called for a judgement based on the topography of the DEM. The first step was “Slope Discretization”. Under this, two options were given. These were the “Single Slope” and the “Multiple Slope” functionalities. The latter was chosen first.

During the Multiple Slope Discretization, all slope classes were falling in one class, that is, the first class. Five, four, three and two classes were used and still yielded the same results, all slope falling in one class. This was evident from the elevation differences in DEM used. The difference between the maximum and minimum elevation was minimal hence the reason for all elevation classes to be lumped in one class. With this in mind, the Single Slope Discretization was later used.

Once all the three functionalities in HRUs formation are exhausted, that is, land use data, soil data and slope, then the overlay process begins. This was done by a single click of the overlay button and the HRUs were delineated. A full HRU map delineated during HRU Analysis is given in Figure 3.20.

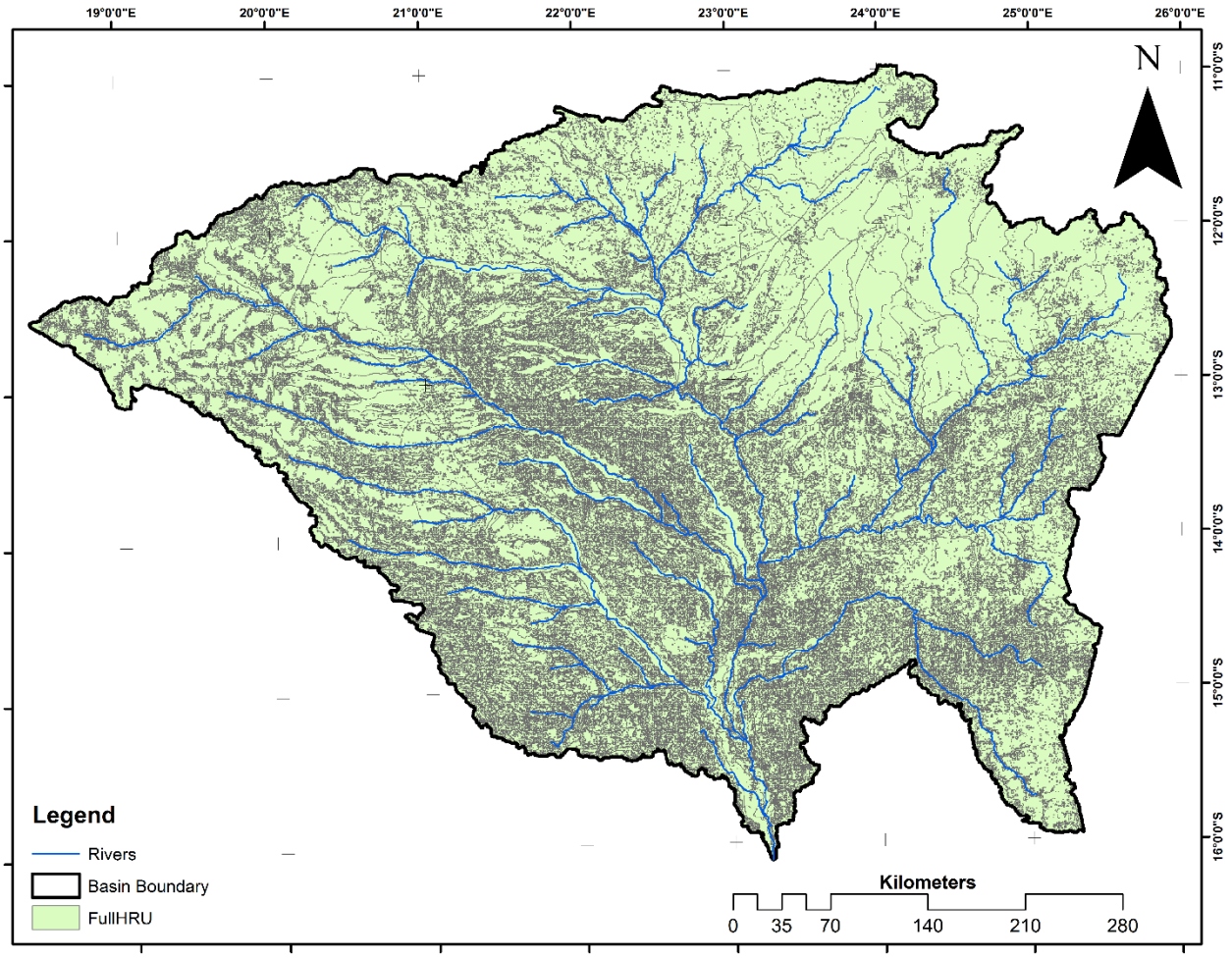

Figure 3.20: Full HRUs delineated during the HRU Analysis Stage, Barotse Floodplain, Western Zambia

3.4.5 Importing Weather Data

Weather data used in the watershed simulation was imported after the HRU distribution was completely defined. The data was loaded using the first command in the "Write Input Table" menu item situated on the Arc SWAT toolbar. This tool allows loading weather station locations into the project and assigning weather data to sub-watersheds.

Before we proceed with how to load data into the model, it is appropriate at this point to know how and where this data was acquired, including the processing steps.

Firstly, the address http://swat.tamu.edu/ was entered in the search engine and Arc SWAT webpage was opened. Under this page, five (5) menus (headings) were shown (first row). These were: software; documentations; workshops; conferences; publications and developers. Each of

these when clicked gave extra details in line with each heading. Underneath this first row was the second row with three (3) headings. These were: software downloads; upcoming workshops and 2015 conferences. The heading of interest here was software downloads. Under this column scrolling downward, a link named Climate Change Data (http://globalweather.tamu.edu/cmip) was clicked that led to the page of interest. This page had the heading named "Climate Change Data for SWAT (CMIP3). CMIP3 stands for Climate Model Simulation. This website allows users to download CMIP3 data in SWAT file format for a given location and time period. The steps which were followed are:

(i) Selection of the bounding box;
(ii) Defining time period for collecting data;
(iii) Selection of climate change model;
(iv) Selection of what type of data to collect; and finally
(v) How the data can be delivered.

A bounding box helped in the selection of the area of interest by zooming in and inputting the coordinates enclosing the region. The period for collecting data was from 1979 to 2013, a thirty-five (35) year period. About nine (9) climate change models were available to choose from in the third step indicated above. The model chosen was from the Meteorological Institute of the University of Bonn (MIUB), Germany. The type of data selected and downloaded was temperature, relative humidity, precipitation, wind speed and solar radiation. This data was delivered via email. A display of Figure 3.21 shows the window used in selecting the region of interest by panning and putting up of a bounding box or simply entering the four bounding coordinates for the region of interest.

Figure 3.21: Selection window for the region of interest in downloading weather data for a preferred region of interest. In this case the western part of Zambia was selected, specifically Western Zambia

3.4.6 Data Format and Processing

Once the data was received via email, it was in two formats. These were:

(i) Comma Separated Values (C.S.V.) and

(ii) Text Documents (.txt), to be opened by MS Excel and Notepad respectively.

These were representing a total of 270 weather stations. However, only 240 weather stations falling within the bounds of the study area were selected due to processing time for the 35 years.

This download data was useful in developing a custom made "userwgn". A Weather Generator (WGEN) is a table in database format that contains weather data for the area of interest with respect to the period and location of weather stations. The interface does not allow the user to perform other input data processing until the Weather Generator Data is defined.

The table developed had the following weather data information in the first row which corresponded to the values in the columns. Field names and their definitions for the "userwgn" developed following the required Arc SWAT format are given in Table 3-2.

Table 3-2: Summary of field names and their definitions which were entered into the database (Arc SWAT Documentation, 2009) used in this study

Field Name(s)	Definition
TMPMX1 to TMPMX12	Average maximum air temperature (^{0}C) for each month from January to December
TMPMN1 to TMPMN12	Average minimum air temperature (^{0}C) for each month from January to December
TMPSTDMX1 to TMPSTDMX12	Standard deviation of maximum air temperature (^{0}C) for each month from January to December
TMPSTDMN1 to TMPSTDMN12	Standard deviation of minimum air temperature (^{0}C) for each month from January to December
PCPMM1 to PCPMM12	Average precipitation (mm/day) for each month from January to December
PCPSTD1 to PCPSTD12	Standard deviation for daily precipitation (mm/day) for each month from January to December
PCPSKW1 to PCPSKW12	Skew coefficient for daily precipitation for each month from January to December
PR_W1_1 to PR_W1_12	Probability of wet day following dry day for January to December
PR_W2_1 to PR_W2_12	Probability of wet day following wet day from January to December
PCPD1 to PCPD12	Average number of days of precipitation from January to December
RAINHHMX1 to RAINHHMX12	Maximum 0.5 h rainfall from January to December for entire period of record (mm)
SOLARAV1 to SOLARAV12	Average solar radiation for January to December (MJ/m2/day)
DEWPT1 to DEWPT12	Average dew point for each month from January to December (^{0}C)
WNDAV1 to WNDAV12	Average wind speed in from January to December (m/s)

A summary of the processing steps for the weather data is as follows:

(i) Calculating four (4) statistical parameters of daily air temperature data using Pivot Table (MS Excel);

(ii) Calculating six (6) statistical parameters of daily air precipitation data using pcpSTAT.exe software;

(iii) Calculating maximum 0.5-hour rainfall in entire period of record for month using Pivot Table (MS Excel);

(iv) Calculating average daily solar radiation using Pivot Table (MS Excel);

(v) Calculating average dew point temperature using Dew Point Calculator software; and

(vi) Calculating average wind speed using Pivot Tables (MS Excel).

Once these calculations are done, a total of fourteen (14) statistical parameters of daily weather data used by the weather generator of the SWAT (WGEN_user table) model are ready.

The programmes pcpSTAT.exe and Dew Point Calculator (i.e., dew.exe and dew02.exe) were designed by Liersch (2003). PcpSTAT.exe calculates statistical parameters of daily precipitation data used by weather generator of the SWAT model (userwgn.dbf) while dew.exe and dew02.exe are designed to calculate the average daily dew point temperature per month using daily air temperature and humidity data. These programmes made long calculations faster than using Pivot Table approach in MS Excel. Once the data was ready for use, it was imported into SWAT via "Weather Data Definition Dialogue Box". Ideally, for each type of weather data loaded, each sub-watershed is linked to one gauge. However, as was mentioned, only two hundred and forty (240) stations were used in this project due to processing time. More stations can be used for greater accuracy in modelling.

3.4.7 Running the Model

With the other five (5) menus of the Arc SWAT interface complete, the sixth and final menu was the "SWAT Simulation". This menu allows the setting up and running of the model. Instructions and commands on running the model were given via the Set Up and Run SWAT Model Simulation dialog box.

Due to a lot of gaps in the data obtained from the DWA/DWRD, the starting date for the model had to be set at 1st October 1986. Three years were skipped to warm up the model. These were 1986, 1987 and 1988. This implied that 1989 was the first year to yield results or give a report. The month of October was selected as it is the end and start of a new hydrological cycle. The model was run for ten (10) years, that is, 1989 to 1999. The years 2000 to 2005 were left for validation of the model. Two separate simulations were done. One on a yearly time step (Sim2-Yearly) and the other one on a monthly time step (Sim2-Monthly). Rainfall distribution was left at skewed normal and SWAT.exe Version set to 64-bit, release. The setup SWAT Run command was clicked after which the Run SWAT command followed. The final alert window read, "SWAT run successful". This marked the end of this stage.

3.4.8 Acceptable Model Constituents

The following are the steps needed nowadays in order to develop an acceptable hydrological model that merits to be published as scientific paper. These include:

(i) Model building;
(ii) Calibration;
(iii) Validation;
(iv) Sensitivity analysis; and
(v) Uncertainty analysis.

A few of these are explained in the proceeding subsections so as to comprehend their significance in hydrological modelling.

3.4.9 Hydrological Model Flow Mechanism

In this model, calibration and validation was achieved by using the Soil and Water Assessment Tool-Calibration and Uncertainty Parameters (SWAT-CUP) which is a separate software with its own Graphical User Interface (GUI). SWAT-CUP is a public domain programme, and as such may be used and copied freely (Abbaspour et al, 2015). The programme links Sequential Uncertainty Fitting version 2 (SUFI-2), Particle Swarm Optimization (PSO), Parameter Solution (ParaSol), Generalized Likelihood Uncertainty Estimations (GLUE), and Markov Chain Monte Carlo (MCMC) procedures to SWAT. It enables sensitivity analysis, calibration, validation and uncertainty analysis of SWAT models (Abbaspour et al, 2015).

In order to be able to calibrate and validate the results of the model, it is important to also have an idea of what processes precede the calibration and validation stages. Hence, based on the brief outline given in the previous subsection, the following are some explanations of the hydrological flow mechanism with respect to the components:

(i) Model buildup, entirely done within the Arc SWAT environment. This is where (the environment or GUI) field measured datasets are combined with remotely sensed datasets. The buildup of the model starts from model set up, watershed delineation dialogue box, incorporation of land use/land cover/slope data including soil dataset from FAO and later merged with imported weather datasets. This is as explained previously in Figures 3.12 through to 3.21 above. These are meant to reveal a sequence of the steps in the development or model buildup;

(ii) Calibration, the adjusting of model inputs (parameters, structures, variables, etc.) with the purpose of achieving the best simulation match with observation. In other words best match between what the model gives and what you observe (Abbaspour, 2015). As indicated earlier, three (3) years were used for model warm up period, that is, 1986 through to 1989. Then 1989 through to 1999 was used for calibrating the model. Senanga Hydrometric Station had discharge historical data from 1949 to 2005 with a lot of gaps in the data. Hence the rationale in selecting 1989 to 1999 was based on diminished gaps in the data. In essence, calibration was based on the optimization of an objective function. For example, some kind of error between the observed data and the simulated data should be calculated. So the idea was to reduce the error and catch the dynamics of the observations. Recall equation (3) (Abbaspour, 2015, p.57) where SSQR is the sum of squares of the difference of the measured and simulated values after ranking:

$$\text{Minimize: } SSQR = \left(\frac{1}{n}\right)\sum_{i=1}^{n}[Q_{i,m} - Q_{i,s}]^2 \quad \ldots\ldots\ldots \textit{(eqn 3)}$$

There are many different types of objective functions to enhance performance of the model. As for SWAT-CUP, 10 different objective functions are currently allowed. Equations 4, 5 and 6 are the Coefficient of Determination, Kling-Gupta efficiency and the modified Nasch-Sutcliffe efficiency factor respectively (Gupta et al., 2009 and Abbaspour, 2015, p.57). However, in this research, the coefficient of determination was used. The equations mentioned are:

$$\text{Maximize: } R^2 = \frac{[\sum_i (Q_{m,i} - \bar{Q}_{\cdot m})(Q - Q)]^2}{\sum_i (Q_{m,i} - \bar{Q}_m)^2 \sum_i \left(Q_{s,i} - \bar{Q}_s\right)^2} \quad \ldots\ldots\ldots \textit{(eqn 4)};$$

Maximize: $KGE = 1 - \sqrt{(r-1)^2 + (\alpha-1)^2 + (\beta-1)^2}$ ..... *(eqn 5)* and

Maximize: $NS = 1 - \frac{\sum_i |Q_m - Q_s|_i^p}{\sum_i |Q_{m,i} - \bar{Q}_m|_i^p}$ ..... *(eqn 6).*

Of interest is equation 4, where R^2 stands for coefficient of determination and Q is a variable (e.g., discharge), and ***m*** and ***s*** stand for measured and simulated, ***i*** is the ***i^{th}*** measured or simulated data;

(iii) Validation, the process of testing the calibrated parameters with an independent set of data without further changes to the parameters (Abbaspour, 2015). Once the model was calibrated, a certain amount of observed data was used. This was discharge data from 2000 to 2005. This was done to show that the model is not just conditioned on those observations used for calibration, but it can also simulate beyond that input used to calibrate the model. So, this is why part of the data needed to be saved so that part of it is used for validating the model. Once calibration was done, no further adjustments were made to the parameters. The model was run based on the values of the calibrated parameters. In other words, the validation process was the use of an independent dataset to the one used for calibration. This independent dataset was the discharge data from 2000 to 2005 and not the 1989 to 1999 data, which was already used in the calibration process. The use of an independent dataset is essential for avoiding biased conclusions and to inspire confidence in the results when a similar pattern or signal is reproduced with a different dataset;

(iv) Sensitivity analysis, the process of determining the significance of one or a combination of parameters with respect to an objective function or a model output. We can also say that it is a process where you define which one of your parameters has the highest impact on the objective function that you are using (Abbaspour, 2015). Thirteen (13) parameters were used and according to Abbaspour et al (2015) parameters represent processes. Inputting of these parameters revealed the most sensitive parameters represented the most dominant processes in the watershed. With these parameters set and using the t-stat and p-value analysis, the most sensitive parameters would be observed. This was through a global sensitivity analysis. However, others may prefer to use one at a time sensitivity analysis. An example of the parameters used was the Curve Number, (CN2). CN2 is the

factor that sort of partitions rainfall into infiltration and runoff. So, it is a very important parameter. This is the parameter to adjust in order to control the peaks in the discharge against time hydrograph; and

(v) Finally, we have uncertainty analysis. Basically, uncertainty comes from the fact that we do not know about the parameters or that our measurements are very little, that is, number of measurements we make. An example of this is the spatial soil heterogeneity. The heterogeneity of the system is so large such that even if you take a hundred soil samples and determine hydraulic conductivity, you still don't know what the hydraulic conductivity of the soil is.

Calibration and uncertainty analysis are two different processes, and they are different from each other. However, these two are intimately linked that you cannot separate them. To capture the two, a 95 Percentage Prediction Uncertainty (95PPU) enveloping curve was used.

As was stated earlier, there are different objective functions that you may use to calibrate the model. These objective functions gave some sort of performance of the model. Some kind of index or indication to the performance of the model developed. And there are many different, i.e., Root Mean Square Error (RMSE), Coefficient of Determination (R2), Nash-Sutcliffe (NS), Coefficient of Determination multiplied by the Coefficient of the Regression (bR2) and so on and so forth. Each of these has a set of good solutions with one being the best.

When we use different types of objective functions, we will have different best solutions. A question arises on which of these is the best solution. The problem is that different sets of parameters can give us similarly good solutions and then we do not know which one is better. Some results are relatively close to each other for individual parameters. However, a problem comes in for those which have large variations. Therefore, to mitigate this, one objective function was used.

3.5 Limitations of the study

(i) Lack of historical sediment measurements and installation of new sediment traps was beyond the budget plan, hence, prioritization was applied. This means that the model developed was only calibrated for river flow which is the first phase of calibration. The sediment yields and distributions are based on the first calibration. In future, the

WARMA and researchers needs to set up sediment traps so that the second phase of calibration and validation can be done; and

(ii) Certain software could only be used as trial or student version; hence the analysis of data was in a way restricted. An example of such a software was the Soil and Water Assessment Tool for Calibration and Uncertainty Parameter (SWAT-CUP). This software is capable of carrying out parallel processing that improves the simulation time and results, however, this requires a licensed product (Abbaspour *et al*, 2015).

CHAPTER 4: RESULTS AND DISCUSSION

This chapter presents the results of this study and analysis of the various data obtained from water, soils and hydrological modelling. The analysis is mainly based on a total of 124 surface water samples. These were analysed for their physical, chemical and bacteriological characteristics using graphical and statistical charts to infer their variations, patterns and trends. Furthermore, field sediment samples as well as those predicted by SWAT were analysed to explain the spatial distribution. A discussion of the results is covered after each subsection of results presented.

4.1 Water Quality

Water quality analysis of bacteriological, physical and chemical characteristics are presented in subsequent sections.

4.1.1 Bacteriological Parameter Distribution

Three transects were done for bacteriological analysis on the Barotse Floodplain, with each transect having a different number of samples collected. The transects were Mongu – Kalabo, Sioma – Kalabo and Mongu – Senanga with ten, twelve and seven samples collected, respectively (Figure 4.1 a, b and c). It was observed that on the Mongu – Kalabo Transect (Figure 4.1-a) had two locations out of ten, which recorded Too – Numerous – To – Count (TNTC). These locations were Mapungu (IB14) and Nguya (IB15). It was further observed that IB9 and IB11 (unnamed areas) recorded the lowest levels of bacteriological contamination. On the Sioma – Kalabo Transect (Figure 4.1-b), three samples out of the twelve had TNTC values observed. All these three points were located on basic schools, that is, Nakatwelenge (IB28), Sinungu (IB31) and Sikana (IB32). As for the Mongu – Senanga Transect, six out of the seven samples collected recorded TNTC values (Figure 4.1-c). Furthermore, some of the hot spots along this transect included Sianda Stream (IB 18), Sefula Rice Irrigation Scheme (IB 19), Litoya Bridge (IB 20) and a sewerage disposal site (IB 23) which is connected to a sewer line from Senanga Secondary School.

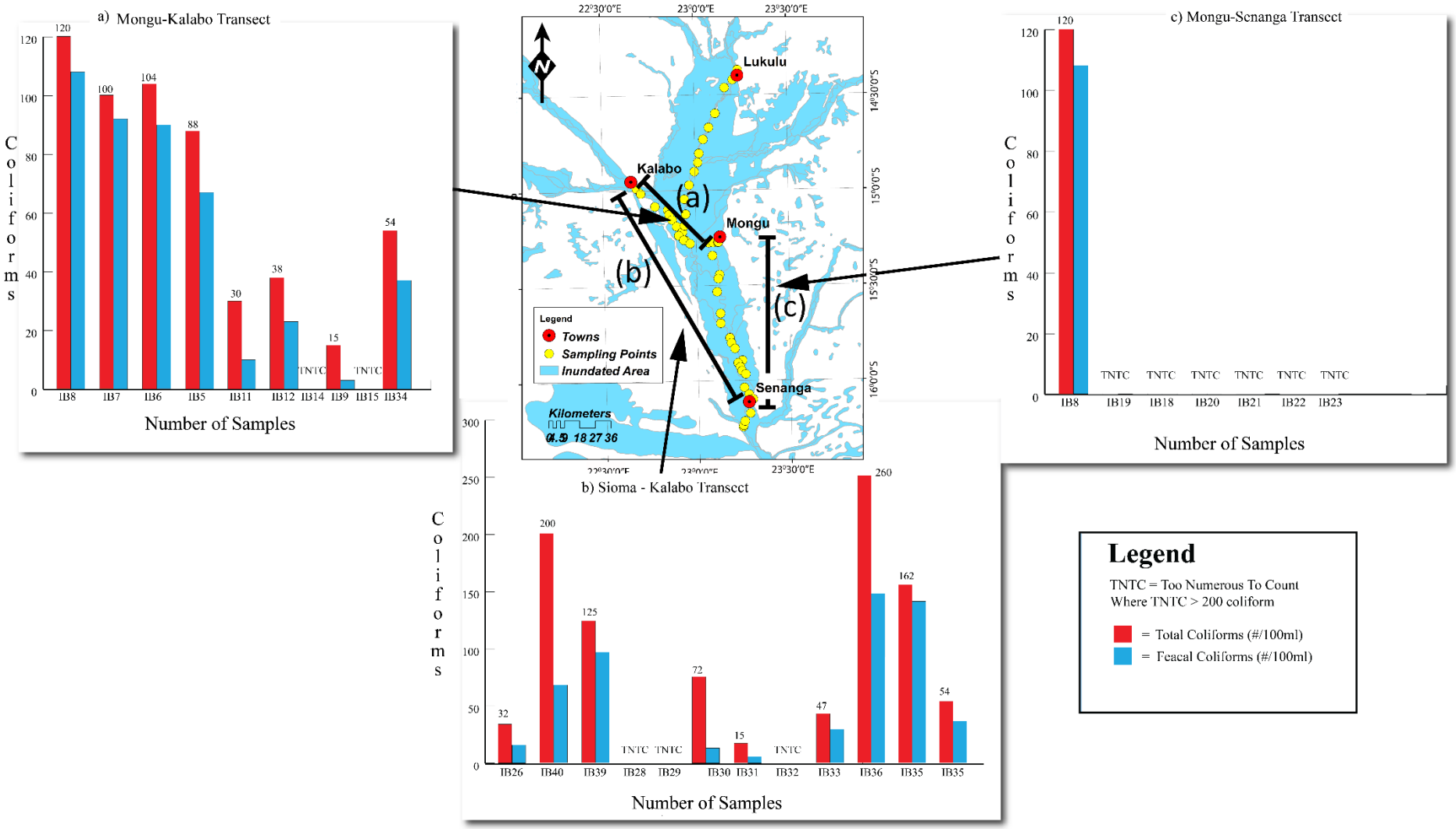

Figure 4.1: Variations of total and feacal coliforms along the 3 transects labeled as **a**, **b** and **c**, Barotse Floodplain, Western Zambia

4.1.2 Discussion of Bacteriological Results

The Mongu – Senanga Transect (Figure 4.1-a above) had the highest levels of coliform concentrations (TNTC >200 coliforms), which resulted from a combination of various water quality perturbation induced by anthropogenic activities such as livestock rearing, sewerage discharges and open defecation. Similarly, the few locations on the other two transects (Mongu – Kalabo and Sioma – Kalabo) which recorded TNTC where located on settled areas. The results of this study can be compared to the work by Mulamattathil *et al* (2014) in South Africa. Mulamattathil *et al* (2014) studied the levels of environmental bacteria from different sources of drinking water in Mafikeng, a province in the north – west bordering with Botswana. Samples were collected on the Modimola Reservoir and Molopo Eye. The water samples collected by Mulamattathil *et al* (2014) were for both raw and treated water and their bacteriological analysis used four indictors namely Feacal Coliform, Total Coliform, Heterotrophic Bacteria and Aeromonas to show the average number of microorganisms isolated. However, in this study, only raw water samples were analysed and the bacteriological analysis used two indicators (Total Coliform and Feacal Coliform). Furthermore, results by Mulamattathil *et al* (2014) showed that coliforms were most prevalent on the Modimola Rerservoir because it is located near settled areas characterised by several anthropogenic activities similar to the results of this study (Figure 4.1 above).

The quantity of coliforms per 100 ml is affected by the difference in water levels between the wet and dry seasons in that the concentration of coliforms is higher during the dry season and lower during the rainy season. The levels of bacteriological contamination on the Mongu – Kalabo, Sioma – Kalabo and Mongu – Senanga Transects were evaluated by percentages as mentioned earlier. These percentages indicated the variation of population and anthropogenic activities among the three river stretches/transects with Mongu – Senanga having the highest percentage (85.7%). This is evident as rice farming, cattle rearing, saw milling industries and municipal sewerage discharges were observed on this transect. Research work by Mutonga (2012) also indicates that waterborne diseases were mostly prevalent in dense areas such as Mongu. On the Kalabo – Mongu transect, the recorded 20% TNTC can be associated to the increased activities on the section during the construction of the Mongu – Kalabo Bridge.

4.1.3 Physiochemical Parameter Distribution

The parameters collected for physical and chemical analysis included pH, turbidity, electrical conductivity, total suspended solids and total dissolved solids. A representative water sampling was carried out from each location during the wet and dry season and the results were as follows:

i) *Hydrogen Ion Concentration (pH)* – Samples were collected in four different transects. These transects were Mongu – Kalabo, Sioma – Kalabo, Mongu – Senanga and Mongu – Lukulu indicated as a, b, c and d respectively in Figure 4.2. These samples were all collected during the 2014 field campaigns for both the wet and dry season.

The Mongu – Kalabo Transect had seventeen sampling points which generally showed lower pH values in the dry season with the lowest reading of 4.3 at Matongo Platform Hydrometric Station (IB1). Conversely, Mapungu (IB14) located on the Luanginga River en route to Kalabo from Mongu, north – west of Matongo Platform had the highest pH value in the dry season of 7.8. As for the wet season, pH values generally ranged within 6.8 to 7.5. However, a sharp peak was observed at IB9 (unnamed area and no settlements) south – east of Mapungu (IB14).

The Sioma – Kalabo Transect had twelve sampling points. This transect had no low – flow samples collected. The peak pH value (8.0) on this transect was at Nakatwelenge Basic School (IB 28). In contrast, the lowest pH (6.5) was recorded at IB35, a point below Ndoka Bridge (Figure 4.2-b).

The Mongu – Senanga Transect had seven pH samples collected for both wet and dry seasons (Figure 4.2-c). pH values for the high – flow period had a peak of 8.0 at a tributary called Sianda (IB 18) joining the Zambezi River south – east of Mongu and on the eastern bank of the floodplain called Kataba Settlement. The lowest value (6.8) for the high flow was recorded at Senanga High School sewerage discharge point (IB23). The site was characterized by several gardens and a sawmill. As for the dry season, the main irrigation canal in Sefula (IB19) recorded the lowest pH value of 6.2.

The Mongu – Lukulu Transect with twenty-two samples collected in the dry season no samples collected during the high flow period. The peak (7.3) and lowest (5.8) values

where located on Ngulwana Area (IB71) and Lukulu Habour (IB60) respectively (Figure 4.2-d). The Mongu – Lukulu Transect in Figure 4.2-d was trimmed to only show values starting from the confluence of the Luanginga and the Zambezi Rivers to Lukulu. Hence only twelve samples are given in the graph from the confluence northwards along the Zambezi River all the way to Lukulu. The results for the transect between Mongu and the confluence are given in Figure 4.2-a. The two transects, that is, Mongu – Lukulu and Mongu – Kalabo intersected at the confluence and hence results between the confluence and Mongu were reported once to avoid repetition.

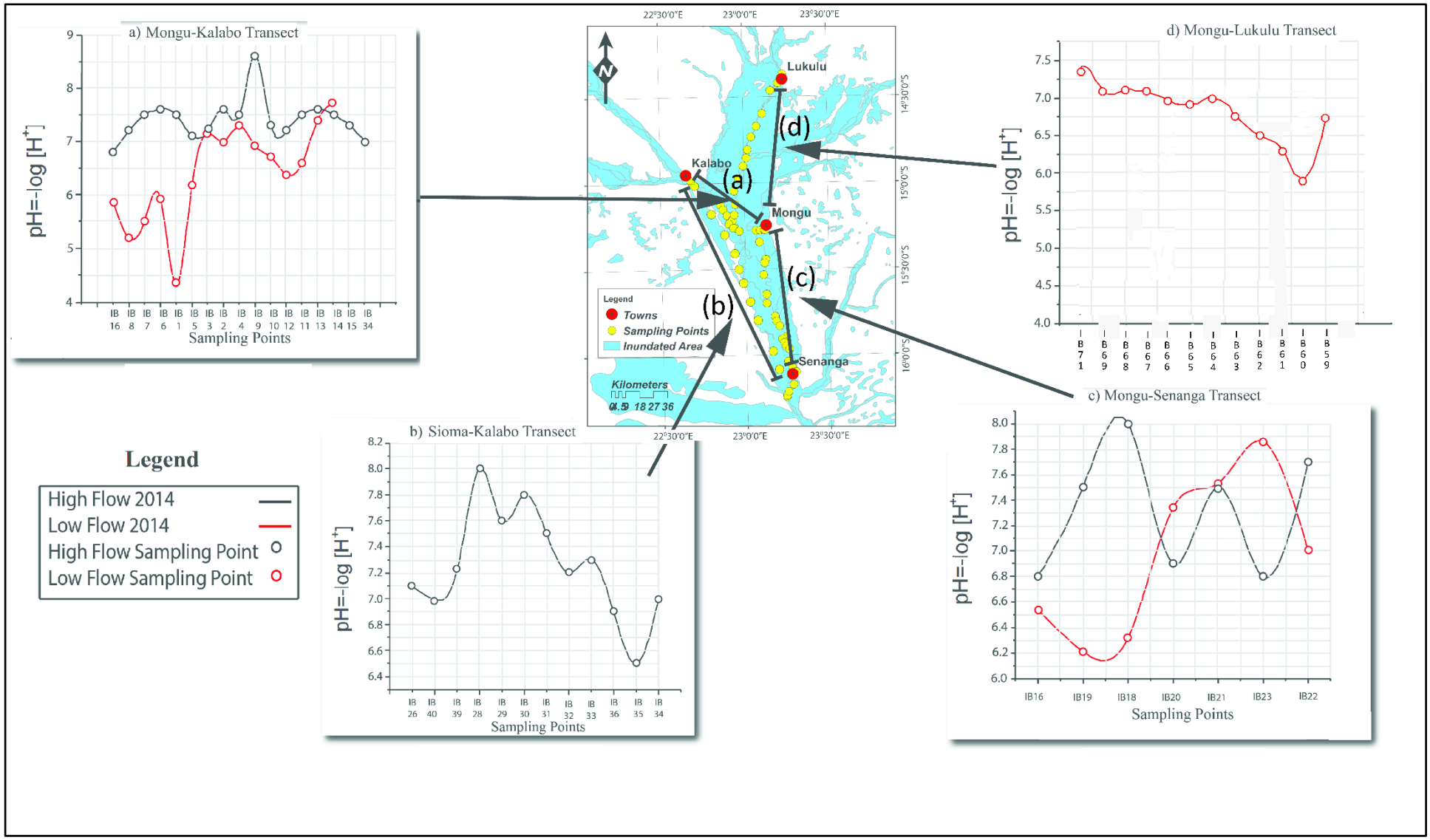

Figure 4.2: Variations of pH along the 4 different transects labeled as **a**, **b**, **c** and **d**, Barotse Floodplain, Western Zambia

One transect was chosen as an example to show the changes in the pH results (Figure 4.3). A general trend of low pH during the dry season and a high pH during the wet season was observed. This behaviour in the system is illustrated in two separate examples (Figure 4.3 and 4.4) and the interpretation and discussion of this will be given in next subsection. The first example is as in Figures 4.3 taken on the Mongu – Senanga Transect 2015 field campaign.

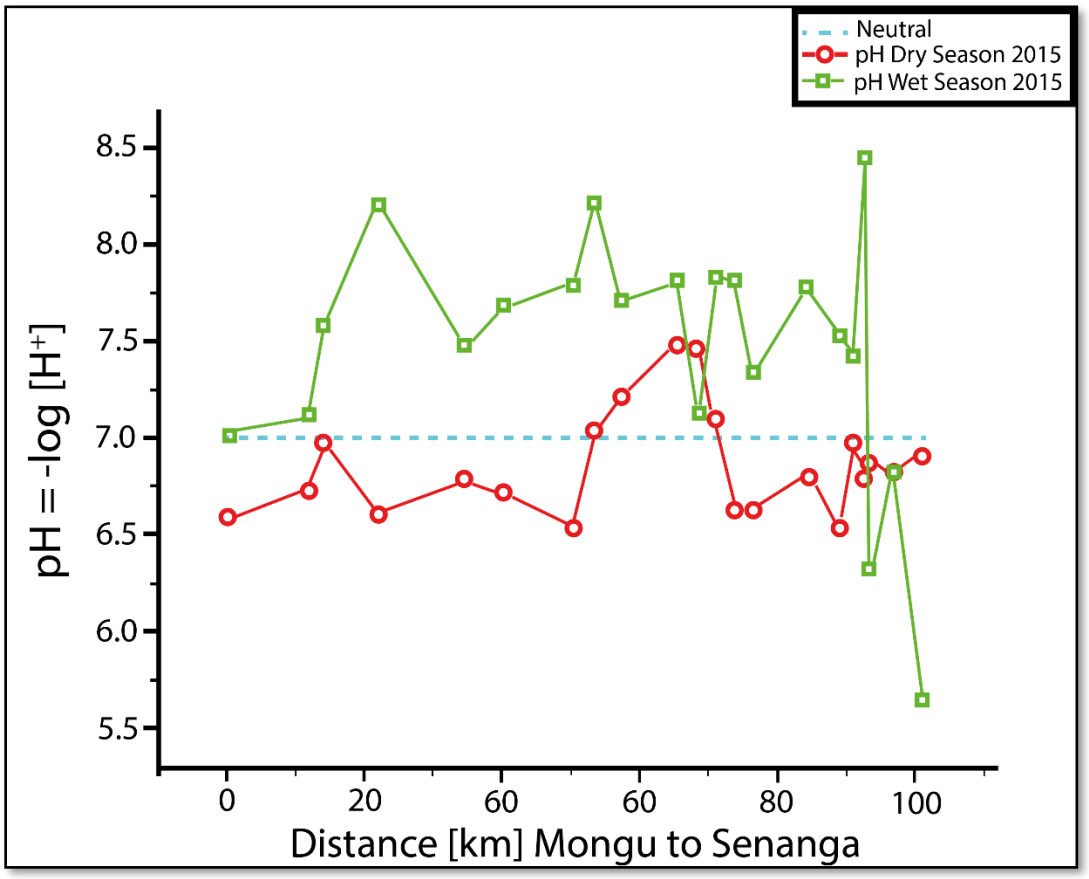

Figure 4.3: An example of pH variations on the Mongu - Senanga Transect for wet and dry seasons of 2015, Barotse Floodplain, Western Zambia

The figure above (Figure 4.3) is a graphical representation of the pH scale for the Mongu – Senanga Transect showing the changes in pH relative to distance. The values of pH are compared for dry and wet seasons of 2015 field campaign. During the wet season, pH values ranged between 7.0 - 8.5. The mean value for this period was 7.43. However, results for the dry season gave a pH range of 6.5 - 7.5 with a mean value of

6.87. It can also be observed that at about 95km from Mongu towards Senanga, pH values dramatically dropped.

The second example were two models developed by ordinary kriging for both seasons, where pH predicted distribution surfaces was generated using the pH readings of the measured points (Figure 4.4). Using the legend that combines both low–flow and high–flow, it was observed that the range was from 6.5 to 8.2.

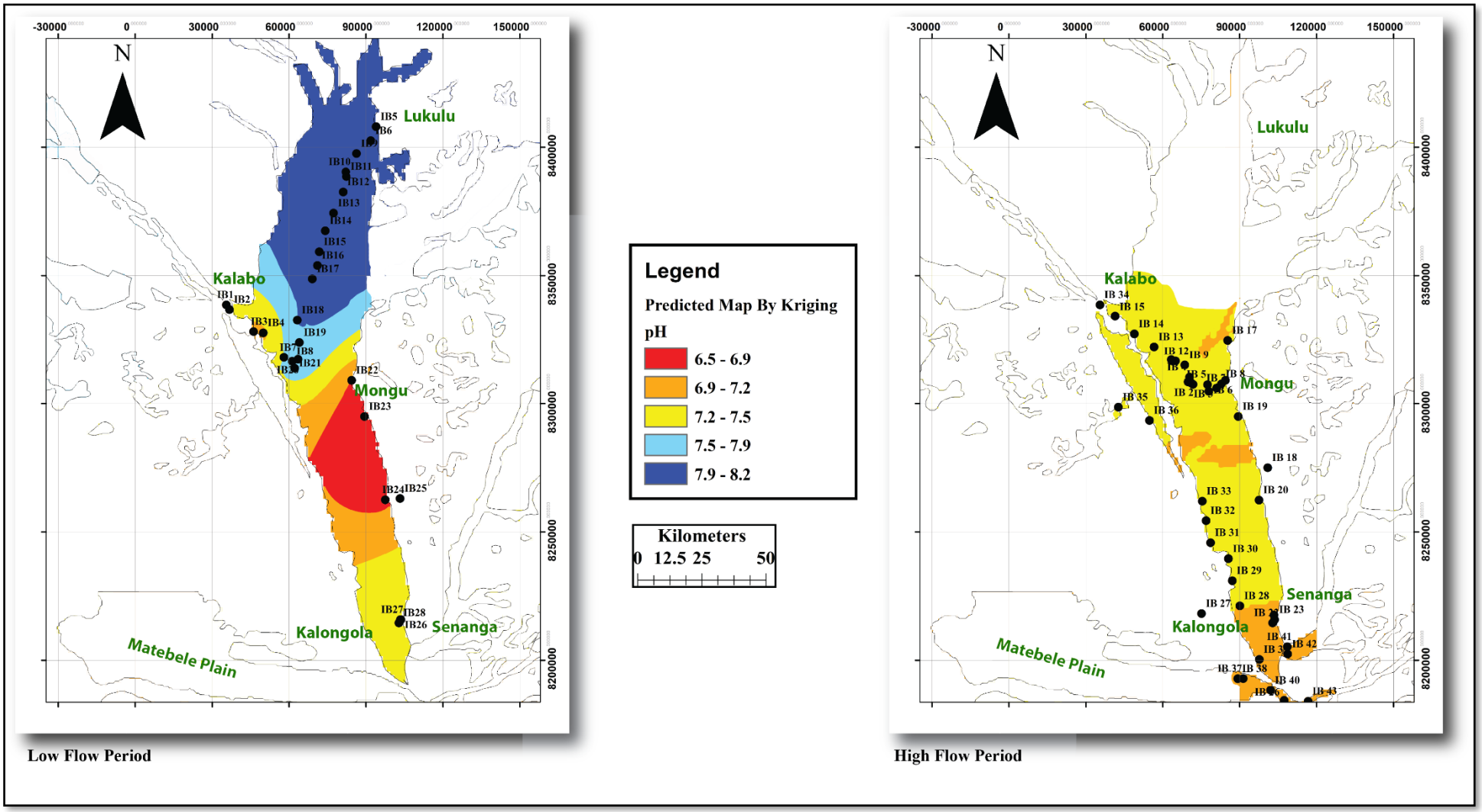

Figure 4.4: pH variations between samples collected in the low-flow and high–low periods, Barotse Floodplain, Western Zambia

From the two diagrams (Figure 4.4), the low flow period indicates that, from north to south, the pH is dropping from 7.9 to 6.9 (blue to orange colour) until Mongu (IB22) - Senanga (IB23) areas. These areas had a pH range of 6.5 to 6.9 (red colour) and were characterised by farming, saw milling and sewerage discharge points. This region also included the old pontoon at Katima Mulilo (IB24) and the site where a bridge was being constructed on the Senanga – Sesheke Zambezi River crossing (IB25). There after the pH begins to climb to 7.2 to 7.5 (Orange to yellow colour). Notice that IB22, IB23, IB24 and IB25 were located on sites characterized by various anthropogenic activities ranging from farming to schools (Appendix 8).

For the high flow (north to south), the pH for the basin ranged from 7.2 to 7.5 except in some parts where it was between 6.9 to 7.2 (settled areas). These areas where Chauteni River in Limulunga (IB17), somewhere between Kataba (IB18) and Sefula agricultural area (IB19) and the whole of Senanga area (IB 23) (Figure 4.4 above).

ii) *Turbidity* – Samples were collected on three different transects. These transects were Mongu – Kalabo, Mongu – Lukulu and Mongu – Senanga indicated as a, b and c respectively in Figure 4.5. These samples were collected during the 2014 field campaign. Each of these three graphs was plotted with respect to cumulative distance from the first sampling point to the last.

The Mongu – Kalabo Transect was characterized by high turbidity when compared to the other two (Figure 4.5-a). At the beginning of the transect, the turbidity was 0.89 NTU. A sharp increase of 47.2 NTU was immediately recorded after a short distance of less than 1km from the first sampling point into the main river system in Mongu District. The next points had lower turbidity values ranging from 1.64 to 10.99 NTU. However, upon joining the Luanginga River, the turbidity values rose all the way to Kalabo with a maximum value of 87.9 NTU.

The Mongu – Lukulu Transect had high turbidity values for the first 65km distance (Figure 4.5-b). After the confluence of the Luanginga and Zambezi River, the turbidity levels recorded a sharp drop.

The Mongu – Senanga Transect was characterised by an alternating rise and fall in turbidity values (Figure 4.5-c). The peak values show a decline from 1.35 NTU at sampling point IB78 to 0.33 NTU at sampling point IB92, whereas the lower values vary from 0.3 NTU to 0.16 NTU from sampling point IB76 to IB93.

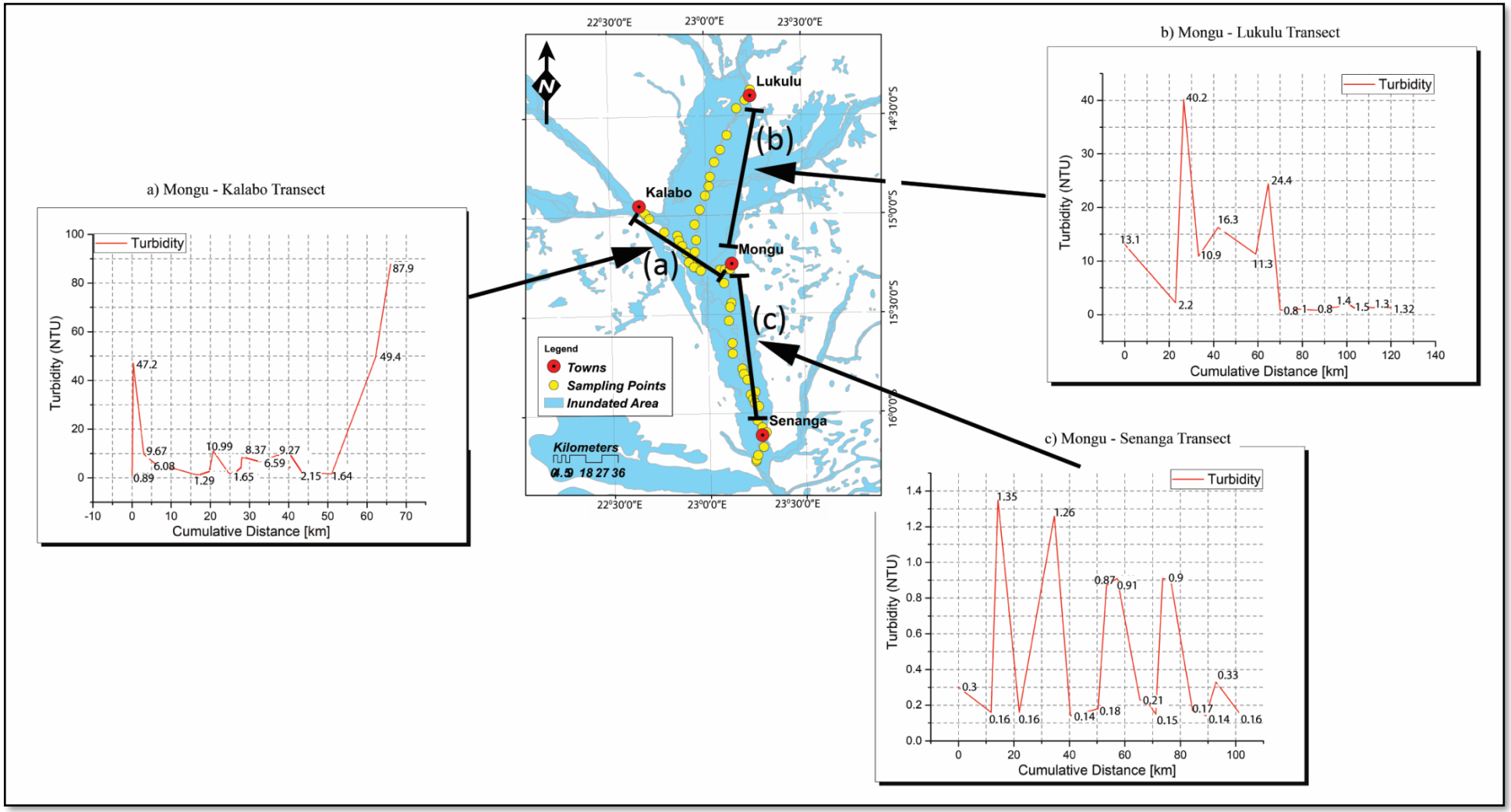

Figure 4.5: Variations of turbidity along the 3 different transects labeled as **a**, **b** and **c**, Barotse Floodplain, Western Zambia

In summary, Figure 4.6 shows the changes in turbidity from Lukulu to the confluence, and from the confluence to Mongu. The figure further illustrates the changes in turbidity from Kalabo to the confluence and from the confluence to Mongu. Finally, the figure also shows the combined flow as Luanginga (Kalabo to confluence) joins the Zambezi passing through Mongu and all the way to Senanga. The reason why turbidity was high in the Luanginga River (Mongu - Kalabo Transect) and main Zambezi River after the confluence with the Luanginga southwards is explained in the next subsection.

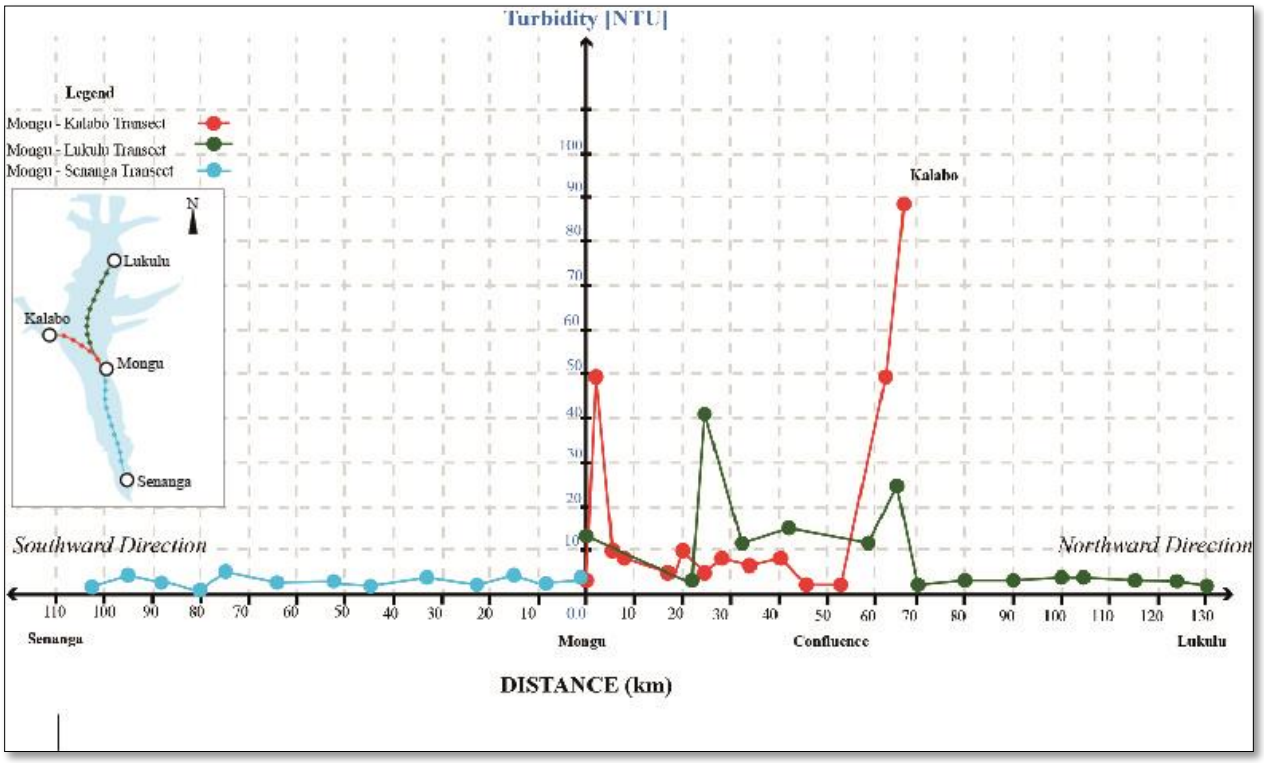

Figure 4.6: Turbidity on the Luanginga River (Mongu–Kalabo Transect - red line), main Zambezi River (Mongu-Lukulu Transect – green line) compared to main Zambezi River along the Mongu-Senanga Transect – blue line

iii) *Electrical Conductivity* – Samples were collected on four different transects. These were Mongu – Kalabo, Sioma – Kalabo, Mongu – Senanga and Mongu - Lukulu labelled as a, b, c and d respectively in Figure 4.7.

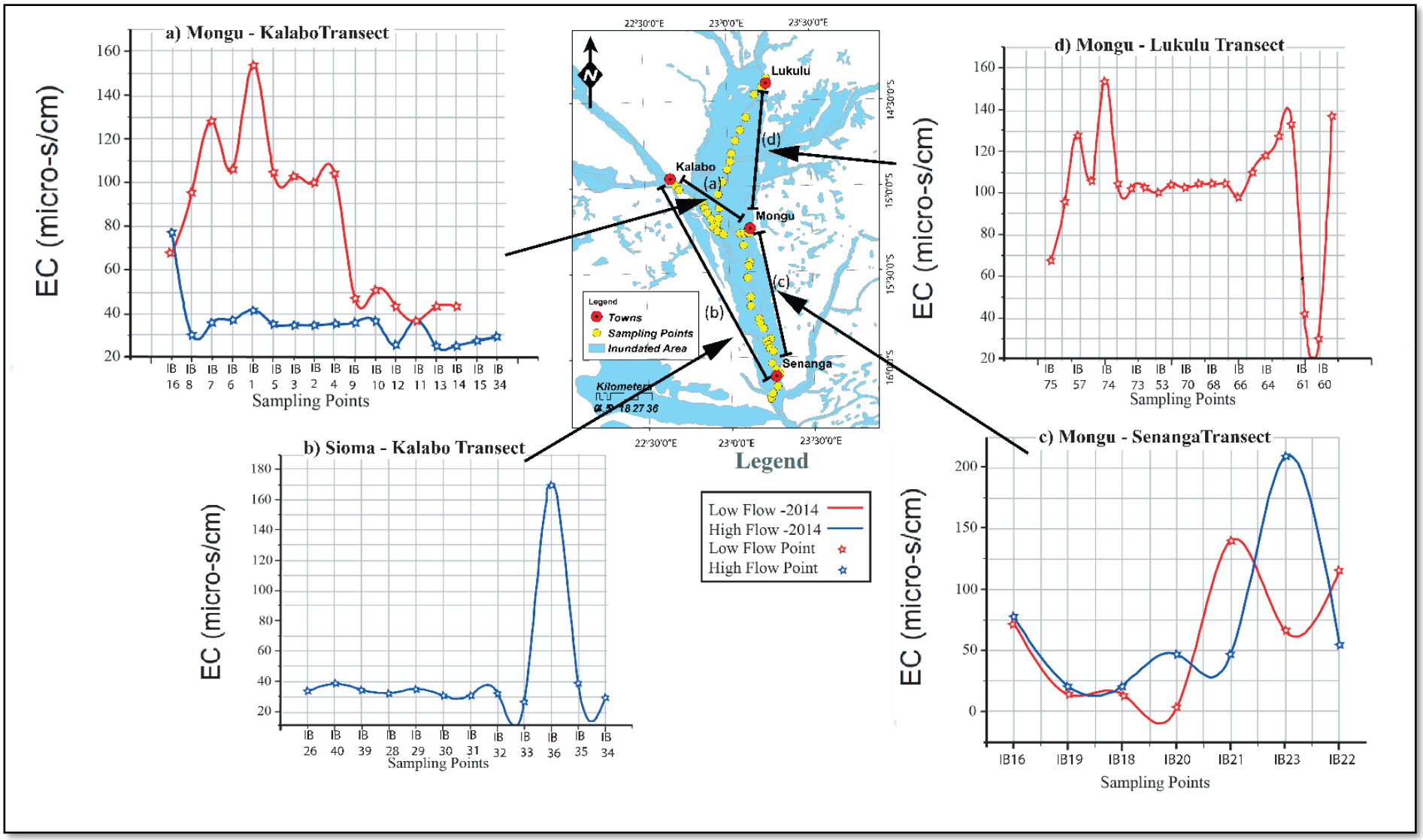

Figure 4.7: Variations of electrical conductivity along the 4 different transects labeled as **a**, **b**, **c** and **d**, Barotse Floodplain, Western Zambia

The Kalabo – Mongu Transect had seventeen samples collected for both wet and dry seasons labelled as high flow and low flow in Figure 4.7 above. It was noted that all points except IB17 (Chauteni River in Limulunga) for the high flow were lower than those of the low flow period.

Since EC is related to the total dissolved solids (TDS), a comparison was done on the Mongu - Lukulu Transect to verify this by plotting the two parameters using a double-Y graph (Figure 4.8).

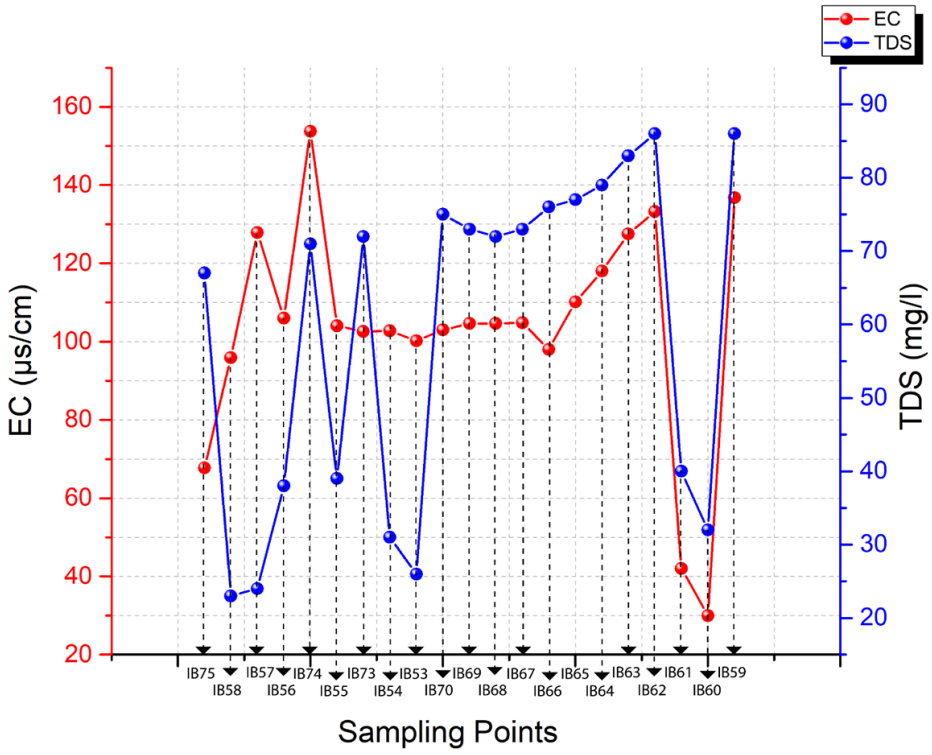

Figure 4.8: Relationship of EC and TDS on the Mongu - Lukulu Transect, Barotse Floodplain, Western Zambia

In Figure 4.8 above, it was observed that EC was rising and falling in a similar way as TDS except for 6 out of 21 sampling points. These points were IB53, IB54, IB55, IB57 and IB58 (unnamed areas) as can be observed on the left-hand side of Figure 4.8.

The Sioma – Kalabo Transect had twelve samples all collected during the wet season of 2014. EC in this season ranged between 30 to 40 µs/cm except for one outlier at borehole at Lukona Basic School (IB36) of value 169.8 µs/cm.

On the Mongu – Senanga Transect, seven samples were collected. These were for both the low – flow and high – flow period. Unlike the Mongu – Kalabo Transect, Mongu – Senanga Transect had high EC levels ranging from 0 to 210 µs/cm for both seasons. However, the wet season showed slightly higher EC values up to 210 µs/cm than the dry season's maximum of 140 µs/cm. This transect was characterized by several anthropogenic activities which included farming, saw-milling and sewerage discharges into the Zambezi River.

The last transect was Mongu – Lukulu, which had 21 samples collected during the dry season. Since there were no samples collected in the wet season, no comparison has been made. EC was high with a maximum value of 154 µs/cm recorded on this transect except for only two points, IB60 (10 µs/cm) and IB61 (41 µs/cm).

iv) *Dissolved Oxygen (DO) and Temperature* - Temperature and DO at all the sampling stations in the Barotse Floodplain were collected, coalescence, plotted and analyzed on a linear graph (Figure 4.9). Notice that the key sampling points discussed have dotted green lines emerging both from the y and x – axis. It is observed that the DO was lowest (1.24 mg/l) at Sinungu Basic School (IB31) indicated by a green line pointing on a blue DO line. On the other hand, DO is highest (7.62 mg/l) at Sesheke-Senanga Bridge (IB25). The temperature did not vary much from Matongo Platform (IB1) to somewhere near Senanga (IB21), Figure 4.9. It is after this point in a southward direction that fluctuations in the temperature are observed.

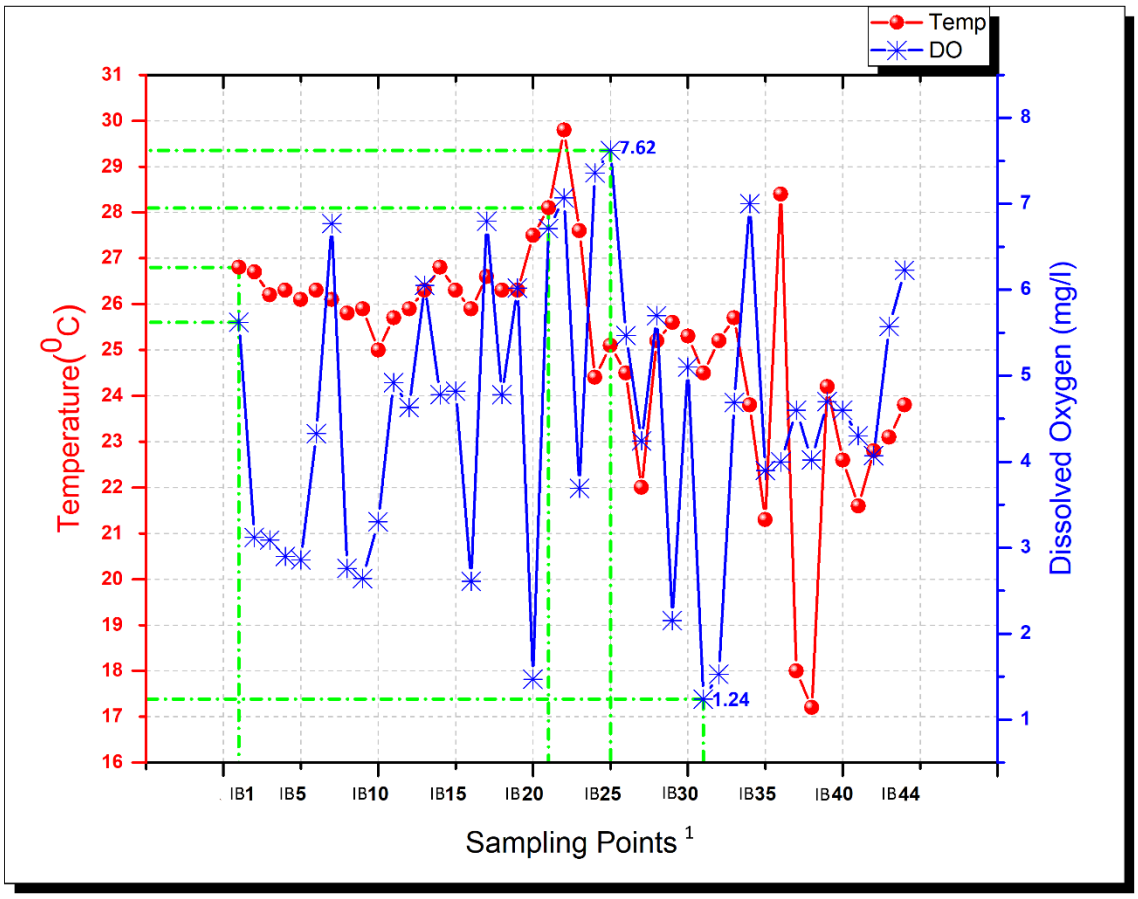

Figure 4.9: Dissolved oxygen and temperature variation in 2014 at different sampling points on the Barotse Floodplain, Western Zambia

v) *Sediment Analysis in Terms of Solids in Water* – A further analysis was done on the water quality samples collected from the field campaigns of 2014 and 2015. This analysis was on the Total Solids (TS), which are a sum of Total Suspended Solids (TSS) and Total Dissolved Solids (TDS) along the flood waters of the Barotse Floodplain and rivers flowing into the floodplain (Figure 4.20). The samples were collected from Mongu via the Little Zambezi River into the Main Zambezi River and eventually the Luanginga River. The last sample was collected at Kalabo Habour. Results show that the Mongu-Kalabo Transect had more TS being transported during the wet season (April 2014) than the dry season (September 2014). Only between 20km-27km and beyond 60km were the TSs values of the wet season lower than those of the dry season (Figure 4.10).

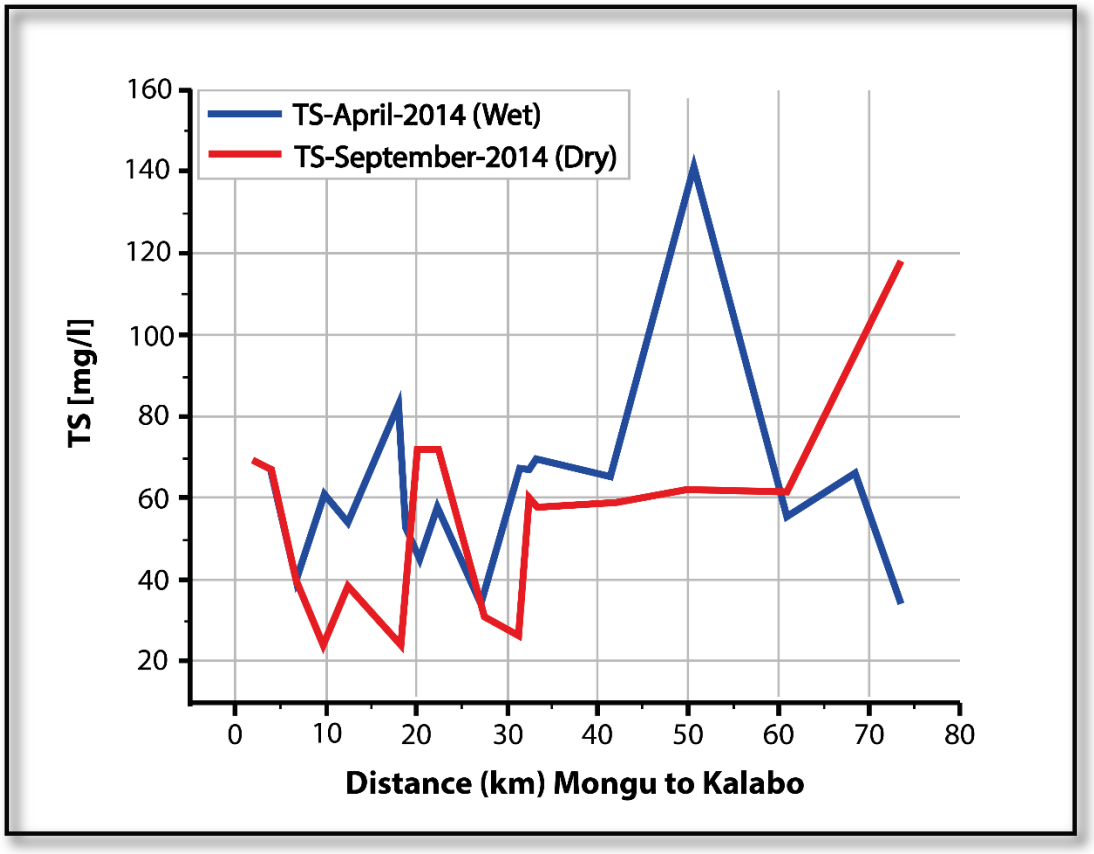

Figure 4.10: TS comparison between Mongu and Kalabo route for both the wet and dry seasons of 2014. These samples were collected along the Zambezi River into the Luanginga River all the way to Kalabo. The concentration of TS during the wet season was generally higher than that of the dry season, Barotse Floodplain, Western Zambia

From Figure 4.10, peak values for the wet and dry seasons were 140mg/l and 120mg/l respectively. These were from two different locations. It was also observed that TS for the dry season were higher than those of the wet as we approached Kalabo.

On the Mongu –Senanga Transect, it was observed that the TS transported during the dry season (October 2015) were more than those transported during the wet season (June 2015) contrary to the Mongu-Kalabo Transect (Figure 4.11).

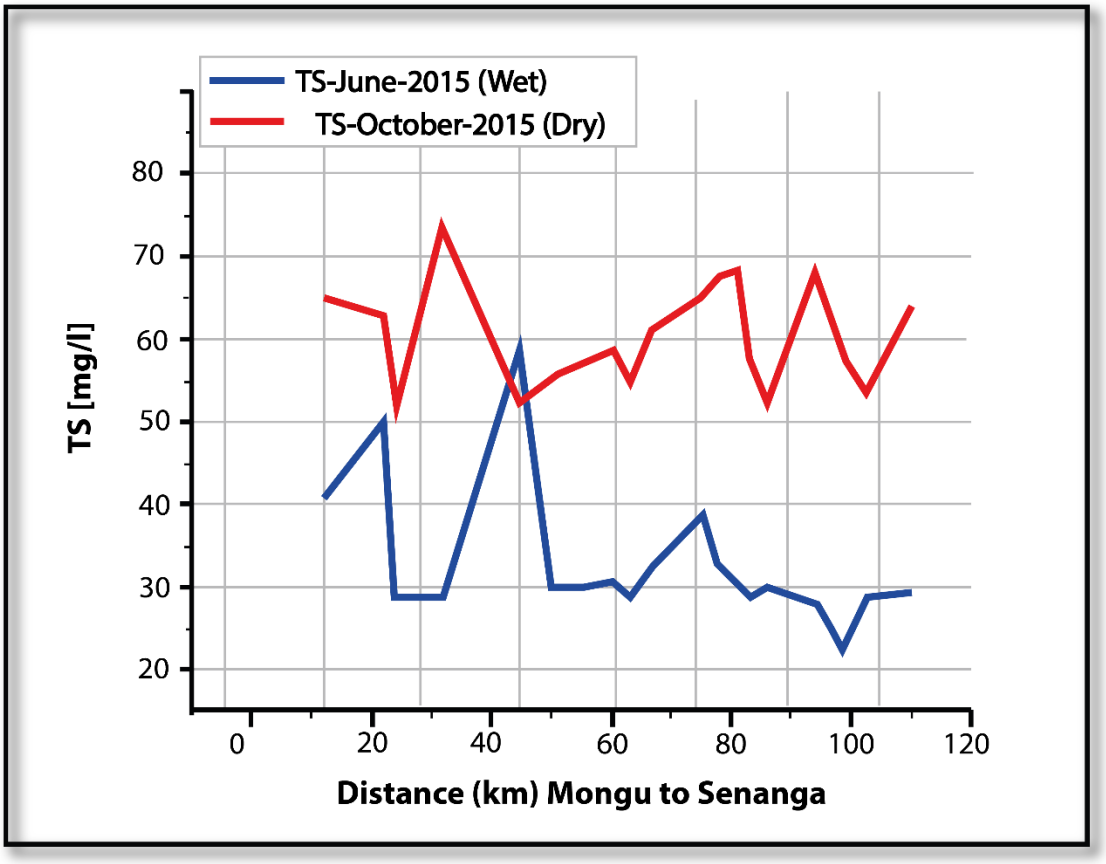

Figure 4.11: TS comparison between Mongu and Senanga route for both the wet and dry seasons of 2015. These samples were collected along the Zambezi River all the way to Senanga with TS concentration of the dry season being greater than that of the wet season (TS_{dry}), Barotse Floodplain, Western Zambia

TS values for the wet and dry seasons ranged from 27mg/l to 60mg/l and 54mg/l to 74mg/l, respectively.

vi) *Variability of Agricultural Nutrients in Water* - Among the agricultural nutrients, nitrate was found to be relatively higher, particularly in the 2014 wet season which experienced higher floods than the 2015 wet season (Figure 4.12).

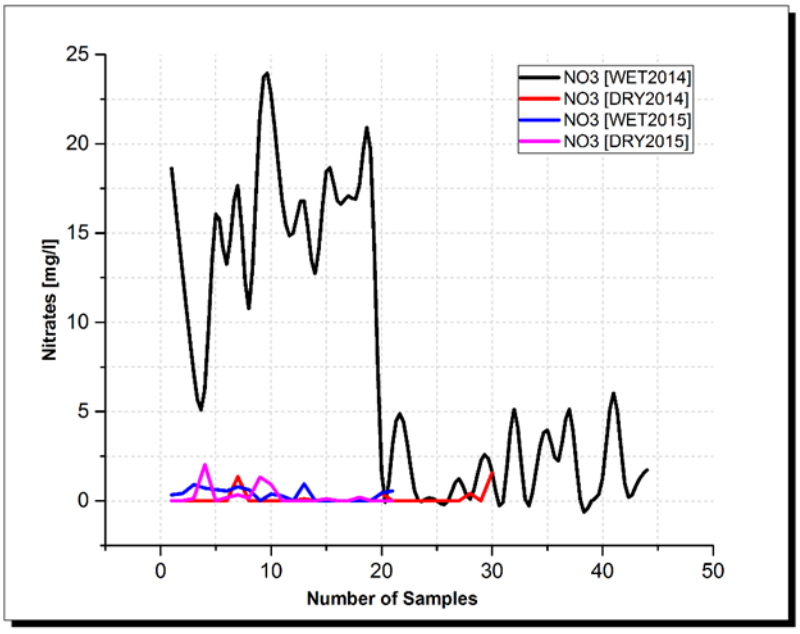

Figure 4.12: A general comparison of nitrate trends dissolved in water collected during the wet and dry seasons of 2014, Barotse Floodplain, Western Zambia

Others such as total phosphates (< 0.01mg/l) and nitrites (< 0.001mg/l) were not detected in the samples analysed.

4.1.4 Discussion of Physiochemical Parameters

i) *Hydrogen Ion Concentration (pH)* - Although pH usually has no direct impact on consumers, it is one of the most important operational water quality parameters (WHO, 2003). Acidic pH readings were associated with settlement areas, such as sewerage discharge points in Senanga and runoff from agricultural areas IB19 (Sefula). The latter is seen in a study on the Ismailia Canal in Egypt by Stahl and Ramadan (2008), showing how pH can be affected by agricultural runoff. In this study, some of the lowest pH values were recorded at Matongo Platform (IB1, pH = 4.3), Sefula agricultural area (IB19, pH = 6.2) and Senanga High School Sewerage discharge (IB23, pH = 6.8). Wamulume et al, (2011) and Nyoni (2014) further explain that the lowering of pH is due to respiration of organic matter (e.g saw milling in Senanga, IB23) as well as in several settlement areas such as Ndoka Bridge (IB35), Nakatwelenge Primary School (IB 28) and Libonda Area (IB71). The high rates of respiration were accompanied by the decomposition of waste material from dish washing and bathing on riverbanks. Further, calcium carbonate ($CaCO_3$) and

other bicarbonates can combine with both hydrogen or hydroxyl ions to reduce the pH in water (geogenic interactions) (Nyoni, 2014). Calcium carbonates from results of this study were present both in the soils and water samples.

Following the WHO (2003) guidelines for drinking water which ranges between 6.5 and 8.5, it is generally concluded that the water is safe for human and animal consumption. Only a few cases were observed with pH values falling outside of the WHO (2003) guideline range (6.5 – 8.5) for drinking water are given in Figure 4.3 above. Lastly, according to the Ramsar Treaty of 1971 mentioned in Chapter 2, pH values for wetlands are expected to be in the range of 7.0-9.0. However, only the wet season results for the Barotse Floodplain conform to this requirement;

ii) *Turbidity* – Among the three transects mentioned, Mongu -Kalabo was observed to have had the highest turbidity results. The causes for such high levels of turbidity can be compared to Ndungu et al, (2014). In that study, the causes were excess sediment input from eroded catchment soils, eutrophication, increased algal biomass and re-suspension from the benthic layer as a result of the water movement. From Ndungu et al, (2014), the most probable cause of turbidity in the Barotse Floodplain case was the erosion of catchment soils due to loss of land cover from deforestation and cutting of reeds for fencing and construction purposes. Furthermore, the soils were sandy and loose, hence easily detached and carried by water. According to Nyoni (2014), with such high levels of turbidity, the amount of light available for photosynthetic reactions is reduced. This may eventually lead to a loss of habitat for small fish and invertebrates including the much-needed dissolved oxygen (DO). In Figure 4.6, we observe the changes in turbidity before and after the confluence of the Zambezi and Luanginga Rivers. This was attributed to the large amount of sediments from various tributaries upstream of the Luanginga and the river itself. However, within the main floodplain, vegetation acted as a sediment trap leading to deposition on the river banks and within the floodplain. This resulted in less turbidity along the Mongu - Senanga Transect;

iii) *Electrical Conductivity and Total Solids* – Samples were collected from four different transects as earlier indicated in Figure 4.7. High EC values occurred during the dry

season especially on settlements along river stretches and increased temperatures during the dry season leading to high rates of evaporation and hence concentrating the salts in the remaining water. Nyoni (2014) indicates that higher EC values are an indication of higher ionic activities. This is true for this study as Figures 4.13 to 4.16 in the next subsection show this. Obarrio's (2005) results for studies done on the Lake Cuitzeo, a wetland in Mexico, indicated high salt values leading to high EC readings. In this study, high EC values were observed (Figure 4.7 above) and the relationship between EC and TDS was validated in Figure 4.8. EC was observed to be proportional to TDS in that the conductance of water was higher in water with a higher dissolved salt content (TDS). On the other hand, distilled water with no dissolved salts (TDS = 0) had no effect on EC. In summary, EC values were directly related to the TDS values. Higher values of EC were mostly in the dry season due to evaporation. Lastly, Figures 4.10 and 4.11 show the seasonal variation in TS between wet and dry seasons. Mongu – Kalabo Transect (Figure 4.10) recorded higher TS in the wet season than in the dry season. This could be explained by the loss of land cover in the nearby areas and the larger catchment itself. Due to insufficient canopy cover during the wet season, the rainfall runoff is characterized by a brown color (turbidity) and a number of dissolved chemicals. Meinhardt *et al*, (2018) point out how the topographical changes and land use changes from the Angolan Bie' Plateau to the Luanginga sub-basin have also exacerbated the rates of erosion, hence leading to high level of turbidity and TS in the water. Conversely, the Mongu - Senanga Transect (Figure 4.11) showed higher TS in the dry season, unlike the Mongu – Kalabo Transect. This could be attributed to the timing of the wet season trip. By June, the surface runoff would have ceased considering the type of soil (sandy soils have high infiltration) in the floodplain;

iv) *Dissolved Oxygen and Temperature* – According to Yingyi *et al* (2016), the temperature and DO are related, in that lower temperature favour DO more than higher temperatures. The results in this study showed that DO was very low in several places (Figure 4.9 above). This might have been due to high levels of salts in water, excess algae and a large mass of decomposing biotic materials (Nyoni, 2014). Examples of places with two contrasting DO results where Sinungu Basic School (IB31 at 1.24mg/l) and Sesheke Bridge (IB25 at 7.62mg/l). This variation was due to the difference in the levels of human induced

activities at the two dissimilar sites. The depletion in DO at Sinungu Basic School (IB31) is attributed to the oxygen being used in the reaction with the cow dung as cattle manure is used in the gardens nearby. On the other hand, DO is highest (7.62 mg/l) at Sesheke-Senanga Bridge (IB25) because of the absence of anthropogenic materials which depletes DO;

v) *Sediment Analysis in Terms of Solids in Water* – This can possibly be attributed to the numerous activities along the banks of the river, as many settlements are located on the banks as we approached Kalabo and that the water levels at this time were low. High TS could be attributed to several agricultural activities on the river banks and possibly cattle rearing in the transect. Ndungu *et al* (2014) also alludes to the fact that agricultural practices that are close to the riverbank have a way of increasing TS especially cattle. The results in Figures 4.10 and 4.11 were later compared with the WHO (2003) standards for TS in water for drinking (1000mg/l). From the results, it was observed that both for 2014 and 2015 field campaigns had TS value below 100mg/l which is far below the WHO (2003) guidelines for drinking water (1000mg/l);

vi) *Variability of Agricultural Nutrients in Water* - From the results in Figure 4.12 above, nitrates were considered to be the highest main nutrient supporting the growth of agricultural crops such as maize and vegetables grown in the Barotse Floodplain. Figure 4.12 also suggests that nitrate and nutrients are significantly mobilised and replenished during higher flood seasons. Scientists have clearly shown in recent decades how urban and agricultural development in catchments increases nutrient runoff, for a number of reasons (Tanner *et al*.,2007 and Meinhardt *et al.,* 2018). Catchment development increases water flows, erosion, and sedimentation and intense eutrophication. The source of nitrates in this study was suspected to be agriculture-related activities around the floodplain. For instance, the local people (mainly Lozi) keep a lot of cattle within the floodplain during the dry season and also practice a complex flood agriculture system. The animals are moved to the highlands and margins of the floodplain during the wet season. It was noted that the year 2014 experienced higher flood levels than 2015. The observed higher concentration of nitrates shown in Figure 4.12 above was therefore attributed to increased mobilisation and recruitment of this element from anthropogenic sources during the higher

floods of 2014, whereas in 2015 the source was restricted to small areas around the floodplain. According to Tanner *et al*. (2007), nutrient mobilisation in wetlands come from a variety of sources including streams, creeks and drains, groundwater from the surrounding catchment, from the air in rainfall and spray drift. Once in a wetland, nutrients tend to stay there and accumulate, initially in the soil, then in the plants, and then in the surface water. This accumulation of nutrients (eutrophication) in wetlands is what leads to prolific vegetation growth hence blocking water-ways and increasing sediment build-up as is the case for this study (Sorrell *et al*., 2004).

4.2 Distribution of Elements for the Wet and Dry Seasons

Earlier on, water quality was defined as the measure of the state or condition of water resources relative to the requirements of the biotic species and human needs (Johnson *et al*., 1997) or as the physical, chemical, biological and organoleptic (taste-related) characteristic of water (United Nations, 2007 and Ndungu *et al*., 2014). In this subsection, the latter definition is used. This specifically looks at the results of the physical and chemical parameters of the Barotse Floodplain for the 2014 and 2015 field campaigns.

From the water samples collected in the 2014 wet season, three elements had the highest concentrations. These were calcium (Ca) (65mg/l), magnesium (Mg) (48mg/l) and chlorine (Cl) (30mg/l). The lowest concentration levels were reported for iron (Fe) (2.5mg/l) and manganese (Mn) (0mg/l), indicating that these elements are the least absorbed in water. Apart from the three most concentrated elements, the rest had concentration values ranging between 0-15mg/l.

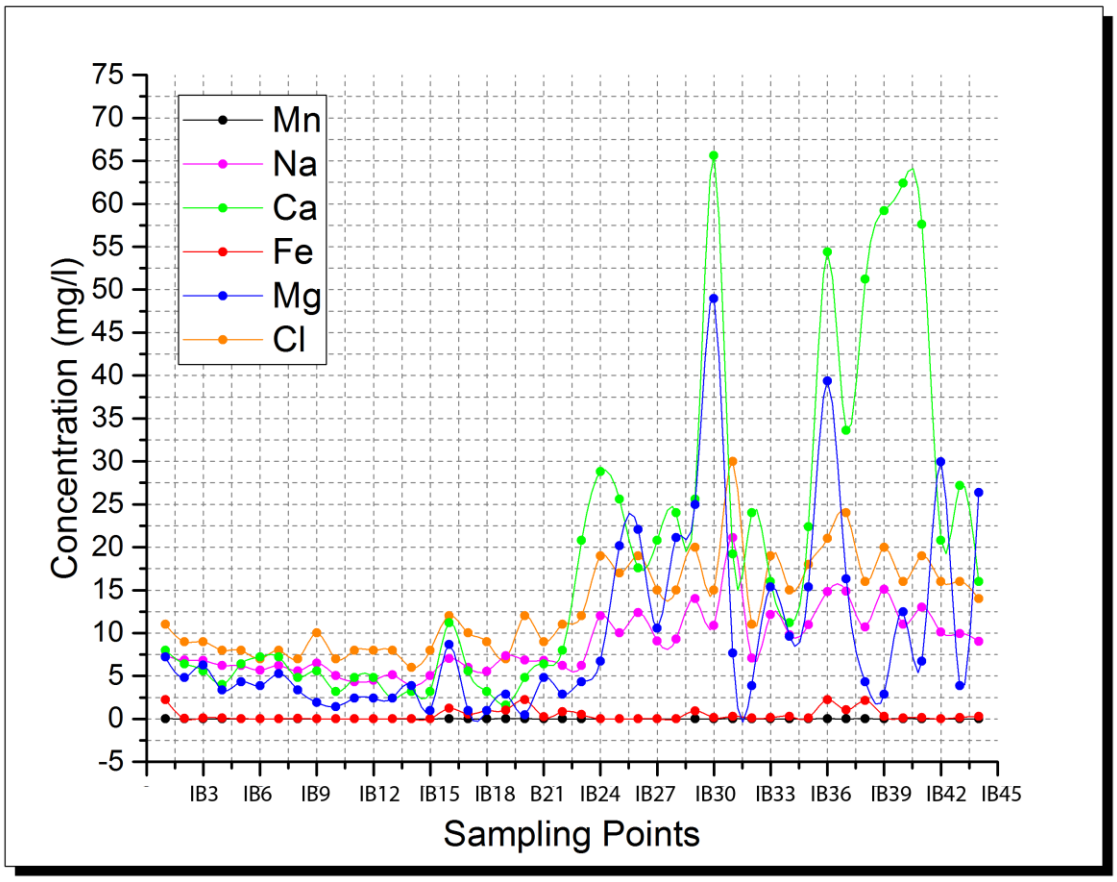

Figure 4.13: Element variation during 2014 high flow period (wet season) in the Barotse Floodplain, Western Zambia

The concentration of Ca, Cl and Mg increased after Musama in Senanga District (IB21), Figure 4.13. It was observed that values ranged from 0 to 15mg/l before Musama (IB21) and Litoya (IB20) to 65mg/l after this point. Sodium (Na) also increased from 5.5mg/l to 23mg/l, however, not to a comparable extent of the other three elements mentioned earlier.

Weathering of minerals is a significant natural source for Ca and Mg for freshwaters. For example, Ca containing minerals like calcium carbonate (CaCO3), which combines with carbonic acid (H2CO3) from atmospheric and soil respiration sources, can be found in significant proportions in soils and rocks in the catchments of water bodies. Furthermore, chloride found in places where it does not naturally occur may be the result of water pollution. Some sources could have come from runoff of rock salt (NaCl). Other sources could come from potash fertilizer, animal waste, water softener regeneration, and effluent from septic tanks (KCl) (Weyhenmeyer et al, 2019).

The same analysis was done for the wet season. The differences noticed were in the distribution patterns. Generally, dry season concentrations ranged between 0 and 25mg/l (Figure 4.14). The highest peak recorded during this period was about 39mg/l for Cl at a canal in Mongu (IB3), Figure 4.14). This was less than the highest concentration peak value for the wet season (Figure 4.13). Calcium (27mg/l), chlorine (39mg/l) and this time sodium (25.5mg/l) had the highest concentration recordings. Figures 4.13 and 4.14 confirm that more elements and sediments are transported during the wet season. Iron was at 3mg/l while manganese was not present in any of the analysed samples.

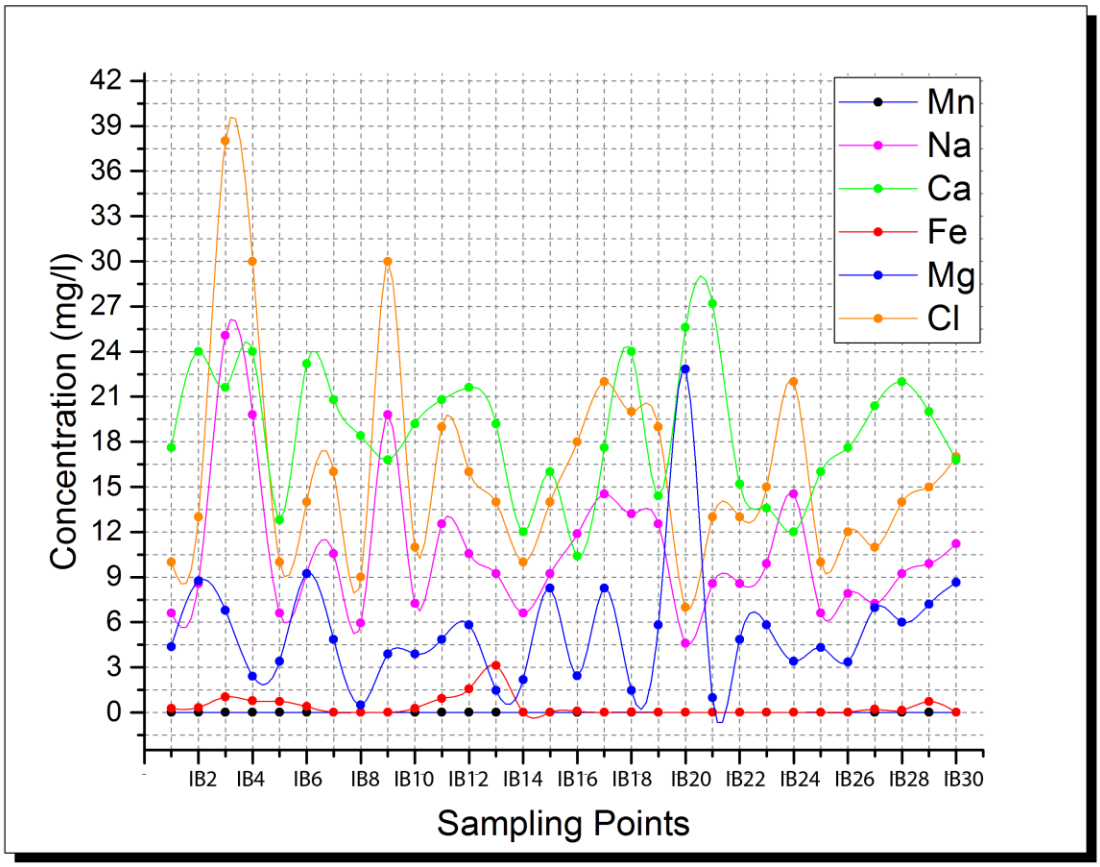

Figure 4.14: Element variation during low flow (dry season) 2014, Barotse Floodplain, Western Zambia

The linear graph for 2015 wet season illustrates Ca (17.8mg/l) as the predominant element (Figure 4.15). This was followed by Mn (6.5mg/l), which was the lowest in 2014. In the wet season 2015, Ca (17.8mg/l) again was the main element in the water. However, the concentration for 2015 wet season was much lower than that of 2014 wet season probably as evidence to show

that the 2015 floods (wet season) were lower than that of 2014. Fe as was the case for 2014 field campaigns was on the lower part of the linear graphs followed by Cl.

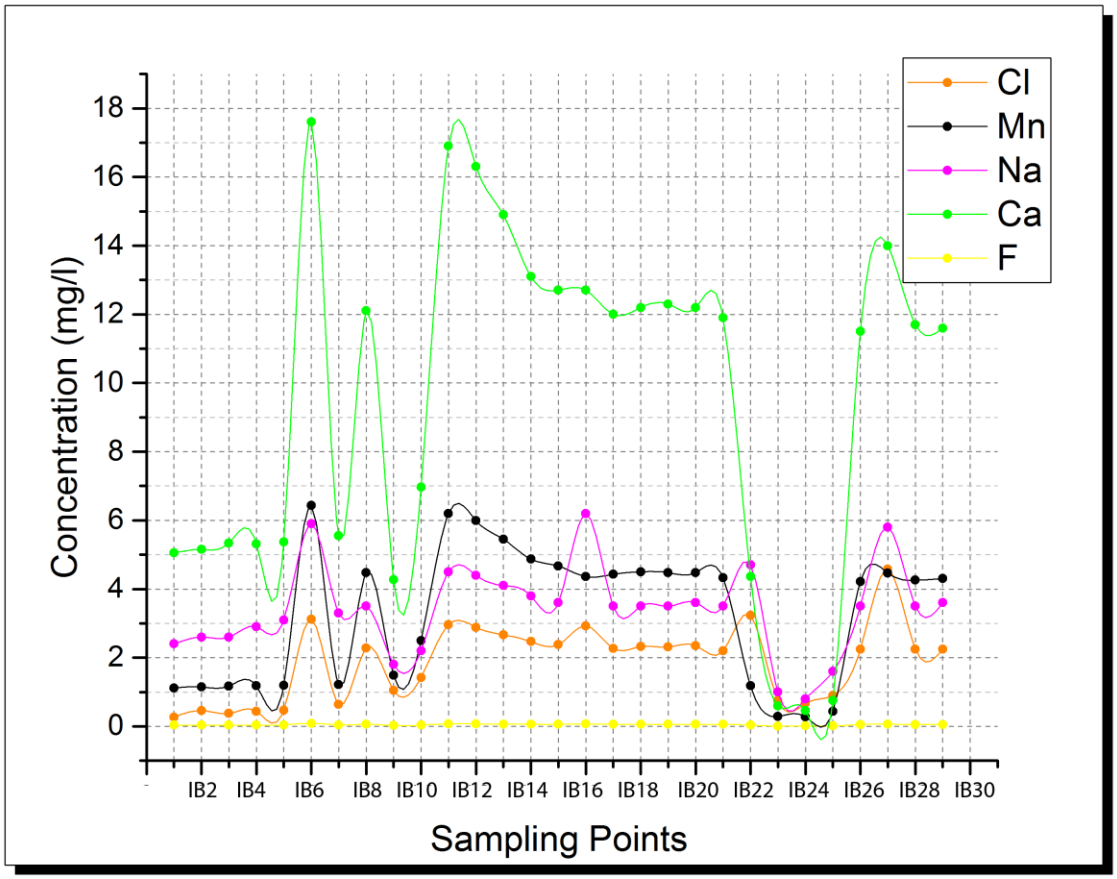

Figure 4.15: Element variation during 2015 wet season, Barotse Floodplain, Western Zambia

The fourth and last analysis for the element distribution was done on the samples collected during the 2015 dry season. The concentration of the elements was higher than that of the wet season because during the wet season there was more water and therefore, there was a dilution effect. Ca (24mg/l) was again the most concentrated element as given in Figure 4.13. In contrast, Fe again was undetectable from all the samples. The instrument used was not able detect anything less than 0.01mg/l.

In summary based on Figures 4.13 to 4.16, the order of abundance in terms of element concentration in the Barotse Floodplain was Ca, Cl and Mg (noticeable higher curves on graphs). Mn was on the lower end for all the seasons except for the 2015 wet seasons as given in Figure 4.15 above.

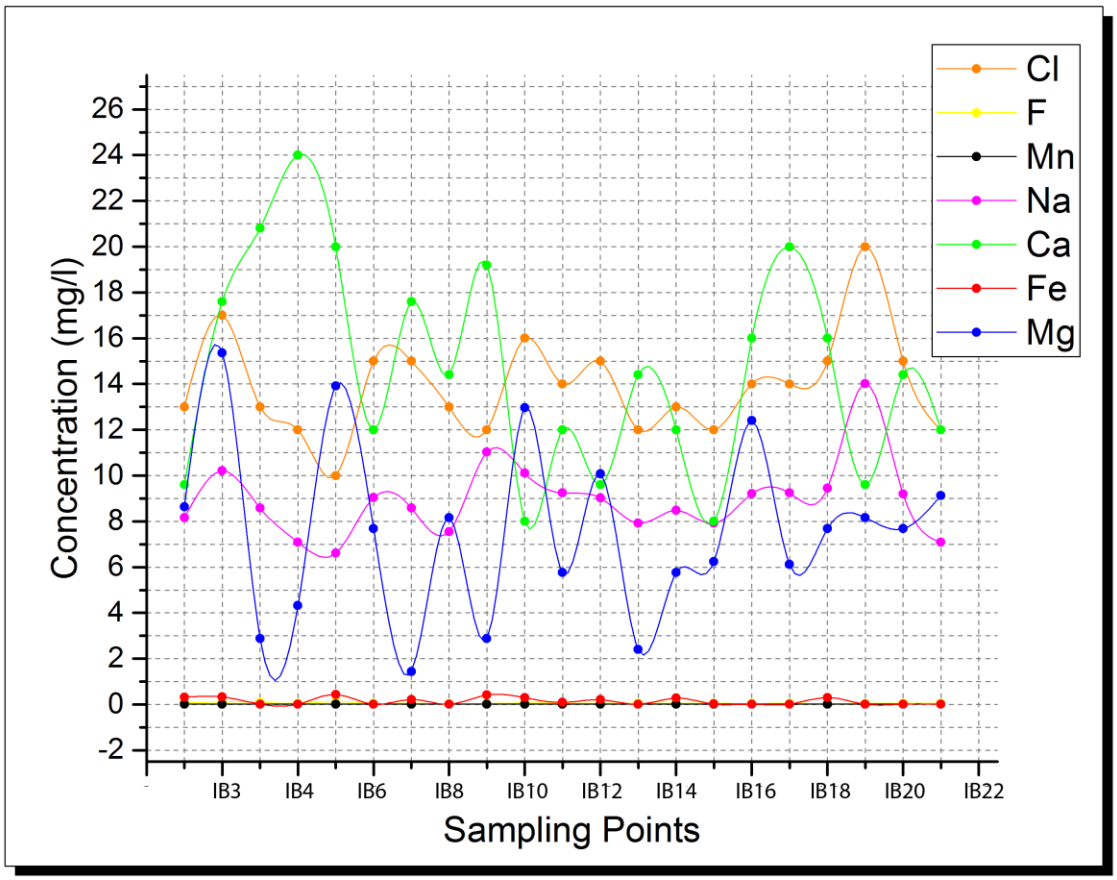

Figure 4.16: Element variation during 2015 dry season, Barotse Floodplain, Western Zambia

4.2.1 A Focus on Calcium

Seasonal trend analysis of these elements was carried out to understand their variability. In this study, however, we present such an analysis using calcium, which was frequently the most abundant element in samples analysed for both wet and dry seasons (Figure 4.17). Calcium's presence was detected both in water and stream sediments samples.

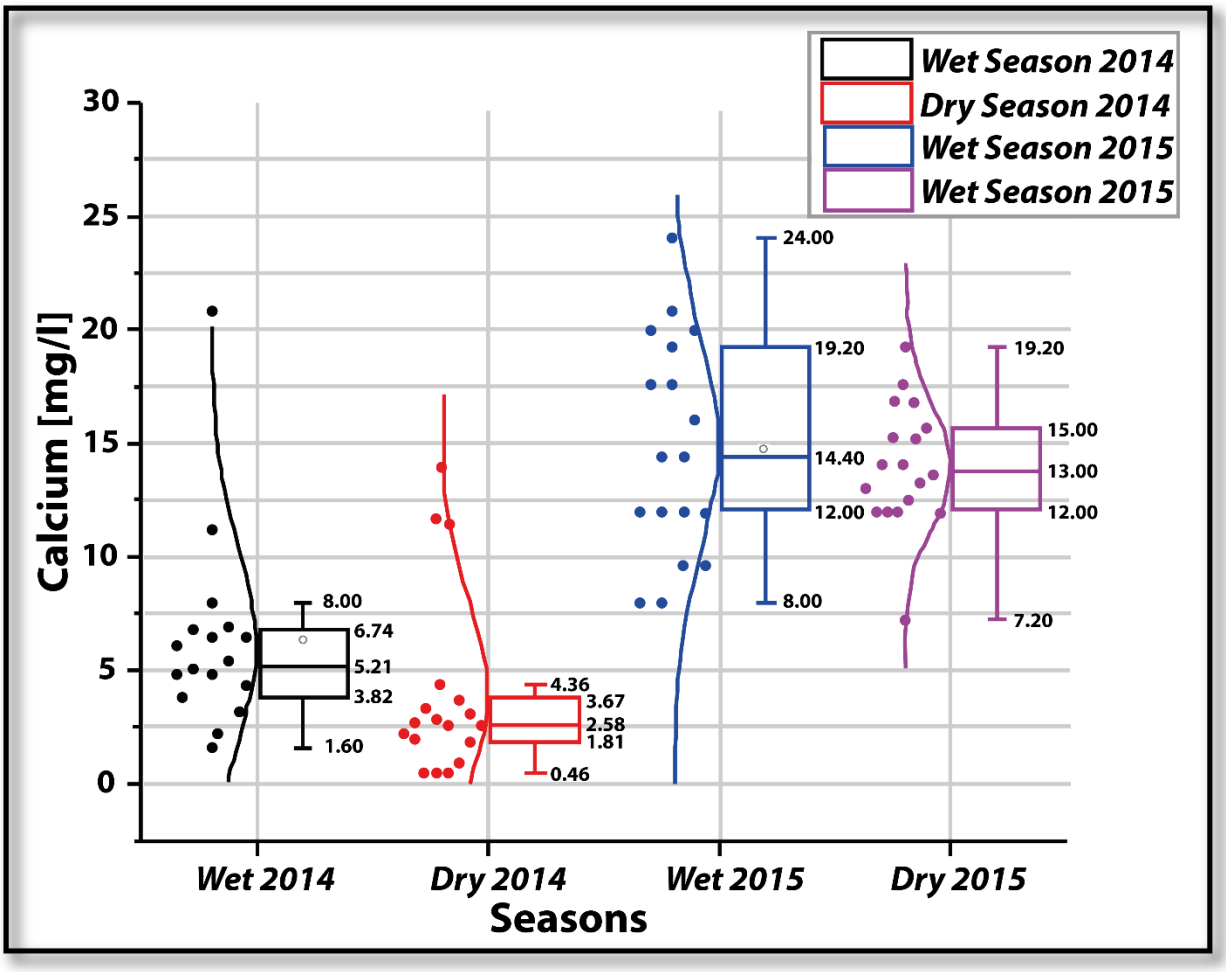

Figure 4.17: Boxplot distribution of calcium concentrations along the Zambezi River, Mongu to Senanga (Southern direction) transects for both wet and dry seasons of 2014 and 2015

The trends in calcium concentration on the Mongu - Senanga Transect indicated that the medians were Q_{2wet} = 5.2 mg/l and Q_{2dry} = 2.6 mg/l for the wet and dry seasons of 2014, respectively, and Q_{2wet} = 14.4 mg/l and Q_{2dry} = 13.0 mg/l for the wet and dry seasons of 2015, respectively. This transect indicated a positive skewness for both seasons, that is, $Q_3 - Q_2 > Q_2 - Q_1$, or mode < median < mean (Figure 4.17 above), where Q stands for quartiles, that is, upper (Q_3), median (Q_2), and lower quartiles (Q_1). It was observed that there was a considerable increase in calcium concentration from the 2014 wet season to the 2015 wet season. Similar trends were observed from the 2014 dry season to the 2015 dry season. However, there was a general decrease in calcium concentration for seasonal changes within the years (Table 4-1).

Table 4-1: Comparison of percentage changes of calcium concentration on the Mongu-Senanga Transect based on 2014 and 2015 yearly changes (Δ) as well as within the year seasonal changes (Δ). The changes (Δ) are in percentages showing an increase or a decrease by a percentage

Mongu-Senanga Transact				
2014 Wet Season		***2015 Wet Season***		***Yearly %*** Δ
Q_3	6.7358	Q_3	19.2	+185.0%
Q_2	5.20544	Q_2	14.4	+176.6%
Q_1	3.81584	Q_1	12	+214.5%
2014 Dry Season		***2015 Dry Season***		
Q_3	3.67434	Q_3	15	+308.2%
Q_2	2.5768	Q_2	13	+404.5%
Q_1	1.814	Q_1	12	+561.5%
Seasonal %Δ 2014	-45.5%	**Seasonal %Δ 2015**	-21.9%	
	-50.5%		-9.7%	
	-52.5%		0.0%	

Table 4-1 above shows that calcium concentration was increasing from 2014 to 2015 wet seasons (reading quartile values from left to right hand side). The yearly percentage increase is given in the last column (***Yearly %*** Δ) with a positive sign showing increase. The same analysis was done for the 2014 to 2015 dry seasons. This time, it is observed that the yearly percentage increase (***Yearly %*** Δ) was higher than that of the wet season. Table 4 -1 also shows that the concentration of calcium was decreasing down the table (from top to bottom) for the same year. Twenty-fourteen (2014) wet to dry seasons show a negative seasonal percentage change (**Seasonal %Δ 2014)** and so does 2015 seasons. However, Mongu to Kalabo Transect was different. The median concentration of calcium for 2014 field campaign were Q_{2wet} = 5.600mg/l and Q_{2dry} = 20.800mg/l for wet and dry seasons respectively. This transect indicated negative skewness, that is, $Q_3 - Q_2 < Q_2 - Q_1$ (Figure 4.18).

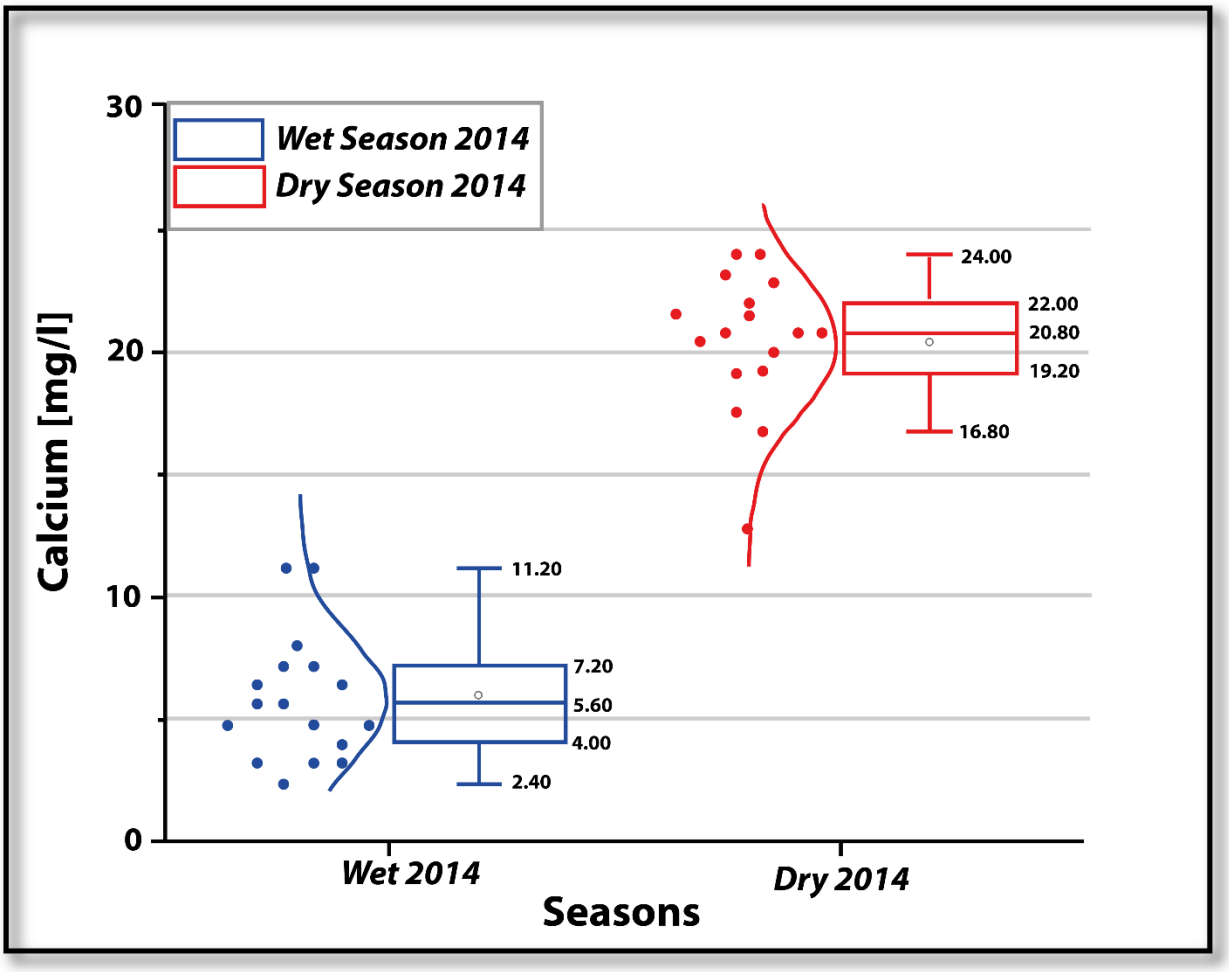

Figure 4.18: Boxplot distribution of calcium concentration along the Luanginga River, Mongu to Kalabo Transect for 2014 wet and dry seasons, Barotse Floodplain, Western Zambia

Trends here show that there is a dramatic increase in calcium concentration from 2014 wet season to 2014 dry season. However, in 2015 samples were not collected to have a yearly comparison of the Mongu – Kalabo Transect (Table 4-2).

Table 4-2: Comparison of percentage changes of calcium concentration on the Mongu-Kalabo transact based on 2014 seasonal changes (Δ), that is, wet and dry season. The changes (Δ) are in percentages showing an increase by a positive (+) designation.

Mongu-Kalabo Transact				
2014 Wet Season		*2014 Dry Season*		*Seasonal %Δ*
Q_3	7.2	Q_3	22	+205.6%
Q_2	5.6	Q_2	20.8	+271.4%
Q_1	4	Q_1	19.2	+380.0%

From Table 4-2 above, calcium concentration was increasing (quartile values from left to right hand side). The percentage increases were +205.6%, +271.4% and +380.0% for the upper, median and lower quartiles respectively. This behaviour in the system was opposite to that observed on the Mongu – Senanga Transect.

4.2.2 Heavy Metals

On the environmental impact of upstream large-scale copper mining, particularly in the Kabombo River Basin of north-western Zambia – a tributary of the Zambezi River upstream of the Barotse Floodplain, it was found that concentration of heavy metals (i.e. copper, lead, cadmium, mercury, arsenic, zinc and chromium) was negligible (< 0.002mg/l) and within the World Health Organisation (WHO) and Zambia Bureau of Standards (ZABS) standards for portable water in both the water and stream sediment samples. This indicated that water quality within the floodplain is still in its natural state in relation to mining contaminants.

4.2.3 Interpretation and Discussion on the Distribution of Elements

The observed seasonal changes in calcium concentration were attributed to complex factors such as variations in the flow regimes between the wet and the dry seasons, and plant uptake of calcium. For instance, calcium is brought into the floodplain system through overland flows and is used up by plants in the formation of new tissues such as roots and shoots. El Habbasha & Ibrahim, (2016) give more insight stating that, "calcium, up taken as Ca^{2+}, is an essential element for the growth of the plants and fruit development, and it is important in the resistance of diseases on plants due to its ability to uphold a physical barrier against pathogens. Calcium plays important biochemical functions and supports many metabolic processes, in addition to activating several enzymatic systems, thus contributing to the proper development of plants". Furthermore, the seasonal variation of calcium was also attributed to changes in the physical parameters of the water, particularly pH. According to Dyrness &Van Cleve (1993), lower pH favours the dissolution of calcium and hence validating Figure 4.3 and 4.4. It was noted that the pH was mostly lower than 6.9 along the Mongu - Senanga transect (Figure 4.3 above) during the low flows (i.e., dry season) of 2015, which coincided with a period when the concentration of calcium was high (~15mg/l).

From a general perspective, sodium and chloride, which lead to salty water, were found to be high in isolated ponds. These form salt pans as a result of the high rates of evaporation during the dry season. An example of such a feature is the Sisima salt pan, located on the Matebele Plain. One of the water quality samples [Sisima Salt Pond (IB 37)] was taken from this location and contained

some of the highest amounts of sodium and chloride. These elements were also found to be high in places where intensive anthropogenic activities such as gardening were taking place [e.g., Sinungu Basic School (IB 31)]. High concentrations of magnesium were associated with the presence of organic materials and animal waste at some sampling locations [e.g., Libuba Stream at Nambwae Basic School (IB 30)]. It was also suspected, however, that geogenic factors could be influencing high concentrations of magnesium. For instance, a high concentration of magnesium was found in one of the samples [Lukona Basic School (IB 36)], which was taken from a borehole. All these activities ranging from schools, salt pans and boreholes support Nyairo, Owuor & Kengara, (2015) results who concluded that anthropogenic activities were impacting the quality of water in the two tributaries studied he studied in East Africa.

As for the heavy metals, it was found that the concentrations of heavy metals (i.e., copper, lead, cadmium, mercury, arsenic, zinc, and chromium) were mostly below detection limits (< 0.002 mg/l) and fell within the World Health Organization (WHO) and Zambia Bureau of Standards (ZABS) guidelines for drinking water which is shown in studies by Zuijdgeest *et al*., (2015) and Nyambe et al., (2018). The both clearly conclude that the Barotse Floodplain is still pristine.

4.3 Soils

Samples from alluvial soils were also analysed by AAS and XRF as soils act as sinks for precipitation elements in the water. Figures 4.19 and 4.20a illustrates the spatial locations and associated line graph for the samples collected in the floodplain. Thirteen samples were collected from AB1 to AB13. The names of these places were Lukulu River Confluence with the Zambezi River (A1), Lukulu Habour (AB2), Mangongole Area (AB3), Sibanda Area (AB4), Yuka Mission Gauge Station (AB5), Kakuli Wamalilo Area (AB6), Liloyele near crossing of Zambezi River and Mongu – Kalabo Bridge (AB7), cassava gardens within Mongu District (AB8), Senanga Gauge Station (AB12) and an island-like piece of land about five 500m from Senanga Gauge Station. The points AB9, AB10 and AB11 were unnamed areas, but heaps of sediments on the banks of the Zambezi en route to Senanga. The samples were collected in Lukulu in the North all the way to Senanga in the South. This also included parts of the Kalabo District. This was done by digging pits of 1mx1mx1m in dimension. Examples of some pictures of some of the localities are given in Figure 4.19.

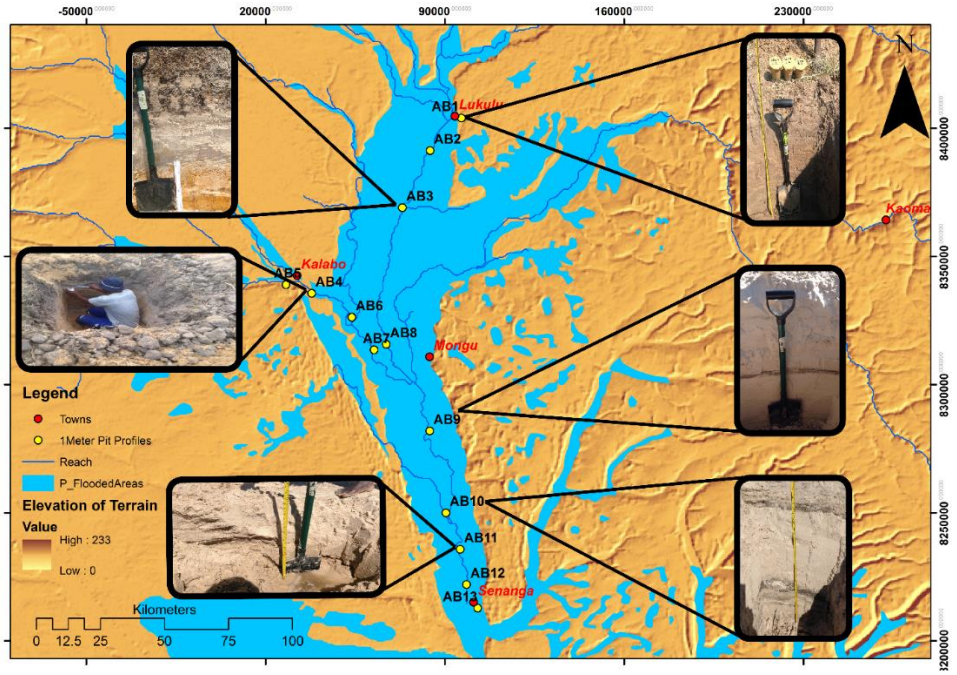

Figure 4.19: Locations of 1 meter pits dug within the Barotse Floodplain for XRF analysis with examples of photographs of the geo-tagged pits during the field campaign in the Barotse Floodplain, Western Zambia

It is observed that the predominant elements in the alluvium were iron (17,000mg/kg) and titanium (7,500mg/kg) respectively (Figure 4.20a). These were higher in the northern part of the floodplain from Lukulu River Confluence with the Zambezi River (AB1) to Kakuli Wamalilo Area (AB6). Two peaks can be observed at AB2 and AB6. After these peaks, the iron and titanium decreased to below 3,000mg/kg. Sand (silica) was the most abundant in this part of the floodplain varying from 72.89% at Nakatwelenge Basic School (IB28) to 91.23% at Sisma Salt Lake (IB37) with alternating layer of silica rich sand and laminae of iron-rich material (Appendix 5).

Figure 4.20b gives samples analysed by the AAS-method. This method showed calcium (12,750mg/kg), iron (5,300mg/kg) and sodium (3,000mg/kg) to have had the highest concentration in the alluvial soils for the labeled sampling points.

In summary, calcium's signature was present both in water and alluvial soils making it the most abundant element. Iron too was in abundance in the alluvial soils and undetectable in the water.

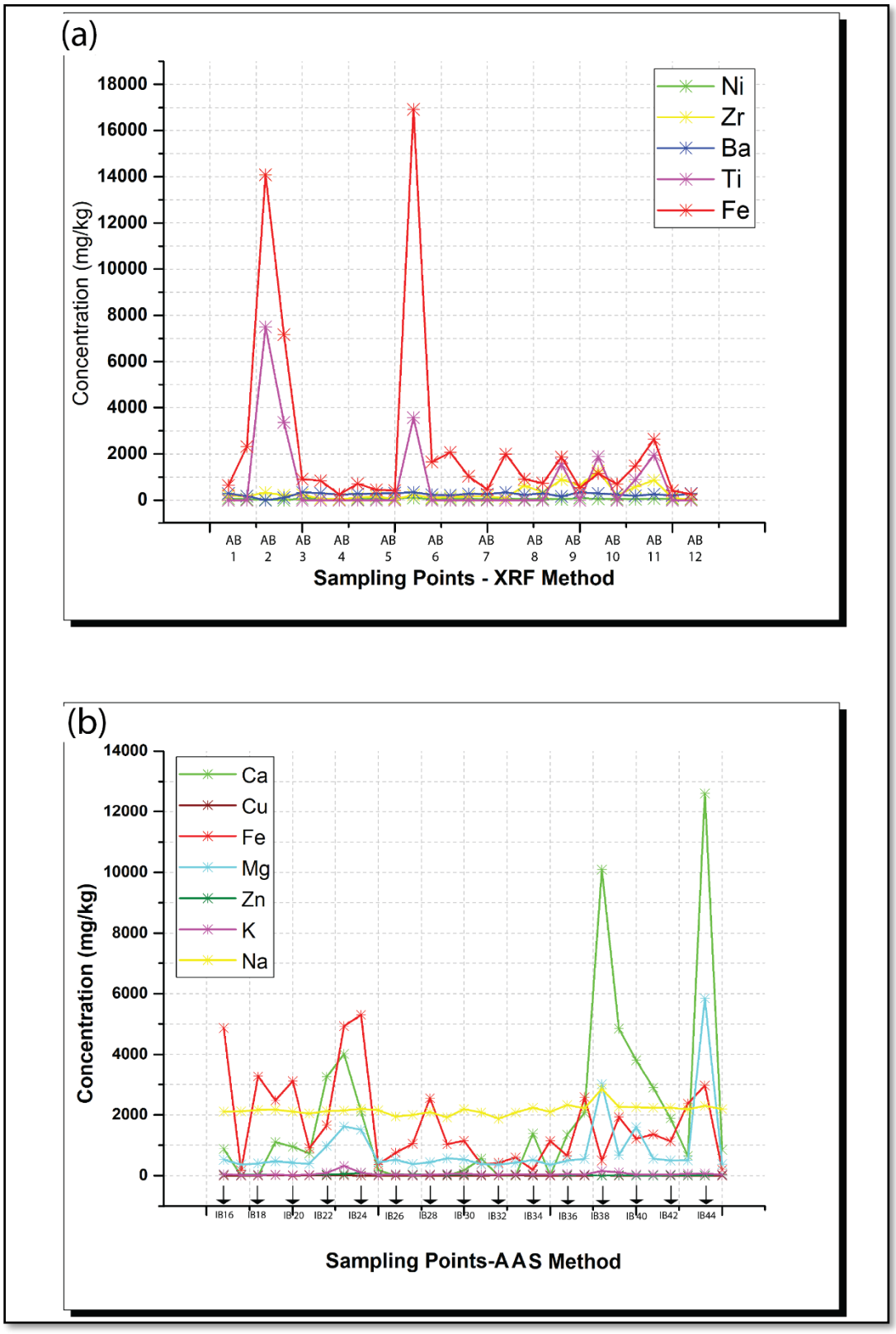

Figure 4.20: (a) XRF and (b) AAS analysis of alluvial soil's elemental constituents and concentration for the Barotse Floodplain, Western Zambia.

4.3.1 A Focus on Two Points for Soil Samples

Riverbed sediments were analyzed by the AAS and XRF methods as indicated earlier (Figure 4.20 above). These were collected in the same location as the water samples as mentioned in Chapter 3. However, the riverbed sediment parameters (most heavy metals) analyzed by the Geochemical Laboratory at the School of Mines were different from those tested in the water samples, hence no comparison could be made and most of the heavy metals both in water and sediments were less than the Limit of Detection (LOD) (see Appendix 9).

Results from the XRF were viewed through a Spectra View Mode (SVM). SVM enabled a visual inspection of the fluorescent x-ray peaks obtained from the samples. This was also viewed directly on the XRF screen as the sample was being analyzed. In SVM, the spectrum was displayed using a linear energy scale along the x-axis with the count rate auto-scaled logarithmically on the y-axis so that the highest peak on the screen reached the top of the scale (Fisher & Niton, 2010). The counts per unit of time were in response to the amount or concentration of the elements in each soil or sediment sample. Some examples of samples of riverbank profiles, that is, graph compared to the field taken photographs are given in Figures 4.21 and 4.22.

1 meter Pit Profile	Graph

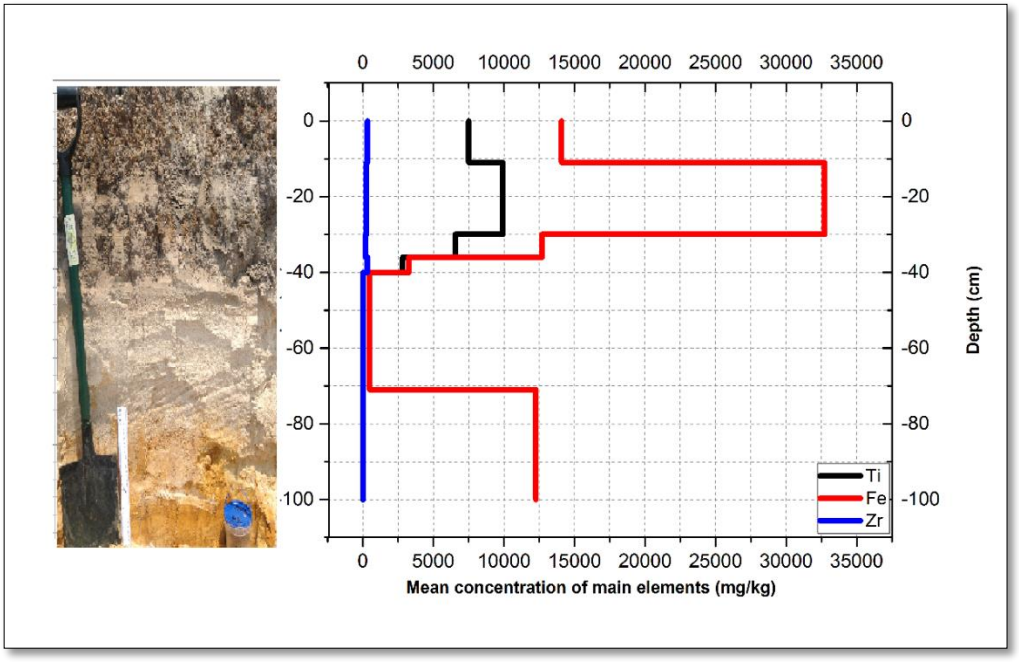

Figure 4.21: Graph (right hand side) showing the variation of concentration of Ti, Fe and Zr elements in the alluvium (left hand side) with depth in a pit dug at Mangongole (AB3) within the Barotse Floodplain, Western Zambia

It was observed from Figure 4.21 above that a relationship exists between soil pigmentation and the levels of concentration. This is similar to Figure 4.22 showing a riverbank profile at a location near Senanga Gauge Station (AB10). The red peaks in Figure 4.21 above are iron, which corresponds to the dark brown horizontal layers in the soil profiles as observed in the photographs taken in the field.

1 meter River Bank Profile	Graph

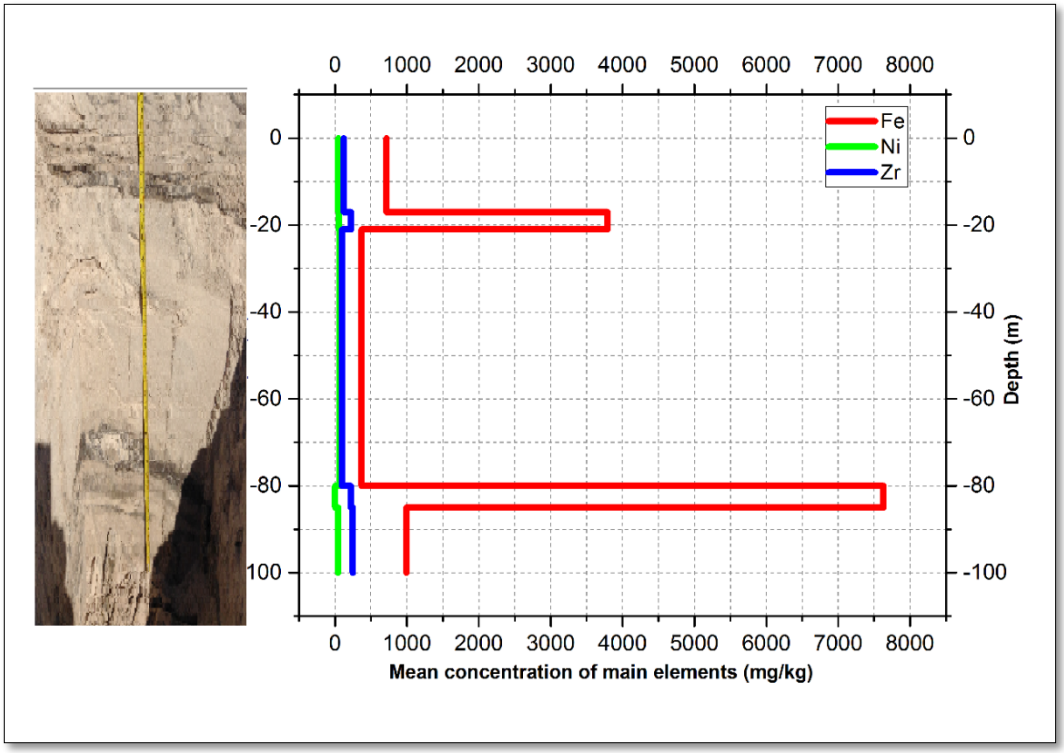

Figure 4.22: Graph (right hand side) showing the variation of concentration of Fe, Ni and Zr elements in the soil profile (left hand side) with depth in pit dug at location a location near Senanga Gauge Station (AB10) within the Barotse Floodplain, Western Zambia

4.3.2 Interpretation and Discussion on Soil Results

The Southern part of the floodplain was characterised by a layer of silica being above the iron layer, as in the case of AB10 (Figure 4.22). However, the soil/sediment samples collected in the Northern part of the floodplain had layers of iron before the silica layer as in the case of AB3 (Figure 4.21). This is because sediment transport is not constant. The inconsistency of sediment deposition caused by changes in water levels and flow regimes, larger particles are carried faster at higher flows. Settling often occurs when the water flow slows down or stops, and heavy particles can no longer be supported by the bed turbulence. According to Dingman (2009), to understanding the movement and settling of particles (sediments) in natural rivers, one needs to understand fluvial hydraulics. Geomorphologically, the floodplain slope reduces and widens moving from North to South. This leads to a loss in velocity, allowing for the settling of heavier particles. The transmission between turbulent flow (in the North) to laminar flow (in the South) is responsible for this phenomenon called Reynolds effect (Dingman, 2009).

4.4 Calibration, Validation and Sensitivity Analysis in SWAT-CUP

Figure 4.23 gives three hydrographs generated after running three (3) successive iterations each with five hundred (500) simulations. This was done in SWAT-CUP environment using SUFI-2 algorithm.

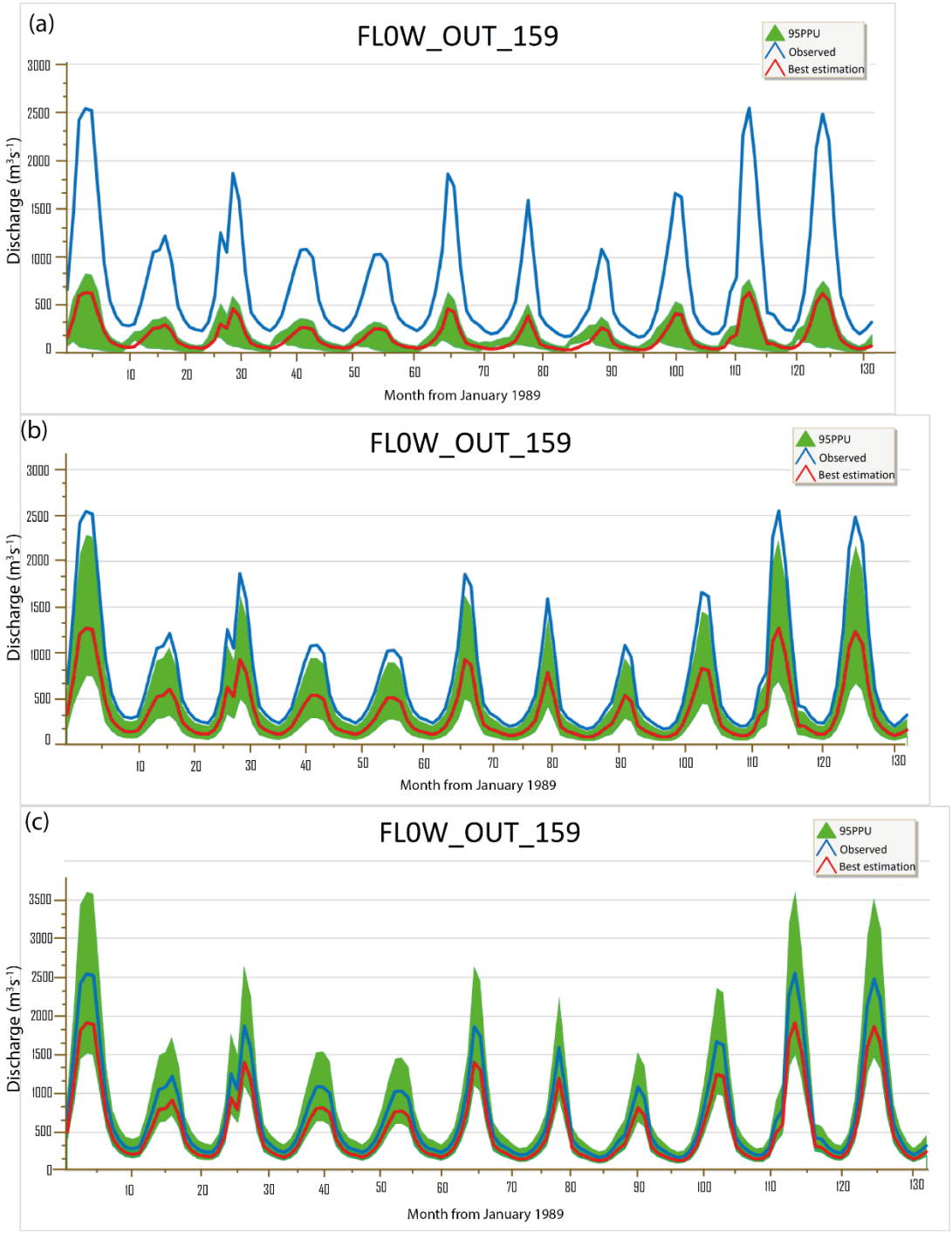

Figure 4.23: Hydrographs generated after running three (3) successive iterations each with five hundred (500) simulations during the calibration of the SWAT model in SWAT-CUP

The first three (3) iterations were calibration based whereas the fourth was used for validation. The years used were 1989 to 1999 on a monthly time step indicated by 132 data points on the abscissa of Figure 4.23 (a), (b) and (c). The three iterations were also viewed through a statistical summary window within SWAT-CUP as given in Figure 4.24 (a), (b) and (c).

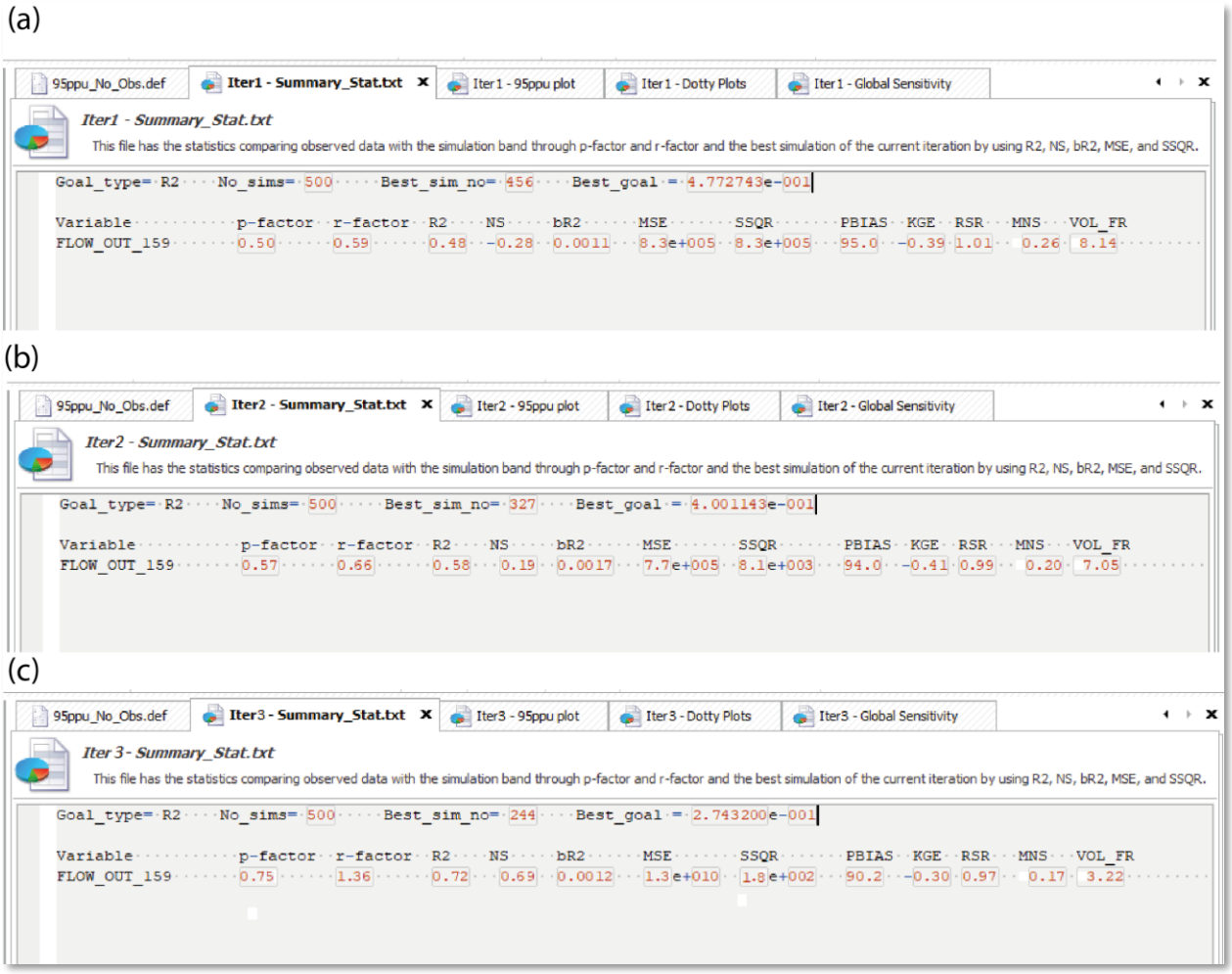

Figure 4.24: Summary statistics comparing observed data with the simulation band through P-factor and R- factor and the best simulation of the current iteration by using Coefficient of Determination (R^2), Nash Sutcliffe (NS), Modified Coefficient of Determination (bR^2), Mean Square Error (MSE), Sum of Square Residual (SSQR), Percent Bias (PBIAS), Kling-Gupta Efficiency (KGE), Root Mean Square Error (RSR), and the Overall Water Balance Fraction (VOL_FR). This was for the three iterations (a), (b) and (c)

An independent dataset from 2000 to 2006 was reserved for the validation of the model. This dataset was about one-third of the entire period less the years used in warming up the model (NYSKIP). Figure 4.25 gives an illustration of the full SWAT-CUP output showing the observed, the best simulation, and the 95% prediction uncertainty (95PPU). P-factor is the percentage of observations points bracketed by the prediction uncertainty band, and R-factor is the average thickness of the band divided by the standard deviation of the observed values showing the degree of uncertainty.

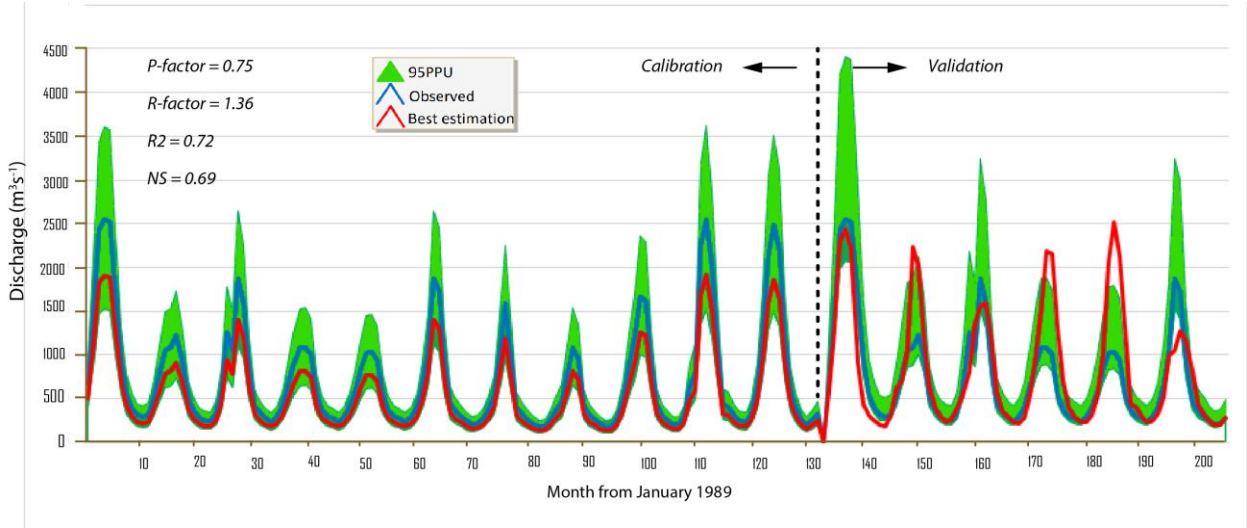

Figure 4.25: Hydrograph combining calibration and validation data. The calibration data is from the third iteration. A total of 204 data points representing the number of months for the entire period are plotted on the abscissa

A sensitivity analysis was further used in the SWAT model developed to try and understand which processes controlled the system. A total of 21 parameters were used during the calibration and validation phases. These, their meanings, and their range of validity are listed below (Table 4-3).

Table 4-3: Parameters used during the calibration and validation stages in SWAT-CUP

Parameter	Meaning	Validity Range	
ALPHA_BF	Baseflow alpha factor (days).	0	1
GW_DELAY	Groundwater delay (days).	0	500
GW_REVAP	Groundwater "revap" coefficient	0.02	0.2
GWQMN	Threshold depth of water in the shallow aquifer required for return flow to occur (mm).	0	5000
REVAPMN	Threshold depth of water in the shallow aquifer for "revap" to occur (mm).	0	500
RCHRG_DP	Deep aquifer percolation fraction.	0	1
OV_N	Manning's "n" value for overland flow.	0.01	30
SLSUBBSN	Average slope length.	10	150
LAT_TTIME	Lateral flow travel time.	0	180
SLSOIL	Slope length for lateral subsurface flow.	0	150
ESCO	Soil evaporation compensation factor.	0	1
EPCO	Plant uptake compensation factor.	0	1
SOL_K	Saturated hydraulic conductivity.	0	2000
SOL_AWC	Available water capacity of the soil layer.	0	1
SURLAG	Surface runoff lag time.	0.05	24
CN2	SCS runoff curve number	35	98
CH_N2	Manning's "n" value for the main channel.	-0.01	0.3
CH_K2	Effective hydraulic conductivity in main channel alluvium.	-0.01	500
CH_D	Average depth of main channel.	0	30
ALPHA_BNK	Baseflow alpha factor for bank storage.	0	1
CH_W2	Average width of main channel.	0	1000

Two types of sensitivity analysis are allowed in SWAT-CUP, One-at-a-time sensitivity and Global Sensitivity. The letter was used, and the results are given below (Figure 4.26).

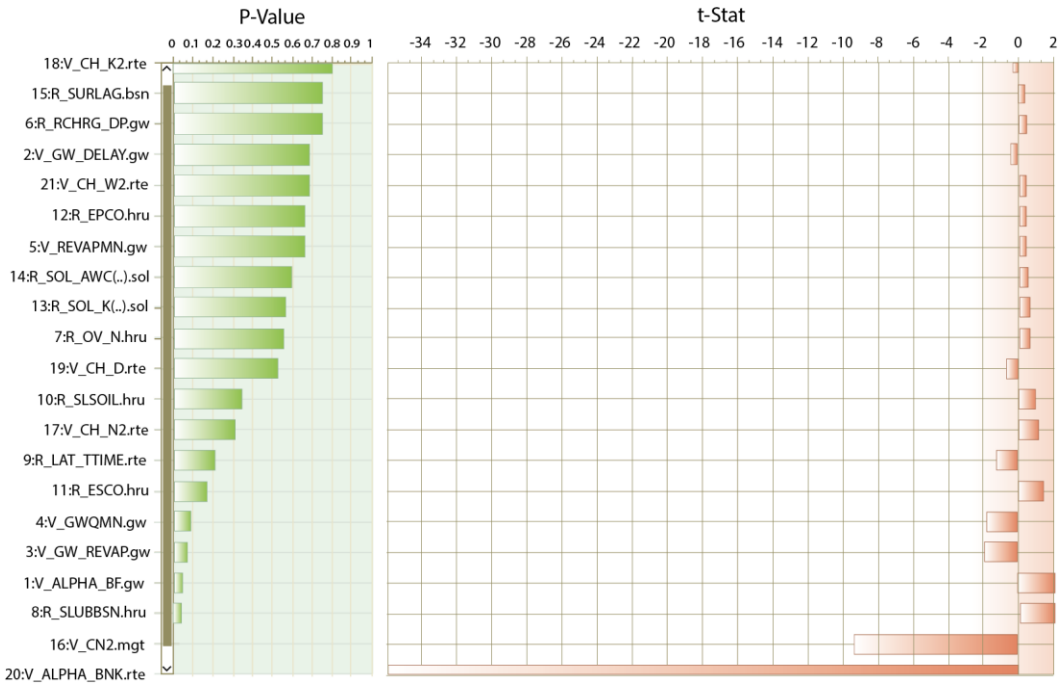

Figure 4.26: Order of sensitivity for the 21 parameters representing processes in the SWAT model. These are analysed by two statistical parameters, P-Value and t-Stats. The order of sensitivity is from bottom to top

From Figure 4.26, ALPHA_BNK (Baseflow alpha factor for bank storage) was the most sensitive parameter according to the model and its respective dotty plot is given below (Figure 4.27).

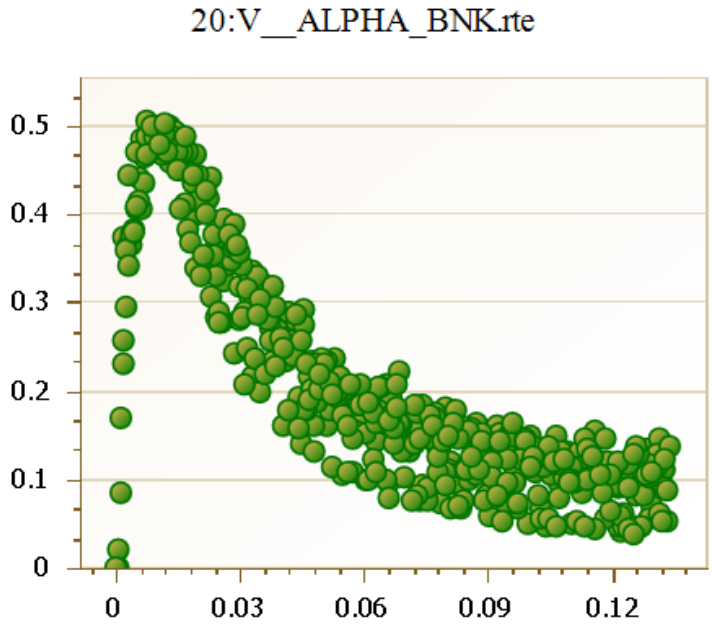

Figure 4.27: Dotty plot for ALPHA_BNK showing its sensitivity relative to the objective function

4.4.1 Discussion on the Model Calibration, Validation and Sensitivity Analysis

According to Dingman (2009), discharge measurements are invaluable for calibrating and validating hydrological models, and they are the only means of forecasting the effects of land use and climate change on water resources in large and complex areas. This is why we also used historical discharge data measured at Senanga Hydrometric Station to try and understand the hydrodynamics taking place in the Barotse Floodplain. However, hydrological models are subject to the expertise of their developers and are prone to error (Abbaspour *et al.*, 2015). For this reason, the data presented in this study has undergone calibration and validation processes according to the knowledge of the developer/author.

During the three-stage iterative calibration process, eleven (11) years of data were used using SWAT – CUP environment from 1989 to 1999 to produce a time series of simulated and observed flows (Figure 4.23). The reason why the iterations were done in phases, was to allow for the monitoring process for the progression to the convergence of the signals (Abbaspour *et al.*, 2015). Figure 4.24 shows the statistical summary of the hydrographs in Figure 4.23. It can be observed from Figure 4.24 that 500 simulations were used for each iteration. This is as per requirement from the SWAT-CUP Manual (Abbaspour *et al*., 2015). A summary of the final key statistical variables with respect to other similar studies is given in Table 4-4.

Table 4-4: Comparison of key statistical variables (performance indicators) for this study with other studies

			Variable Number				**Size of Study Area (km^2)**
			1	2	3	4	
		Variable Name/Symbol	P-factor	R-factor	R^2	NS	
Study Number	1	This study (final iteration)	0.750	1.360	0.720	0.690	264,312
	2	Abbaspour *et al*, (2015)	0.690	1.390	0.780	0.740	92,090
	3	Habte *et al*, (2013)	0.210	0.250	0.720	0.710	1,600
	4	Phomcha, *et al*, (2011)	-	-	0.805	0.848	357
	5	Duan *et al*, (2007)	-	-	0.930	0.810	1,850
	Ideal value		>0.70	<1.5	1.00	1.00	

From the five (5) studies listed in Table 4-4, study 1 (this study) has the largest catchment area. This meant that the model had more spatial uncertainties compared to the other four studies.

Abbaspour *et al* (2015), explain that it is not possible to account for every soil type, slope and land use, hence some soil groups/slope/land use are classified together. This process becomes even more complex for bigger areas. Further, studies 2 and 3, that is, Abbaspour *et al* (2015) and Habte *et al* (2013) in Table 4-4 are the closest studies related to this study in that both use SWAT-CUP for inverse modeling (calibration and validation). Using this basis, statistical parameters relating to the performance of the model were analysed. According to Abbaspour *et al* (2015), the desired values for P-factor and R-factor when simulating discharge should be greater than 0.70 (>0.70) and less than 1.5 (<1.5) respectively. This shows that our P-factor (0.75) and R-factor (1.36) fall within this acceptable range. However, Habte *et al* (2013) had 0.210 and 0.250 as P and R-factors respectively. These results were relatively smaller than those of this study and those of Abbaspour *et al* (2015). When the results by Habte *et al* (2013) were further analysed, it was observed that the optimization algorithm used was not the semi-automated Sequential Uncertainty Fitting (SUFI-2), but fully automated Parameter Solution (ParaSol). Normally, we expect the P and R-factor to be similar as the objective functions or performance indicators used were almost the same. A final analysis of the results by Habte *et al* (2013) showed that their calibration was sediment based and not discharge based. This observation made further explained one of Abbaspour's *et al* (2015) uncertainty principles which explains that a model calibrated for one parameter does not necessary mean that it is calibrated for another. Questions on this study are still being asked whether a single model calibrated for one parameter can work for discharge, sediment as well as water quality (Abbaspour *et al*, 2015) as the case is in this study. Duan *et al* (2007) and Phomcha *et al* (2011), used the trial-and-error calibrations techniques described in SWAT's user manual (Arnold *et al*, 2012). As observed, this method seems to produce better performance indicators (Table 4-4) when compared to SUFI-2. However, the downside to this method is its incapacity to account for uncertainties as SUFI-2 does through the 95PPU (Abbaspour *et al*, 2015 and Abbaspour *et al*, 2017). The 95PPU is the solution to inverse modelling as there are numerous combinations of parameters that can give a signal falling within the green band, that is, 95PPU (Figures 4.23 and 4.25). Furthermore, SWAT-CUP allows for 10 objective functions to be used as shown in Figure 4.24, however, only R^2 and NS are used as most studies only use these two to optimize their models (Abbaspour *et al*, 2015).

Figure 4.25 shows a hydrograph combining the calibration and validation period. It can be observed that the best estimation during the validation period showed over-estimation of the model

through the peak flows towards the end. This same behavior can be seen throughout the calibration to validation by the 95PPU (green band defined by the P and R-factor). This is why a sensitivity analysis was conducted to ascertain the most sensitive parameters (Figures 4.26 and 4.27). The most sensitive parameters in this model were ALPHA_BNK and CN2 (Table 4-3). According to Arnold *et al*, (2012), bank flow is simulated with a recession curve similar to that used for ground water if the model is running well. This further confirms the reliability of the model as Figure 4.27 resembles the recommended description by Arnold *et al*, (2012) other than the performance indicators alone. ALPHA_BNK has a maximum value of about 0.5 at about 0.01 (Figure 4.27) and falls sharply to all values greater or less than 0.01 on either side. The reason for the high peaks simulated in the hydrographs can be attributed to CN2, which is related to runoff and infiltration from excess runoff (Emam *et al*, 2017).

4.5 Limitations of the Model

No historical dataset for sediment monitoring were available hence, sediment calibration and validation could not be done, therefore, the results depended on the first level calibration, that is discharge data. According to Arnold et al, (2012) and Betrie *et al*., (2001), the progressive stages of calibration are discharge calibration, sediment calibration and then water quality calibration.

4.6 Sediment Distributions, Yields and Spatial Visualization

These were analysed using the SWAT model in Arc GIS environment after the model calibration and validation. This means that both qualitative (as given in Subsection 4.3) and quantitative aspects (sediment yields) were analyzed in order to further understand the soil water relationships. Sediment yield and spatial visualization are explained by starting with the general distribution of sediments in the entire basin and then narrowing the focus on the Barotse Floodplain.

4.6.1 General Distribution of Sediments in the Entire Basin

The years considered in this approach were 2001, 2002, 2003, 2004 and 2005, as given in the methodology. The spatial distribution of sedimentation of five (5) different sub-basin classes for the entire watershed for five (5) consecutive years are given throughout this subsection in the form of maps and bar graphs. The classification maps capture the dynamics and changes per year in terms of sedimentation patterns (Figure 4.28). Discretization of the basin as per methodology gave 159 sub-basins each depicting different rates of sedimentation. The sediments were measured in

tons per annum. Furthermore, respective bar graphs were included showing the differences among sub-basins as described herein.

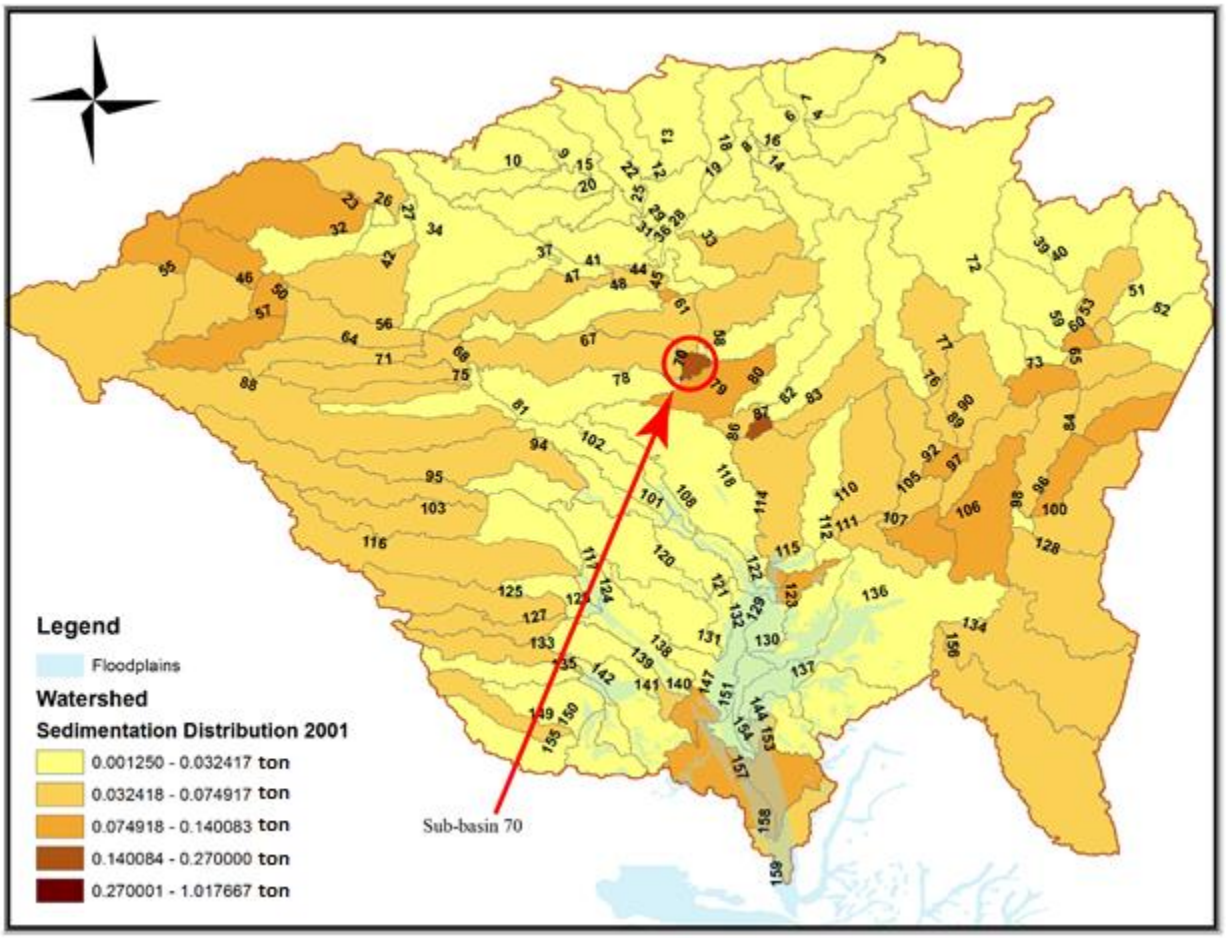

Figure 4.28: Spatial sedimentation pattern/distribution for the UZB as simulated by SWAT for 2001, Western Zambia. Note sub-basin 70 had the highest sedimentation rate

The map in Figure 4.28 gives an increasing colour intensity as you move down the legend. The colours moved from yellow, orange to dark brown. This indicated increasing rates of sediment accumulation for each sub-basin. The lighter the colour, the less the accumulation of sediments per sub-basin. Similarly, the darker the colour, the greater the rate of sediment accumulation per sub-basin.

For 2001 sediment yield distribution patterns are given in Figures 4.28 and 4.29. Sub-basin 70 had the highest sediment deposition, which is along the Zambezi River, directly north of the floodplain. It was seconded by sub-basin 87 south - east of sub-basin 70 (Figure 4.28). The yields for the two

sub-basins were about 1.02 and 0.27tons for sub-basin 70 and 87 respectively, which indicated a huge difference of 0.75tons, (7,500kg).

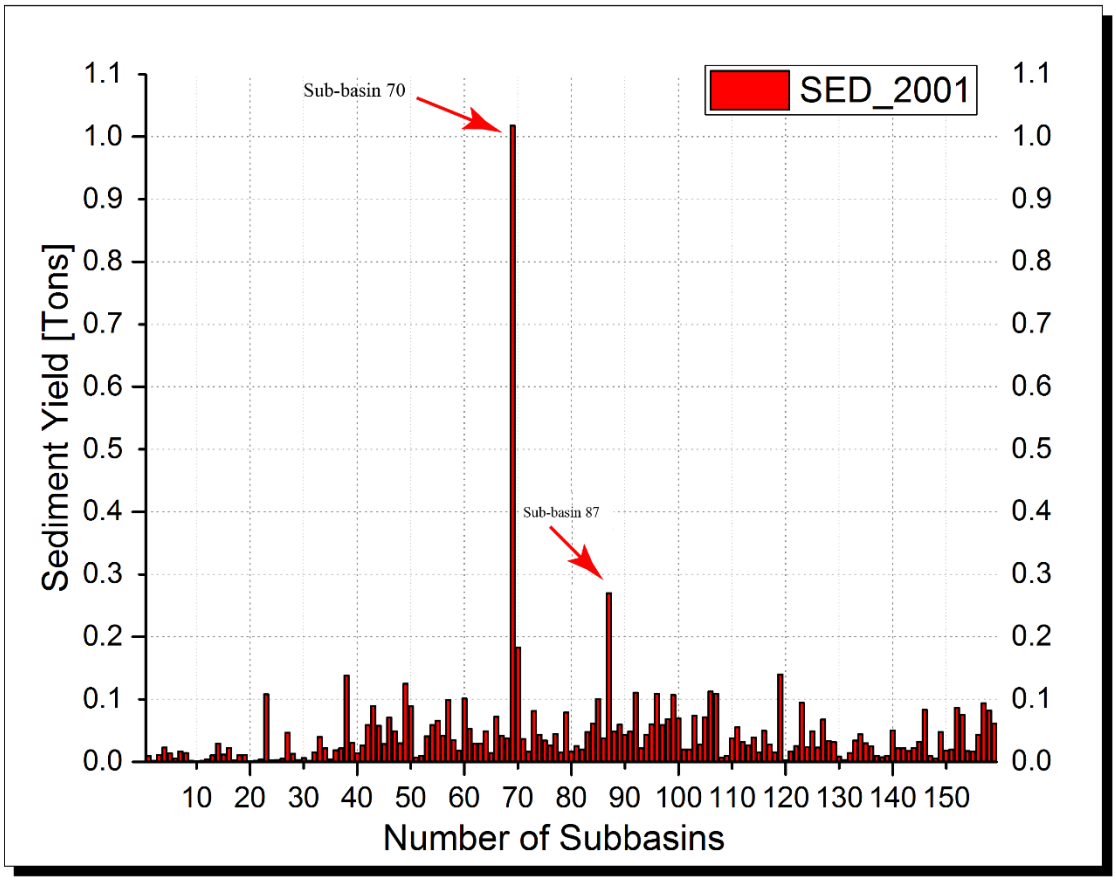

Figure 4.29: Bar graphs showing sub-basin sediment accumulation for each sub-basin for 2001 simulation, Barotse Floodplain, Western Zambia. Sub-basin 70 is the most affected.

For 2002 sediment yield distribution patterns are similarly given in Figures 4.30 and 4.31. Here the pattern of sedimentation changed. Sub-basin 70 still had the highest sediment deposition, located along the Zambezi River, directly north of the floodplain. It was seconded by two sub-basins, sub-basin 38 north – west of sub-basin 70 and sub-basin 87 south - east of sub-basin 70. Sub-basin 70 and 87 were along the Zambezi River. However, the values of sub-basin 38 and 87 are almost the same as indicated in Figure 4.31 giving readings of 0.28 tons and 0.27 tons respectively.

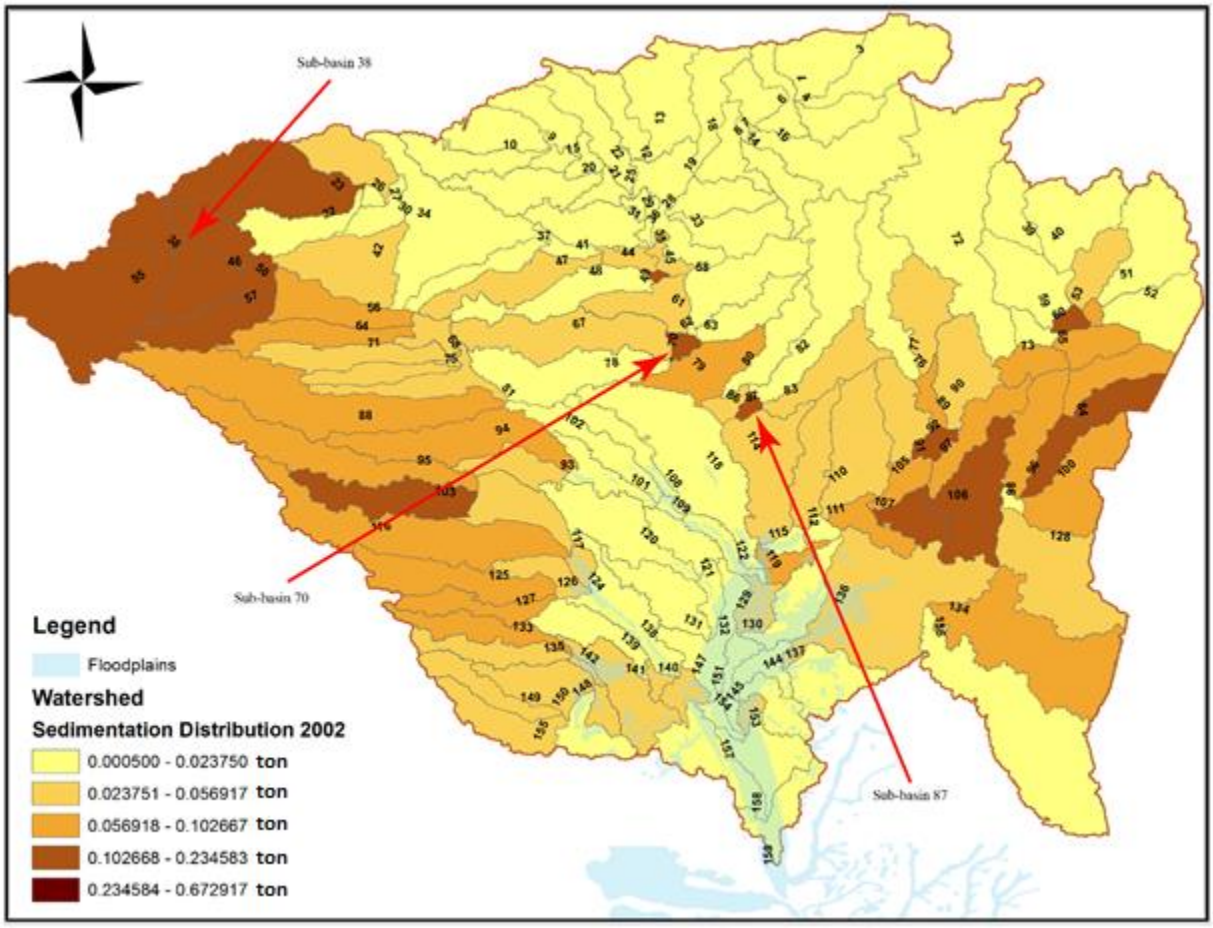

Figure 4.30: Spatial sedimentation pattern/distribution for the entire catchment as simulated by SWAT for 2002, Barotse Floodplain, Western Zambia. Sub-basin 70 had the highest sedimentation rate.

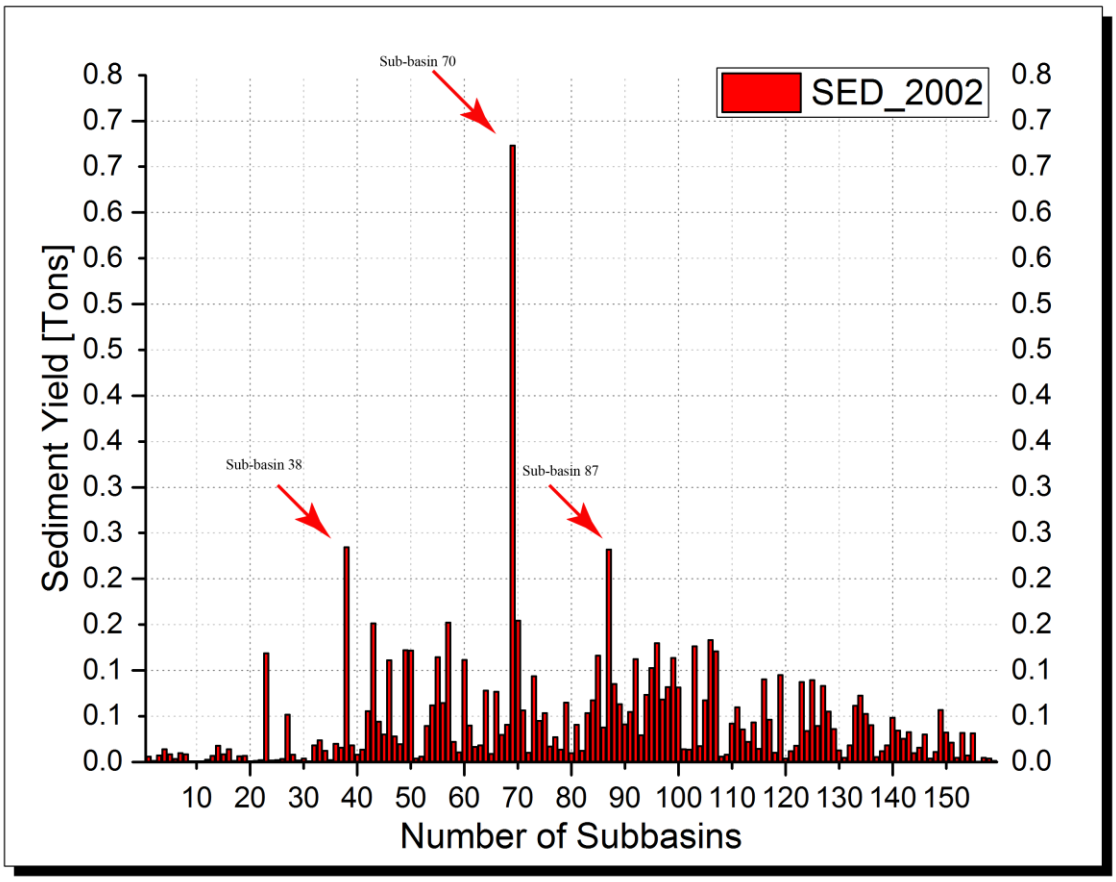

Figure 4.31: Bar graphs showing sub-basin sediment accumulation for each sub-basin for 2002 simulation, Barotse Floodplain, Western Zambia. Sub-basin 70 is the most affected

Comparing the sedimentation effects of 2001 and 2002, the pattern is similar along the Zambezi River, however, the same results indicate an intensified sedimentation pattern on the north - western side of the basin in Angola. Portions of increased sedimentation rates were also visible in the north - eastern direction towards Kaoma into Kafue National Park (sub-basins 84 and 96). This could have been due to the spatial changes in the land cover. Examples include clearing for farms, farming itself, cattle rearing plus increase in settlements. Deforestation and the intensity of rainfall in the area are likely to be the main causes of erosion.

Sediment yield distribution patterns for the year 2003 are given in Figures 4.32 and 4.33. Sub-basin 70 had the highest sedimentation effects, which was along the Zambezi River, directly North

of the floodplain. This was seconded by sub-basin 38 north - west of sub-basin 70. Other affected areas included the north - western region of the catchment in Angola.

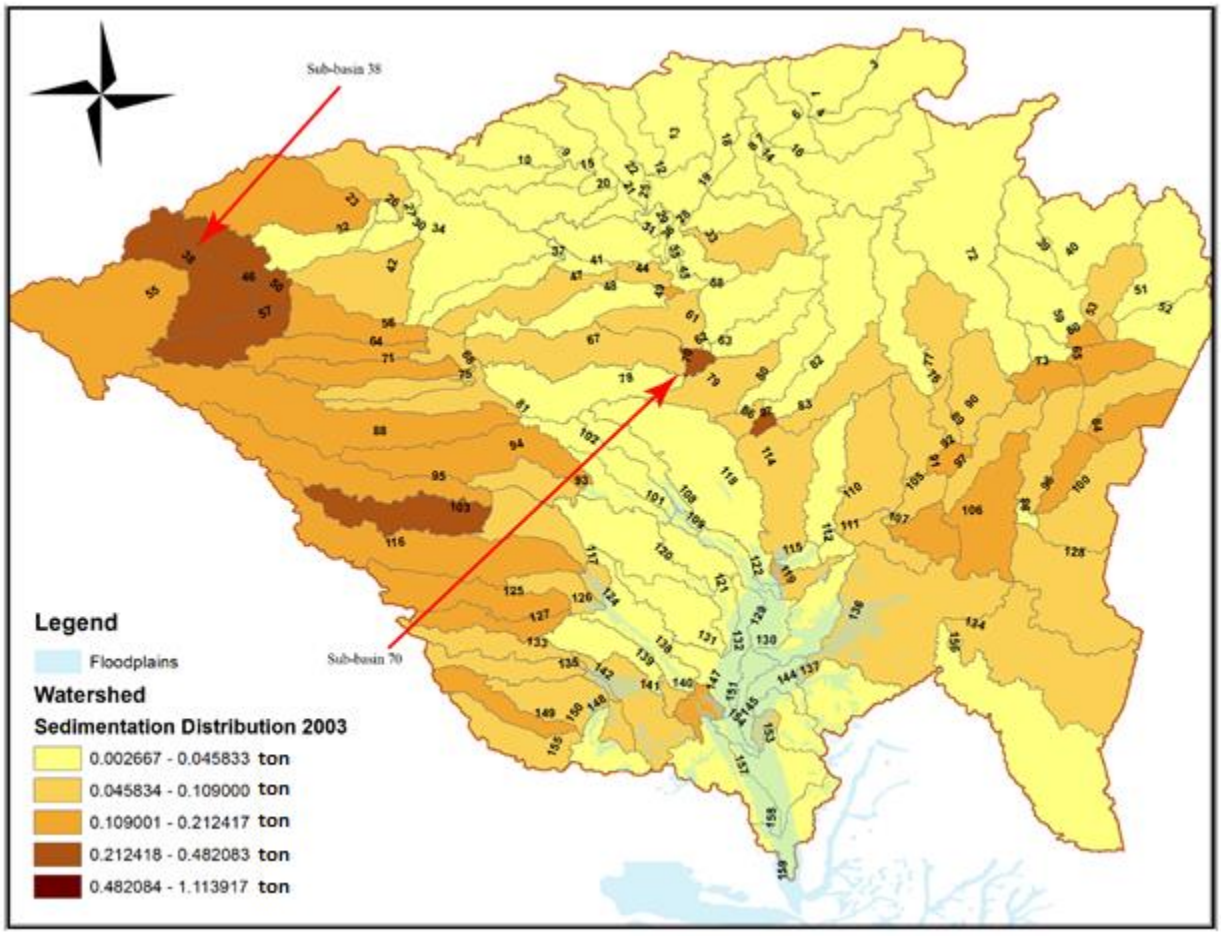

Figure 4.32: Spatial sedimentation pattern/distribution for the entire catchment as simulated by SWAT for 2003, Barotse Floodplain, Western Zambia. Sub-basin 70 is the most affected

Figures 4.30 and 4.32 represents the sedimentation patterns of 2002 and 2003, respectively. These appeared to be similar, however, 2002 sediment distribution was more on the eastern part of the entire basin when compared to 2003. The sub-basin distinguishing the two (Figure 4.30 and 4.32) were 60,84, 97 and 106.

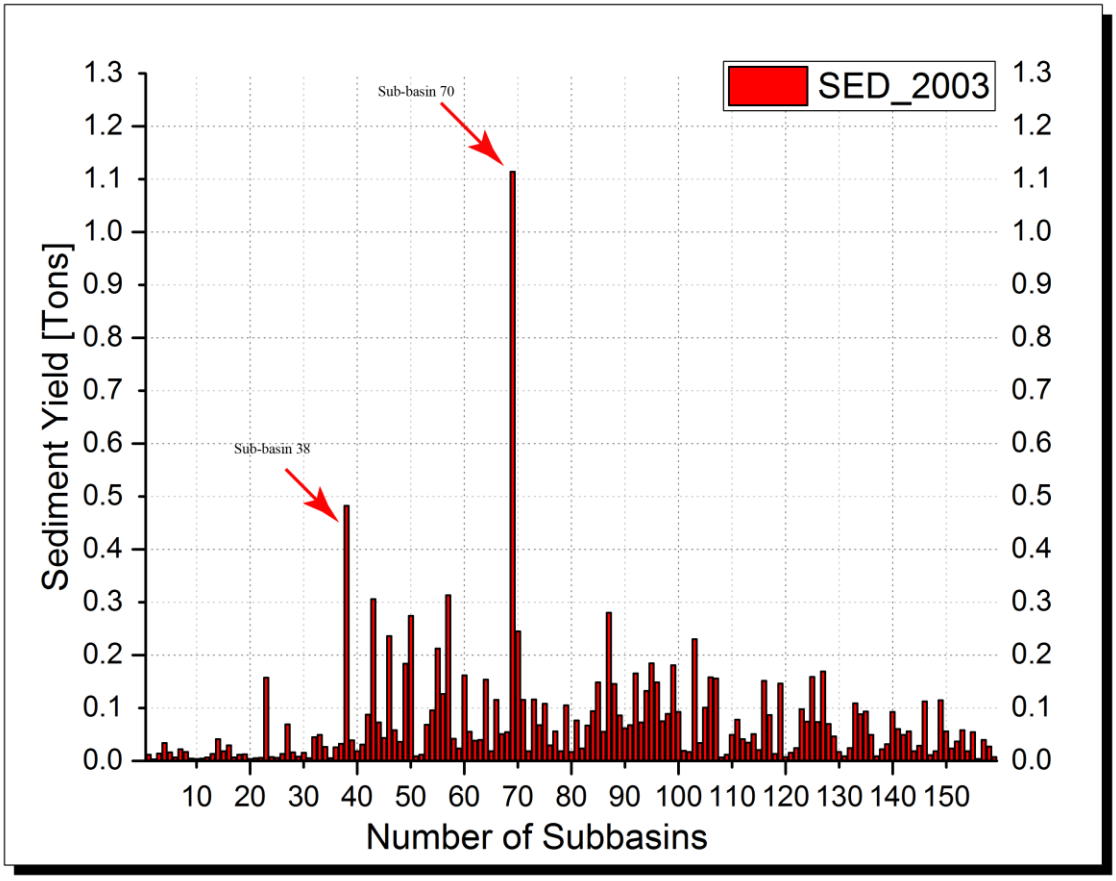

Figure 4.33: Bar graphs showing sub-basin sediment accumulation for each sub-basin for 2003 simulation, Barotse Floodplain, Western Zambia. Sub-basin 70 is the most affected

Figures 4.29 and 4.33 were similar, however, Figure 4.33 showed more sediment yields in the sub-basins before sub-basin 70. Those that stood out were sub-basins 38, 43 and 57.

A change in the distribution of sediments was also observed in Figures 4.34 and 4.35 for the 2004 simulation in SWAT. The map in Figure 4.34 gives a total shift of the worst areas of sedimentation to the North West of the catchment in Angola as indicated by the darker colours in this part of the catchment. From the North West into the western region and south wards, the colour intensity reduces, hence, predicting a reduction in sediment accumulation.

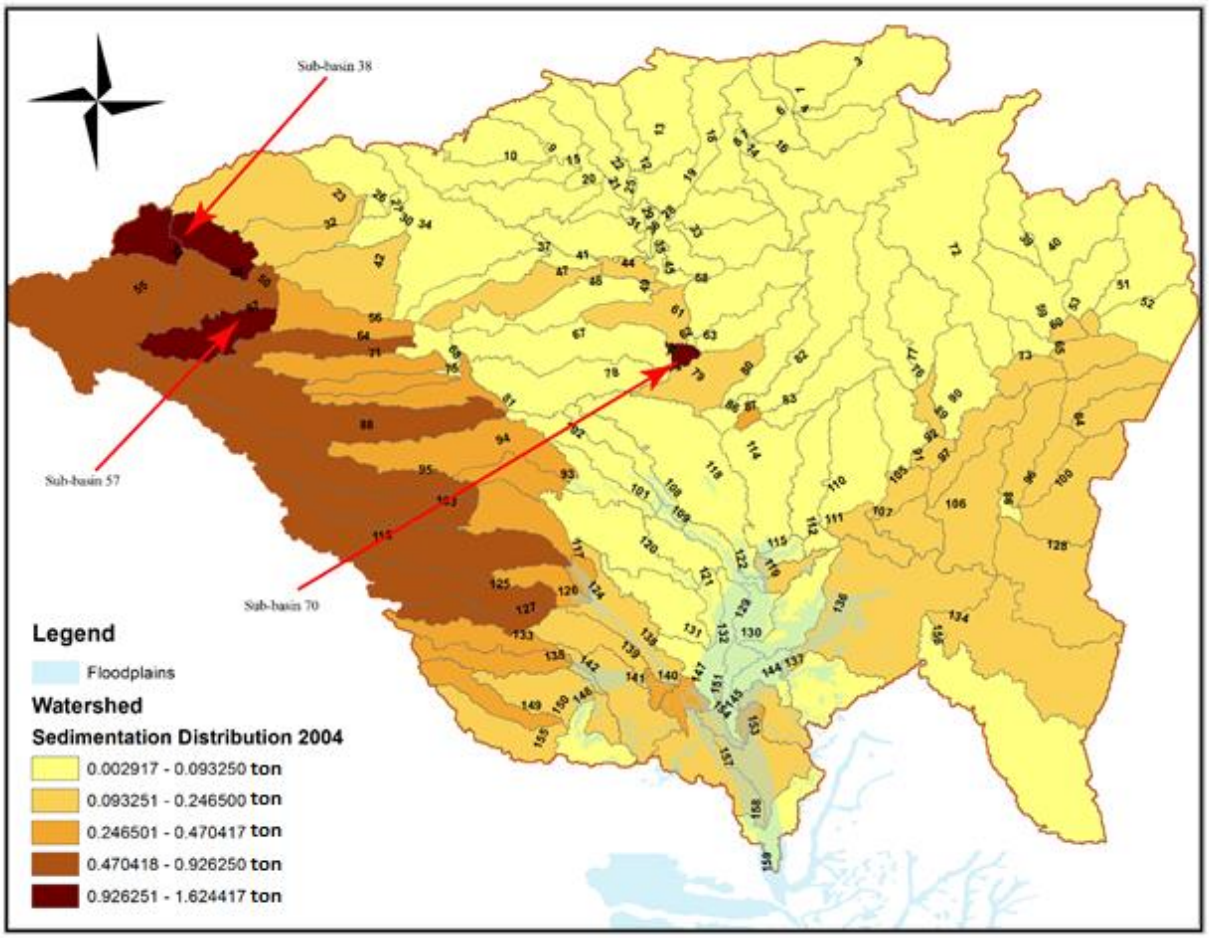

Figure 4.34: Spatial sedimentation pattern/distribution for the entire catchment as simulated by SWAT for 2004, Barotse Floodplain, Western Zambia. Sub-basin 38 is the most affected

The worst affected sub-basin has now changed to sub-basin 38 with a yield of about 1.63tons seconded by sub-basin 70 with a yield of 1.48tons. Other sub-basins with higher yields were sub-basins 57 and 43, which were just below sub-basin 38 in the North West with a yield of about 1.08 tons and 1.05 tons respectively (Figure 4.34 above).

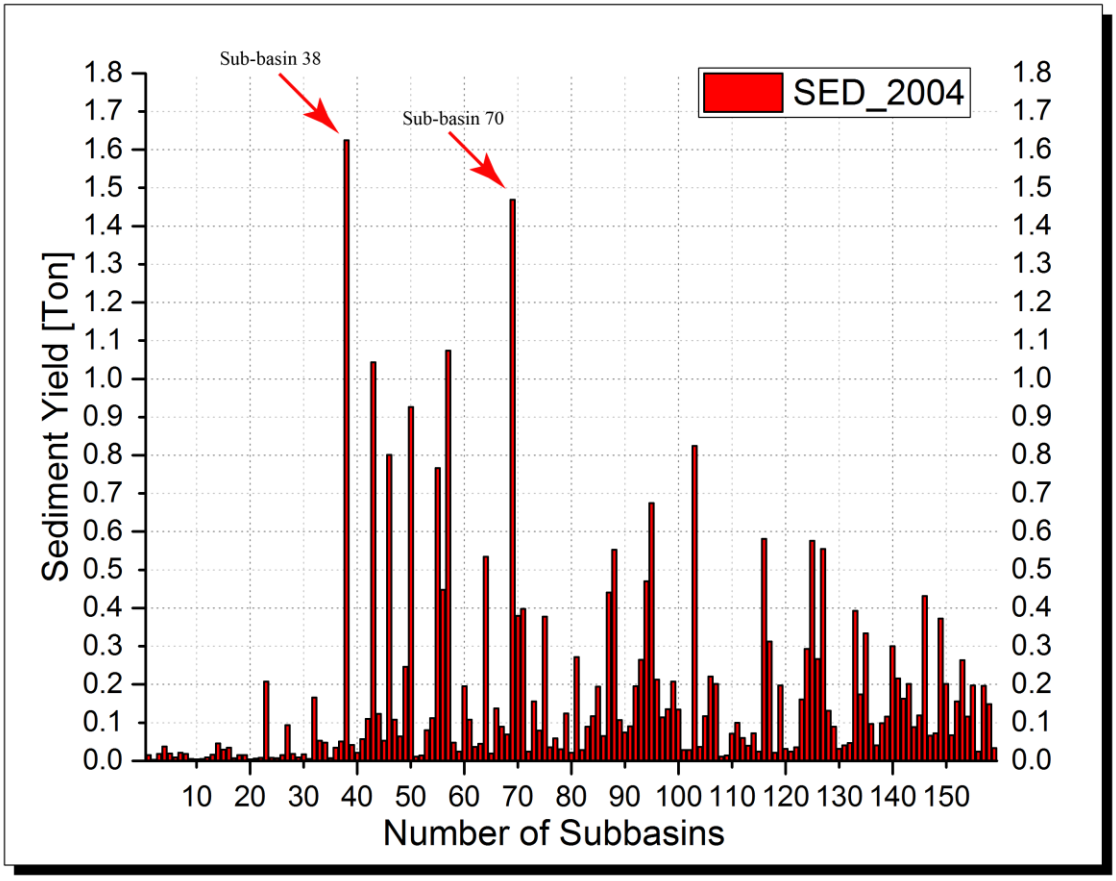

Figure 4.35: Bar graphs showing sub-basin sediment accumulation for each sub-basin for 2004 simulation, Barotse Floodplain, Western Zambia. Sub-basin 38 and 70 are the most affected

In the final year of 2005 simulation, the distribution of the sediments was similar to 2003, where the sediments were on the North-Western side (Figure 4.36). The sub-basins on the North Western side of the catchment were 38, 46, 50, 55 and 57. These fell in the same colour range from 0.295 to 0.676 tons. To the South of these sub-basins, sub-basin 103 is within this same colour code range. The sub-basins mentioned here are in two red circles, that is, sub-basins 38, 46, 50, 55 and 57 in one circle and sub-basin 103 in the other (Figure 4.36) for quick identification.

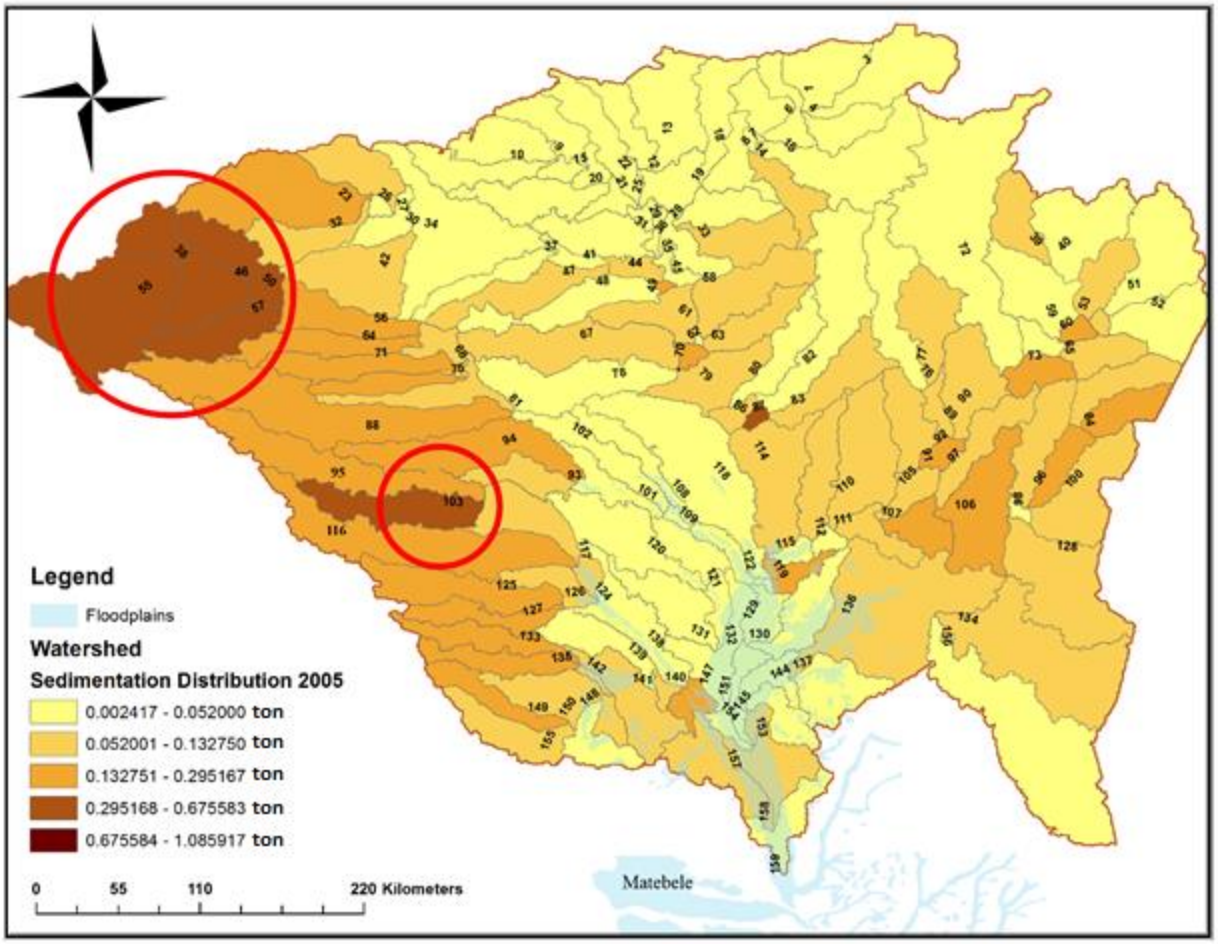

Figure 4.36: Spatial sedimentation pattern/distribution for the entire catchment as simulated by SWAT for 2005, Barotse Floodplain, Western Zambia. Sub-basins in red circles were the most affected

Figure 4.36 above showing the spatial distribution of sediments in 2005 simulation is supported by the bar graph (Figure 4.37) giving the yield associated to each sub-basin for the entire basin.

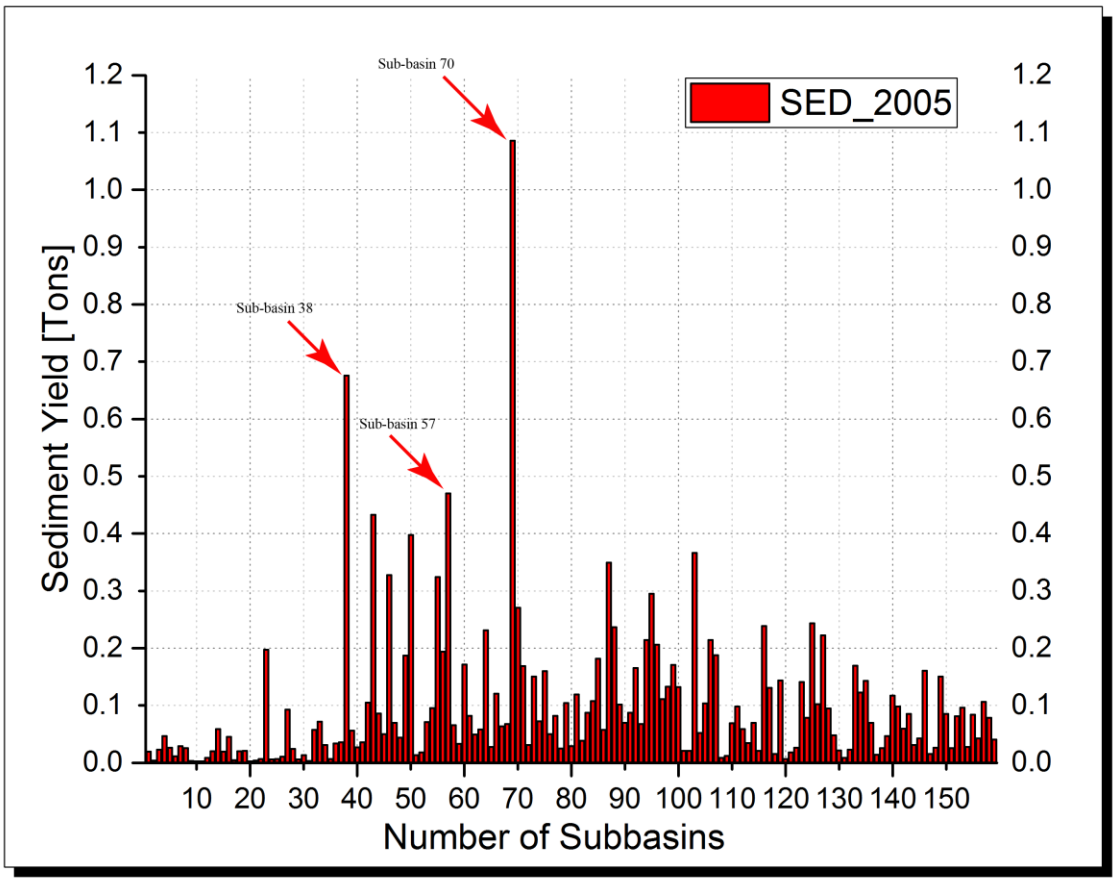

Figure 4.37: Bar graphs showing sub-basin sediment accumulation for each sub-basin for 2005 simulation, Barotse Floodplain, Western Zambia. Sub-basin 70, 38 and 57 were the most affected respectively

The series of maps and bar graphs from Figures 4.28 to 4.37 gave a general overview of the changes in the sedimentation patterns in terms of accumulation per sub-basin. As earlier indicated, the sub-basins with the greatest sedimentation were 70 and 38 along the Zambezi and Luanginga rivers respectively.

4.6.2 Distribution of Sediments in the Barotse Floodplain

From the results of the SWAT model, the focus was now directed on the Barotse Floodplain by observing how many of the sub-basins occurred in the floodplain when spatially overlaid on the same map using the Barotse Floodplain Shape-file (Figure 4.38).

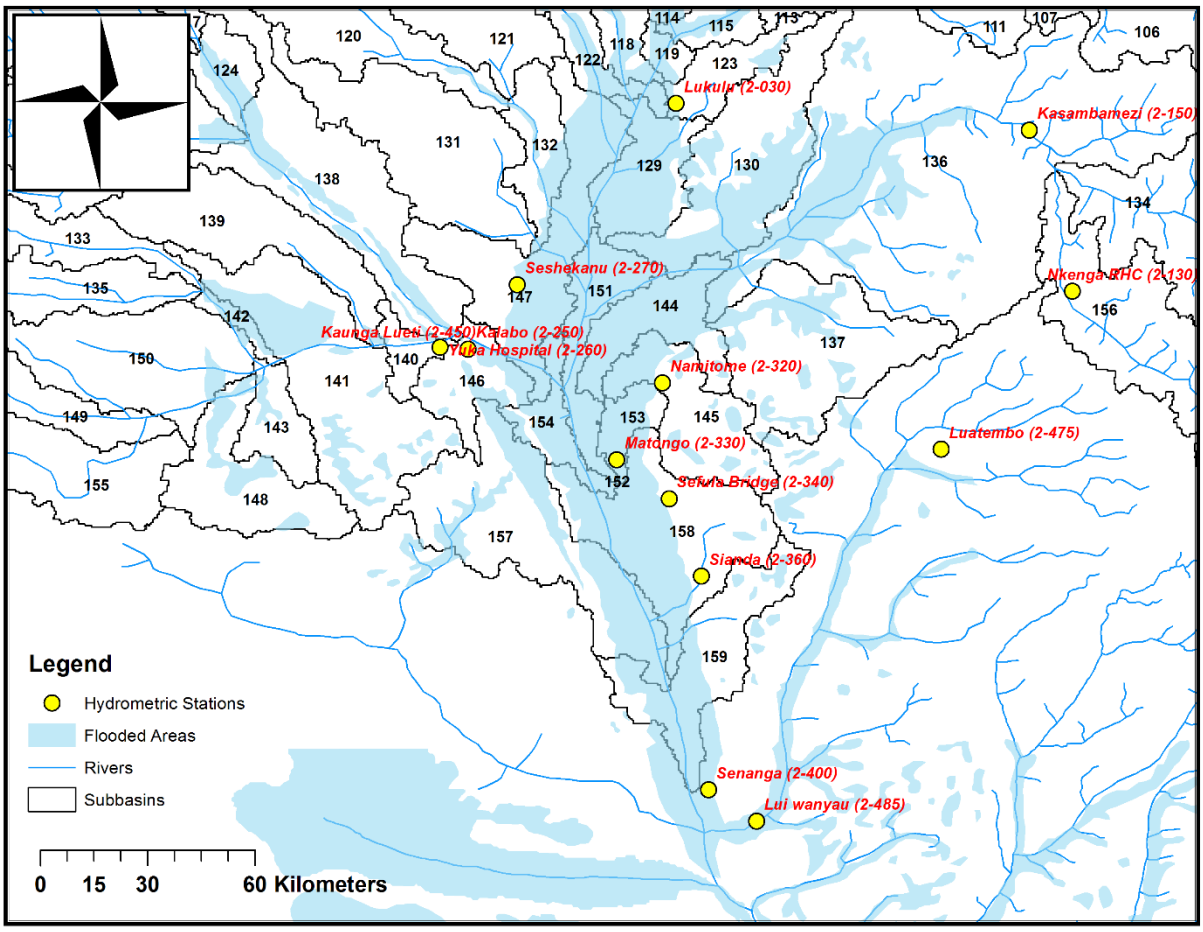

Figure 4.38: A map of the Barotse Floodplain showing how the entire basin is partitioned into sub-basins with Senanga Hydrometric Station (2-400) as the model outlet, Western Zambia

Figure 4.38 above shows an overlay of discretized sub-basins and the inundated area of the floodplain. This discretization of the floodplain into sub-basins was done using SWAT at a set threshold mentioned in the methodology. Notice that the basin closes at Senanga Hydrometric Station coded as 2-400 by Department of Water Resources Development (DWRD).

Four scenarios of decreasing sedimentation order were analysed to show how sedimentation occurs on the floodplain. This was based on the same results from SWAT, however, this time as indicated earlier the focus was on the floodplain. Sub-basins with the highest sediment yields were highlighted or coloured first, that is, from the worst sediment prone basins to the least affected (Figure 4.39).

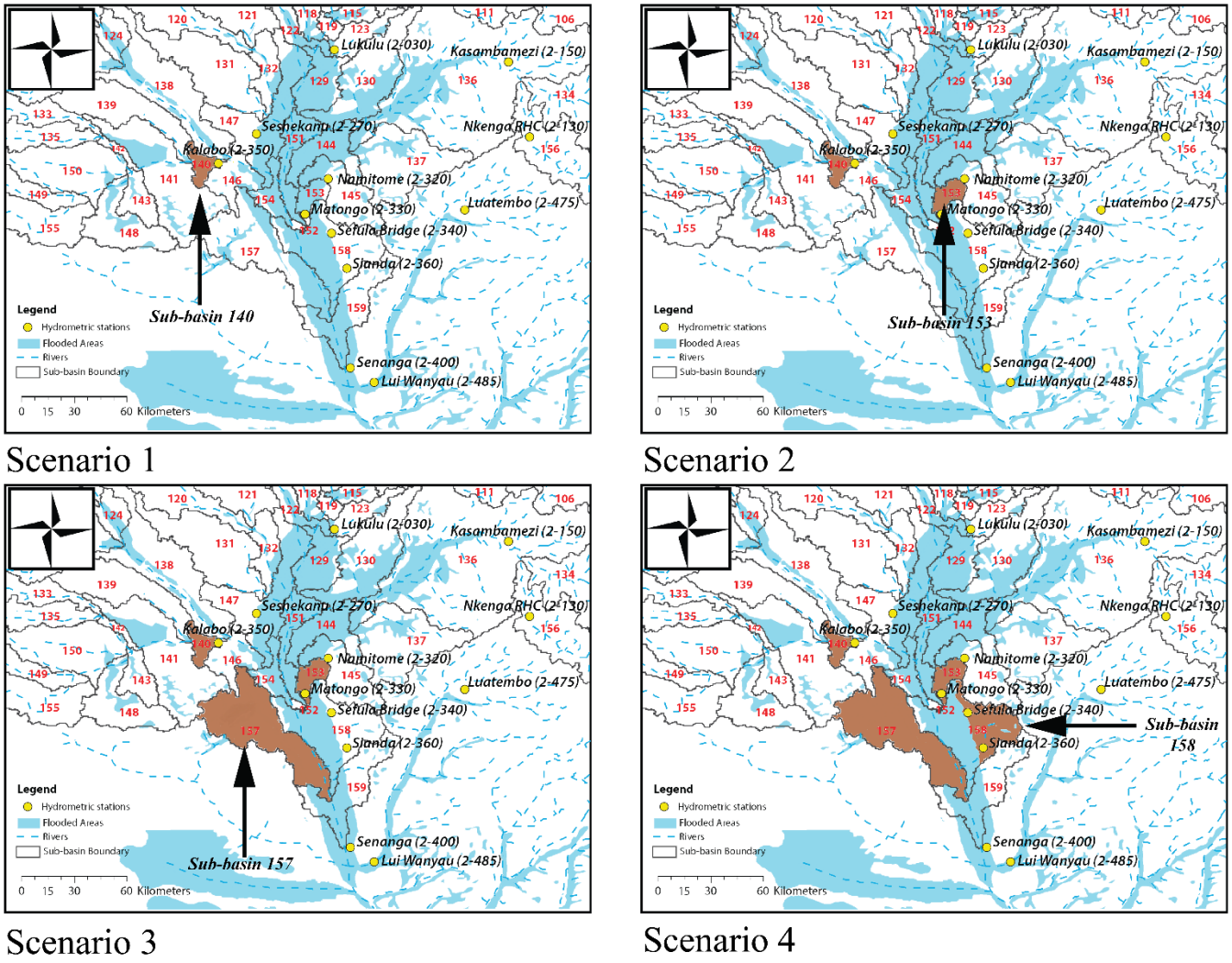

Figure 4.39: Maps of the Barotse Floodplain showing scenarios of the first four sub-basins having the highest sediment yield (in brown colour) starting with the worst scenario 1 to scenario 4, Western Zambia

From Figure 4.39 above, scenario 1 shows sub-basin 140 having the highest sediment yield of 0.609 tons. The results for these were obtained from the calibrated SWAT output files. Only those sub-basins occurring within the floodplain had their sedimentation yield totals calculated this time. These were total sediment yields for each sub-basin within the floodplain for the years 2001 to 2005. Sub-basin 140 was located along the Luanginga River, a river described by the local people to contain 'dark waters' due to the high levels of turbidity. These modelled results confirm that the field data results given in Figures 4.5(a) and 4.6 above correspond to the high turbidity levels in the Luanginga River.

Scenario number 2 (Figure 4.39) gives two highlighted sub-basins. The yield for Sub-basin 140 was seconded by 153 with a yield of 0.524 tons. Luanginga River's flow meets the Zambezi River at an acute angle. Using resultant vector relationships, the resultant hydrodynamic force pushes the water in the Zambezi River in a South East direction into Liyeyelo area, carrying along with it sediments and nutrients. Part of the resultant hydrodynamic force pushes the water, sediments and nutrients on the western bank, hence depositing sediments on the same bank. This forms part of sub-basin 157 (scenario 3 in Figure 4.39).

Finally, scenario 4 (Figure 4.39) gives the fourth affected sub-basin 158 in terms of decreasing sediment accumulation levels within the floodplain. Sub-basin 158 occurs within Sefula area, having a total sediment yield of 0.340 tons.

Sub-basin 140 scenario 1 (Figure 4.39) was the worst affected basin arising from the erosion of sediments in the Luanginga River sub-catchment which is relatively steep depositing the sediments on its way to the confluence with the Zambezi River. The sediments deposition was influenced by the availability of sediments, slope and flow velocity.

Figures 4.40 and 4.41 give summaries of the total sedimentation patterns in the floodplain as indicated by a bar-graph and a photograph taken in Sefula Agriculture Area respectively. From the photographs, sediments are mobilised from the agricultural activities leading to high sediment yields in sub-basin 158. Notice that the colour coding used for the bar-graph is a reflection of the figures given above for easier illustration (Figures 4.31, 4.33, 4.35, 4.37 and 4.39).

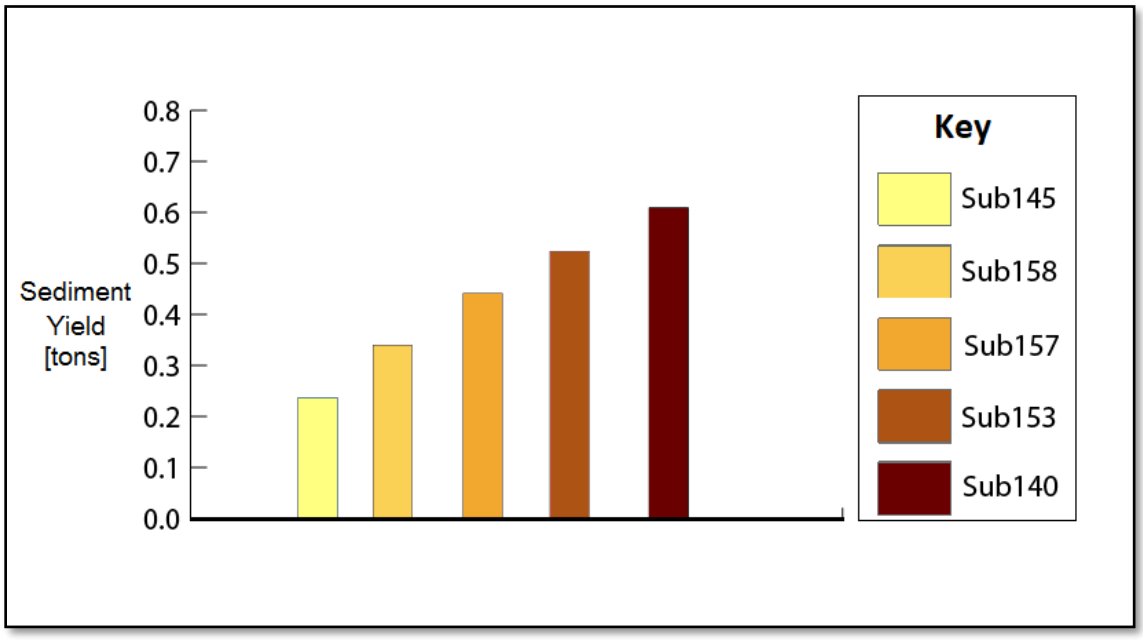

Figure 4.40: Bar graph of sedimentation totals for the years 2001 to 2005 for the sub-basins occurring within the Barotse Floodplain. These were the most affected sub-basins

Figure 4.41: Sefula Agricultural Area which occurs within sub-basin 158, Barotse Floodplain. The photograph was taken on 23rd October 2015

4.6.3 Discussion on Water-Sediment Distribution

Results from modelling indicated that deposition mostly occurred on riverbanks and floodplains (Figure 4.39) where there are several anthropogenic activities. The most affected sub-basins according to SWAT modelling where those sub-basins occurred on the Luanginga River with an annual mean yield of 0.609 tons for the years 2001 to 2005 indicating high levels of turbidity due to both geogenic and anthropogenic activities. Meinhardt *et al*. (2018) and Nyambe *et al*., (2018) show in their studies in the Luanginga catchment and the Barotse Floodplain, respectively, that these areas experience high levels of turbidity and as sedimentation as shown in this study. The mapping of sediment deposition in such a manner is similar to that of Betrie *et al*., (2011) who used SWAT to implement Best Management Practices (BMPs). Using this approach, BMP can also be implemented on the Barotse Floodplain using the four scenarios developed in this study. Note that only areas with the greatest amounts of sediment yields where mapped in this study and that the difference between this study and Betrie *et al*., (2001) was in the calibration process. Betrie *et al*., (2001) used a two-step calibration process which involves calibration for water quantity then followed by calibration of sediment data. These two processes require historical datasets for water quantity and sediments to calibrate, however, for this study, only historical water quantity data (water levels and flows) were available. This is why only a one-step calibration process was done, and the results (R^2 and NS) were quite reasonable when compared to other studies like Abbaspour *et al*, (2015), Habte *et al*, (2013), Phomcha, *et al*, (2011) and Duan *et al*, (2007) (Table 4-4). However, when the study by Duan *et al.*, (2007) are singled out, their SWAT plots were different from those of this study in that Duan et al., (2007) plotted for soil losses (erosion prone areas). Meanwhile, in this study, the areas plotted were for deposition and not for soil losses (erosion).

CHAPTER 5: CONCLUSION AND RECOMMENDATIONS

This chapter gives conclusions and recommendations based on findings of this study following the two primary objectives.

5.1 Conclusions

The conclusions of this study were:

i) The order of bacteriological contamination for the three transects was Mongu - Senanga at 85.7%, Mongu -Kalabo at 20.0% and Sioma – Kalabo at 16.7% based on the TNTC readings for each transect;

ii) The potential of hydrogen (pH) under physiochemical parameters showed an acidic inclined pH for the dry season ranging from 6.5 to 6.9 in hot spot areas and basic during the wet season ranging from 6.9 to 7.5. When these two ranges are compared to the WHO and ZABS guidelines for drinking water which are 6.5 to 8.5 and 6.5 to 8.0, respectively, the Barotse Floodplain is still safe;

iii) Turbidity in the floodplain varied with the Luanginga River showing the highest value of 87.9 NTU and the lowest value of 0.8 NTU observed in the Zambezi between Lukulu and the confluence with the Luanginga. In the Luanginga River, the observed turbidity was higher than the maximum permissible turbidity value (5.0 NTU) for drinking water according to WHO as well as ZABS;

iv) Nitrates are mostly transported during the wet season (decayed plant and animal remains moved by higher velocity) which had a mean value of 17.5mg/l (Figure 4.12). In contrast, the mean value of nitrates during the dry season was 1.5mg/l, which showed a decrease from 17.5mg/l, suggesting that small amounts of nutrients were transported during the dry season;

v) The Mongu – Senanga Transect had the highest EC values from the analysis of the four transects. This analysis was based on both the wet and dry seasons. The high EC values were due to the high levels of salts and anthropogenic activities along this transect;

vi) There were no traces of heavy metals in both water and sediment samples for the two years except for elements like calcium which were predominant; and

vii) The plots extracted from SWAT output files showed that sub-basin 140 along the Luanginga River hand the worst sedimentation yields (0.609 tons). This was followed by sub-basin 153 (0.524 tons) in Liyeyelo, sub-basin 157 (0.441 tons) on the western bank and sub-basin 158 (0.340 tons) in Sefula. The yields were calculated from the 2001 to 2005 annual totals.

5.2 Recommendations

The following recommendations are entirely based on the in-situ observations, modelling inadequacies and findings while in the field in the Barotse Floodplain, Western Zambia:

(i) The shifting of the hydrometric station from Senanga Hydrometric Station to Kalongola so that entire flow coming from upstream can be fully captured. The shifting of the station can be done by WARMA whereas maintaining the station at Senanga as it has a lot of historical data that can be useful to compare with Kalongola, if it is established;

(ii) Setting up sediment monitoring stations would help in calibrating and validating such models. This would thereby increase the amount of certainty in modelling and later on, help in forecasting due to improved model accuracy. WARMA in the Zambezi Catchment can choose areas that are critical like Sefula as predicted by the model for sediment monitoring as this is also a key agricultural area;

(iii) Future studies should look at relationships between sedimentation and degradation with the changes in land cover. This should also include the spatial distribution of rainfall patterns in comparison to land cover and degradation;

(iv) Emanating from (ii) and (iii), there is also the need for consistent water quality monitoring to cover the entire floodplain system to add to this baseline water quality database. This, in turn, will aid in improving model accuracy if both sediments and water quality parameters are consistently collected, thereby improving the accuracy of the model. Furthermore, water quality analysis for future research needs to be holistic and representative, that is, to cover all areas of the floodplain. This would improve the accuracy of the surfaces produced by interpolation for predicting the state of water quality in unreached areas. It would also be good to monitor water quality parameters from upstream and downstream of individual river stretches to see if there are any changes; and

(v) In Zambia, the Ministry of Agriculture needs to partner with universities to develop digital soil maps that are representative of Zambia for better modelling in the future.

(vi) Due to the high bacteriological contamination in densely populated areas characterised by farming and unmonitored sewerage disposals, it would be prudent to put water treatment before discharging into the river as a requirement.

REFERENCES

Abbaspour, K.C., Rouholahnejad, E., Vaghefi, S., Srinivasan, R., Yang, H., Kløve, B (2015). A continental-scale hydrology and water quality model for Europe: Calibration and uncertainty of a high-resolution large-scale SWAT model.. SWAT - CUP SWAT Calibration and Uncertainty Programs. Elsevier B.V,J. Hydrol. 2015, 524, pp.733–752

Abbaspour, K. C. (2015). SWAT - CUP SWAT Calibration and Uncertainty Programs. Eawag. Swiss Federal Institute of Aquatic Science and Technology, pp. 1-100.

Abbaspour, K., Vaghefi, S., Srinivasan, R (2017). A guideline for successful calibration and uncertainty analysis for soil and water assessment: A review of papers from the 2016 International SWAT Conference. Water 2018, pp.6 - 10.

Ahiablame, L., Chaubey, I. & Smith, D., (2010). Nutrient Content at the Sediment-Water Interface of Tile-Fed Agricultural Drainage Ditches. , pp.411–428.

Anon, (2012). Estimation of sediment yield in Kiliyar Sub-Watershed using SWAT Model. Anna University, College of Engineering, pp.1-36.

Arnold, J.G., Kiniry, J.R., Srinivasan, R., William, J.R., Haney, E. B., Neitsch, S. L. (2012). SWAT input/output Documentation. Version 2012. Texas Water Resources Institute , TR-439.

Baidu-Forson, J.J., Phiri, N., Ngu'ni, D., Mulele, S., Simainga, S., Situmo, J., Ndiyoi, M., Wahl, C., Gambone, F., Mulanda, A., Syatwinda, G. (2014). Assessment of agrobiodiversity resources in the Borotse flood plain, Zambia. CGIAR Research Program on Aquatic Agricultural Systems. Penang, Malaysia. Working Paper: AAS-2014-12, pp. 1-198.

Bakir, M. and Xingnan, Z., (2008). GIS-Based Hydrological Modelling: A comparative study of HEC-HMC and the Xinanjiang Model. *Twelfth International Water Technology Conference, IWTC12.* Alexandria, Egypt. Journal of Science and Technology 53 (5A). pp 189-195

Banda, S., Namafe. C.M., and Chakanika. W.W. (2015). Traditional Environmental Knowledge among Lozi Adults in Mitigating Climate Change in the Barotse Plains of Western Zambia.

International Journal of Humanities Social Sciences and Education (IJHSSE). Volume 2, Issue 9, pp.222-239.

Basin, Z. R. (2003). *ZAMBIA : local economic dependence on wetland resources Integrating Wetland Economic Values into River Basin Management*. *May*.

Barotseland Post, (2018). The Barotseland Post, Zambia battles cholera as BRE calls for measures to prevent it spreading to Barotseland. Available from: < http://barotselandpost.com/top-stories/zambia-battles-cholera-as-bre-calls-for-measures-to-prevent-it-spreading-to-barotseland >. [3rd April 2019]

Bayern, P. V. (2002). Handbuch der Technischien Gewasserraufsicht, Bayerisches Landesamt fur Wasserwitschaft, pp.106-129.

Balek, J., (1971). *Water Balance of the Zambezi Basin, Technical Report 15*. Lusaka, Zambia: National Council for Scientific Research. International Rivers, pp.1-46

Beilfuss, R., (2012). *A Risky Climate for Southern African Hydro Assessing Hydrological Risks and a Risky Climate for Southern African Hydro*, International Rivers, pp.2-46

Betrie, G. D. and Van Griensven, A., (2011). *Sediment management modelling in the Blue Nile Basin using SWAT model*, Hydrology and Earth System Sciences, pp.807-818.

Biagi, L., Brovelli, M. and Zamboni, G., 2011. A DTM multi-resolution compressed model for efficient data storage and network transfer. *Int Arch Photogramm Remote Sens Spat Inf Sci*, *38*, pp.7-13.

Bilotta, G.S. and Brazier, R.E., (2008). Understanding the influence of suspended solids on water quality and aquatic biota. *Water research*, *42*(12), pp.2849-2861.

Bilotta, G.S., Burnside, N.G., Cheek, L., Dunbar, M.J., Grove, M.K., Harrison, C., Joyce, C., Peacock, C. and Davy-Bowker, J., (2012). Developing environment-specific water quality guidelines for suspended particulate matter. *Water Research*, *46*(7), pp.2324-2332.

Brooks, E.S., Dobre, M., Elliot, W.J., Wu, J.Q. and Boll, J., 2016. Watershed-scale evaluation of the Water Erosion Prediction Project (WEPP) model in the Lake Tahoe basin. *Journal of Hydrology*, *533*, pp.389-402.

Brunner, G.W., 2016. HEC-RAS River Analysis System, User â€™ s Manual, Version 5.0., (5), pp.1–960.

Burt R., Weber T., Park S., Yochum S., and Ferguson R., (2011). "Trace Element Concentration and Speciation in Selected Mining-Contaminated Soils and Water in Willow Creek Floodplain, Colorado," Applied and Environmental Soil Science, vol. 2011, Article ID 237071, pp.1-20.

Central Statistics Office of Zambia (CSO), (2012). Agriculture Statistics of Zambia, Western Province. Accessed from: http://Zambia.opendataforaforafrica.org/ZMAGSTB2016/agriculture-statistical-bulletin-of-zambia-2012.

Change, C. & Basis, T.S., (2001). CLIMATE CHANGE 2001: Intergovernmental Panel on Climate Change, pp.1-94

Chileshe, P., Trottier, J. and Wilson, L., (2005, January). Translation of water rights and water management in Zambia. In *International workshop on African water laws: plural legislative frameworks for rural water management in Africa* (pp. 26-28).

Ciach, G.J. (2003). Local random errors in tipping-bucket rain gauge measurements. *Journal of Atmospheric and Oceanic Technology* 20(5): pp.752-759.

Clark, I. (1979). Practical Geostatistics. London, Applied Science Publishers LTD, Elsevier Science and Technology, pp. 1-141.

Dingman, L.S. (2009), Fluvial hydraulics, Oxford University Press, USA, New York, pp.3-559

Duan, Z., Song, X., & Liu., J., 2007. Application of SWAT for sediment yield estimation in a mountainous agricultural basin. Chinese Academy of Sciences, pp.20-25.

Dyrness, C.T. and Cleve Van K. (1993). Control of surface soil chemistry in early-successional floodplain soils along the Tanana River, interior Alaska. Canadian Journal of Forest Research, 1993, 23(5): 979-994, https://doi.org/10.1139/x93-126

Emam,A. R., Kappas, M., Linh, NHK, Renchin T (2017) 'Hydrological Modeling and Runoff Mitigation in an Ungauged Basin of Central Vietnam Using'. doi: 10.3390/hydrology4010016.

Easton, Z.M., Fuka, D.R., White, E.D., Collick, A.S., Biruk Ashagre, B., McCartney, M., Awulachew, S.B., Ahmed, A.A. and Steenhuis, T.S., 2010. A multi basin SWAT model analysis of runoff and sedimentation in the Blue Nile, Ethiopia. *Hydrology and earth system sciences*, *14*(10), pp.1827-1841.

El Habbasha. S. F, and Ibrahim, F. M. (2016) 'Calcium : Physiological function , deficiency and absorption Calcium : Physiological Function , Deficiency and Absorption', 2016(January 2015). ISSN: 0974-4290Vol.8, No.12pp196-202

Fanshawe, D., (2010). Vegetation Description of the Upper Zambezi Districts of Zambia, Famona, Bulawayo, Zimbabwe: Biodiversity Foundation for Africa, pp 1-20.

FAO/UNESCO (2009) Soil Classification.URL: http://www.fao.org/nr/Water/docs/Harm-World-Soil-DBv7cv.pdf. pp.1-43

Fisher, T. & Niton, S., (2010). Themo Fisher Science Niton Analyzers XL2 [niton@thermofisher.com]. Billerica Publishers, USA, pp. 1-191.

Flaxman, E. M. (1975) *Sediment and its effect on water*. New Mexico. American Geophysical Union, p78.

Fontaine, T.A., Cruickshank, T.S., Arnold, J.G. and Hotchkiss, R.H., (2002). Development of a snowfall–snowmelt routine for mountainous terrain for the soil water assessment tool (SWAT). *Journal of hydrology*, *262*(1-4), pp.209-223.

Francos, A., Bidoglio, G., Galbiati, L., Bouraoui, F., Elorza, F.J., Rekolainen, S., Manni, K. and Granlund, K., (2001). Hydrological and water quality modelling in a medium-sized coastal

basin. *Physics and chemistry of the earth, part B: Hydrology, Oceans and Atmosphere*, *26*(1), pp.47-52.

Fuka, D.R., Walter, M.T., MacAlister, C., Degaetano, A.T., Steenhuis, T.S. and Easton, Z.M., 2014. Using the Climate Forecast System Reanalysis as weather input data for watershed models. *Hydrological Processes, 28*(22), pp.5613-5623.

Gassman, P.W., Reyes, M.R., Green, C.H. and Arnold, J.G., 2007. The soil and water assessment tool: historical development, applications, and future research directions. *Transactions of the ASABE, 50*(4), pp.1211-1250.

Gotway, C. A., Helsel, D. R. and Hirsch, R. M. (1994) 'Statistical Methods in Water Resources', Technometrics, 36(3), p. 323. doi: 10.2307/1269385.

Gray, N. F., (2008). Drinking water quality: Problems and Solutions, second ed. Cambridge University Press, New York, p. 520.

Gregory, S.V. and Swanson, F.J. (1991). An Ecosystem Perspective of Riparian Zones. Bio-Science 40: pp.540-551.

GRZ, (2013). Ministry of Finance and National Planning. Investment Projects for the Barotse and Kafue Sub-basins under the Strategic Programme for Climate Resilience in Zambia Environmental and Social Management Framework. Final Draft Volume I. NIRAS, pp.1-134.

Habib, E, Aduvala, A.V., Meselhe E.A., (2008). Analysis of radar-rainfall error characteristics and implications for stream flow simulation uncertainity. *Hydrological Science Journal* 53(3): pp.568-587.

Habte, K., Mamo, M. & Jain, M.K., (2013). Runoff and Sediment Modelling Using SWAT in Gumera. , 2013(October), pp.196–205.

Haddon, I.G. & McCarthy, T.S., (2005). The Mesozoic-Cenozoic interior sag basins of Central Africa: The Late-Cretaceous-Cenozoic Kalahari and Okavango basins. *Journal of Africa Earth Sciences*, 43, pp.316-333.

Inchell, M.W., Rinivasan, R.S. & Uzio, M.D.I.L., (2010). Arc SWAT Interface for SWAT 2009 User's Guide, p.495

IRI Climate Library Satellite Rainfall Data, viewed 16 July (2016) http://iridl.ldeo.columbia.edu/SOURCES/

IUCN, (2003). Case Studies in Wetland Valuation #2; Barotse Floodplain, Zambia: Local Economic Dependence on Wetland Resources. *Integrating Wetland Economic Values into River Basin Management*, pp.1-6

Japan International Cooperation Agency (JICA) (1995). The study on the national water resources master plan in the Republic of Zambia. Final report. Supporting report Vol. I (D): Hydrogeology. D-10

Johnson, D. L., Ambrose, S. H., Bassett, T. J., Bowen, M. L., Crummey, D. E., Isaacson, J. S., Johnson, D. N., Lamb, P., Saul, M., and Winter-Nelson, A. E. (1997). Meaning of Environmental Terms. J. Environ. Qual. 26, pp.581-589.

Taylor, D.O.U.G.L.A.S., 2002. The Ramsar convention on wetlands. *Parks*, *12*(3), pp.42-49.

Timberlake, J., 2000. *Biodiversity of the Zambezi basin* (p. 23). Bulawayo, Zimbabwe: Biodiversity Foundation for Africa.

Jozef, R. and Bobáľ, P. (2010). Simulation of Sediment Transport in Catchment Using ArcSWAT 2005 Dynamic Erosion Model Exemplified by the Catchment of the Ostravice River, Technical University of Ostrava, pp.27-35.

Kaleab, H. M. M. and Manoj, K. J. (2013). Runoff and Sediment Modelling Using SWAT in Gumera Catchment, Ethiopia. *Open Journal of Modern Hydrology*, pp.196-205

Kouwen, N., Danard, M., Bingeman, A., Luo, W., Seglenieks, F.R., Soulis, E.D., (2005). Case study: watershed modelling with distributed weather model data. *Journal of Hydrologic Engineering* 10(1): pp.23-38.

Liersch, S., (2003). The Program pcpSTAT. User's Manual. Berlin. Accessed from: https://wenku.baidu.com/view/9e478e4a767f5acfa1c7cd53?_wkts_=1674575523327

Loucks, D.P. and Van Beek, E., 2017. *Water resource systems planning and management: An introduction to methods, models, and applications*. Springer.

Lovett, S., Price, P. & Edgar, B. (eds) (2007). Salt, nutrient, sediment and interactions. Findings from the National River Contaminants Program, Land & Water Australia, Canberra, p.150.

Mehta, V.K., Walter M.T., Brooks B.S., Steenhuis T.S., Walter M.F., Johnson M., Bull J., Thongs D., (2004). Evaluation and application of SMR for watershed modelling in the Catskill Mountains of New York State. *Environmental Modelling and Assessment* **9**(2): pp.77-89.

Meinhardt, M., Fleischer, M., Fink, M., Kralisch, S., Kenabatho, P., de Clercq, W.P., Zimba, H., Phiri, W. & Helmschrot, J. (2018) Semi-arid catchments under change: Adapted hydrological models to simulate the influence of climate change and human activities on rainfall-runoff processes in southern Africa. In: Climate change and adaptive land management in southern Africa – assessments, changes, challenges, and solutions (ed. by Revermann, R., Krewenka, K.M., Schmiedel, U., Olwoch, J.M., Helmschrot, J. & Jürgens, N.), pp. 114-130, Biodiversity & Ecology, 6, Klaus Hess Publishers, Göttingen & Windhoek. doi:10.7809/b-e.00313

Miller, C.L. and La Flamme, R.A., (1958). Photogrammetric Engineering and Remote Sensing. The Digital Terrain Model-Theory and Application, 24, pp.433-442.

Money, N.J., (1972). An Outline of the Geology of Western Zambia. Records of the Geological Survey, Republic of Zambia No.12, pp. 103-123.

Mongu MET Climate Normals, (1961 – 1991). National Oceanic and Atmospheric Administration. Retrieved April 5, 2015 (https://www.yr.no/place/Zambia/Western/Mongu/statistics.html).

Mulamattathil, S.G., Bezuidenhout, C., Mbewe, M. and Ateba, C.N., (2014). Isolation of environmental bacteria from surface and drinking water in Mafikeng, South Africa, and characterization using their antibiotic resistance profiles. *Journal of pathogens, 2014*.

Mutenyo, I., Nejadhashemi, A.P., Woznicki, S.A. and Giri, S., (2013). Evaluation of SWAT performance on a mountainous watershed in tropical Africa. Hydrol. Curr. Res.

Mutonga, M., (2012). 'An Ethical Assessment of Human Adaptation to Annual Floods in Mongu's Barotse Floodplain and its Impact on Environment'. Lusaka: University of Zambia, pp.1-81.

Muzumara, M., Sichingabula, H.M., Bauer-Gottwein, P. and Nyambe, I.A., 2014. APPLICATION OF THE SOIL WATER ASSESSMENT TOOL (SWAT) USING REMOTE SENSED DATA ON THE KABOMPO RIVER BASIN, ZAMBIA. *Journal of Natural and Applied Sciences*, *1*(1), pp.4-19.

Nachtergaele, F., Velthuizen, H. Van & Verelst, L., (2008). Harmonized world soil database. *Food and Agriculture*, p.43. Available at: http://www.fao.org/nr/Water/docs/Harm-World-Soil-DBv7cv.pdf.

Naiman, R.J., Bechtold, J.S., Drake, D.C., Latterell, J.J., O'Keefe, T.C. and Balian, E.V., (2005). Origins, patterns, and importance of heterogeneity in riparian systems. In Ecosystem function in heterogeneous landscapes (pp. 279-309). Springer, New York, NY.

Naimen, R.J. and De ´camps, H. eds. (1997). The Ecology of Interfaces-Riparian Zones. Annual Review of Ecology and Systematics 28: pp.621-658.

Ndomba, P. M. & Griensven, A. Van, (2010). Suitability of SWAT Model for Sediment Yields Modelling in the Eastern Africa. In Tech, pp.631-684.

Nicholas V. C. Polunin (ed.) (2008). *Aquatic Ecosystems*. [Online]. Cambridge: Cambridge University Press. Available from: Cambridge Books Online <http://dx.doi.org/10.1017/CBO9780511751790> [Accessed 17 April 2015].

National Oceanic & Atmospheric Administration, (2016). *Earth System Research Laboratory: Physical Sciences Division*, viewed 23 June 2016, www.esrl.noaa.gov/psd/data/composites/reference.html

Ndungu, J.N. (2014). *Assessing Water Quality in Lake Naivasha*. University of Twente , Netherlands, pp. 1-149

Noe, G.B. & Hupp, C.R., (2007). *Seasonal Variation in Nutrient Retention During Inundation of A Short-Hydroperiod Floodplain* y., 1101(July), pp.1088–1101.

Neitsch, S. L., Anorld, J.G., Kiniry, J. R., Williams, J. R., (2005). Soil and Water Assessment Tool – Theoretical Documentation – Version 2005, Grassland, Soil and Water Research Laboratory, Agricultural Research Service and Blackland Research Centre, Texas Agric exp. station

Nyairo, W.N., Owuor, P.O. & Kengara, F.O (2015). Effect of anthropogenic activities on the water quality of Amala and Nyangores tributaries of River Mara in Kenya. *Journal of Environmental Monitoring and Assessment* 187: 691. https://doi.org/10.1007/s10661-015-4913-8

Nyambe, I., Chabala, A., Banda, K., Zimba, H. & Phiri, W. (2018) Determinants of spatio-temporal variability of water quality in the Barotse Floodplain, western Zambia. In: Climate change and adaptive land management in southern Africa – assessments, changes, challenges, and solutions (ed. by Revermann, R., Krewenka, K.M., Schmiedel, U., Olwoch, J.M., Helmschrot, J. & Jürgens, N.), pp. 96-105, Biodiversity & Ecology, 6, Klaus Hess Publishers, Göttingen & Windhoek. doi:10.7809/b-e.00310

Nyoni, F.C., (2014). *Carbon dynamics in two river systems in Zambia A comparative study of the Zambezi and the Kafue Rivers.* The University of Zambia, School of Mines, Department of Geology, Integrated Water Resources Management Centre, Lusaka, pp.1-102.

Obarrio, M.G. De, (2005). Water Quality and its Spatial Variability in Lake Water Quality and its Spatial Variability in Lake Cuitzeo, Mexico. Institute of Geo-information Science and Earth Observation, pp.1-59.

O'Sullivan, D. and Unwin D., (2003). *Geographic information analysis*. John Wiley & Sons., Inc., Hoboken, New Jersey, pp.1-32.

Phomcha, P., Wirojanagud, P., Vangpaisal, T., Thaveevouthti, T., (2011) 'Predicting sediment discharge in an agricultural watershed : A case study of the Lam Sonthi watershed ', 37, pp. 43–50. doi: 10.2306/scienceasia1513-1874.2011.37.043.

Preksedis, M.N. and Van Griensven, A. (2011). Suitability of SWAT Model for Sediment Yields Modelling in the Eastern Africa, Advances in Data, Methods and Their Applications in Geosciences, Dr.DongMei Chen (Ed.), ISBN:978-953-307-737-6, InTech, Available from: http://www.intechopen.com/books/advances-in-data-methods-and-their-applications-in-geoscience/suitability-of-swat-model-for-sediment-yields-modelling-in-the-eastern-africa, pp.261-284

Qiu, L., Zheng, F. & Yiu, R., (2012). SWAT-based runoff and sediment simulation in a small watershed, the loessial hilly-gullied region of China: capabilities and challenges. *International Journal of Sediment Research*, 27(2), pp.226-234. Available at: http://linkinghub.elsevier.com/retrieve/pii/S1001627912600304 [Accessed August 11, 2014].

Richard, B. (2012). A Risky Climate for Southern African Hydro. Assessing hydrological risks and consequences for Zambezi River Basin Dams, pp.1-46

Richter, B. D., Braun, D. P., Mendelson, M. A., Master, L. L., (2005). Threats to imperiled freshwater fauna. Conservation Biology 11 (5), pp.1081-1093.

Riley, J.S. (1997). *The sediment concentration – turbidity relation: its value in monitoring at Ranger Uranium Mine, Northern Territory*, Australia. Kingswood. University of Western Sydney, Catena 32(1), pp.1-14.

Rukuni, S., (2006). Modelling the response of small multi-purpose reservoirs to hydrology for improved rural livelihoods in the Mzingwane catchment: Limpopo Basin, University of Zimbabwe, pp.1-75

SADC/SARDC and others (2012). *Zambezi River Basin Atlas of the Changing Environment*. SADC, SARDC, ZAMCOM, GRID-Arendal, UNEP. Gaborone, Harare and Arendal, pp.1-148

SASSCAL, (2012). Project Document for Task ID 191. Developing a Water Quality and Quantity Database for Western Zambia, pp.1-6.

Schulze, R.E., (1995). Hydrological Models. IHE Lecture notes No. HH062/95/1.

Sorrell, B. Clarkson, B. and Reeves, P. (2004). Wetland restoration. In: Harding, J., Mosley, P., Pearson, C., and Sorrell, B. (Editors), Freshwaters of New Zealand. New Zealand Hydrological and Limnological Societies, Christchurch, New Zealand.

Shanbehzadeh, S., Vahid Dastjerdi, M., Hassanzadeh, A. and Kiyanizadeh, T., 2014. Heavy metals in water and sediment: a case study of Tembi River. *Journal of environmental and public health, 2014*.

Shaw, E.M. (1983). *Hydrology in Practice.* Van Nostrand Reinhold, United Kingdom. CRC Press, pp.1-546.

Setegn, S.G., Dargahi, B., Srinivasan, R. and Melesse, A.M., 2010. Modeling of Sediment Yield From Anjeni-Gauged Watershed, Ethiopia Using SWAT Model 1. *JAWRA Journal of the American Water Resources Association*, *46*(3), pp.514-526.

Stahl, R. and Ramadan, A. B. (2008). Environmental Studies on Water Quality of the Ismailia Canal/Egypt. Link: https://publikationen.bibliothek.kit.edu/270072585/3815282, pp. 1-58.

SWAT Documentation, T., (2009). Soil & Water Assessment Tool Theoretical Documentation Version 2009. Taxes A and M University. Taxes Water Resource institute, pp.1-597.

SWAT Documentation, T., (2012). Soil & Water Assessment Tool Theoretical Documentation Version 2012. Taxes A and M University. Taxes Water Resource institute, pp.1-597.

Tanner, C., Caldwell, K., Ray, D. and McIntosh, J (2007). Constructing wetlands to treat nutrient-rich inflows to Lake Okaro, Rotorua. Presentation at the South Pacific Stormwater Conference, Auckland.

The Barotse Cultural Landscape, (2009). National Heritage Conservation Commission. Zambia, Western Province. Ref 5428.

Thomas, D. & Shaw, P., 1991a. The deposition and development of the Kalahari Group sediments, Central Southern Africa. *Journal of African Earth Sciences (and the Middle East)*, 10, pp.187-197.

Tockner, K. and Stanford, J.A. (2002). Riverine flood plains: present state and future trends. Environmental Conservation 29: pp.308-330.

Tong, S.T. and Chen, W., 2002. Modeling the relationship between land use and surface water quality. *Journal of environmental management*, *66*(4), pp.377-393.

Turpie, J. Smith, B., Emerton, L., and Barnes, J. (1999). Economic value of the Zambezi Basin wetlands. Zambezi Basin Wetlands Conservation and Resource Utilization Project, IUCN Regional Office for Southern Africa. The Canadian International Development Agency (CIDA). Printed by University of Cape Town, pp.23-28.

United Nations (2007). "Glossary of environmental statistics, studies in methods," An Operational Manual. New York, pp.1-67

Van Liew, M.W., Arnold, J.G. and Bosch, D.D., 2005. Problems and potential of autocalibrating a hydrologic model. *Transactions of the ASAE*, *48*(3), pp.1025-1040.

Veith, T.L. and Ghebremichael, L.T., 2009, August. How to: applying and interpreting the SWAT Auto-calibration tools. In *2009 international SWAT conference, conference proceedings* (Vol. 26).

Wamulume, J., Landert, J., Zurbrügg, R., Nyambe, I., Wehrli, B. and Senn, D.B., (2011). Exploring the hydrology and biogeochemistry of the dam-impacted Kafue River and Kafue Flats (Zambia). *Physics and Chemistry of the Earth, Parts A/B/C*, *36*(14-15), pp.775-788.

Water Resources Management Act, (2011). No.21 of 2011, Government Printers, pp.265-378

Weyhenmeyer, G.A., Hartmann, J., Hessen, D.O., Kopáček, J., Hejzlar, J., Jacquet, S., Hamilton, S.K., Verburg, P., Leach, T.H., Schmid, M. and Flaim, G., 2019. Widespread diminishing anthropogenic effects on calcium in freshwaters. *Scientific Reports*, *9*(1), pp.1-10.

Williams, C.R., Nisbet, B.W., van der Stelt, B. and Richards, M.N., (2009) ZAMBIA: EXPLORATION POTENTIAL FOR IRON OXIDE COPPER–GOLD DEPOSITS AND A RE-EVALUATION OF THE COPPERBELT.

WMO, (1985). Review of requirements for area-average precipitation data, surface-based and space-based estimation techniques, space and time sampling, accuracy and error; data exchange. WCP-100, WMO/TD-No. 115, pp. 57

XL2 User's Guide v 7.1.1, (2010). Thermo Fisher Scientific Niton Analyzers. Revision C.

Yangwen, J., Guangheng, N., Yoshihisa, K. and Tadashi, S., (2001). *Development of WEP model and its application to an urban watershed*. *Hydrology Processes* [online] Available at: onlinelibrary.wiley.com (Accessed 16th July, 2015).

Yingyi Chen, Jing Xu, Huihui Yu, Zhumi Zhen, and Daoliang Li,(2016). "Three-Dimensional Short-Term Prediction Model of Dissolved Oxygen Content Based on PSO-BPANN Algorithm Coupled with Kriging Interpolation," Mathematical Problems in Engineering, vol. 2016, Article ID 6564202, 10 pages, 2016. doi:10.1155/2016/6564202

ZEMA, GRID- Arendal, GRID-Sioux Falls, UNEP (2013). *Zambia Atlas of Our Changing Environment.* ZEMA, GRID- Arendal, GRID-Sioux Falls, UNEP. Lusaka, Arendal, Sioux Falls and Nairobi, pp.12-116.

Zimba, H., Kawawa, B., Chabala, A., Phiri, W., Selsam, P., Meinhardt, M. and Nyambe, I., (2018). Assessment of trends in inundation extent in the Barotse Floodplain, upper Zambezi River Basin: A remote sensing-based approach. *Journal of Hydrology: Regional Studies*, *15*, pp.149-170.

Zuijdgeest, A.L., Zurbrugg, R., Blank, N., Fulcri, R., Senn, D.B., and Wehrli, B., (2015). 'Seasonal dynamics of carbon and nutrients from two contrasting tropical floodplain systems in the Zambezi River basin'. *Biogeosciences*, 12(24), pp.7535–7547.

APPENDICES

Appendix 1a: Samples collected during the first field campaign in April 2014 showing analysed parameters, Barotse Floodplain, Western Zambia

Number	ID	Alkalinity (as mg CaCO3/l)	Ammonia (as NH4-Nmg/l)	Total hardness (as mg CaCO3/l)	Nitrates (as NO3 -Nmg/l)	Nitrites (as NO2 -Nmg/l)	Total phosphates (mg/l)	Total Dissolved Solids (mg/l)	Total Suspended Solids (mg/l)	Turbidity (NTU)	Calcium hardness (as mg CaCO3/l)	Month	Period	Year	Latitude	Longitude
1	IB1	26	<0.01	30	18.62	<0.001	<0.01	69	14.8	133	20	April	High Flow	2014	-15.2754	23.06725
2	IB2	18	<0.01	20	12.68	<0.001	<0.01	58	<1.0	0.95	16	April	High Flow	2014	-15.2644	22.99681667
3	IB3	22	<0.01	26	7.15	<0.001	<0.01	45	<1.0	1.11	14	April	High Flow	2014	-15.2693	23.00903333
4	IB4	12	<0.01	14	6.36	<0.001	<0.01	34	<1.0	1.16	10	April	High Flow	2014	-15.2475	23.00268333
5	IB5	16	<0.01	18	16.06	<0.001	<0.01	53	<1.0	1.18	16	April	High Flow	2014	-15.2736	23.01496667
6	IB6	12	<0.01	16	13.29	<0.001	0.05	54	<1.0	1.32	18	April	High Flow	2014	-15.2989	23.07163333
7	IB7	18	<0.01	22	17.6	<0.001	<0.01	61	<1.0	0.76	18	April	High Flow	2014	-15.2879	23.09993333
8	IB8	10	<0.01	14	10.8	<0.001	0.05	40	<1.0	1.81	12	April	High Flow	2014	-15.2739	23.11758333
9	IB9	18	<0.01	22	21.68	<0.001	0.08	67	<1.0	1.3	14	April	High Flow	2014	-15.2046	22.98616667
10	IB10	12	<0.01	14	22.72	<0.001	0.08	67	<1.0	1.5	8	April	High Flow	2014	-15.19	22.9532
11	IB11	20	<0.01	22	16.78	<0.001	<0.01	65	<1.0	1.7	12	April	High Flow	2014	-15.1852	22.93771667
12	IB12	19	<0.01	22	15.05	<0.001	0.09	69	<1.0	1.4	12	April	High Flow	2014	-15.1904	22.9438
13	IB13	4	<0.01	16	16.76	<0.001	<0.01	141	<1.0	0.8	6	April	High Flow	2014	-15.1384	22.87681667
14	IB14	20	<0.01	24	12.76	<0.001	0.08	55	<1.0	1	8	April	High Flow	2014	-15.0913	22.80635
15	IB15	10	<0.01	12	18.45	<0.001	0.05	66	<1.0	0.8	8	April	High Flow	2014	-15.0276	22.7382
16	IB16	54	<0.01	64	16.82	<0.001	0.04	65	4.2	24.4	28	April	High Flow	2014	-15.2615	23.13323333
17	IB17	16	<0.01	18	17.09	<0.001	<0.01	69	3.4	11.3	14	April	High Flow	2014	-15.1201	23.1441
18	IB18	10	<0.01	12	17.75	<0.001	<0.01	74	3.8	16.3	8	April	High Flow	2014	-15.5712	23.28088333
19	IB19	14	<0.01	16	19.48	<0.001	0.07	71	4.4	10.9	4	April	High Flow	2014	-15.3893	23.17723333
20	IB20	8	<0.01	10	1.51	<0.001	0.09	31	12.6	40.2	12	April	High Flow	2014	-15.6844	23.247
21	IB21	30	<0.01	36	3.16	<0.001	<0.01	31	<1.0	2.2	16	April	High Flow	2014	-16.0894	23.2941

Number	ID	Alkalinity (as mg CaCO3/l)	Ammonia (as NH4-Nmg/l)	Total hardness (as mg CaCO3/l)	Nitrates (as NO3 -Nmg/l)	Nitrites (as NO2 -Nmg/l)	Total phosphates (mg/l)	Total Dissolved Solids (mg/l)	Total Suspended Solids (mg/l)	Turbidity (NTU)	Calcium hardness (as mg CaCO3/l)	Month	Period	Year	Latitude	Longitude
22	IB22	10	<0.01	14	4.39	<0.001	0.03	43	2.8	13.1	20	April	High Flow	2014	-16.1168	23.28866667
23	IB23	66	<0.01	70	0.54	0.004	0.07	79	2	6.7	52	April	High Flow	2014	-16.1056	23.29638333
24	IB24	96	0.84	100	0.11	0.003	<0.01	41	<1.0	2.05	72	April	High Flow	2014	-17.4667	24.24728333
25	IB25	128	<0.01	148	<0.01	0.006	<0.01	38	<1.0	2.74	64	April	High Flow	2014	-16.6718	23.62583333
26	IB26	126	<0.01	136	<0.01	0.014	0.12	37	<1.0	2.7	44	April	High Flow	2014	-16.3908	23.32511667
27	IB27	92	<0.01	96	1.23	0.008	0.09	53	<1.0	4.28	52	April	High Flow	2014	-16.0792	23.02993333
28	IB28	140	<0.01	148	0.11	0.011	0.06	54	<1.0	2.34	60	April	High Flow	2014	-16.0547	23.17063333
29	IB29	120	<0.01	168	2.26	0.003	<0.01	39	3	6.53	64	April	High Flow	2014	-15.966	23.14498333
30	IB30	210	0.09	368	1.63	0.006	<0.01	44	2	4.02	164	April	High Flow	2014	-15.8891	23.1326
31	IB31	74	0.11	80	<0.01	0.002	<0.01	35	2.9	4.7	48	April	High Flow	2014	-15.8309	23.06768333
32	IB32	36	<0.01	44	5.11	<0.001	<0.01	34	<1.0	1.69	60	April	High Flow	2014	-15.7533	23.05296667
33	IB33	100	<0.01	104	0.09	<0.001	<0.01	30	<1.0	2.42	40	April	High Flow	2014	-15.6846	23.04038333
34	IB34	62	0.13	68	1.84	0.002	<0.01	34	<1.0	1.86	28	April	High Flow	2014	-14.9872	22.68306667
35	IB35	116	0.08	120	3.94	0.004	<0.01	39	<1.0	3.85	56	April	High Flow	2014	-15.3485	22.74348333
36	IB36	248	0.03	300	2.26	0.013	0.09	84	5.8	9.46	136	April	High Flow	2014	-15.3973	22.85498333
37	IB37	146	<0.01	152	5.11	0.094	0.14	169	3.6	5.5	84	April	High Flow	2014	-16.3104	23.17816667
38	IB38	140	<0.01	146	<0.01	0.032	0.08	197	6.3	10.2	128	April	High Flow	2014	-16.3106	23.15818333
39	IB39	158	<0.01	160	<0.01	<0.001	0.13	44	<1.0	3.11	148	April	High Flow	2014	-16.2442	23.23766667
40	IB40	200	<0.01	208	1.34	0.03	<0.01	62	2.8	4.04	156	April	High Flow	2014	-16.3539	23.27646667
41	IB41	168	0.11	172	6.02	0.136	0.05	166	3.9	7.82	144	April	High Flow	2014	-16.2015	23.34011667
42	IB42	154	0.07	160	0.96	0.017	<0.01	62	<1.0	1.34	52	April	High Flow	2014	-16.227	23.34096667
43	IB43	78	0.14	84	0.84	0.009	<0.01	77	2.6	5.02	68	April	High Flow	2014	-16.3958	23.41213333
44	IB44	148	<0.01	152	1.72	0.032	<0.01	48	3.8	7.84	40	April	High Flow	2014	-16.6335	23.55756667

Appendix 1b: Samples collected during the first field campaign in Barotse Floodplain, Western Zambia showing comparison of in-situ results and the laboratory ones

Number	ID	pH-InSitu	pH-Lab	Temp(^{0}C)-InSitu	DO(mg/l)-InSitu	EC (µs/cm)-InSitu	EC (mMhos/cm)-Lab	Month	Period	Year	Latitude	Longitude
1	IB1	7.5	6.02	26.8	5.62	41.6	140	April	High Flow	2014	-15.2754	23.06725
2	IB2	7.6	6.22	26.7	3.12	34.5	115	April	High Flow	2014	-15.2644	22.996817
3	IB3	7.2	5.59	26.2	3.09	34.8	90	April	High Flow	2014	-15.2693	23.009033
4	IB4	7.5	6.11	26.3	2.9	35	70	April	High Flow	2014	-15.2475	23.002683
5	IB5	7.1	6.21	26.1	2.86	35.2	106	April	High Flow	2014	-15.2736	23.014967
6	IB6	7.6	6.62	26.3	4.33	37.3	108	April	High Flow	2014	-15.2989	23.071633
7	IB7	7.5	6.31	26.1	6.77	46.6	122	April	High Flow	2014	-15.2879	23.099933
8	IB8	7.2	6	25.8	2.76	29.9	61	April	High Flow	2014	-15.2739	23.117583
9	IB9	8.6	4.96	25.9	2.64	35.9	135	April	High Flow	2014	-15.2046	22.986167
10	IB10	7.3	5.87	25	3.3	36.5	139	April	High Flow	2014	-15.19	22.9532
11	IB11	7.5	5.94	25.7	4.92	37	126	April	High Flow	2014	-15.1852	22.937717
12	IB12	7.2	5.85	25.9	4.63	25.6	139	April	High Flow	2014	-15.1904	22.9438
13	IB13	7.6	5.67	26.3	6.05	25	141	April	High Flow	2014	-15.1384	22.876817
14	IB14	7.5	5.99	26.8	4.78	25.4	105	April	High Flow	2014	-15.0913	22.80635
15	IB15	7.3	5.7	26.3	4.82	27.9	136	April	High Flow	2014	-15.0276	22.7382
16	IB16	6.8	4.02	25.9	2.61	77.2	131	April	High Flow	2014	-15.2615	23.133233
17	IB17	6.6	4.77	26.6	6.8	32.5	137	April	High Flow	2014	-15.1201	23.1441
18	IB18	8	5.63	26.3	4.78	20.9	151	April	High Flow	2014	-15.5712	23.280883
19	IB19	7.5	5.6	26.3	6.02	20.9	143	April	High Flow	2014	-15.3893	23.177233
20	IB20	6.9	5.74	27.5	1.47	41.7	62	April	High Flow	2014	-15.6844	23.247
21	IB21	7.5	5.95	28.1	6.71	47.1	64	April	High Flow	2014	-16.0894	23.2941
22	IB22	7.7	5.38	29.8	7.07	54.2	87	April	High Flow	2014	-16.1168	23.288667
23	IB23	6.8	5.97	27.6	3.69	208	156	April	High Flow	2014	-16.1056	23.296383
24	IB24	7.3	6.66	24.4	7.36	36.5	83	April	High Flow	2014	-17.4667	24.247283
25	IB25	8.1	6.42	25.1	7.62	36.1	78	April	High Flow	2014	-16.6718	23.625833
26	IB26	7.1	6.4	24.5	5.47	33.1	75	April	High Flow	2014	-16.3908	23.325117

Number	ID	pH-InSitu	pH-Lab	Temp(^{0}C)-InSitu	DO(mg/l)-InSitu	EC (µs/cm)-InSitu	EC (mMhos/cm)-Lab	Month	Period	Year	Latitude	Longitude
27	IB27	7.4	6.68	22	4.24	69.4	106	April	High Flow	2014	-16.0792	23.029933
28	IB28	8	6.6	25.2	5.7	31.9	108	April	High Flow	2014	-16.0547	23.170633
29	IB29	7.6	6.06	25.6	2.15	34.7	80	April	High Flow	2014	-15.966	23.144983
30	IB30	7.8	6.09	25.3	5.1	30.7	88	April	High Flow	2014	-15.8891	23.1326
31	IB31	7.5	6.17	24.5	1.24	30.7	72	April	High Flow	2014	-15.8309	23.067683
32	IB32	7.2	6.15	25.2	1.53	32.2	68	April	High Flow	2014	-15.7533	23.052967
33	IB33	7.3	6.12	25.7	4.69	25.9	59	April	High Flow	2014	-15.6846	23.040383
34	IB34	7	6	23.8	7	29.1	67	April	High Flow	2014	-14.9872	22.683067
35	IB35	6.5	6.31	21.3	3.9	38.5	78	April	High Flow	2014	-15.3485	22.743483
36	IB36	6.9	6.72	28.4	4	169.8	165	April	High Flow	2014	-15.3973	22.854983
37	IB37	7.2	7.24	18	4.6	307	342	April	High Flow	2014	-16.3104	23.178167
38	IB38	6.9	7.19	17.2	4.02	345	392	April	High Flow	2014	-16.3106	23.158183
39	IB39	7.23	6.4	24.2	4.7	34.4	87	April	High Flow	2014	-16.2442	23.237667
40	IB40	6.99	6.63	22.6	4.6	38.9	123	April	High Flow	2014	-16.3539	23.276467
41	IB41	7.1	7.34	21.6	4.3	282	335	April	High Flow	2014	-16.2015	23.340117
42	IB42	6.7	6.71	22.8	4.07	31.8	125	April	High Flow	2014	-16.227	23.340967
43	IB43	7.1	6.84	23.1	5.57	86.6	151	April	High Flow	2014	-16.3958	23.412133
44	IB44	7.5	6.48	23.8	6.23	44.1	94	April	High Flow	2014	-16.6335	23.557567

Appendix 2a: Samples collected during the second field campaign in Barotse Floodplain (September 2014), Western Zambia showing laboratory analysed parameters

Total hardness (as mg CaCO3/l)	Total phosphates (mg/l)	Total Dissolved Solids (mg/l)	Total Suspended Solids (mg/l)	Turbidity (NTU)	Month	Period	Year	Latitude	Longitude
1	<0.01	78	40.4	87.9	September	Low Flow	2014	-14.9872	22.68307
2	<0.01	73	22.5	49.4	September	Low Flow	2014	-15.0143	22.70544
3	<0.01	61	<1.0	1.64	September	Low Flow	2014	-15.0827	22.7812
4	<0.01	62	<1.0	2.15	September	Low Flow	2014	-15.101	22.84967
5	<0.01	59	<1.0	9.33	September	Low Flow	2014	-15.1254	22.85673
6	<0.01	58	<1.0	9.27	September	Low Flow	2014	-15.153	22.873
7	<0.01	60	<1.0	6.59	September	Low Flow	2014	-15.188	22.896
8	<0.01	26	<1.0	8.37	September	Low Flow	2014	-15.2149	22.92658
9	<0.01	31	<1.0	1.65	September	Low Flow	2014	-15.2174	22.92762
10	<0.01	39	<1.0	1.66	September	Low Flow	2014	-15.262	22.9437
11	<0.01	38	<1.0	6.08	September	Low Flow	2014	-15.2754	23.06725
12	<0.01	24	<1.0	9.67	September	Low Flow	2014	-15.275	23.092
13	<0.01	23	18.2	47.2	September	Low Flow	2014	-15.2739	23.11758
14	<0.01	86	<1.0	3.41	September	Low Flow	2014	-14.3702	23.23707
15	<0.01	32	<1.0	8.46	September	Low Flow	2014	-14.4221	23.20994
16	<0.01	40	<1.0	6.6	September	Low Flow	2014	-14.4633	23.16501
17	<0.01	86	<1.0	3.55	September	Low Flow	2014	-14.5979	23.11344
18	<0.01	83	<1.0	1.84	September	Low Flow	2014	-14.6714	23.07758
19	<0.01	79	<1.0	7.52	September	Low Flow	2014	-14.7331	23.04686
20	<0.01	77	<1.0	4.18	September	Low Flow	2014	-14.8064	23.02354
21	<0.01	76	<1.0	1.92	September	Low Flow	2014	-14.8544	23.01596
22	<0.01	73	<1.0	3.68	September	Low Flow	2014	-14.9014	22.99663
23	0.13	72	<1.0	5.71	September	Low Flow	2014	-14.9717	22.96722
24	<0.01	73	<1.0	5.33	September	Low Flow	2014	-15.0454	22.93968
25	<0.01	75	<1.0	6.17	September	Low Flow	2014	-15.1242	22.94587
26	<0.01	74	<1.0	9.99	September	Low Flow	2014	-15.1841	22.93905

Total hardness (as mg CaCO3/l)	Total phosphates (mg/l)	Total Dissolved Solids (mg/l)	Total Suspended Solids (mg/l)	Turbidity (NTU)	Month	Period	Year	Latitude	Longitude
27	<0.01	71	<1.0	1.98	September	Low Flow	2014	-15.2363	22.90664
28	<0.01	72	<1.0	10.99	September	Low Flow	2014	-15.2601	22.93303
29	<0.01	71	<1.0	1.29	September	Low Flow	2014	-15.2789	22.96766
30	<0.01	67	<1.0	0.89	September	Low Flow	2014	-15.2735	23.12013

Appendix 2b: Samples collected during the second field campaign in September 2014 in Barotse Floodplain, Western Zambia showing comparison of in-situ results and the laboratory ones

Number	ID	pH-InSitu	pH-Lab	Temp(^{0}C)-InSitu	DO(mg/l)-InSitu	EC (µs/cm)-InSitu	EC (mMhos/cm)-Lab	Month	Period	Year	Latitude	Longitude
1	IB46	7.73	8.27	21.9	0.20%	43.2	156	September	Low Flow	2014	-14.9872	22.68307
2	IB47	7.4	8.38	22.6	0.10%	43.19	145	September	Low Flow	2014	-15.0143	22.70544
3	IB48	6.6	8.21	23.5	0.50%	36.7	121	September	Low Flow	2014	-15.0827	22.7812
4	IB49	6.38	8.2	22.9	0.30%	43.6	124	September	Low Flow	2014	-15.101	22.84967
5	IB50	6.72	8.6	23.8	0.30%	50.9	119	September	Low Flow	2014	-15.1254	22.85673
6	IB51	6.92	8.45	24.4	0.40%	47.1	116	September	Low Flow	2014	-15.153	22.873
7	IB52	7.3	8.05	24	0.40%	104	120	September	Low Flow	2014	-15.188	22.896
8	IB53	7.35	8.07	24	0.50%	100.2	52	September	Low Flow	2014	-15.2149	22.92658
9	IB54	6.35	8.06	24.3	0.60%	102.8	61	September	Low Flow	2014	-15.2174	22.92762
10	IB55	6.188	8.15	24.1	0.30%	104.6	78	September	Low Flow	2014	-15.262	22.9437
11	IB56	5.934	8.17	25.5	0.30%	106	76	September	Low Flow	2014	-15.2754	23.06725
12	IB57	5.52	8.2	26.2	0.40%	127.9	48	September	Low Flow	2014	-15.275	23.092
13	IB58	5.2	8.06	23.5	0.30%	95.9	47	September	Low Flow	2014	-15.2739	23.117583
14	IB59	5.631	8	24.3	0.60%	136.8	181	September	Low Flow	2014	-14.3702	23.23707
15	IB60	6.73	8.33	24.6	1.40%	30	71	September	Low Flow	2014	-14.4221	23.20994
16	IB61	5.9	8.18	24.6	0.50%	42	81	September	Low Flow	2014	-14.4633	23.16501
17	IB62	6.322	8.02	25.5	0.40%	133.2	173	September	Low Flow	2014	-14.5979	23.11344
18	IB63	6.5	8.04	25.4	0.40%	127.5	170	September	Low Flow	2014	-14.6714	23.07758
19	IB64	6.76	8.02	25.9	0.30%	118	160	September	Low Flow	2014	-14.7331	23.04686
20	IB65	7	8.03	26	0.10%	110.1	155	September	Low Flow	2014	-14.8064	23.02354
21	IB66	6.9	8.07	26.1	0.30%	98	154	September	Low Flow	2014	-14.8544	23.01596
22	IB67	6.97	8.18	25.6	0.10%	104.8	148	September	Low Flow	2014	-14.9014	22.99663
23	IB68	7.08	8	27.1	0.30%	104.6	147	September	Low Flow	2014	-14.9717	22.96722
24	IB69	7.1	8.05	25.8	0.40%	104.6	147	September	Low Flow	2014	-15.0454	22.93968
25	IB70	7.1	8	25.8	0.30%	103	151	September	Low Flow	2014	-15.1242	22.94587
26	IB71	7.09	8.12	25.6	0.20%	104.5	147	September	Low Flow	2014	-15.1841	22.93905

Number	ID	pH-InSitu	pH-Lab	Temp(^{0}C)-InSitu	DO(mg/l)-InSitu	EC (µs/cm)-InSitu	EC (mMhos/cm)-Lab	Month	Period	Year	Latitude	Longitude
27	IB72	7	8.19	25.7	0.30%	100.1	142	September	Low Flow	2014	-15.2363	22.90664
28	IB73	7.15	8.08	25.8	0.30%	102.6	143	September	Low Flow	2014	-15.2601	22.93303
29	IB74	4.32	8.08	26.2	0.20%	153.7	143	September	Low Flow	2014	-15.2789	22.96766
30	IB75	5.877	8.05	30	0.40%	67.7	133	September	Low Flow	2014	-15.2735	23.12013

Appendix 3: Samples collected during the third field campaign in October 2014 in Barotse Floodplain, Western Zambia showing comparison of in-situ results and the laboratory ones

Number	ID	pH-InSitu	pH-Lab	Temp(^{0}C)-InSitu	DO(mg/l)-InSitu	EC (µs/cm)-InSitu	EC (mMhos/cm)-Lab	Month	Period	Year	Latitude	Longitude
1	IBG1	7.49	7.49	25.5		51.8	51.8	October	Low Flow	2014	-14.987	22.68337
2	IBG2	7.16	7.16	25.8		107.43	107.43	October	Low Flow	2014	-15.0037	22.69434
3	IBG3	6.96	6.96	26		127.63	127.63	October	Low Flow	2014	-15.0827	22.78112
4	IBG4	6.54	6.54	26.6		155.57	155.57	October	Low Flow	2014	-15.0877	22.81598
5	IBG5	8.16	8.16	26.6		164.64	164.64	October	Low Flow	2014	-14.3701	23.23702
6	IBG6	8.31	8.31	28.7		168.3	168.3	October	Low Flow	2014	-14.4193	23.21702
7	IBG7	7.01	7.01	28.3		57.93	57.93	October	Low Flow	2014	-15.176	22.88893
8	IBG8	8.08	8.08	27.2		108.4	108.4	October	Low Flow	2014	-15.1903	22.91833
9	IBG9	7.53	7.53	27.6		47.96	47.96	October	Low Flow	2014	-14.4634	23.16494
10	IBG10	7.72	7.72	27.9		67.34	67.34	October	Low Flow	2014	-14.5275	23.12451
11	IBG11	8.39	8.39	28.4		158.57	158.57	October	Low Flow	2014	-14.5438	23.12649
12	IBG12	8.24	8.24	28.4		152.04	152.04	October	Low Flow	2014	-14.5979	23.11345
13	IBG13	8.03	8.03	28		142.45	142.45	October	Low Flow	2014	-14.6714	23.07759
14	IBG14	8.07	8.07	28.2		128.52	128.52	October	Low Flow	2014	-14.7333	23.04652
15	IBG15	8.18	8.18	28.6		125.65	125.65	October	Low Flow	2014	-14.8064	23.02355
16	IBG16	8.41	8.41	28.9		132.59	132.59	October	Low Flow	2014	-14.8544	23.01585
17	IBG17	8.08	8.08	28.2		118.71	118.71	October	Low Flow	2014	-14.9014	22.99663
18	IBG18	8.08	8.08	27.7		117.28	117.28	October	Low Flow	2014	-15.0452	22.93986
19	IBG19	8.02	8.02	27.7		118.78	118.78	October	Low Flow	2014	-15.1242	22.94576
20	IBG20	8.11	8.11	27.6		118.75	118.75	October	Low Flow	2014	-15.184	22.93999
21	IBG21	8.1	8.1	27.4		114.64	114.64	October	Low Flow	2014	-15.2149	22.92672
22	IBG22	6.54	6.54	23.1		72.71	72.71	October	Low Flow	2014	-15.2615	23.13323
23	IBG23	6.21	6.21	23.6		14.138	14.138	October	Low Flow	2014	-15.3893	23.17723
24	IBG24	6.32	6.32	25		14.36	14.36	October	Low Flow	2014	-15.6834	23.247
25	IBG25	7.34	7.34	25.3		2.9	21	October	Low Flow	2014	-15.6796	23.30075
26	IBG26	7.86	7.86	26.8		66.01	66.01	October	Low Flow	2014	-16.1056	23.2941

Number	ID	pH-InSitu	pH-Lab	Temp(^{0}C)-InSitu	DO(mg/l)-InSitu	EC (µs/cm)-InSitu	EC (mMhos/cm)-Lab	Month	Period	Year	Latitude	Longitude
27	IBG27	7.53	7.53	28		139.58	139.58	October	Low Flow	2014	-16.1056	23.29638
28	IBG28	7	7	26.6		114.5	114.5	October	Low Flow	2014	-16.1168	23.28867
29	IBG29	6.94	6.94	27.6		115	115	October	Low Flow	2014	-17.4667	24.24812
30	IBG30	7.08	7.08	28.3		114		October	Low Flow	2014	-16.3908	23.32512
31	IBG31	7.13	7.13	33.5		28.963		October	Low Flow	2014	-16.3926	23.32533

Appendix 4a: Samples collected during the fifth field campaign in June 2015 in Barotse Floodplain Western Zambia. Laboratory analysed results were counted as high flow and not mid flow as indicated in the table since comparison between low and high flows only

Number	ID	Alkalinity (as mg CaCO3/l)	Ammonia (as NH4-Nmg/l)	Total hardness (as mg CaCO3/l)	Total phosphates (mg/l)	Total Dissolved Solids (mg/l)	Total Suspended Solids (mg/l)	Turbidity (NTU)	Calcium hardness (as mg CaCO3/l)	Month	Period	Year	Latitude	Longitude
1	IB76	58	<0.01	60	<0.01	40	2.8	0.3		June	Mid Flow	2015	-15.3432	23.08716
2	IB77	92	0.04	108	<0.01	50	2.2	0.16		June	Mid Flow	2015	-15.4437	23.12351
3	IB78	60	<0.01	64	0.03	32	<1.0	1.35		June	Mid Flow	2015	-15.4644	23.11641
4	IB79	60	0.03	78	<0.01	33	<1.0	0.16		June	Mid Flow	2015	-15.5335	23.10908
5	IB80	104	<0.01	108	<0.01	58	2.9	1.26		June	Mid Flow	2015	-15.6465	23.12534
6	IB81	58	<0.01	62	<0.01	33	<1.0	0.14		June	Mid Flow	2015	-15.6988	23.12571
7	IB82	52	<0.01	50	0.03	33	1.6	0.18		June	Mid Flow	2015	-15.7757	23.17382
8	IB83	60	<0.01	70	<0.01	32	<1.0	0.87		June	Mid Flow	2015	-15.8026	23.18146
9	IB84	52	1	60	<0.01	33	3.3	0.91		June	Mid Flow	2015	-15.832	23.19986
10	IB85	76	0.81	74	0.11	39	2.8	0.23		June	Mid Flow	2015	-15.894	23.24036
11	IB86	68	<0.01	54	<0.01	36	<1.0	0.21		June	Mid Flow	2015	-15.9075	23.21539
12	IB87	68	0.14	66	<0.01	34	<1.0	0.15		June	Mid Flow	2015	-15.9288	23.22762
13	IB88	40	<0.01	46	<0.01	32	<1.0	0.91		June	Mid Flow	2015	-15.9491	23.23688
14	IB89	50	<0.01	54	<0.01	32	2.2	0.9		June	Mid Flow	2015	-15.9666	23.25673
15	IB90	42	<0.01	46	<0.01	32	<1.0	0.17		June	Mid Flow	2015	-16.037	23.24769
16	IB91	86	<0.01	92	0.02	27	<1.0	0.14		June	Mid Flow	2015	-16.0729	23.27302
17	IB92	82	<0.01	88	0.01	33	<1.0	0.33		June	Mid Flow	2015	-16.0982	23.29454
18	IB93	68	<0.01	72	<0.01	32	1.8	0.16		June	Mid Flow	2015	-16.243	23.2386
19	IB94	52	0.01	58	<0.01	32	<1.0	0.41		June	Mid Flow	2015	-16.2352	23.2405
20	IB95	62	0.01	68	<0.01	33	<1.0	0.37		June	Mid Flow	2015	-16.2133	23.24854
21	IB96	60	<0.01	68	<0.01	32	<1.0	0.12		June	Mid Flow	2015	-16.1717	23.27931

Appendix 4b: Samples collected during the fifth field campaign in June 2015, Barotse Floodplain, Western Zambia showing in-situ parameter for the stretch between Mongu and Senanga

Number	ID	pH-InSitu	pH-Lab	Temp(^{0}C)-InSitu	DO(mg/l)-InSitu	EC (µs/cm)-InSitu	EC (mMhos/cm)-Lab	Month	Period	Year	Latitude	Longitude
1	IB76	7.14	6.54	20.3	3.66	62.3	79	June	Mid Flow	2015	-15.3432	23.08716
2	IB77	7.203	6.87	20.5	4.52	59.7	100	June	Mid Flow	2015	-15.4437	23.12351
3	IB78	7.505	6.85	21.2	5.58	57.5	64	June	Mid Flow	2015	-15.4644	23.11641
4	IB79	7.931	6.79	21.1	5.61	57.8	65	June	Mid Flow	2015	-15.5335	23.10908
5	IB80	7.443	7.13	20.9	5.31	58.3	116	June	Mid Flow	2015	-15.6465	23.12534
6	IB81	7.568	6.89	21.2	6.07	58.2	60	June	Mid Flow	2015	-15.6988	23.12571
7	IB82	7.65	6.88	21.2	4.6	57.6	67	June	Mid Flow	2015	-15.7757	23.17382
8	IB83	7.929	6.81	21.1	4.58	57.4	63	June	Mid Flow	2015	-15.8026	23.18146
9	IB84	7.592	6.85	21.2	4.66	57.57	66	June	Mid Flow	2015	-15.832	23.19986
10	IB85	7.674	6.83	20.7	4.83	56.9	77	June	Mid Flow	2015	-15.894	23.24036
11	IB86	7.208	6.88	21.3	4.82	56.8	71	June	Mid Flow	2015	-15.9075	23.21539
12	IB87	7.683	6.84	21.2	5.64	57	67	June	Mid Flow	2015	-15.9288	23.22762
13	IB88	7.663	6.81	21.4	6.4	56.9	64	June	Mid Flow	2015	-15.9491	23.23688
14	IB89	7.345	6.75	21.2	4.4	56.1	62	June	Mid Flow	2015	-15.9666	23.25673
15	IB90	7.636	6.88	21.1	4.79	56.7	63	June	Mid Flow	2015	-16.037	23.24769
16	IB91	7.47	6.95	21.1	4.33	56.7	53	June	Mid Flow	2015	-16.0729	23.27302
17	IB92	7.4	7.08	21.1	4.42	56.4	64	June	Mid Flow	2015	-16.0982	23.29454
18	IB93	8.08	6.79	20.3	4.44	56.1	63	June	Mid Flow	2015	-16.243	23.2386
19	IB94	6.684	6.74	20.3	4.24	56.1	65	June	Mid Flow	2015	-16.2352	23.2405
20	IB95	7.012	6.95	20.5	5.53	56.5	63	June	Mid Flow	2015	-16.2133	23.24854
21	IB96	6.23	6.99	20.4	4.9	56.5	65	June	Mid Flow	2015	-16.1717	23.27931

Appendix 5: Samples analysed by Atomic Spectroscopy (AS) showing elemental constituents of the river bed sediments for the Barotse Floodplain, Western Zambia. These where picked at the same locations as the water quality samples

ID	Al ppm	Ag	As	Au	Ca ppm	Cd	Co	Cr	Cu	Fe	Hg	Mg	Mn	Ni	Pb	Sn	Zn	K ppm	Na	% SiO2
---mg/kg---																				
IB 16	977.29	<0.002	<0.03	<0.01	872.28	<0.002	<0.005	<0.006	5.68	4866.04	<0.2	516.64	0.43	0.04	<0.01	<0.1	35.95	49.20	2107.85	78.93
IB 17	947.64	<0.002	<0.03	<0.01	<0.001	<0.002	<0.005	<0.006	3.57	174.86	<0.2	363.28	<0.002	<0.01	<0.01	<0.1	31.96	19.74	2109.62	81.27
IB 18	895.76	<0.002	<0.03	<0.01	<0.001	<0.002	<0.005	<0.006	5.44	3268.17	<0.2	398.17	<0.002	<0.01	<0.01	<0.1	34.13	23.99	2155.90	73.44
IB 19	3406.04	<0.002	<0.03	<0.01	1101.46	<0.002	<0.005	<0.006	19.64	2473.45	<0.2	470.27	<0.002	<0.01	<0.01	<0.1	31.58	33.56	2170.35	77.98
IB 20	2671.21	<0.002	<0.03	<0.01	945.34	<0.002	<0.005	<0.006	5.97	3105.71	<0.2	423.50	0.05	<0.01	<0.01	<0.1	24.63	24.63	2100.03	79.8
IB 21	1246.10	<0.002	<0.03	<0.01	724.86	<0.002	<0.005	<0.006	8.18	898.48	<0.2	396.72	<0.002	<0.01	<0.01	<0.1	29.23	35.07	2037.22	85.66
IB 22	1709.05	<0.002	<0.03	<0.01	3252.99	<0.002	<0.005	<0.006	10.44	1646.90	<0.2	972.67	<0.002	<0.01	<0.01	<0.1	36.06	90.15	2119.00	79.94
IB 23	1702.91	<0.002	<0.03	<0.01	4017.48	<0.002	<0.005	<0.006	15.05	4931.65	<0.2	1618.45	1.23	<0.01	<0.01	<0.1	56.31	320.39	2143.69	84.66
IB 24	1651.98	<0.002	<0.03	<0.01	2100.27	<0.002	<0.005	<0.006	4.17	5303.86	<0.2	1510.76	1.62	<0.01	<0.01	<0.1	90.04	107.10	2192.21	75.69
IB 25	2214.16	<0.002	<0.03	<0.01	188.97	<0.002	<0.005	<0.006	6.20	369.82	<0.2	438.90	0.49	<0.01	<0.01	<0.1	30.54	20.04	2152.13	76.77
IB 26	0.03	<0.002	<0.03	<0.01	<0.001	<0.002	<0.005	<0.006	5.72	748.05	<0.2	516.04	<0.002	<0.01	<0.01	<0.1	49.57	43.85	1937.08	89.9
IB 27	200.23	<0.002	<0.03	<0.01	<0.001	<0.002	<0.005	<0.006	7.03	1042.36	<0.2	381.15	<0.002	<0.01	<0.01	<0.1	37.54	25.03	1994.61	73.66
IB 28	0.03	<0.002	<0.03	<0.01	<0.001	<0.002	<0.005	<0.006	5.61	2548.93	<0.2	437.51	<0.002	<0.01	<0.01	<0.1	43.28	31.47	2084.19	72.89
IB 29	165.66	<0.002	<0.03	<0.01	<0.001	<0.002	<0.005	<0.006	4.77	1027.09	<0.2	565.08	0.18	<0.01	<0.01	<0.1	35.08	58.47	1915.81	79.83
IB 30	0.03	<0.002	<0.03	<0.01	172.46	<0.002	<0.005	<0.006	2.23	1142.70	<0.2	533.08	0.05	<0.01	<0.01	<0.1	43.58	68.61	2182.66	81.23
IB 31	0.03	<0.002	<0.03	<0.01	559.62	<0.002	<0.005	<0.006	1.85	378.28	<0.2	386.36	0.05	<0.01	<0.01	<0.1	32.17	35.10	2075.66	83.58
IB 32	0.03	<0.002	<0.03	<0.01	<0.001	<0.002	<0.005	<0.006	8.90	418.81	<0.2	361.99	<0.002	<0.01	<0.01	<0.1	31.93	27.10	1871.49	76.34
IB 33	0.03	<0.002	<0.03	<0.01	<0.001	<0.002	<0.005	<0.006	8.77	593.52	<0.2	431.01	<0.002	<0.01	<0.01	<0.1	41.87	46.86	2076.77	77.99
IB 34	1152.64	<0.002	<0.03	<0.01	1375.58	<0.002	<0.005	<0.006	5.60	191.54	<0.2	510.77	<0.002	0.03	<0.01	<0.1	34.15	47.43	2227.49	85.81
IB 35	767.97	<0.002	<0.03	<0.01	<0.001	<0.002	<0.005	<0.006	4.15	1136.23	<0.2	352.71	0.20	<0.01	<0.01	<0.1	27.98	33.77	2098.41	78.97
IB 36	1692.08	<0.002	<0.03	<0.01	1340.31	<0.002	<0.005	<0.006	4.09	647.33	<0.2	494.63	0.50	0.04	<0.01	<0.1	21.92	60.79	2320.88	76.96
IB 37	1115.80	<0.002	<0.03	<0.01	2071.51	<0.002	<0.005	<0.006	5.75	2571.32	<0.2	546.33	<0.002	<0.01	<0.01	<0.1	32.59	40.26	2211.46	91.23
IB 38	2559.88	<0.002	<0.03	<0.01	10086.08	<0.002	<0.005	<0.006	14.97	488.21	<0.2	3011.79	0.50	<0.01	<0.01	<0.1	5.61	160.93	2856.47	86.63
IB 39	2372.51	<0.002	<0.03	<0.01	4843.34	<0.002	<0.005	<0.006	4.63	1922.20	<0.2	669.04	0.44	<0.01	<0.01	<0.1	18.32	107.97	2254.89	77.97
IB 40	1537.20	<0.002	<0.03	<0.01	3805.04	<0.002	<0.005	<0.006	1.73	1205.25	<0.2	1593.92	0.26	<0.01	<0.01	<0.1	6.73	39.42	2247.64	87.33

ID	Al ppm	Ag	As	Au	Ca ppm	Cd	Co	Cr	Cu	Fe	Hg	Mg	Mn	Ni	Pb	Sn	Zn	K ppm	Na	% SiO2
IB 41	1175.24	<0.002	<0.03	<0.01	2889.44	<0.002	<0.005	<0.006	4.01	1354.00	<0.2	551.87	0.13	0.07	<0.01	<0.1	4.77	43.88	2235.05	84.69
IB 42	1138.38	<0.002	<0.03	<0.01	1874.65	<0.002	<0.005	<0.006	3.21	1125.17	<0.2	496.20	0.01	<0.01	<0.01	<0.1	9.44	36.81	2228.62	86.75
IB 43	1537.95	<0.002	<0.03	<0.01	645.19	<0.002	<0.005	<0.006	3.73	2365.61	<0.2	503.81	0.36	<0.01	<0.01	<0.1	10.51	64.04	2179.32	78.96
IB 44	4726.57	<0.002	<0.03	<0.01	12610.98	<0.002	<0.005	<0.006	7.09	2966.49	<0.2	5839.73	1.83	<0.01	<0.01	<0.1	15.54	73.82	2291.40	83.96
Kalabo H	697.33	<0.002	<0.03	<0.01	845.79	<0.002	<0.005	<0.006	3.91	197.19	<0.2	378.07	<0.002	<0.01	<0.01	<0.1	35.16	33.21	2188.69	73.67
Unknown	0.03	<0.002	<0.03	<0.01	<0.001	<0.002	<0.005	<0.006	<0.003	2217.08	<0.2	<0.0003	<0.002	<0.01	<0.01	<0.1	<0.001	<0.003	<0.0002	ND
SDA	0.03	<0.002	<0.03	<0.01	<0.001	<0.002	<0.005	<0.006	<0.003	1957.14	<0.2	<0.0003	<0.002	<0.01	<0.01	<0.1	<0.001	<0.003	<0.0002	ND
IB 28	0.03	<0.002	<0.03	<0.01	<0.001	<0.002	<0.005	<0.006	<0.003	2202.34	<0.2	<0.0003	<0.002	<0.01	<0.01	<0.1	<0.001	<0.003	<0.0002	ND
IB 30	0.03	<0.002	<0.03	<0.01	<0.001	<0.002	<0.005	<0.006	<0.003	1684.97	<0.2	<0.002	<0.002	<0.01	<0.01	<0.1	<0.001	<0.003	<0.0002	ND
IB 40		<0.002	<0.03	<0.01	<0.001	<0.002	<0.005	<0.006	<0.003	1569.20	<0.2	<0.0003	<0.002	<0.01	<0.01	<0.1	<0.001	<0.003	<0.0002	ND

Appendix 6: The following are the 159 sub-basins according to Arc SWAT discretization were each sub-basin is given a description for July 2013 for the Barotse Floodplain, Western Zambia. Please note that not all parameters are given here as this is an extract from the database developed by Arc SWAT. The database years range from 1989 to 2013

SUB	YEAR	MON	AREAkm2	PRECIPmm	SNOWMELTmm	PETmm	ETmm	SWmm	PERCmm	SURQmm	GW_Qmm	WYLDmm	SYLDt_ha
1	2013	7	1846.6	0	0	180.02	0	0	0	0	0	2.161	0
2	2013	7	0.405	0	0	180.33	0	0	0	0	0	2.135	0
3	2013	7	2801.6	0	0	179.7	0	0	0	0	0	2.161	0
4	2013	7	1158.3	0	0	179.96	0	0	0	0	0	2.164	0
5	2013	7	1015.7	0	0	180.12	0	0	0	0	0	2.182	0
6	2013	7	1062.7	0	0	180.12	0	0	0	0	0	2.158	0
7	2013	7	32.603	0	0	180.28	0	0	0	0	0	2.198	0
8	2013	7	112.39	0	0	180.22	0	0	0	0	0	2.197	0
9	2013	7	1605	0	0	180.31	27.36	9.261	0	0.113	0	0.3	0
10	2013	7	1515.3	0	0	180.27	27.361	9.215	0	0.504	0	0.691	0
11	2013	7	1301.7	0	0	180.34	27.359	9.27	0	0.141	0	0.328	0
12	2013	7	1140.9	0	0	180.29	9.335	3.205	0	0	0	1.513	0
13	2013	7	2850.8	0	0	180.22	2.792	0.992	0	0	0	1.995	0
14	2013	7	1211.6	0	0	179.75	0	0	0	0	0	2.176	0
15	2013	7	340.81	0	0	180.36	26.148	16.941	0	0	0	0.187	0
16	2013	7	3952.4	0	0	179.51	0	0	0	0	0	2.166	0
17	2013	7	411.89	0	0	180.37	27.357	9.356	0	0	0	0.187	0
18	2013	7	1645.9	0	0	180.15	0	0	0	0	0	2.2	0
19	2013	7	1166	0	0	180.19	0	0	0	0	0	2.191	0
20	2013	7	1968.1	0	0	180.33	27.359	9.25	0	0.594	0	0.781	0
21	2013	7	486.4	0	0	180.38	27.357	9.324	0	0.004	0	0.191	0
22	2013	7	1839.5	0	0	180.33	16.566	5.637	0	0.01	0	0.992	0
23	2013	7	4414.3	0	0	179.62	0.147	0	0	0	0	2.159	0
24	2013	7	7.29	0	0	180.4	27.354	9.421	0	0	0	0.186	0

SUB	YEAR	MON	AREAkm2	PRECIPmm	SNOWMELTmm	PETmm	ETmm	SWmm	PERCmm	SURQmm	GW_Qmm	WYLDmm	SYLDt_ha
25	2013	7	1164.6	0	0	180.36	13.096	4.496	0	0	0	1.236	0
26	2013	7	180.23	0	0	180.24	27.358	9.485	0	0	0	0.188	0
27	2013	7	1740.5	0	0	180.04	5.619	3.348	0	0	0	1.761	0
28	2013	7	1306.9	0	0	180.18	0	0	0	0	0	2.189	0
29	2013	7	228.01	0	0	180.39	27.355	9.407	0	0	0	0.189	0
30	2013	7	798.66	0	0	180.21	23.173	8.077	0	0	0	0.491	0
31	2013	7	1809.7	0	0	180.37	27.358	9.297	0	0.117	0	0.304	0
32	2013	7	1540	0	0	174.04	0	0	0	0	0.055	2.478	0
33	2013	7	1717.2	0	0	180.04	0	0	0	0	0	2.222	0
34	2013	7	4940.2	0	0	180.25	21.782	19.706	0	0.148	0	0.505	0
35	2013	7	230.24	0	0	180.39	7.916	2.741	0	0	0	1.617	0
36	2013	7	939.2	0	0	180.32	0	0	0	0	0	2.18	0
37	2013	7	1163.8	0	0	180.24	22.808	19.488	0	0	0	0.411	0
38	2013	7	1220.1	0	0	173.8	0	0	0	0	0.045	2.41	0
39	2013	7	1465.9	0	0	179.41	0	0	0	0	0	2.165	0
40	2013	7	2781.5	0	0	179.7	0	0	0	0	0	2.108	0
41	2013	7	411.89	0	0	180.37	25.186	13.348	0	0.001	0	0.19	0
42	2013	7	2907.1	0	0	179.92	2.519	2.379	0	0	0	1.989	0
43	2013	7	1387.3	0	0	173.86	0	0	0	0	0.048	2.427	0
44	2013	7	484.79	0	0	180.38	15.225	7.749	0	0	0	0.984	0
45	2013	7	362.48	0	0	180.31	0	0	0	0	0	2.18	0
46	2013	7	2000.3	0	0	173.78	0	0	0	0	0.047	2.426	0
47	2013	7	1999.5	0	0	180.26	21.468	23.53	0	0	0	0.276	0
48	2013	7	2140.8	0	0	180.3	21.735	23.676	0	0.002	0	0.288	0
49	2013	7	77.355	0	0	180.32	0	0	0	0	0	2.144	0
50	2013	7	607.5	0	0	174.01	0	0	0	0	0.05	2.44	0
51	2013	7	3076.4	0	0	179.65	0	0	0	0	0	2.105	0
52	2013	7	2150.1	0	0	179.8	0	0	0	0	0	2.173	0
53	2013	7	1327	0	0	179.86	0.991	0	0	0	0	2.099	0

SUB	YEAR	MON	AREAkm2	PRECIPmm	SNOWMELTmm	PETmm	ETmm	SWmm	PERCmm	SURQmm	GW_Qmm	WYLDmm	SYLDt_ha
54	2013	7	181.44	0	0	180.04	0	0	0	0	0	2.188	0
55	2013	7	6435.7	0	0	173.62	0	0	0	0	0.047	2.422	0
56	2013	7	1915.9	0	0	174.2	0	0	0	0	0.05	2.441	0
57	2013	7	1925.2	0	0	173.76	0	0	0	0	0.046	2.415	0
58	2013	7	2465.6	0	0	179.85	0	0	0	0	0	2.216	0
59	2013	7	2299.6	0	0	179.94	0	0	0	0	0	2.166	0
60	2013	7	312.05	0	0	180.1	0	0	0	0	0	2.192	0
61	2013	7	1482.3	0	0	180.31	5.526	8.868	0	0	0	1.547	0
62	2013	7	41.715	0	0	180.31	0	0	0	0	0	2.197	0
63	2013	7	1353.5	0	0	179.81	0	0	0	0	0	2.173	0
64	2013	7	1698.4	0	0	173.97	0	0	0	0	0.049	2.437	0
65	2013	7	511.11	0	0	180.12	0	0	0	0	0	2.205	0
66	2013	7	1111.9	0	0	179.9	0	0	0	0	0	2.198	0
67	2013	7	3473.1	0	0	180.28	17.099	25.857	0	0	0	0.595	0
68	2013	7	644.35	0	0	180.12	0.224	0.107	0	0	0	2.184	0
69	2013	7	5.4675	0	0	180.39	0	0	0	0	0	1.952	0
70	2013	7	280.46	0	0	180.3	2.696	8.248	0	0	0	1.71	0
71	2013	7	1753.7	0	0	174.08	0	0	0	0	0.05	2.444	0
72	2013	7	8606.5	0	0	179.45	0	0	0	0.001	0	2.178	0
73	2013	7	891.2	0	0	180.12	0	0	0	0	0	2.212	0
74	2013	7	81.202	0	0	180.17	0	0	0	0	0	2.166	0
75	2013	7	1038.6	0	0	174.15	0	0	0	0	0.049	2.443	0
76	2013	7	2524.4	0	0	179.62	0	0	0	0	0	2.196	0
77	2013	7	2032.7	0	0	179.87	0	0	0	0	0	2.214	0
78	2013	7	3181.7	0	0	180.3	4.425	5.524	0	0	0.001	1.882	0
79	2013	7	1984.3	0	0	180.33	0.444	0.576	0	0	0	2.133	0
80	2013	7	1534.1	0	0	180.04	0	0	0	0	0	2.196	0
81	2013	7	1447.1	0	0	174.32	0	0	0	0	0.048	2.432	0
82	2013	7	4153.5	0	0	179.72	0	0	0	0	0	2.2	0

SUB	YEAR	MON	AREAkm2	PRECIPmm	SNOWMELTmm	PETmm	ETmm	SWmm	PERCmm	SURQmm	GW_Qmm	WYLDmm	SYLDt_ha
83	2013	7	1940.2	0	0	180.13	0	0	0	0	0	2.167	0
84	2013	7	1475.8	0	0	179.78	0	0	0	0	0	2.205	0
85	2013	7	1187.3	0	0	179.85	0	0	0	0	0	2.173	0
86	2013	7	421.61	0	0	180.41	0	0	0	0	0	2.194	0
87	2013	7	184.07	0	0	180.38	0	0	0	0	0	2.083	0
88	2013	7	6629.4	0	0	173.99	0	0	0	0	0.045	2.41	0
89	2013	7	487.01	0	0	180.22	0	0	0	0	0	2.168	0
90	2013	7	2173.6	0	0	180.13	0	0	0	0	0	2.231	0
91	2013	7	1566.5	0	0	180.19	0	0	0	0	0	2.162	0
92	2013	7	435.17	0	0	180.22	0	0	0	0	0	2.157	0
93	2013	7	1117.2	0	0	174.59	0	0	0	0	0.052	2.477	0
94	2013	7	3517.2	0	0	174.39	0	0	0	0	0.041	2.398	0
95	2013	7	3728.6	0	0	174	0	0	0	0	0.046	2.415	0
96	2013	7	982.53	0	0	180.08	0	0	0	0	0	2.181	0
97	2013	7	1577.9	0	0	180.07	0	0	0	0	0	2.194	0
98	2013	7	1877.4	0	0	180.04	0	0	0	0	0	2.193	0
99	2013	7	1.62	0	0	180.3	0	0	0	0	0	2.165	0
100	2013	7	2798.8	0	0	180.04	0	0	0	0	0	2.192	0
101	2013	7	1011.5	0	0	180.39	0	0	0	0	0.002	2.229	0
102	2013	7	1593.3	0	0	180.36	0	0	0	0	0.002	2.207	0
103	2013	7	2418.3	0	0	174.15	0	0	0	0	0.043	2.403	0
104	2013	7	160.38	0	0	180.19	0	0	0	0	0	2.251	0
105	2013	7	774.97	0	0	180.24	0	0	0	0	0	2.182	0
106	2013	7	3137.7	0	0	180.05	0.352	0	0	0	0	2.194	0
107	2013	7	1113.5	0	0	180.19	0.553	0	0	0	0	2.193	0
108	2013	7	1202.4	0	0	180.38	0	0	0	0	0.004	2.31	0
109	2013	7	142.76	0	0	180.46	0	0	0	0	0.002	2.275	0
110	2013	7	3095	0	0	180.24	0	0	0	0	0	2.156	0
111	2013	7	983.34	0	0	180.29	0.453	0	0	0	0	2.194	0

SUB	YEAR	MON	AREAkm2	PRECIPmm	SNOWMELTmm	PETmm	ETmm	SWmm	PERCmm	SURQmm	GW_Qmm	WYLDmm	SYLDt_ha
112	2013	7	1808.5	0	0	180.3	0	0	0	0	0	2.154	0
113	2013	7	315.09	0	0	180.41	0	0	0	0	0	2.191	0
114	2013	7	3190	0	0	180.38	0	0	0	0	0	2.165	0
115	2013	7	338.38	0	0	180.48	0.098	0	0	0	0	2.236	0
116	2013	7	5200	0	0	174.29	0	0	0	0	0.042	2.397	0
117	2013	7	1807.9	0	0	174.59	0	0	0	0	0.042	2.392	0
118	2013	7	5438.3	0	0	180.42	0	0	0	0	0.003	2.291	0
119	2013	7	149.85	0	0	180.51	0	0	0	0	0.001	2.114	0
120	2013	7	2709.7	0	0	174.77	0	0	0	0	0.073	2.621	0
121	2013	7	1124.9	0	0	180.47	0	0	0	0	0.003	2.233	0
122	2013	7	697.01	0	0	180.49	0	0	0	0	0.001	2.182	0
123	2013	7	492.08	0	0	180.42	1.227	0	0	0	0	2.118	0
124	2013	7	395.89	0	0	174.8	0	0	0	0	0.019	2.281	0
125	2013	7	2597.7	0	0	174.39	0	0	0	0	0.042	2.396	0
126	2013	7	923.8	0	0	174.71	0	0	0	0	0.034	2.363	0
127	2013	7	1267.9	0	0	174.43	0	0	0	0	0.04	2.361	0
128	2013	7	4100	0	0	178.01	0.112	0	0	0	0	2.236	0
129	2013	7	782.26	0	0	178.55	0.024	0	0	0	0.005	2.224	0
130	2013	7	1755.1	0	0	178.47	0.035	0	0	0	0.013	2.365	0
131	2013	7	1897.6	0	0	174.84	0	0	0	0	0.064	2.568	0
132	2013	7	567	0	0	178.53	0	0	0	0	0.004	2.226	0
133	2013	7	1513.9	0	0	174.46	0	0	0	0	0.044	2.407	0
134	2013	7	5751.8	0	0	178.04	0.192	0	0	0	0	2.217	0
135	2013	7	1352.7	0	0	174.5	0	0	0	0	0.041	2.391	0
136	2013	7	7001	0	0	178.28	0.203	0	0	0	0.026	2.477	0
137	2013	7	1865	0	0	175.55	0	0	0	0	0.112	2.861	0
138	2013	7	2080.1	0	0	174.84	0	0	0	0	0.05	2.479	0
139	2013	7	1490	0	0	174.8	0	0	0	0	0.078	2.638	0
140	2013	7	256.36	0	0	174.85	0	0	0	0	0.04	2.329	0

SUB	YEAR	MON	AREAkm2	PRECIPmm	SNOWMELTmm	PETmm	ETmm	SWmm	PERCmm	SURQmm	GW_Qmm	WYLDmm	SYLDt_ha
141	2013	7	2240.3	0	0	174.82	0	0	0	0	0.057	2.508	0
142	2013	7	128.99	0	0	174.83	0	0	0	0	0.025	2.28	0
143	2013	7	474.66	0	0	174.82	0	0	0	0	0.049	2.459	0
144	2013	7	794	0	0	175.69	0	0	0	0	0.013	2.058	0
145	2013	7	1024	0	0	175.58	0	0	0	0	0.097	2.678	0
146	2013	7	608.51	0	0	173.72	0	0	0	0	0.048	2.294	0
147	2013	7	1722.3	0	0	173.75	0	0	0	0	0.06	2.441	0
148	2013	7	1120.2	0	0	174.8	0	0	0	0	0.065	2.555	0
149	2013	7	1286.1	0	0	174.52	0	0	0	0	0.038	2.343	0
150	2013	7	1734.6	0	0	174.72	0	0	0	0	0.05	2.463	0
151	2013	7	670.48	0	0	178.59	0	0	0	0	0	1.948	0
152	2013	7	1.215	0	0	173.22	0	0	0	0	0	1.87	0
153	2013	7	283.5	0	0	175.72	0	0	0	0	0.002	1.963	0
154	2013	7	406.42	0	0	173.79	0	0	0	0.001	0.028	2.208	0
155	2013	7	1731.4	0	0	174.65	0	0	0	0	0.056	2.494	0
156	2013	7	7004.3	0	0	176.09	0	0	0	0.001	0	1.888	0
157	2013	7	2064.1	0	0	173.15	0	0	0	0	0.006	2.063	0
158	2013	7	1787.7	0	0	173.13	0	0	0	0	0.063	2.412	0
159	2013	7	1210.1	0	0	176.6	0	0	0	0	0.017	2.116	0

Appendix 7: Soil and Land Use Tables developed for the Barotse Floodplain, Western Zambia. These were in ASCII text format that SWAT can read

LOOK-UP TABLES				
SOILS			LANDUSE	
Value	NAME		Value	Landuse
39	Fo28-3ab-39		20	AGRL
522	Fo66-2-3b-522		30	AGRL
531	Fo74-2-3a-531		40	FRSD
537	Fo76-2-3a-537		50	FRSD
568	Fr12-2-3a-568		60	FRSD
569	Fr13-2ab-569		110	FRST
570	Fr14-3a-570		120	FRST
593	Fx20-2a-593		130	RNGE
594	Fx21-2ab-594		140	RNGE
599	Fx26-1-2a-599		150	RNGE
600	Fx26-1a-600		160	WETF
612	Ge25-1a-612		180	WETL
614	Ge27-1a-614		200	WATR
615	Ge28-1a-615		210	WATR
616	Ge29-1a-616			
618	Ge31-1a-618			
621	Ge33-2-3a-621			
646	I-F-c-646			
686	Je49-2-3a-686			
859	Ph5-1a-859			
866	Qc23-1a-866			
867	Qc24-1a-867			
869	Qc25-1a-869			
870	Qc26-1a-870			
874	Qc29-1a-874			
899	Qf23-1a-899			
903	Qf26-1a-903			

Appendix 8: Laboratory findings for the first trip with photographs in the Barotse Floodplain, Western Zambia. The locations are the same as June 2015 trip

ID	LAT (Deg Min)	LONG (Deg M)	Elev (m)	DATE & TIME	TEMP (oC)	PH	Cond (µs/cm)	DO (mg/l)	SAMPLING SITE DESCRIPTION	PICTURE
IB 1	15 16.521'	23 04.035'	1013	26-04-14 12:46	26.8	7.5	41.6	5.62	Matongo hydrometric station which is maintained by Zambezi River Authority located along the Mongu canal	
IB 2	15 15.861'	22 59.809'	1015	26-04-14 14:03	26.7	7.6	34.5	3.12	Along the Mongu Canal; Area surrounded by Hippo grass	
IB 3	15 16.158	23 00.542'	1012	26-04-14 14:59	26.2	7.2	34.8	3.09	Along Mongu canal; area surrounded by grasses	
IB 4	15 14.849 '	23 00.161'	1016	26-04-14 15:31	26.3	7.5	35.0	2.90	Along the Mongu Canal; Area surrounded by water lillies	
IB 5	15 16.414'	23 00.898'	1013	26-04-14 16:07	26.1	7.1	35.2	2.86	Along the Mongu Canal; near the Seventh Day Adventist Church	
IB 6	15 17.936'	23 04.298'	998	26-04-14 17:20	26.3	7.6	37.3	4.33	Along the Mongu Canal at Nibubela Village settlement	
IB 7	15 17.272'	23 05.996	1004	26-04-14 17:46	26.1	7.5	46.6	6.77	Along Mongu Canal; Under the big tree settled by birds	
IB 8	15 16.432'	23 07.055'	1010	26-04-14 17:55	25.8	7.2	29.9	2.76	Near Mongu Habour at Mulambwa village; Pit latrine near the banks	

ID	LAT (Deg M)	LONG (Deg M)	Elev (m)	DATE & TIME	TEMP (ºC)	PH	Cond (µs/cm)	DO (mg/l)	SAMPLING SITE DESCRIPTION	PICTURE
IB 9	15 12.273'	22 59.170'	1012	27-04-14 10:23	25.9	8.6	35.9	2.64	Barotse flood plains en route to Kalabo	
IB 10	15 11.401'	22 57.192'	1014	27-04-14 10:34	25.0	7.3	36.5	3.30	Barotse flood plains en route to Kalabo	
IB 11	15 11.110'	22 56.263'	1013	27-04-14 10:47	25.7	7.5	37.0	4.92	Barotse flood plains en route to Kalabo	
IB 12	15 11.426'	22 56.628'	1011	27-04-14 10:49	25.9	7.2	25.6	4.63	Barotse flood plains en route to Kalabo	
IB 13	15 08.302'	22 52.609'	1019	27-04-14 11:04	26.3	7.6	25.0	6.05	Barotse flood plains en route to Kalabo	
IB 14	15 05.475'	22 48.381'	1017	27-04-14 11:23	26.8	7.5	25.4	4.78	Barotse flood plains en route to Kalabo (Village with pigs, Mapungu)	
IB 15	15 01.655'	22 44.292'	1013	27-04-14 11:44	26.3	7.3	27.9	4.82	Barotse plains near Kalabo Habour (Nguya Area)	
IB 16	15 15.692'	23 07.994'	1010	28-04-14 13:42	25.9	6.8	77.2	2.61	Kabule walk-over bridge about 200m from tarred road; brick moulding and banana plants around	

ID	LAT (Deg Min)	LONG (Deg M)	Elev (m)	DATE & TIME	TEMP (oC)	PH	Cond (µs/cm)	DO (mg/l)	SAMPLING SITE DESCRIPTION	PICTURE
IB 17	15 07.207'	23 08.646'	1111	28-04-14 14:45	26.6	6.6	32.5	6.80	Sampling point at Chauteni River in Limulunga; Area used for bathing and washing of dishes	
IB 18	15 34.273'	23 16.853'	1014	28-04-14 16:55	26.3	8.0	20.9	4.78	Sampling point at Sianga River in kataba	
IB 19	15 23.358'	23 10.634'	1008	28-04-14 18:05	26.3	7.5	20.9	6.02	Sefula irrigation main canal	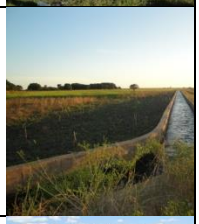
IB 20	15 41.064'	23 14.820'	1002	29-04-14 13:42	27.5	6.9	41.7	1.47	Litoya bridge 6 km off the main road; Cattle grazing around the river	
IB 21	16 05.365'	23 17.646'	994	29-04-14 14:53	28.1	7.5	47.1	6.71	River Zambezi at Senanga Musama area	
IB 22	16 07.009'	23 17.320'	987	29-04-14 15:15	29.8	7.7	54.2	7.07	Rice fields in Senanga were the Zambezi narrows	
IB 23	16 06.334'	23 17.783'	992	29-04-14 15:40	27.6	6.8	208.0	3.69	Senanga High School sewerage discharge point into Zambezi River; Saw milling upstream and some vegetable gardens	

ID	LAT (Deg Min)	LONG (Deg M)	Elev (m)	DATE & TIME	TEMP (oC)	PH	Cond (µs/cm)	DO (mg/l)	SAMPLING SITE DESCRIPTION	PICTURE
IB 24	17 28.001'	24 14.837'	935	15-05-14 13:25	24.4	7.3	36.5	7.36	Old Pontoon site at the banks of the Zambezi River at Katima Mulilo, Sesheke ; Algae around the place	
IB 25	16 40.306'	23 37.550'	976	15-05-14 15:35	25.1	8.1	36.1	7.62	The Senanga-Sesheke new Bridge site at the Zambezi River; Still under construction; Quarzite rock and sand deposites around	
IB 26	16 23.450'	23 19.507'	999	15-05-14 17:40	24.5	7.1	33.1	5.47	Nangweshi point; Hippo grass and washing of plates nearby	
IB 27	16 04.750'	23 01. 796'	1010	16-05-14 10:26	22.0	7.4	69.4	4.24	New bridge point at Lueti River; construction of the bridge by the Zambia Army on-going	
IB 28	16 03.282'	23 10.238'	996	16-05-14 12:20	25.2	8.0	31.9	5.7	Nakatwalenge Basic Sch; Abstraction point for drinking water for the school and village; Algae aroung around the place	
IB 29	15 57.961'	23 08.699'	997	16-05-14 13:01	25.6	7.6	34.7	2.15	Mapungu Basic Sch;Barotse flood plain; Slow movement of water in the lagoon; Fertiliser applied in the nearby gardens	

ID	LAT (Deg Min)	LONG (Deg M)	Elev (m)	DATE & TIME	TEMP (oC)	PH	Cond (µs/cm)	DO (mg/l)	SAMPLING SITE DESCRIPTION	PICTURE
IB 30	15 53.348'	23 07.956'	1000	16-05-14 14:23	25.3	7.8	30.7	5.1	Libubawe River near Nambwae Basic Sch ; bathing and washing of dishes nearby	
IB 31	15 49.853'	23 04.061'	998	16-05-14 15:44	24.5	7.5	30.7	1.24	Sinungu Basic Sch; gardens nearby using cow and chicken manure	
IB 32	15 45 198'	23 03 178'	1000	16-05-14 16:35	25.2	7.2	32.2	1.53	Sikana basic Sch; place surrounded by grass; washing of clothes, dishes and drinking water point for animals neraby by	
IB 33	15 41.077'	23 02.423'	1010	16-05-14 17:52	25.7	7.3	25.9	4.69	Liliachi Basci Sch at Malana stream; bathing and washing of dishes nearby	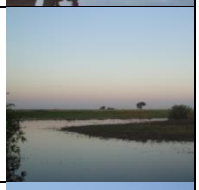
IB 34	14 59.232'	22 40.984'	1012	17-05-14 10:19	23.8	7	29.1	7	Kalabo Habour; water lilies and algae around: pumping machine nearby	
IB 35	15 20.912'	22 44.609'	1027	17-05-14 12:18	21.3	6.5	38.5	3.9	Ndoka bridge; animals grazing and fishing around	
IB 36	15 23.839'	22 51.299'	1057	17-05-14 13:11	28.4	6.9	169.8	4	Borehole about 42 m at Lukona Basic Sch; Indian Mark II pump enclosed in wooden fence	

ID	LAT (Deg Min)	LONG (Deg M)	Elev (m)	DATE & TIME	TEMP (oC)	PH	Cond (µs/cm)	DO (mg/l)	SAMPLING SITE DESCRIPTION	PICTURE
IB 37	16 18.625'	23 10.690'	995	18-05-14 8:37	18	7.2	307.0	4.6	Sisma salt lake/pond upstream of the Matebele Plain; Surrounded by grass	
IB 38	16 18.633'	23 09 491'	994	18-05-14 9:05	17.2	6.9	345	4.02	Muyoyoma salt lake upstream of Matebele Plains: surrounded by mulilima plants and grasses	
IB 39	16 14.652'	23 14.260'	999	18-05-14 11:32	24.2	7.23	34.4	4.7	Kalongola Habour; dead matter in water, washing and bathing done nearby	
IB 40	16 21.232'	23 16.588'	996	18-05-14 12:31	22.6	6.99	38.9	4.6	Matebele plains at the Bridge; washing and bathing done nearby	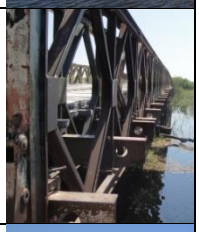
IB 41	16 12.088'	23 20.407'	983	19-05-14 10:06	21.6	7.1	282.0	4.3	Lulonga river near the Bridge; surrounded by grasses	
IB 42	16 13.619'	23 20.458'	991	19-05-14 10:29	22.8	6.7	31.8	4.07	Lui River at the Bridge; Washing and bathing done nearby	
IB 43	16 23.746'	23 24.728'	995	19-05-14 11:11	23.1	7.1	86.6	5.57	kakenge River at the bridge: bathing and washing of dishes done here; surrounded by grass and water lillies	

ID	LAT (Deg Min)	LONG (Deg M)	Elev (m)	DATE & TIME	TEMP (oC)	PH	Cond (µs/cm)	DO (mg/l)	SAMPLING SITE DESCRIPTION	PICTURE
IB 44	16 38.007'	23 33.454'	986	19-05-14 11:48	23.8	7.5	44.1	6.23	Kalongola pontoon at the Zambezi River; old construction debri around the area	

Appendix 9: An extract from the XRF readings of the different soil layers/horizons for Barotse Floodplain, Western Zambia

Reading No	39	40	41	42	43	44	45	46	47	48	49	50
Time	4/9/2015 10:47	4/9/2015 10:49	4/9/2015 10:49	4/9/2015 15:12	4/9/2015 15:14	4/9/2015 15:16	4/9/2015 15:16	4/9/2015 15:33	4/9/2015 15:35	4/9/2015 15:37	4/9/2015 15:37	4/9/2015 15:52
Type	Soil Profile	Soil Profile	Soil Profile	Soil Profile	Soil Profile	Soil Profile	Soil Profile	Soil Profile	Soil Profile	Soil Profile	Soil Profile	Soil Profile
Duration	120	120	360	120	120	120	360	120	120	120	360	120
Units	ppm	ppm	ppm	ppm	ppm	ppm	ppm	ppm	ppm	ppm	ppm	ppm
SAMPLE	AC_6	AC_6		AC_6	AC_6	AC_6		AC_6	AC_6	AC_6		AC_6
LOCATION	-14.51945,23.14388	-14.51945, 23.14388	-14.51945, 23.14388	-14.51945, 23.14388	-14.51945, 23.14388	-14.51945, 23.14388	-14.51945, 23.14388	-14.51945, 23.14388	-14.51945, 23.14388	-14.51945, 23.14388	-14.51945, 23.14388	-14.51945, 23.14388
INSPECTOR	Anthony Chabala	Anthony Chabala	Anthony Chabala	Anthony Chabala	Anthony Chabala	Anthony Chabala	Anthony Chabala	Anthony Chabala	Anthony Chabala	Anthony Chabala	Anthony Chabala	Anthony Chabala
COR 1	L1	L1	L1	L2	L2	L2	L2	L3	L3	L3	L3	L4
COR 2	L1ofL6	L1ofL6	L1ofL6	L2ofL6	L2ofL6	L2ofL6	L2ofL6	L3ofL6	L3ofL6	L3ofL6	L3ofL6	L4ofL6
AVERAGE			Avg of 38-40				Avg of 42-44				Avg of 46-48	
Ti	<LOD	<LOD	<LOD	<LOD	<LOD	<LOD	<LOD	670.16	711.8	977.64	786.53	<LOD
Ti Error	608.75	607.04	607.89	587.11	599.57	605.21	597.3	444.84	442.07	439.17	442.02	616.93
Cr	<LOD	<LOD	<LOD	<LOD	<LOD	<LOD	<LOD	<LOD	<LOD	<LOD	<LOD	<LOD
Cr Error	45.41	45.14	45.3	45.7	46.2	45.31	45.73	46.45	47.48	46.71	46.88	46.78
Mn	81.64	77.48	67.2	56.46	62.94	52.61	57.33	46.39	49.7	56.62	50.9	<LOD
Mn Error	24.08	23.9	23.71	23.45	23.79	23.55	23.6	24.38	24.29	24.24	24.3	34.69
Fe	1998.97	2059.34	1990.25	3157.22	3119.59	3180.06	3152.29	3076.62	3119.56	3138.99	3111.72	361.71
Fe Error	45.47	45.92	45.53	55.88	55.64	56.44	55.99	58.62	57.93	57.6	58.05	24.63
Co	<LOD	<LOD	<LOD	<LOD	<LOD	<LOD	<LOD	<LOD	<LOD	<LOD	<LOD	<LOD
Co Error	20.42	20.28	20.24	23.47	23.63	23.7	23.6	25.29	24.78	24.79	24.95	14.05
Ni	86.85	84.76	78.93	74.1	85.56	91.33	83.66	63.65	64.18	73.82	67.22	101.77
Ni Error	15.61	15.53	15.56	15.39	15.61	15.8	15.6	16.41	16.09	16.09	16.2	16.51
Cu	<LOD	<LOD	<LOD	<LOD	<LOD	<LOD	<LOD	<LOD	<LOD	<LOD	<LOD	<LOD
Cu Error	9.79	9.52	9.73	9.54	9.23	9.62	9.46	10.7	10.24	10.42	10.45	10.28
Zn	<LOD	<LOD	<LOD	<LOD	<LOD	<LOD	<LOD	<LOD	6.7	<LOD	5.5	<LOD
Zn Error	4.93	4.93	4.96	4.74	4.81	4.84	4.8	5.44	3.64	5.35	3.61	5.15
As	<LOD	<LOD	<LOD	<LOD	<LOD	<LOD	<LOD	<LOD	<LOD	<LOD	<LOD	<LOD
As Error	2.97	3.04	3.02	3.05	3.09	3.06	3.07	3.44	3.33	3.21	3.33	3.11
Se	<LOD	<LOD	<LOD	<LOD	<LOD	<LOD	<LOD	<LOD	<LOD	<LOD	<LOD	<LOD
Se Error	1.83	1.91	1.9	1.86	1.93	1.86	1.88	1.99	2.03	1.94	1.98	2
Rb	1.62	1.87	1.82	2.83	1.55	2.62	2.33	4.42	5.18	5.27	4.96	<LOD
Rb Error	0.98	0.98	0.99	1.01	0.98	1.01	1	1.12	1.12	1.12	1.12	1.5
Sr	2.74	2.85	3.23	4.62	4.55	3.43	4.2	5.3	4.64	5.69	5.21	<LOD
Sr Error	1.34	1.34	1.35	1.37	1.37	1.36	1.37	1.49	1.45	1.46	1.47	2.06
Zr	95.05	94.48	93.79	65.45	65.84	65.71	65.67	335.66	347.89	343.52	342.36	156.82
Zr Error	4.69	4.67	4.7	4.47	4.48	4.51	4.49	6.57	6.52	6.44	6.51	5.3
Pd	5.57	<LOD	4.46	4.48	<LOD	5.2	4.5	<LOD	<LOD	<LOD	<LOD	4.89

Continuation extract of element readings from XRF												
Pd Error	2.84	4.22	2.84	2.82	4.23	2.86	2.83	4.46	4.41	4.38	4.42	2.94
Ag	<LOD	<LOD	<LOD	<LOD	<LOD	<LOD	<LOD	<LOD	<LOD	<LOD	<LOD	<LOD
Ag Error	76.76	78.27	74.63	63.79	75.29	84.95	74.68	49.57	55.27	54.78	53.21	83.48
Cd	17.96	15.3	16.31	14.61	14.04	21.16	16.6	14.36	18.57	18.06	17	22.97
Cd Error	4.62	4.59	4.63	4.59	4.59	4.67	4.62	4.89	4.84	4.79	4.84	4.84
Sn	32.75	34.7	34.19	31.03	38.13	31.15	33.44	25.37	29.4	29.45	28.07	42.25
Sn Error	6.92	6.91	6.95	6.88	6.95	6.97	6.93	7.29	7.19	7.13	7.2	7.25
Sb	40.15	38.69	38.53	23.36	36.26	49.64	36.42	28.42	23.18	29.86	27.15	46.9
Sb Error	7.61	7.58	7.63	7.5	7.58	7.71	7.6	8.04	7.87	7.84	7.92	7.94
Ba	343.48	360.58	347.56	314.14	359.89	393.27	355.77	248.96	272.45	255.53	258.98	380.55
Ba Error	23.86	23.85	23.97	23.73	23.92	24.18	23.94	25.08	24.73	24.45	24.76	24.9
W	<LOD	<LOD	<LOD	<LOD	<LOD	<LOD	<LOD	<LOD	<LOD	<LOD	<LOD	<LOD
W Error	20.16	20.29	20.45	21.1	20.55	20.81	20.82	22	21.64	21.8	21.81	21.86
Au	9.32	7.43	7.4	<LOD	10.53	<LOD	7.21	<LOD	<LOD	9.4	<LOD	<LOD
Au Error	4.71	4.66	4.68	6.9	4.79	6.92	4.67	7.29	7.11	4.96	7.28	7.09
Hg	<LOD	<LOD	<LOD	<LOD	<LOD	<LOD	<LOD	<LOD	<LOD	<LOD	<LOD	<LOD
Hg Error	4.01	4.01	4.05	4.06	4	4.07	4.04	4.37	4.28	4.38	4.34	4.26
Pb	<LOD	<LOD	<LOD	<LOD	<LOD	<LOD	<LOD	<LOD	<LOD	<LOD	<LOD	<LOD
Pb Error	4.25	4.28	4.29	4.24	4.37	4.21	4.28	4.7	4.74	4.61	4.68	4.42

Appendix 10: Laboratory findings from the University of Zambia Laboratory for the final trip in the Barotse Floodplain, Western Zambia. The locations are the same as June 2015 trip

SCHOOL OF ENGINEERING
CIVIL ENGINEERING DEPARTMENT
ENVIRONMENTAL ENGINEERING LABORATORY
P.O Box 32379, Lusaka
Direct Telefax: 260-1-290962

PHYSICAL/CHEMICAL EXAMINATION OF WATER

Attn : IWRM Centre
UNZA
Lusaka
Sampled by : Client
Sampling date : 27.10.2015
Report date : 20.11.2015

Laboratory Results

Parameter	**IB 77B**	**IB 78B**	**IB 79B**	**IB 80B**	WHO Guideline (Maximum Permissible value for drinking water)
pH	6.59	6.74	6.97	6.60	6.5- 8.5
Turbidity (NTU)	6.70	5.77	11.10	8.91	5.0
Conductivity (mMhos/cm)	128	106	143	107	1500
Total Dissolved Solids (mg/l)	64	53	72	54	1000
Total Suspended Solids (mg/l)	<1.0	<1.0	2.1	<1.0	-
Total hardness (as mg $CaCO_3$/l)	60	108	64	78	500
Chromium(mg/l)	<0.01	<0.01	<0.01	<0.01	0.05
Alkalinity (as mg $CaCO_3$/l)	52	100	58	70	500
Iron (mg/l)	0.11	0.02	0.91	0.07	0.30
Ammonia (as NH_4-Nmg/l)	0.21	<0.01	<0.01	<0.01	1.50
Chlorides (mg/l)	15.0	15.0	17.0	13.0	250
Nitrites (as NO_2 –Nmg/l)	<0.001	<0.001	<0.001	0.001	0.100
Nitrates (as NO_3 –Nmg/l)	<0.01	<0.01	0.14	2.04	10.0
Total phosphates (mg/l)	<0.01	<0.01	<0.01	<0.01	5.0
Magnesium (mg/l)	6.96	5.04	8.64	7.20	-
Calcium (mg/l)	14.0	12.4	15.2	7.2	200
Fluorides (mg/l)	0.14	0.15	0.18	0.11	1.50
Sodium (mg/l)	9.90	9.95	11.22	8.58	-
Manganese (mg/l)	<0.01	<0.01	<0.01	<0.01	0.50
Bacteriological Results					
Total coliforms (#/100ml)	70	80	0	0	0
Feacal coliforms (#/100ml)	60	45	0	0	0

Tests carried out in conformity with " Standard Methods for the Examination of water and Wastewater APHA, 1998".

SCHOOL OF ENGINEERING
CIVIL ENGINEERING DEPARTMENT
ENVIRONMENTAL ENGINEERING LABORATORY
P.O Box 32379, Lusaka
Direct Telefax: 260-1-290962

PHYSICAL/CHEMICAL EXAMINATION OF WATER

Attn : IWRM Centre
UNZA
Lusaka
Sampled by : Client
Sampling date : 27.10.2015
Report date : 20.11.2015

Laboratory Results

Parameter	**IB 81B**	**IB 82B**	**IB 83B**	**IB 84B**	WHO Guideline (Maximum Permissible value for drinking water)
pH	6.79	6.72	6.54	7.04	6.5- 8.5
Turbidity (NTU)	12.20	10.10	8.20	8.02	5.0
Conductivity (mMhos/cm)	108	117	113	123	1500
Total Dissolved Solids (mg/l)	55	59	56	62	1000
Total Suspended Solids (mg/l)	2.2	1.7	<1.0	<1.0	-
Total hardness (as mg $CaCO_3$/l)	56	54	54	74	500
Chromium(mg/l)	<0.01	<0.01	<0.01	<0.01	0.05
Alkalinity (as mg $CaCO_3$/l)	50	48	49	67	500
Iron (mg/l)	0.66	<0.01	<0.01	0.37	0.30
Ammonia (as NH_4-Nmg/l)	<0.01	0.25	<0.01	<0.01	1.50
Chlorides (mg/l)	13.0	13.0	15.0	14.0	250
Nitrites (as NO_2 –Nmg/l)	<0.001	<0.001	<0.001	<0.001	0.100
Nitrates (as NO_3 –Nmg/l)	<0.01	0.18	0.34	0.15	10.0
Total phosphates (mg/l)	<0.01	<0.01	<0.01	<0.01	5.0
Magnesium (mg/l)	6.24	5.04	5.76	7.60	-
Calcium (mg/l)	12.0	13.2	12.0	17.6	200
Fluorides (mg/l)	0.08	0.12	0.10	0.15	1.50
Sodium (mg/l)	8.58	8.55	8.52	9.95	-
Manganese (mg/l)	<0.01	<0.01	<0.01	<0.01	0.50
Bacteriological Results					
Total coliforms (#/100ml)	0	0	0	0	0
Feacal coliforms (#/100ml)	0	0	0	0	0

Tests carried out in conformity with " Standard Methods for the Examination of water and Wastewater APHA, 1998".

SCHOOL OF ENGINEERING
CIVIL ENGINEERING DEPARTMENT
ENVIRONMENTAL ENGINEERING LABORATORY
P.O Box 32379, Lusaka
Direct Telefax: 260-1-290962

PHYSICAL/CHEMICAL EXAMINATION OF WATER

Attn : IWRM Centre
UNZA
Lusaka
Sampled by : Client
Sampling date : 27.10.2015
Report date : 20.11.2015

Laboratory Results

Parameter	**IB 85B**	**IB 86B**	**IB 87B**	**IB 88B**	WHO Guideline (Maximum Permissible value for drinking water)
pH	7.21	7.48	7.46	7.10	6.5- 8.5
Turbidity (NTU)	13.00	7.04	18.80	6.48	5.0
Conductivity (mMhos/cm)	126	136	127	117	1500
Total Dissolved Solids (mg/l)	63	68	64	59	1000
Total Suspended Solids (mg/l)	3.2	<1.0	5.3	<1.0	-
Total hardness (as mg $CaCO_3$/l)	72	74	60	58	500
Chromium(mg/l)	<0.01	<0.01	<0.01	<0.01	0.05
Alkalinity (as mg $CaCO_3$/l)	65	68	52	50	500
Iron (mg/l)	0.62	1.30	1.33	0.89	0.30
Ammonia (as NH_4-Nmg/l)	<0.01	<0.01	<0.01	<0.01	1.50
Chlorides (mg/l)	15.0	13.0	13.0	16.0	250
Nitrites (as NO_2 –Nmg/l)	<0.001	<0.001	<0.001	<0.001	0.100
Nitrates (as NO_3 –Nmg/l)	1.34	0.91	<0.01	<0.01	10.0
Total phosphates (mg/l)	<0.01	0.11	<0.01	<0.01	5.0
Magnesium (mg/l)	8.16	7.68	6.24	5.52	-
Calcium (mg/l)	15.2	16.8	13.6	14.0	200
Fluorides (mg/l)	0.18	0.16	0.09	0.16	1.50
Sodium (mg/l)	9.94	8.56	8.59	10.56	-
Manganese (mg/l)	<0.01	<0.01	<0.01	<0.01	0.50
Bacteriological Results					
Total coliforms (#/100ml)	0	0	0	0	0
Feacal coliforms (#/100ml)	0	0	0	0	0

Tests carried out in conformity with " Standard Methods for the Examination of water and Wastewater APHA, 1998".

SCHOOL OF ENGINEERING
CIVIL ENGINEERING DEPARTMENT
ENVIRONMENTAL ENGINEERING LABORATORY
P.O Box 32379, Lusaka
Direct Telefax: 260-1-290962

PHYSICAL/CHEMICAL EXAMINATION OF WATER

Attn : IWRM Centre
UNZA
Lusaka
Sampled by : Client
Sampling date : 27.10.2015
Report date : 20.11.2015

Laboratory Results

Parameter	**IB 89B**	**IB 90B**	**IB 91B**	**IB 92B**	WHO Guideline (Maximum Permissible value for drinking water)
pH	6.64	6.63	6.80	6.54	6.5- 8.5
Turbidity (NTU)	5.70	12.00	7.17	1.53	5.0
Conductivity (mMhos/cm)	107	130	117	109	1500
Total Dissolved Solids (mg/l)	54	65	59	55	1000
Total Suspended Solids (mg/l)	<1.0	4.2	<1.0	<1.0	-
Total hardness (as mg $CaCO_3$/l)	70	68	56	68	500
Chromium(mg/l)	<0.01	<0.01	<0.01	<0.01	0.05
Alkalinity (as mg $CaCO_3$/l)	66	53	47	65	500
Iron (mg/l)	0.38	1.29	0.76	1.14	0.30
Ammonia (as NH_4-Nmg/l)	<0.01	<0.01	<0.01	<0.01	1.50
Chlorides (mg/l)	13.0	15.0	12.0	13.0	250
Nitrites (as NO_2 –Nmg/l)	<0.001	<0.001	<0.001	<0.001	0.100
Nitrates (as NO_3 –Nmg/l)	<0.01	<0.01	0.12	<0.01	10.0
Total phosphates (mg/l)	<0.01	<0.01	<0.01	0.02	5.0
Magnesium (mg/l)	9.60	38.76	29.76	7.68	-
Calcium (mg/l)	12.0	15.6	12.0	13.0	200
Fluorides (mg/l)	0.11	0.14	0.14	0.16	1.50
Sodium (mg/l)	8.55	9.94	7.92	8.57	-
Manganese (mg/l)	<0.01	<0.01	<0.01	<0.01	0.50
Bacteriological Results					
Total coliforms (#/100ml)	79	0	0	0	0
Feacal coliforms (#/100ml)	50	0	0	0	0

Tests carried out in conformity with " Standard Methods for the Examination of water and Wastewater APHA, 1998".

SCHOOL OF ENGINEERING
CIVIL ENGINEERING DEPARTMENT
ENVIRONMENTAL ENGINEERING LABORATORY
P.O Box 32379, Lusaka
Direct Telefax: 260-1-290962

PHYSICAL/CHEMICAL EXAMINATION OF WATER

Attn : IWRM Centre
UNZA
Lusaka
Sampled by : Client
Sampling date : 27.10.2015
Report date : 20.11.2015

Laboratory Results

Parameter	**IB 93B**	**IB 94B**	**IB 95B**	**IB 96B**	WHO Guideline (Maximum Permissible value for drinking water)
pH	6.97	6.80	6.87	6.82	6.5- 8.5
Turbidity (NTU)	8.94	12.30	7.41	14.40	5.0
Conductivity (mMhos/cm)	129	109	109	114	1500
Total Dissolved Solids (mg/l)	65	55	55	57	1000
Total Suspended Solids (mg/l)	<1.0	1.8	<1.0	2.8	-
Total hardness (as mg $CaCO_3$/l)	70	58	56	64	500
Chromium(mg/l)	<0.01	<0.01	<0.01	<0.01	0.05
Alkalinity (as mg $CaCO_3$/l)	62	50	44	57	500
Iron (mg/l)	0.78	0.97	0.04	<0.01	0.30
Ammonia (as NH_4-Nmg/l)	<0.01	<0.01	<0.01	<0.01	1.50
Chlorides (mg/l)	11.0	14.0	10.0	14.0	250
Nitrites (as NO_2 –Nmg/l)	<0.001	<0.001	<0.001	<0.001	0.100
Nitrates (as NO_3 –Nmg/l)	<0.01	0.20	<0.01	<0.01	10.0
Total phosphates (mg/l)	<0.01	<0.01	<0.01	<0.01	5.0
Magnesium (mg/l)	5.28	6.72	5.76	5.28	-
Calcium (mg/l)	19.2	12.0	12.8	16.8	200
Fluorides (mg/l)	0.20	0.22	0.14	0.18	1.50
Sodium (mg/l)	7.22	9.31	6.68	9.22	-
Manganese (mg/l)	<0.01	<0.01	<0.01	<0.01	0.50
Bacteriological Results					
Total coliforms (#/100ml)	90	20	50	TNTC	0
Feacal coliforms (#/100ml)	48	0	28	TNTC	0

Tests carried out in conformity with " Standard Methods for the Examination of water and Wastewater APHA, 1998".

Appendix 11: The following chart shows the solubilities of various compounds, in water, at a pressure of 1 atm and at room temperature (approx. 293.15 K)

	Chloride Cl^-	Bromide Br^-	Iodide I^-	Carbonate CO_3^{2-}	Chlorate ClO_3^-	Hydroxide OH^-	Nitrate NO_3^-	Oxide O^{2-}	Phosphate PO_4^{3-}	Sulfate SO_4^{2-}	Dichromate $Cr_2O_7^{2-}$
Lithium Li^+	S	S	S	sS	S	S	S	R	?	S	S
Sodium Na^+	S	S	S	S	S	S	S	R	S	S	S
Potassium K^+	S	S	S	S	S	S	S	R	S	S	S
Ammonium NH_4^+	S	S	S	S	S	S	S	?	S	S	S
Beryllium Be^{2+}	S	S	R	?	?	?	S	R	?	S	?
Magnesium Mg^{2+}	S	S	S	I	S	I	S	I	I	S	I
Calcium Ca^{2+}	S	S	S	I	S	sS	S	R	I	sS	I
Strontium Sr^{2+}	S	S	S	I	S	S	S	R	?	I	?
Barium Ba^{2+}	S	S	S	I	S	S	S	R	S	I	?
Zinc Zn^{2+}	S	S	S	I	S	I	S	I	I	S	I
Iron(II) Fe^{2+}	S	S	S	I	S	I	S	I	I	S	I
	Chloride Cl^-	Bromide Br^-	Iodide I^-	Carbonate CO_3^{2-}	Chlorate ClO_3^-	Hydroxide OH^-	Nitrate NO_3^-	Oxide O^{2-}	Phosphate PO_4^{3-}	Sulfate SO_4^{2-}	Dichromate $Cr_2O_7^{2-}$

	Chloride Cl^-	Bromide Br^-	Iodide I^-	Carbonate CO_3^{2-}	Chlorate ClO_3^-	Hydroxide OH^-	Nitrate NO_3^-	Oxide O^{2-}	Phosphate PO_4^{3-}	Sulfate SO_4^{2-}	Dichromate $Cr_2O_7^{2-}$
Copper(II) Cu^{2+}	S	S	?	I	S	I	S	I	I	S	I
Aluminium Al^{3+}	S	S	X	?	S	I	S	R	I	S	I
Iron(III) Fe^{3+}	S	S	?	X	S	I	S	I	I	sS	I
Lead(II) Pb^{2+}	sS	sS	I	I	S	I	S	I	?	I	?
Silver Ag^+	I	I	I	I	S	sS	S	sS	I	sS	I

Key:	
S	soluble
I	insoluble
sS	slightly soluble
X	other
R	reacts with water
?	unavailable

Source (https://en.wikipedia.org/wiki/Solubility_chart, 18th August, 2017)